Scuola Internazionale Superiore Studi Avanzati
(SISSA)
Neurobiology sector

From misfolded recombinant proteins *in vitro* to pathological agents *in vivo*

Candidate: Le Tran Thanh Nhat
Supervisor: Giuseppe Legname

A thesis submitted for the degree of
Doctor of Philosophy
in Functional and Structural Genomics

Trieste, 27th March 2014

Acknowledgements

First and foremost I would like to express my gratitude to my supervisor, Prof. Dr. Giuseppe Legname for giving me a good opportunity to work in his group and for his continuous support in my PhD study. His understanding, patience and encouragement helped me to overcome the challenges not only in my work but also in my Italian life.

I warmly thank Erica Sarnataro for her kind help and assistance throughout English correction in this thesis and my PhD study.

I sincerely thank Dr. Fabio Moda, Dr. Ilaria Campagnani, Dr. Olivier Andreoletti, Dr. Alpan Bek, Prof. Dr. Chiara Zurzolo and Saida Abounit for great collaboration works and insightful discussions.

I also would like to thank all my friends in Prof. Legname's group, specially Dr. Tran Hoang Ngoc Ai, Dr. Joanna Narkiewicz, Dr. Gabriele Giachin, Dr. Ilaria Poggiolini, Dr. Lisa Gasperini, Dr. Mai Phuong Thao, Andrea Raspadori, Suzana Aulic, and Tran Thanh Hoa for their kind help, stimulating discussions in work and unforgettable experiences in my four PhD years.

Finally but importantly, I must deeply thank my grand mom, my parents, my husband and my lovely daughter for their constant support, encouragement, help, sacrifice and love to me throughout the years.

Sincerely yours,

Table of contents

ABSTRACT

The pathogenesis of a disease involves a stochastic refolding of the etiologic protein into a misfolded infectious state known as prion. Recently, there has been renewed interest in the possibility that proteins causing neurodegeneration are all prions. The β-sheet rich pathological α-synuclein (α-syn) can cross from the neurons of transplanted patients into the grafted cells, and induce a change in the structure of α-syn in Parkinson's disease (PD) is an example. The convergence of studies showing the presence of prions in the pathogenesis of common neurodegenerative maladies has since been remarkable. Studies on synthetic prions showed that recombinant (rec) prion protein (PrP) is refolded into infectious conformations *in vitro*. This synthetic prion protein stimulates the conversion of cellular PrP into nascent pathological PrP and induces the accumulation of the isoform that causes neurodegeneration *in vivo*.

Using defined biophysical and biochemical conditions *in vitro*, we developed methods for the pathological conversion of recPrP into PrP^{Sc}, and we established whether synthetic pathological agents of rec human α-syn amyloids can be infectious, as Legname *et al*. showed for the first time in production of mammalian synthetic prions. The pathological conversion process of both PrP and α-syn required only purified recombinant proteins and common chemicals. We generated putative infectious materials that possess different conformational structures. Moreover, we designed a novel build-in screening methodology for amyloid preparations to achieve putative infectious materials using amyloid-infected-cell culture assay.

At fifth cell passage after single infection, prion amyloid fibrils from different preparations induced endogenous PrP^{C} to convert into PrP^{Sc} in both non-infected mouse hypothalamic GT1 and mouse neuroblastoma N2a cell lines. Moreover, these variant synthetic proteinaceous infectious agents can replicate and be detected by protein misfolding cyclic amplification (PMCA). Through this methodology that was used to obtain synthetic mammalian prions, we also tested whether recombinant human α-syn amyloids can infect neuronal cell lines *in vitro*, and wild-type mice *in vivo*. A single exposure to amyloid fibrils of human α-syn was sufficient to induce aggregation of endogenous α-syn in human neuroblastoma SH-SY5Y cells, mouse hypothalamic GT1 cells and mouse brains. Interestingly, we found pathological phosphorylated α-syn in amyloid-infected cells and in neurons and neurites of mice. These results suggest that recombinant human α-syn amyloids can promote endogenous α-syn aggregation and pathological post-translational modification. Upon subsequent passages, mice inoculated with either human α-syn amyloid or diseased mouse brain homogenates showed marked neurological symptoms resembling those of PD, as well as neuropathological α-syn inclusions in neurons.

LIST OF FIGURES

LIST OF TABLES

LIST OF ABBREVIATIONS

AD: Alzheimer disease

ALS: Amyotrophic Lateral Sclerosis

Aβ: Amyloid-β

BDNF: Brain-derived neurotrophic factor

BMDC: Bone marrow-derived dendritic cell

BSA: Bovine serum albumin

BSE: Bovine spongiform encephalopathy

CJD: Creutzfeldt-Jakob disease

CNS: Central nervous system

CWD: Chronic Wasting Disease

DC: Dendritic cell

DLB: Dementia with Lewy bodies

DNA: deoxyribonucleic acid

ENS: Enteric nervous system

EUE: Exotic Unregulated Encephalopathy

fCJD: familial Creutzfeldt-Jakob disease

FDC: follicular dendritic cell

FFI: Fatal familial insomnia

FSE: feline spongiform encephalopathy

GALT: gut-associated lymphatic tissue

GCIs: Glial Cytoplasmic inclusions

Gnd-HCl: Guanidine hydrochloride

GPI: glycosylphosphatidylinositol

GSS: Gerstmann-Sträussler-Scheinker syndrome

GTP: guanosine triphosphate

HD: Huntington's disease

Htt: Huntingtin

Hu: human

IBs: inclusion bodies

iCJD: iatrogenic Creutzfeldt-Jakob disease

IHC: immunohistochemistry

LBs: Lewy bodies

LNs: Lewy neuritis

M: molar

Mo: mouse

mRNA: messenger RNA

MSA: Multiple System Atrophy

NAC: non-amyloid-β component

OR: octapeptide repeat

PAF: Pure Autonomic Failure

PD: Parkinson's disease

PIPLC: phosphatidylinositol-specific phospholipase C

PK: proteinase K

PMCA: protein misfolding cyclic amplification

PNS: peripheral nervous system

polyQ: polyglutamine

Prion: proteinaceous infectious particle

PrP^{C}: cellular (i.e. wild type) prion protein

PrPres: PK-resistant PrP

PrP^{Sc}: scrapie (i.e. infectious) prion protein

Rec: recombinant

ROS: reactive oxygen species

RT: Room temperature

sCJD: sporadic Creutzfeldt-Jakob disease

SDS: sodium dodecyl sulfate

SHa: Syrian hamster

SOD: Superoxide dismutase

$sPrP^{Sc}$: PK-sensitive PrP^{Sc}

TGN: trans-Golgi-network

ThS: Thioflavin S

ThT: Thioflavin T

TME: transmissible mink encephalopathy

TNT: tunneling nanotubes

TSE: transmissible spongiform encephalopathy

vCJD: variant Creutzfeldt-Jakob disease

WB: Western Blot

α-syn: α-synuclein protein

INTRODUCTION

1. Neurodegenerative diseases: findings on protein misfolding

1.1. Structural information on protein aggregates in neurodegeneration

1.1.1. Amyloid structure

Amyloids were first described in 1854 as deposits in human tissue that resembled carbohydrate starches when stained with iodine. It is well established that amyloid is predominantly composed of a β-sheet structure [1] based on the detailed structure deduced for cross-β silk [2]. Amyloid is a distinct β-sheet-rich fold that many peptides or proteins can acquire. Despite great variation in primary sequence, many proteins can assemble into amyloid fibrils [3]. However, all amyloids share several distinguishing biophysical properties. Proteins or peptides that adopt the amyloid fold assemble into β-sheet-rich fibrils, where the individual β-strands are oriented perpendicular to the fibril axis [4][5] (Figure 1). The cross-β structure and texture form a robust, stable structure in which the protein chains are held together securely by repetitive hydrogen-bond that extends the length of the fibrils. Fibrilization is initiated by self-aggregation of protein monomers into oligomers, which accumulate over time and nucleate the self-assembly cascade of fibril polymerization (Figure 2) characterized by the stacking of parallel or anti-parallel β-sheet secondary structure; this transition can be detected by circular dichroism (CD) spectroscopy. Once formed, amyloid fibrils are robust, extremely stable and difficult to solubilize [6]; they can also resist disassembly by enzymatic or chemical digestion. They show characteristic FTIR and X-ray diffraction patterns (Figure 1), and can bind to specific dyes such as Congo red (CR) and thioflavin T (ThT) resulting in a red shift and green birefringence under polarized light, leading to increased fluorescence at certain wavelengths, respectively [7]. Colorimetric and biochemical analyses of amyloids are often coupled because CR and ThT can bind other molecules, such as cellulose and amorphous aggregates, respectively [8]. Fibrilization is very sensitive even to small modifications of the peptide backbone [9]. The assembly of amyloid fibers does not require energy because amyloid proteins can "seed" their own oligomerization [10] (Figure 2).

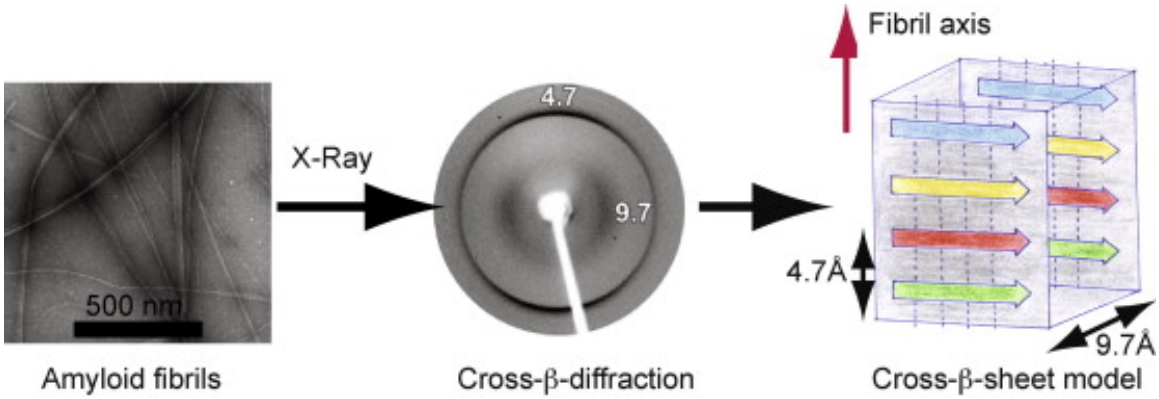

Figure 1. Amyloid fibrils are composed of long filaments as shown by the transmission electron micrograph. In the fiber diffraction pattern they show a meridional reflection at 4.7 Å and an equatorial reflection at around 8–11 Å, which suggest the presence of a cross-β-sheet structural motif as depicted in the drawing [11]

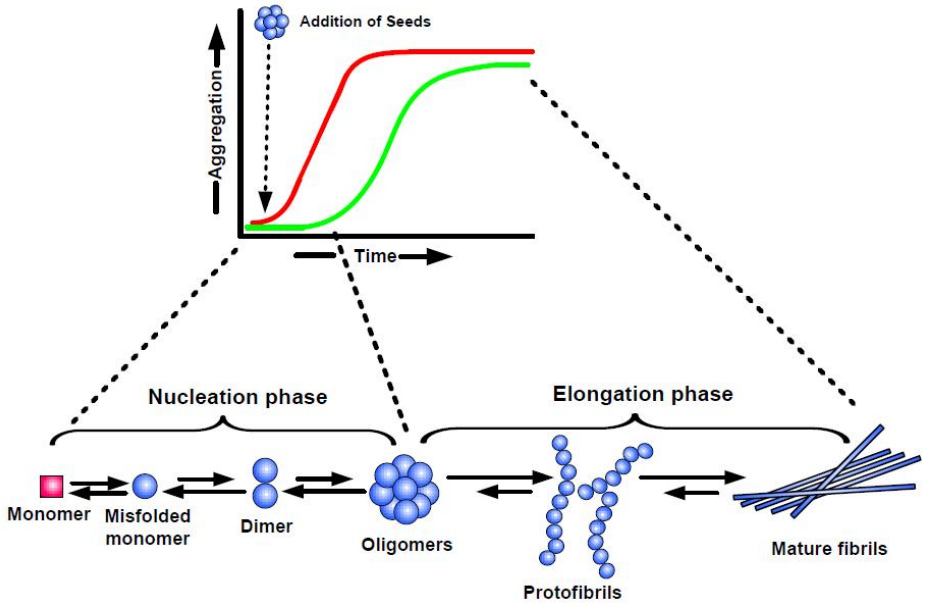

Figure 2. Nucleation-dependent polymerization model of amyloid aggregation. Amyloid formation consists of two phases: (i) a nucleation phase/lag phase, in which monomers undergo conformational change/misfolding and associate to form oligomeric nuclei, and (ii) an elongation phase/growth phase, in which the nuclei rapidly grow by further addition of monomers and form larger polymers/fibrils until saturation. The "nucleation phase", is thermodynamically unfavorable and occurs gradually, whereas the "elongation phase" is a much more favorable process and proceeds quickly. Thus, kinetics of amyloid formation is well represented by a sigmoidal curve with a lag phase followed by rapid growth phase (green curve). The rate-limiting step in the process is the formation of nuclei/seeds to promote aggregation. Thus, amyloid formation can be substantially speeded up by adding preformed seeds (nuclei). The addition of seeds reduces the lag time and induces faster aggregate formation (red curve) [12]

1.1.2. Abnormal protein aggregation in neurodegeneration

Despite the important differences in clinical manifestation, neurodegenerative disorders share some common features such as their appearance late in life, the extensive neuronal loss and synaptic abnormalities, and especially the presence of cerebral deposits of misfolded protein aggregates [13]. This is the reason why they are called "protein misfolding diseases". The formation of these insoluble inclusions is a hallmark of neurodegenerative diseases, and although the main protein component is different in each one, they have similar morphological, structural, and staining characteristics (Figure 3). Aggregation of misfolded proteins is one of the disease characteristics, and it is believed to occur through nucleated polymerization and fibril elongation that involves the addition of precursors [14]. In the early stages of disease, a key protein undergoes a major conformational change from its normal cellular structure to an alternative state, which forms amorphous and/or fibrillar aggregates. In most cases this transformation involves a partial unfolding of the native state and refolding into a β-sheet-rich conformation. These abnormal forms are traditionally considered to lie at the basis of protein misfolding diseases that affect humans, including prion diseases, Alzheimer's, Parkinson's and Huntington's diseases. [13][15].

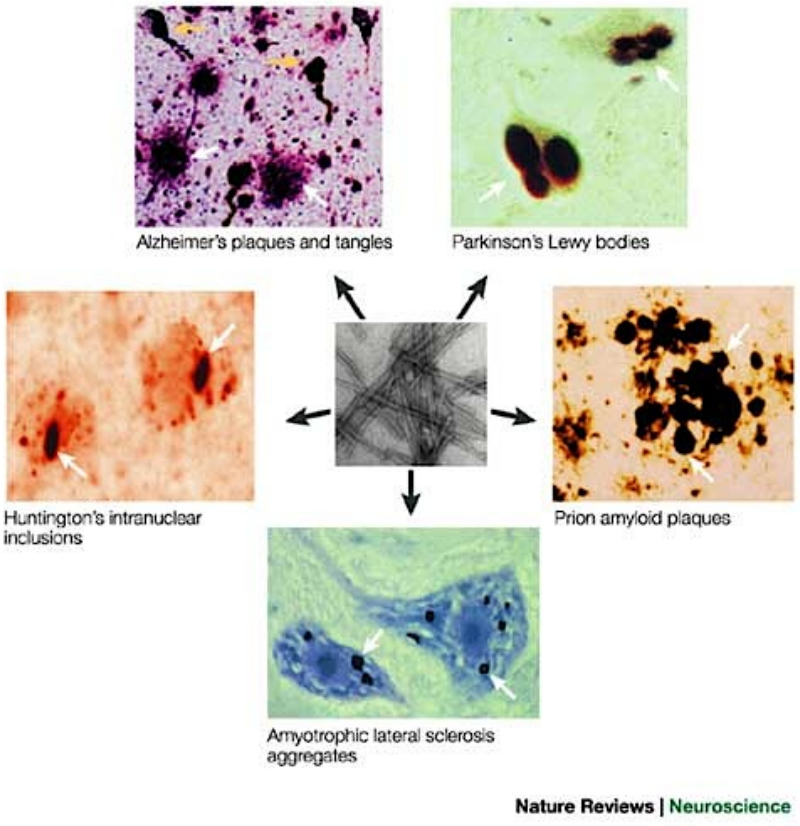

Figure 3. Cerebral aggregates in neurodegenerative diseases. Extracellular amyloid plaques (white arrows) and intracytoplasmic neurofibrillary tangles (yellow arrows) are the pathological signature of Alzheimer's disease. Intracytoplasmic aggregates are typically present in the neurons of people affected by Parkinson's disease and amyotrophic lateral sclerosis. Intranuclear inclusions of huntingtin are observed in Huntington's disease patients, and extracellular prion amyloid plaques that are located in different brain regions are present in some cases of transmissible spongiform encephalopathy. In spite of the different protein compositions, the ultrastructure of these deposits seems to be similar and composed mainly of a network of fibrillar polymers (center) [13]

Insoluble deposits and diffusible oligomers from different diseases are composed of individual amyloidogenic proteins as different as amyloid β-protein (Aβ), tau, prion protein (PrP), α-synuclein (α-syn) and huntingtin. In Alzheimer's disease there are two types of protein deposits: (i) Amyloid plaques are deposited extracellularly in the brain parenchyma and around the cerebral vessel walls, and their main component is a 40- to 42-residue peptide termed Aβ [16]; (ii) Neurofibrillary tangles are located in the cytoplasm of degenerating neurons and are composed of aggregates of hyperphosphorylated tau protein [17]. In patients with Parkinson's disease, Lewy bodies are observed in the cytoplasm of *substantia nigra* neurons. The major constituents of these aggregates are fragments of α-syn [18]. In patients with Huntington's disease, intranuclear deposits of a polyglutamine-rich version of huntingtin protein are a typical feature of the brain [19]. Patients with amyotrophic lateral sclerosis (ALS) have aggregates mainly composed of superoxide dismutase (SOD) in cell bodies and axons of motor neurons

[20]. Finally, the brains of humans and animals with diverse forms of transmissible spongiform encephalopathy (TSE) are characterized by accumulation of protease-resistant aggregates of the prion protein (PrP) [21]. Although the proteins implicated in each of these pathologies and the clinical manifestations of the diseases differ, the molecular mechanism of protein misfolding is strikingly similar. These diseases might share common structural epitopes and common mechanisms of neurotoxicity and memory impairment [22].

1.2. A brief overview of some neurodegenerative diseases

This section describes some of most common neurodegenerative diseases. Prion disorders and Parkinson's disease, also mentioned here, will be described and discussed more extensively in Chapter 2 (Prion disorders) and Chapter 5.1 (Parkinson's disease) as they are related to the subject of my PhD work.

1.2.1. Alzheimer's disease

Alzheimer's disease (AD) is the most common form of dementia. This progressive neurologic disease of the brain leads to the irreversible loss of intellectual abilities, including memory and reasoning, which becomes severe enough to impede social or occupational functioning [23]. AD is characterized by loss of neurons and synapses in the cerebral cortex and certain subcortical regions. This results in gross atrophy of the affected regions, including degeneration in the temporal and parietal lobes, and parts of the frontal cortex and cingulate gyrus [24]. Neurofibrillary tangles and amyloid plaques are the classical neuropathological hallmarks of AD [25][26][27]. Indeed, AD has been identified as a protein misfolding disease, caused by accumulation of abnormally folded Aβ known as extracellular aggregates, and intracellular aggregates of amyloid tau proteins in the brain [28][23]. Plaques are made of small peptides, 39–43 amino acids in length, called beta-amyloid (Aβ). Amyloid beta protein is a fragment from a larger protein called amyloid precursor protein (APP), a transmembrane protein that penetrates through the neuron's membrane. APP is critical to neuron growth, survival and post-injury repair [29][30]. AD is also considered a tauopathy due to abnormal aggregation of the tau protein, which stabilizes the microtubules when phosphorylated. In AD, tau undergoes chemical changes, becoming hyperphosphorylated; it then begins to pair with other threads, creating neurofibrillary tangles and disintegrating the neuron's transport system [31]. Most cases of AD are idiopathic (i.e., of an unknown cause), although mutations in the gene encoding APP or in the enzymes (presenilin gene) that sequentially cleave it cause inherited forms of the disease. These forms are relative rare. In sporadic AD, genes do not cause the disease, but they may influence the risk of developing the disease. The best-studied susceptibility gene in sporadic AD is apolipoprotein E (APOE), which is responsible for the production of a protein that transport cholesterol and fats through out the body. The protein may also be involved in structure and function of the fatty membrane surrounding a brain cell [32][33].

1.2.2. Huntington's disease

Huntington's disease (HD) is a neurodegenerative genetic disorder caused by the expansion of a CAG triplet repeat coding for polyglutamine stretch within the N-terminal of huntingtin protein, which gradually damages cells in the brain [34]. Mutations in the gene encoding huntingtin underlie the autosomal dominant inheritance of HD, which is characterized by involuntary movements, personality changes and dementia. These mutations also affect muscle

coordination and lead to cognitive decline and psychiatric problems. Huntingtin protein is made up of 3,144 amino acids, is expressed widely throughout the body and has numerous interacting protein partners. Its normal functions are not fully understood; it has been implicated in anti-apoptosis, neuronal gene transcription, synaptic function, and vesicle and axonal transport [35]. The mutation encodes an expanded polyglutamine tract, which makes the protein (or a fragment of the protein) prone to aggregate and to form intraneuronal inclusion bodies [36][19]. Generally, the number of CAG repeats is related to how much the pathological process is affected and the resulting disease status. A polyglutamine sequence containing 36 repeats in the corresponding disease protein is benign, whereas a sequence with only 2–3 additional glutamines is associated with disease risk. Above this threshold range, longer repeat lengths are associated with earlier disease onset [37][38] because the longer the polyglutamine tract, the more rapid the aggregation [39].

1.2.3. Parkinson's disease

Parkinson's disease (PD) is characterized by the loss of dopaminergic neurons in the *substantia nigra pars compacta* (SNc). The neuropathological hallmarks of this movement disorder are Lewy bodies (LBs) and Lewy neuritis (LNs), which are protein aggregates in the cell body and neuronal processes, respectively. In adult-onset of PD, LBs are found in cytoplasm of neurons, often near the nucleus. The most abundant protein in the aggregates is α-syn. This 140-amino acid presynaptic protein is natively unfolded, interacts with multiple proteins as well as lipids and membranes, and has been suggested to play a part in vesicular transport [40]. LBs can also be labeled for ubiquitin, a synuclein interactor termed synphilin-1, proteasome proteins, and cytoskeletal and other proteins [41]. Although most Parkinson's disease cases are idiopathic, mutations in the α-syn gene underlie rare, inherited forms. Recessive early-onset PD can be caused by mutations in the genes encoding parkin, DJ-1 or PINK 1 etc. [42], and can also be cause by toxins as MPTP, presumably by loss-of-function mechanisms.

1.2.4. Prion diseases

Transmissible spongiform encephalopathies (TSE) or prion diseases are fatal neurodegenerative disorders affecting the brains of both humans and animals. They can be sporadic (spontaneous), familial (genetic/inherited) or acquired (transmitted by infection). Human TSEs are rare neurological maladies including Creutzfeldt-Jakob disease (CJD), Gerstmann-Sträussler-Scheinker (GSS) syndrome, Fatal familial insomnia (FFI) and kuru. Animal TSE infections include scrapie in sheep and goats, bovine spongiform encephalopathy (BSE) in cattle, and chronic wasting disease (CWD) in elk, deer and moose [43][44][45]. Inherited prion diseases include CJD, GSS and FFI. Variant CJD is believed to be acquired from cattle infected with BSE. However, most cases of human prion diseases occur as sporadic CJD (sCJD) [46][47][48]. Acquired prion diseases include iatrogenic CJD, kuru, variant CJD (vCJD) in humans, scrapie in sheep, and bovine spongiform encephalopathy (BSE) in cattle. Both human and animal conditions share common histopathological features that include neuronal loss with deposition of amyloid plaques, spongiform vacuolation of grey matter and astrogliosis [49]. Prion diseases are linked to the misfolding and subsequent aggregation of the normal globular protein PrP^C [50]. PrP^C is encoded by the prion gene (*PRNP*) on human chromosome 20, with equivalent prion genes in animals. The function of PrP^C remains unknown but it may play a role in anti-oxidant systems and cellular copper metabolism. The distinctive feature of

these diseases is the presence of: (i) microscopic vacuolization of the brain tissue, called spongiform degeneration (meaning that the tissue deteriorates, developing a spongy texture); and (ii) an abnormal protein, called scrapie prion protein (PrP^{Sc}), prions or abnormal prion protein. Unlike other known infectious diseases, prions are believed to result from a change in the conformation of PrP^{C}, which is present in large amounts in the brain as well as in other tissues. Since the abnormal prion protein cannot be broken down through the body's normal processes, it aggregates mostly in the brain, causing degeneration and disease. PrP^{Sc} deposition is associated with neuropathological changes such as neuronal loss, astrocytic gliosis, and spongiform change (Figure 4).

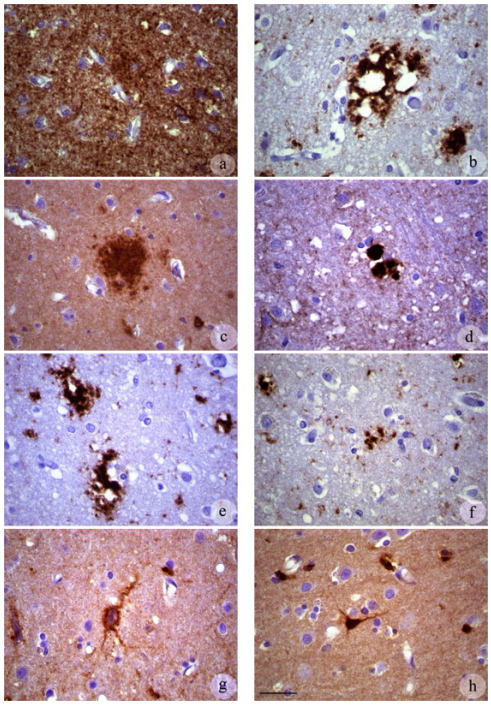

Figure 4. Histological features of prion diseases. Immunohistochemical staining for prion protein on frontal cortices of sCJD (a–d, f–h) and vCJD (e) illustrating deposition of the prion protein in the form of synaptic (a), perivacuolar (b), plaque-like (c), kuru-plaque (d), florid plaque (e), punctuate (f), perineuronal (g), and intraneuronal (h) patterns. Scale bar in h = 50 μm.[51]

2. Transmissible proteins and prion diseases

2.1. Prion diseases in humans

2.1.1. Creutzfeldt-Jakob disease (CJD)

Creutzfeldt-Jakob disease (CJD) is the most common human prion disease. There are three types of CJD: 1) sporadic, also called spontaneous, for which the cause is not known; 2) familial, also called genetic or inherited, which is due to a defect in the prion protein gene; and 3) acquired, which is transmitted by infection due to exposure to the infectious prion from contaminated meat, or from transplant of contaminated tissues or use of contaminated instruments during surgical procedures. In human prion diseases, a common polymorphism at

codon 129 has important effects on susceptibility to disease, the resulting clinical characteristics and the incubation period (in acquired forms). At codon 129 of *PRNP*, an individual may encode for methionine (M) or valine (V) and, therefore, all humans are MM or VV homozygotes or MV heterozygotes.

Sporadic Creutzfeldt-Jakob disease (sCJD) is the most common form of human prion disease, accounting for approximately 85% of all cases, arising from either a spontaneous *PRNP* gene somatic mutation or a stochastic PrP protein structural change. sCJD includes five distinct types, which differ in clinical characteristics (observable physical and subjective symptoms) and neuropathological characteristics (brain tissue changes). The molecular features of the different sCJD types also vary, such as the genotype at codon 129 of the prion protein gene and the length of the scrapie prion protein. As stated above, codon 129 MM is clearly a risk factor for sporadic CJD, with MV heterozygosity affording a partial protection. sCJD typically presents with a rapidly progressive dementia. Other neurological features include cerebellar ataxia and, most characteristically, myoclonus [52][53].

Familial CJD (fCJD) is the second most common type of CJD, accounting for approximately 10-15% of cases worldwide. This hereditary form of CJD is caused by a genetic mutation in the prion protein gene, which causes a change in the amino acid sequence of the normal prion protein. This is believed to cause the mutated prion protein to take on the scrapie prion protein conformations. Currently, there are over 55 mutations of the prion gene, that are known to cause fCJD and other familial prion diseases in humans, including FFI and GSS [736]. The mutations include missense point mutations, octapeptide repeat mutations with insertions of 1, 2 and 4–9 additional repeats, octapeptide repeat mutations with deletion of two repeats and two nonsense mutations. Three missense polymorphisms located at codons 129 (M/V), 171 (N/S), and 219 (E/K), and the deletion of one 24-bp octapeptide repeat is known along with 12 silent polymorphisms [52].

Variant CJD (vCJD) is also a form of acquired CJD, and is thought to be transmitted through the ingestion of contaminated meat [54][55]. vCJD can affect young people, with a mean age at death of 29 years (range 15–73 years) in contrast to a mean age at death of 65 years in sporadic CJD. The early clinical course is dominated by psychiatric symptoms, including depression, withdrawal and anxiety, although a minority of cases has early neurological symptoms in the form of cognitive impairment and, notably, persistent painful sensory symptoms. On average, after six months ataxia develops and this is associated with involuntary movements, which may be choreiform, dystonic, or myoclonic. There is progressive cognitive impairment and other focal signs may occur, including dysphasia, rigidity, hyperreflexia, and primitive reflexes. The later stages are similar to those of sporadic CJD, with terminal akinetic mutism in many cases. The mean survival time is around 14 months, but some patients have survived over three years from the first symptom. Furthermore, vCJD is the only type of prion disease in which a definitive diagnosis can be made with a tonsil biopsy [54][55].

In retrospect, transmission of CJD via neurosurgical instruments probably occurred in the 1950s in three cases operated on in the same theatre, with instruments previously used in cases of CJD. In the 1980s iatrogenic transmission via human pituitary growth hormone and human dura

mater grafts was recognized. Iatrogenic CJD (iCJD) is a form of acquired CJD and one of the least common types, accounting for less than 1% of cases. Both laboratory and clinical research has determined that human-to-human transmission of CJD can occur. [54]. Iatrogenic CJD in humans can have incubation periods longer than 30 years [56]. The route of exposure determines the clinical presentation of iatrogenic CJD. In cases with effective inoculation into the CNS via neurosurgical instruments, for example, the clinical features are indistinguishable from sporadic CJD, with rapidly progressive dementia and myoclonus. Survival is usually measured in months.

2.1.2. Kuru

Kuru was the first human prion disease to be transmitted to experimental animals. As an acquired prion disease, it is virtually extinct. Gajdusek first described it in Papua New Guinea as a disorder linked to ritual cannibalism, caused by a peripheral route of exposure. It also presents with a predominant cerebellar syndrome [57]. The epidemics probably originated from the consumption of contaminated meat from a member of the tribe affected by sporadic CJD. The central clinical feature of kuru is progressive cerebellar ataxia and dementia that is a less prominent and usually late clinical feature. In comparisons of the transmission properties of kuru prions with those isolated from patients with sCJD, iCJD and vCJD in both transgenic and wild-type mice, kuru prions have shown prion strain properties equivalent to those of classical (sporadic and iatrogenic) CJD prions but distinct from vCJD prions [54][58].

2.1.3. Gerstmann-Sträussler-Scheinker syndrome (GSS)

Gerstmann's publications in 1928 and 1936 originally described the syndrome observed in a large Austrian family, with affected members manifesting slowly progressive cerebellar ataxia coupled with cognitive decline at sometime in the course of their illness. According to the clinical symptoms, GSS was classified as prion disease in 1981 [59]. Although this syndrome is somewhat non-specific, all GSS patients share the distinctive underlying neuropathological feature of widespread milticentric amyloid plaques, which equally facilitate delineation of this group of disorders as a discrete entity [60]. GSS is characterized by an early onset between 30 and 60 years of age and slow disease progression extended over a period of 3.5-9.5 years. The *PRNP* polymorphism M129V has been shown to influence the disease phenotype. When linked to V129 allele, P102L, which is the most common cause of GSS, resulted in the predominance of psychiatric signs such as apathy and depression. Following PRNP mutations have been shown to cosegregate with GSS: P102L, P105L, A117V, Y145X, Q160X, F198S, Q217R, Y218N, Y226X and Q227X [61][62][63]. Only patients harboring this mutation have been reproducibly transmissible, but even then in just 40% of such cases [60]. The other less frequent mutations associated with GSS either have not transmitted or have not been assessed [64][65][66].

2.1.4. Fatal familial insomnia (FFI)

The descriptive diagnosis FFI was first used in 1986 to depict an illness afflicting five members of a large Italian family [67] but it was not until 1992 that the disorder was proposed as a novel, genetically determined prion disease [68]. Final nosologic verification as a TSE was achieved with its eventual successful transmission to laboratory animals [66][69]. Since its clarification as a TSE, a number of additional FFI pedigrees have been described. The FFI cases present

between 20 and 72 years with an average of 49 years and may live after the disease onset for 8-72 months with an average of 18.4 months [68][70][71][72][73][74]. The D178N mutation had previously been described as the cause of familial CJD [75][76]. However, FFI was found to segregate with the D178N mutation when combined in *cis* with methionine at codon 129 (D178N–129M), whereas CJD was linked to valine at the latter coding position (D178N–129V) [77]. Detailed studies of kindred containing the D178N mutation have shown sufficient clinicopathological diversity and overlap [78]. Sporadic Fatal insomnia (sFI) has clinical and histopathological features indistinguishable from those of FFI but does not have the mutation on the prion gene that characterizes FFI [52][53].

Table 1. Prion diseases in humans (*G S G Knight, J Neurol Neurosurg Psytriaty, 2004; 75*)

Disease	Abbreviation	Mechanism of pathogenesis	Notes
Creutzfeldt-Jakob disease	CJD	Unknown mechanism	The most common human prion disease. First described in 1921 Exists in four forms: Sporadic Genetic Iatrogenic Variant (described in 1996)
Sporadic CJD	sCJD	Unknown mechanism; possibly somatic mutation or spontaneous conversion of PrP^{C} to PrP^{Sc}	
Variant CJD	vCJD	Infection presumably from consumption of BSE-contaminated cattle products and secondary blood-borne transmission	
Familiar CJD	fCJD	Germline mutations in PrP gene	
Iatrogenic CJD	iCJD	Infection from contaminated corneal and dural grafts, pituitary hormone, or neurosurgical equipment	
Kuru		Infection through ritualistic cannibalism	Confined to Papua New Guinea. Related to cannibalistic mourning rituals
Gerstmann-Sträussler-Scheinker syndrome	GSS	Germline mutations in PrP gene	A rare autosomal dominant hereditary disease
Fatal familial	FFI	Germline mutations in PrP	A rare autosomal dominant hereditary

insomnia	gene	disease

2.2. Prion diseases in animals

Prion diseases occur in many animal species and more frequently as infectious disorders (Table 2). The most known are scrapie in sheep and goat, bovine spongiform encephalopathy (BSE) in cattle, chronic wasting disease (CWD) [79] of mule deer and elk, transmissible mink encephalopathy (TME) and the more recently described feline spongiform encephalopathy (FSE) [80].

Scrapie is the prototype of prion disease. Its name originates from the main clinical symptom, an itching sensation caused by the disease that induces the animal to scrape its fleece off. In 1936, studies demonstrated that scrapie can be transmitted to goat upon injection with scrapie infected brain homogenate. Further transmission experiments demonstrated the ability of scrapie to cross the "species barrier", including the effective transmission to sheep [81], laboratory mice [82] and other species. Up to now, scrapie has never been shown to pose a threat to human health [83].

Bovine spongiform encephalopathy (BSE), commonly known as "mad cow disease", appeared for the first time in 1986 in Great Britain like an epidemic that infected nearly one million cows with prions [84][85]. The clinical signs of BSE may include tremors, gait abnormalities particularly of hind limb (ataxia), aggressive behavior, apprehension, and hyperreactivity to stimuli. PrP^{Sc} accumulation and spongiform vacuolation are usually found in the brain [86]. Brain extracts derived from prion-infected cows can transmit the disease to mice and other species like sheep and pigs after intracerebral inoculation [87][88][89]. At the terminal stages of the disease, BSE prions may also be detected in spinal cord, retina, ileum, adrenal glands, tonsils, bone marrow, peripheral nerves, dorsal root ganglia, trigeminal ganglion and thoracic ganglia. Epidemiological and transmission studies have found no evidence of BSE prions in milk, semen or embryos and there is little or no evidence of its horizontal transmission. However, the offspring of infected animals have shown an increased risk for disease development. The incubation period for BSE is 2 to 8 years and most BSE cases have been found in 4- to 5-year-old dairy cattle [86]. Apart from the BSE strain causing classical BSE, two other strains (H-type and L-type) causing atypical BSE have been described. Most atypical BSE cases have been detected during active surveillance targeting fallen stocks and slaughtered animals [90][91]. More importantly, unlike scrapie, BSE can be transmitted to humans by ingestion of contaminated food, resulting in a new variant of disease, vCJD [92][93]. These atypical BSE cases presented unusual neurophathological features that did not match with CJD cases [50]. Natural cases of BSE transmission have been described in sheep and goats. Such bovid animals may be an additional source of BSE transmission to humans [94][95]. Indeed, transgenic mice expressing human PrP^{C} are more susceptible to sheep-passaged BSE than classical BSE [96]. The origins of BSE are unknown. Although several *PRNP* variants have been described for cattle [97][98], only three amongst these variants — a 23-bp indel in the *PRNP* promoter, a 12-bp indel in the first intron and an E211K polymorphism — are known to confer susceptibility to BSE [99][100][98][101].

Chronic wasting disease (CWD) is a TSE of mule deer, white-tailed deer, black-tailed deer, Rocky Mountain elk, and Shira's moose. To date, CWD has been found mainly in cervids. CWD was first recognized as a clinical "wasting" syndrome in 1967 in mule deer in wildlife, and is typified by chronic weight loss leading to death. Intracerebral transmission of the scrapie agent has been shown to induce the disease in elk [85][102][103]. CWD can also cause these animals to have a rough, dry coat, and patchy retention of the winter coat in summer. In subclinical or early clinical CWD, affected cervids, particularly elk, may also show some other highly subtle symptoms including lassitude, sudden death in deer after handling, a lowered head and drooping ears and behavioral changes such as fixed gaze and lack of fear of humans. With the progression of the disease, more perceptible symptoms may arise: flaccid hypotonic facial muscles, ataxia, head tremors, teeth grinding, repetitive walking close to the boundary of the enclosure, hyperexcitability with handling, excessive salivation due to difficulty swallowing, esophageal dilation or ruminal atony, regurgitation of ruminal fluid, polyuria, polydipsia, syncope, and aspiration pneumonia. Upon histopathological examination, the CNS of affected cervids shows intraneuronal vacuolation, degeneration and loss of neurons, extensive neuropil spongiosis, astrocytic hypertrophy and hyperplasia, and occasional amyloid plaques. Spongiform lesions are mainly observed within the thalamus, hypothalamus, midbrain, pons, medulla oblongata, the olfactory tubercle and cortex. The most consistent histological lesions and PrP_{CWD} immunohistochemical staining are seen within the dorsal motor nucleus of the vagus nerve, which is considered the first site of PrP_{CWD} accumulation. Importantly, the clinical signs of polyuria and polydipsia and the low urine specific gravity in clinically dehydrated animals may be attributed to severe lesions in the supra-optic and paraventricular nuclei, where the production of anti-diuretic hormone occurs [85]. Incubation periods in CWD lie within the range of 16 months to 5 years and the disease equally affects both males and females. Death usually occurs within 1 year after the onset of clinical signs [85]. Epidemiological and experimental data provide evidence that horizontal transmission of CWD can efficiently occur by contact with affected animals or through environmental exposure [85][104][105][106]. So far, the natural transmission of CWD has not been evident in humans nor in domestic bovids such as sheep and cattle. Moreover, transgenic mice expressing either the human, ovine or bovine PrP^{C} coding frames did not develop the disease when inoculated with the CWD agent [85][104][106]. However, other cervids such as red deer and reindeer/caribou are also susceptible to CWD through intracerebral inoculation [107][108]. CWD is also intracerebrally transmissible to cattle, sheep, goats, ferrets, hamsters, bank voles, mink, raccoons and squirrel monkeys [104]. The PrP_{CWD} infectivity can be detected in the nervous system, the lymphoreticular system, the hematopoietic system, skeletal and cardiac muscles, pancreas, fat, retina, and the adrenal and salivary glands of naturally and/or experimentally infected animals [85][104][109][110][111]. Virtually, no tissue in infected cervids should be considered free of the CWD agent. Susceptible animals may acquire the infection from their habitats during feeding on grasses or by drinking water contaminated with PrP_{CWD} which affected cervids excrete or secrete or deposit into the environment, even in the asymptomatic carrier state, in the form of feces, urine, saliva, blood, placenta and carcasses [85][104][112][113]. Acquisition of the infection may be further enhanced by oral abrasions and nasal exposure to PrP_{CWD}-containing droplets and aerosols [114][115]. An important point is that the TSE agents can bind to soil particles, persist there for years still retaining the infectivity, and transmit the disease via oral route with even more

efficiency [116][117]. These investigations provide a plausible explanation for the high incidence of CWD and efficient transmission of the infection among cervids. *PRNP* polymorphisms S96G, M132L and S225F in cervids have been associated with resistance to CWD [104][111][118][119].

Exotic ungulate encephalopathy (EUE) is a TSE of exotic zoo ruminants of the family Bovidae. During a period overlapping with BSE epidemic, 6 greater kudu, 6 elands, 2 each of Arabian oryx and ankole cattle, and 1 each of gemsbok, nyala, scimitar-horned oryx and bison were diagnosed with EUE from the UK. The affected animals had been fed meat and bone derived from ruminants. Indeed, mice inoculated with brain homogenates from greater kudu and nyala with EUE, and from cattle with BSE developed a TSE with similar profiles of neuropathological lesions, and incubation periods. Strain typing studies in these mice also revealed a similarity between the EUE and BSE strains, supporting the hypothesis that EUE is caused by an infection with PrP_{BSE}. The course of EUE and clinical symptoms, according to the species, are distinct from those of BSE and scrapie. All EUE cases died of this disease [85][120][121].

Feline spongiform encephalopathy (FSE) is a TSE of domestic cats and captive wild members of the family Felidae. As most FSE cases occurred in parallel to the BSE epidemic, exposure of affected cats to feed contaminated with PrP_{BSE} was taken as causative of the disease. TSE profiles of neuropathological lesions and incubation periods are similar in mice after inoculation of brain homogenates from cats with FSE and cattle with BSE. Strain typing studies in these mice also revealed a similarity between the FSE and BSE strains, supporting the hypothesis that FSE is caused by an infection with BSE prions [104][122][123]. However, in 1998, a domestic cat and his owner were shown to be affected with a similar strain distinct from PrP_{BSE}. A bifurcation in phenotypes was noted: the man revealed a phenotype reminiscent of sCJD rather than vCJD, and the cat showed a clinical phenotype distinct from FSE. It remains unknown whether this incidence was due to a chance, whether a horizontal transmission occurred between the man and the cat, or if both contracted the disease from the same unknown source [124]. The clinical manifestation of the disease includes severe behavioral changes, depression, restlessness and neglect in coat grooming. The behavioral changes include fear, uncharacteristic aggressiveness or unusual timidity and hiding. Abnormal or hypermetric gait and ataxia, mainly of the hind limbs, are also characteristics of FSE. Affected cats often show poor judgment of distance and hyperesthesia to touch or noise, and may also develop tremors, stare vacantly or circle. In addition, excessive salivation, polyphagia, polydipsia and dilated pupils have been reported as symptoms of FSE. At the end of the disease course, convulsions may occur and somnolence is common. Death occurs after 3-8 and 8-10 weeks of clinical onset of the disease in domestic cats and cheetahs, respectively [85]. Neuropathological profiles of FSE include spongiform degeneration in the neuropil of the brain and spinal cord, with a predominance of the most severe lesions in the medial geniculate nucleus of the thalamus and the basal nuclei. PrP deposits of the FSE agent, with characteristic florid plaques, have been detected by immunohistochemistry in the central and peripheral nervous system, retina, lymphoreticular system, kidney and adrenal glands [85][122][123].

Transmissible mink encephalopathy (TME) is a rare TSE of farmed mink. Mink is a small semi-aquatic wild mammal that is raised in several countries for the production of fur. TME was first

recognized in Wisconsin and Minnesota in 1947. Subsequently, TME outbreaks in US have occurred in the '60s and '70s with the most recent upsurge in 1985 [125]. Although the origin of TME is still unknown, contaminated feed, mainly with the scrapie agent, was presumed to be the main source of infection. Mink inoculated with various strains of the scrapie agent developed TME. Oral infection of minks with the classical BSE agent also caused TME, but animals exhibited docile rather than aggressive behavior. More recently, the L-type BSE agent has been described as the most likely candidate for being causative of TME [126][85]. TME is readily transmissible to raccoons by parenteral, intracerebral and oral routes, and can be transmitted intracerebrally to striped skunks, ferrets, American sable, beech martens, cattle, sheep, goats, hamsters and non-human primates such as rhesus macaque, stump-tailed macaque and squirrel monkey. Non-transgenic mice are not susceptible to TME [85]. TME passaged in cattle has also been transmitted to mink both intracerebrally and orally with incubation periods of only 4-7 months [127]. A bifurcation in clinical phenotypes with distinct incubation periods, neuropathological lesions and biochemical profiles was produced in hamsters on inoculation with TME. Depending on clinical symptoms of the disease, one strain was named as “hyper (HY)” while the other as “drowsy (DY)” [128]. On co-infection of these strains, DY showed a dominant competition for the recruitment of cellular PrP^C into oligomers, and may reduce the incubation time or even block the ability of HY to cause the disease [129].

The clinical manifestation of the disease includes behavioral changes such as increased aggressiveness and hyperesthesia, depression, restlessness, and neglect in parental care and coat grooming. The affected minks often soil the nest or scatter feces in the cage. At the earlier stages of disease they may also exhibit difficulty eating and swallowing. Later, symptoms such as abnormal gait, ataxia, incoordination, occasional tremors, clenching of the jaw, curved tail like those of squirrels, and compulsive biting or mutilation of objects or of the self, particularly of the tail, may be noted. Near the end of the disease course, convulsions may occur, and minks become somnolent and unresponsive, and can be seen to press their heads against the cage for hours. Incubation time in naturally occurring TME may range from 6 to 12 months, and death usually occurs within 2 to 8 weeks [85].

Neuropathological features of TME include extensive spongiform degeneration in the neuropil of the brain; astrocytosis also occurs. Spongiform changes are intense in the cerebral cortex, particularly in the frontal cortex, as well as the corpus striatum, thalamus and hypothalamus, but are less severe in the midbrain, pons and medulla, and usually are not evident in the cerebellum and spinal cord. In addition to CNS, PrP deposits of the TME agent, but not amyloid plaques, have been detected in spleen, intestine, the mesenteric lymph node, thymus, kidney, liver and salivary glands of experimentally infected mink [85].

TSE in non-human primates (NHP). Two Mayotte brown lemurs and 1 each of white fronted brown lemur, mongoose lemur and Rhesus macaque from a zoo and three primate facilities in France were diagnosed with a TSE, from 1996 to 1999. Although a large number of non-human primates are susceptible to experimental exposure to various TSE strains, they have never been reported before to contract a TSE naturally. The affected animals had been fed primate diets likely contaminated with meat. Indeed, lemurs experimentally inoculated with brain homogenates from cattle with BSE developed a TSE with profiles of neuropathological lesions

similar to those seen in naturally infected lemurs. Strain typing studies also revealed a similarity between the two strains. Further, in these naturally and experimentally infected lemurs, immunohistochemical examination showed similar staining patterns and the distribution of PrP^{res} in the brain, spinal cord, tonsils, spleen and various sections of the gut and gut-associated lymphatic tissues [85][130].

Table 2. Prion diseases in animals (*G S G Knight, J Neurol Neurosurg Psytriaty, 2004; 75*)

Disease	Abbreviation	Natural host	Mechanism of pathogenesis	Note
Scrapie		Sheep, goats, mouflon	Infection in genetically susceptible sheep	Naturally occurring disease of sheep and goats
Bovine spongiform encephalopathy	BSE	Cattle	Infection with prion-contaminated feedstuffs	First reported in 1987
Chronic wasting disease	CWD	Mule, deer, white-tailed deer, Rocky Mountain elk	Unknown mechanism; possibly from direct animal contact or indirectly from contaminated feed and water sources	Confined to North America
Exotic ungulate encephalopathy	EUE	Nyala, greater kudu and oryx	Infection with BSE-contaminated feedstuffs	
Feline spongiform encephalopathy	FSE	Domestic and wild cats in captivity	Infection with BSE-contaminated feedstuffs	BSE-related diseases. Transmission of BSE to cats (FSE) and other animals
Transmissible mink encephalopathy	TME	Mink	Infection with prion-contaminated feedstuffs	A disease of farmed mink

2.3. The prion protein gene

The *PRNP* gene encodes the prion protein, which has been implicated in various types of transmissible neurodegenerative spongiform encephalopathies. This gene belongs to the *PRN* gene family that consists of *PRND*, encoding for Doppel protein [131] and *SPRN*, encoding Shadoo [132]. Approximately 15% of human prion diseases are inherited (fCJD, GSS, FFI) and associated with coding mutations in the *PRNP* gene. The cDNA clone corresponding to a pathogenic PrP fragment from a scrapie-infected hamster brain cDNA library was isolated in 1985 [133]. In 1986 Kretzschmar *et al.* isolated a *PRNP* cDNA from a human retina cDNA library [134]. The 253-amino acid protein shared 90% amino acid sequence identity with the hamster protein. In the same year, Basler *et al.* also determined that the pathogenic PrP protein in scrapie and normal cellular PrP are encoded by the same gene [135]. The PrP coding sequence encodes an amino-terminal signal peptide. The primary structure of PrP encoded by the gene of a healthy animal did not differ from that encoded by a cDNA from a scrapie-infected animal, suggesting that the different properties of PrP from normal and scrapie-infected brains are due to posttranslational events. *PRNP* is located in the short arm of chromosome 20 in humans and in a homologous region in mouse chromosome 2 [136]. About gene structure, the open-reading frame (ORF), responsible for transduction of the PrP^C protein, resides in a single exon in all mammalian prions and avian gene *PRNP* [135][137]. However, the *PRNP* gene comprises two to three exons that contain untranslated sequences including the promoter and terminal sequences [61][138][139]. The region 5-prime of the transcriptional start site has GC-rich features commonly seen in housekeeping genes. Mahal *et al.* characterized the promoter region of *PRNP* [140]. This region is highly GC-rich, lacks a canonical TATA box, contains a CCAAT box, and has a number of putative binding sites for transcription factors SP1 [141], AP1, and AP2. *PRNP* transcript is constitutively expressed in different tissues and especially in different brain of different animals, but highly regulated during development [142][133]. In addition, PrP-related mRNA was found at similar levels in normal and scrapie-infected hamster brain, as well as in many other normal tissues during the course of prion disease [133]. High levels of similarities in *PRNP* sequence have been found by aligning more than 40 translated sequences from different species [143]. This highlights the importance of PrP^C protein functions and explains why the gene has been conserved through the evolution, and the risk of prions in transmission within the “species barrier” on the other hand.

2.4 The cellular prion protein

The physiological cellular form PrP^C is a glycosylphosphatidylinositol (GPI) anchored polypeptide present on the outside leaflet of the cellular membrane of most cell types in mammals (Figure 6A). PrP^C expresses early in embryogenesis and is present at a high level in the adult CNS, particularly in neurons but also in glial cells [144][145][146][147]. In neurons, PrP^C is predominant in axons and dendrites [148]. It seems to be excluded from synaptic vesicles but present within the synaptic specialization and perisynaptically [149][150][151]. PrP^C is also found mostly on plasma membranes [152]. In addition, PrP^C is widely expressed in the immune system, in hematopoietic stem cells and mature lymphoid, and myeloid compartments [153]. Also many other tissues and organs like the spleen, intestines, skin, muscles and heart have been found positive for PrP expression.

While most PrP molecules are linked to the plasma membrane exclusively via a GPI anchor, three topological variants have been described: CytoPrP, NtmPrP, and CtmPrP [154]. CytoPrP, in which the polypeptide chain lies entirely in the cytoplasm, is produced at low levels as a result of inefficient translocation into the ER [155]. The amount of CytoPrP can be regulated by cellular stress, a mechanism that has been termed "pre-emptive quality control" [156]. Mice expressing a transgenically encoded form of CytoPrP show a severe neurodegenerative phenotype, indicating that this molecule possesses neurotoxic activity [157]. It has been claimed that prion infection increases production of CytoPrP [158]. At present, the pathogenic role of CytoPrP in prion diseases remains unclear [159]. Two other transmembrane variants of PrP, NtmPrP and CtmPrP, span the lipid layer once via a stretch of hydrophobic amino acids in the central region of protein [159] with opposite sequence orientation with respect to the lumen of the endoplasmic reticulum [160].

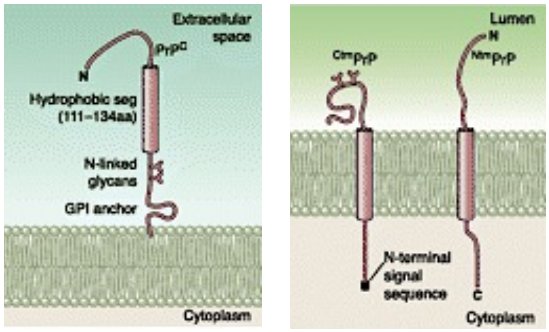

Figure 5. Two transmembrane variants of PrP, NtmPrP and CtmPrP. Mature PrP^C translocates to the outer leaflet of the plasma membrane. Instead, CtmPrP and NtmPrP are unusual transmembrane forms, generated in the ER, which have their COOH or NH_2 terminus in the ER lumen, respectively [89].

Full-length PrP^C is found in non-, mono-, or diglycosylated forms [161]. A rather large variety of N-glycans are found attached to both full-length and truncated PrP^C [162][163], which may be differentially distributed in various areas of the CNS [164][165]. The physiological significance of PrP^C glycosylation is unknown.

2.4.1. PrP^C structure

The pre-pro-protein is composed of 253 amino acids in humans. Removal of 22-amino acid N-terminal and 23-amino acid C-terminal sequences leaves a functional protein, which is 209 amino acids in length and is attached to the cell membrane through a glycophosphatidylinositol (GPI) anchor. Other prominent posttranslational modifications include a disulfide bond between Cys179 and Cys 214, and N-linked glycosylation at Asn 181 and Asn 197 [166] (Figure 6).

Structural and biophysical studies with brain derived PrP^C have been hindered by relative low expression levels and difficulties in obtaining larger quantities of highly purified material. Thus, most structural information about PrP^C has come from studying proteins and polypeptides, which have been prepared through recombinant expression in bacteria or chemical synthesis. Despite the lack of translational modifications such as glycosylation and the GPI anchor, rPrP has been shown to be structurally equivalent to PrP^C found *in vivo* [167].

The part of PrP that is structurally best characterized is the C-terminal domain (residue ~21-231), often referred to as "structured" or "folded" domain. By contrast, the N terminal domain part of the molecule is highly flexible, and early nuclear magnetic resonance (NMR) experiments suggest that it is largely disordered [168][169]. This structurally less-defined NH_2 proximal region consists of residues 23-124 and contains a stretch of several octapeptide repeats (OR) (Figure 6), flanked by two positively charged clusters, CC1 (aa 23-27) and CC2 (aa 95-110), which are important for PrP trafficking. These domains are linked by a hydrophobic stretch of amino acids known as the hydrophobic core (HC) region (aa 111-135) that can be used by PrP^C to assume different transmembrane topologies. As mentioned above, PrP^C presents at least three distinct topological orientations: the fully extracellular form, which is GPI anchored (Figure 6) and two transmembrane isoforms (called Ntm-PrP and Ctm-PrP) [160] (Figure 5). The N-terminal region encompasses five signature OR that coordinate copper and, to a lesser extent, other metal ions. In addition to its ability to bind copper, the OR region has been found to bind polyanions such as glycosaminoglycan, hemin, as well as oligonucleotides and nucleic acid [170][171]. Although the repeats have a propensity to be disordered, they can form β-turn conformations under physiologically relevant conditions [172][173]. Interestingly, the OR region does not appear to be essential for prion infectivity [174]. Although this region has been hypothesized to play a role in self-association of the prion protein [175], it is not a part of the β-sheet rich core of the infectious PrP^{Sc}. Nonetheless, it is perplexing that germline insertion of extra OR results in familial prion disease in humans [176]. This has been corroborated in mouse models in which the insertion of extra OR causes a spontaneous and progressive neurodegenerative disease [177][178][179]. Although not essential for pathogenicity, the OR region appears to play a role in modulating the conversion of prion protein into its pathogenic form [166].

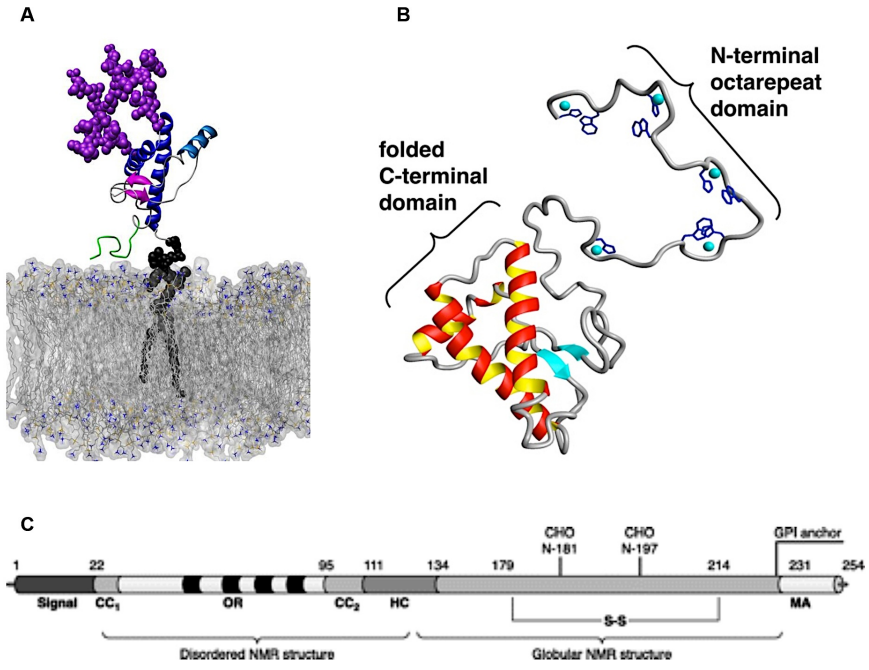

Figure 6. Model PrP^C attaches to the membrane (A). Three-dimensional rendering of PrP(61–231) with coppers included. Intervening regions were built in a relaxed conformation [180] (B). Outline of the primary structure of the cellular prion protein including posttranslational modifications (C). A secretory signal peptide resides at the extreme NH_2 terminus. CC_1 and CC_2 define the charged clusters. OR indicates the octapeptide repeat, and four are present. HC defines the hydrophobic core. MA denotes the membrane anchor region. S-S indicates the single disulfide bridge, and the glycosylation sites are designated as CHO. The numbers describe the position of the respective amino acids [89]

The atomic detail in structures of variant human PrP [181][182][183][184][185][186][187] and at least 14 other vertebrates have been determined by solution NMR [188][189][190]. Collectively, these studies reveal a consensus structure composed of three α-helices in almost 45% of structure and two short β-strands which from an antiparallel β-sheet. Helices 2 and 3 form the bulk of the structure and are covalently bridged by characteristic disulfide bonds between Cys 179 and Cys 214 (residue numbering according to human PrP sequence). PrP^C has an unusually small hydrophobic core, which is mainly found between α-helices 2 and 3, and to a lesser extent between helix 1 and small β-sheet, which wrap around helix 3. Many hydrophilic and charged residues reflective of the sequence of the C-terminal domain dress the surface of the protein. Although PrP structures from different species are strikingly similar, an intriguing difference in the dynamic loop between β-strand 2 and α-helix 2 has been observed, providing insight into a region of potential importance for pathogenicity and barriers to disease transmission across species [191][192]. Interestingly, the majority of the pathogenic germline mutations that have been linked to cases of inherited human prion disease appear within the C-terminal domain, mostly in the region encompassing helix 2 and 3 and the loop between them [193].

2.4.2. PrP^C functions

The physiological function of PrP^C has not been established with certainty. Based on studies in PrP-null mice, Collinge *et al.* concluded that prion protein is necessary for normal synaptic function [194]. They postulated that inherited prion disease may result from a dominant-negative effect with generation of PrP^{Sc}, the posttranslationally modified form of cellular PrP^C, ultimately leading to progressive loss of functional PrP^C [194]. In 1998, Pauly and Harris *et al.* proposed the roles of PrP^C in metal ion trafficking. The preferential localization of PrP^C in lipid rafts suggested its possible involvement in signal transduction, as explained by Mouillet-Richard *et al.* [195][196][197]. Mange *et al.* [198] suggested that PrP^C may also play a role in cell adhesion. A recent report suggests a role for PrP^C in embryonic cell adhesion, based on the phenotype of zebrafish in which expression of a PrP homologue has been knocked down [199]. In further experiments, PrP^C was also suggested to have neuroprotective functions. Indeed, transmembrane or secreted forms of PrP (as discussed in 2.4) mediate these functions, and mutations causing loss of function may be involved in the pathophysiology of prion diseases [200][201]. Several intriguing lines of evidence have emerged recently suggesting that PrP^C may exert a cytoprotective activity against oxidative and pathologic stressors, particularly against stresses (either internal or environmental) that initiate an apoptotic program [202][203]. A recent study has shown that PrP^C protects against cellular stress, and that PrP^{Sc} abrogates this activity by activating stress-related signaling cascades [204]. In addition to its contribution to nervous

system functions, evidence of PrP^C modulating the immune system response has also been published [205][153].

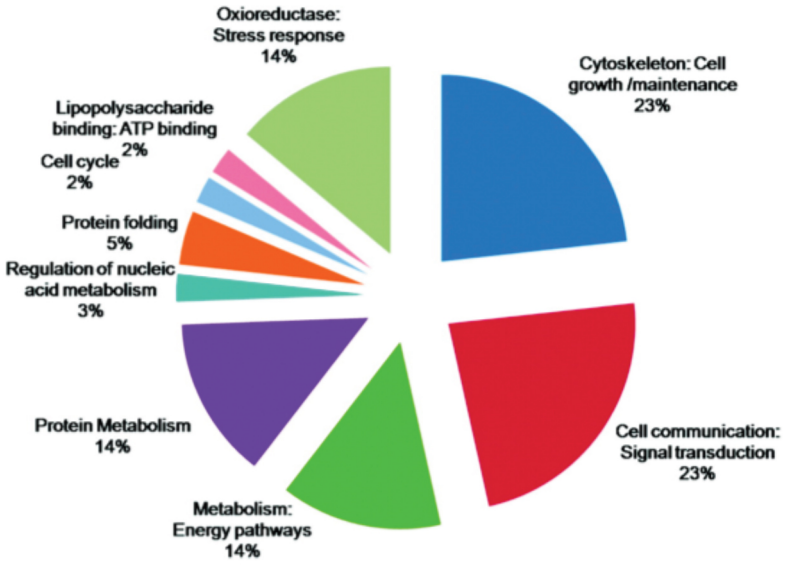

Figure 7. Functional categorization of identified interacting partners of PrP^C [206]

Recent prion research focused on a possible role of the PrP in neuronal differentiation and polarization [201]. As mentioned in paragraph 2.4.1 describing the octapeptide repeat region, prion protein binds Cu^{2+} ions, suggesting that it may be involved in copper homeostasis. A number of studies have explored functional aspects of this interaction, postulating that PrP^C acts as a transporter of copper, a sink for excess cooper, a copper-dependent receptor, or a scavenger of Cu^{2+} generated free radicals [207][208]. Although the principal anomaly of PrP^C is the lack of an intracellular domain activating the cascade of molecular events in response to external stimuli, PrP^C was suggested as a receptor in its signal transduction roles. Therefore, many attempts have been made to identify the physiological ligands of PrP^C that could serve as co-receptors and overcome the absence of transmembrane and cytoplasmic portions [209]. Interestingly, Lauren *et al.* identified PrP^C as an amyloid-beta oligomer receptor [210][211] and concluded that PrP^C is a mediator of amyloid-beta-oligomer-induced synaptic dysfunction. In 2010, axonal prion protein was found to be required for peripheral myelin maintenance [212].

2.5. The infectious prion protein

In 1982, Stanley B. Prusiner hypothesized the existence of prions as infectious proteins able to adopt replicating conformations that would lead to neurodegenerative disease in an affected organism [213][50]. Prion diseases are now widely known to be caused by changes in the conformation of the endogenous normal cellular form PrP^C leading to an abnormally folded, disease-causing form denoted as PrP^{Sc} or prion (Figure 8). According to the "protein only hypothesis" [50][214], the aggregated scrapie form, PrP^{Sc}, is the causative agent of the various TSE-linked diseases. The scrapie conformation can recruit PrP^C and facilitate its conversion to PrP^{Sc}, thus ensuring self-propagation [215]. Conversion to PrP^{Sc} results in a protein that content in β-sheet increase considerably [50][216]. This insoluble form of the PrP protein is derived

posttranslationally from the normal, protease-sensitive PrP^{C} [217]. PrP^{C} and PrP^{Sc} possess the same primary polypeptide sequence, but different secondary and tertiary structures. Residues 90–231 of PrP^{C} are believed to be the major or only infectious unit [50] (Figure 8A). Although structures of mammalian as well as non-mammalian PrP^{C} from a number of species show that residues 90–121 are mostly disordered while the rest of the residues are ordered [190][186][218], as mentioned in 2.4.1, there is no clear structural model for the scrapie form [219][220][221].

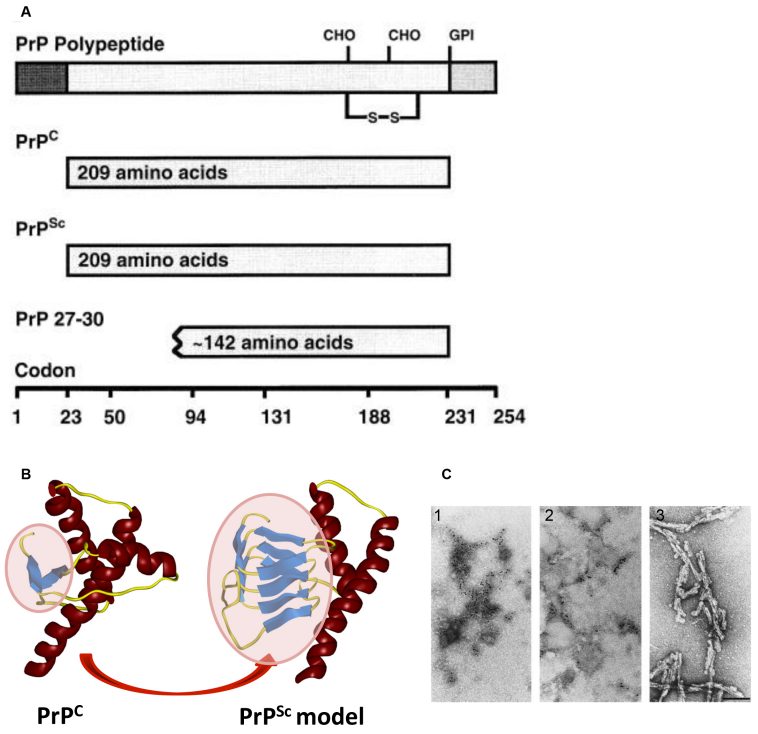

Figure 8. Bar diagram of SHaPrP, which consists of 254 amino acids. Attached carbohydrate (CHO) and a glycosyl-phosphatidylinositol (GPI) anchor are indicated. After processing of the NH2 and COOH termini, both PrP^{C} and PrP^{Sc} consist of 209 residues. After limited proteolysis, the NH2 terminus of PrP^{Sc} is truncated to form PrP 27–30, which is composed of approximately 142 amino acids (A). Model of the PrP^{C} to PrP^{Sc} conversion (B). Electron micrographs of negatively stained and ImmunoGold-labeled prion proteins (C). *(1)* PrP^{C}.*(2)* PrP^{Sc} *(3)* PrP 27-30 the proteinase K-res core of PrP^{Sc} typically appears under the shape of "rods" that indistinguishable from many purified amyloids. (Bar = 100 nm). [50]

PrP^{Sc} tends to aggregate and insoluble, protease-resistant forms can be isolated from prion-infected brains. The protease-resistant isoform of the prion protein (PrP^{res}) is important in the pathogenesis of these diseases [222]. However, protease-sensitive PrP^{Sc} ($sPrP^{Sc}$) oligomers are also predominant in some types of prion disease [223][224][225] and are infectious [226]. Recent studies have revealed a more complex picture about characterization of prions. A proteinase K (PK) sensitive PrP^{Sc} fraction was first described by Safar *et al*. [224] and later isolated and characterized from infected brain tissues [223,227]. Recently, several new strains of protease-resistant synthetic prions have been created from amyloids generated under a variety of conditions and inoculated into mice that overexpress truncated and full-length PrP [214,228]. On the other hand, also in the synthetic prion field, Colby *et al*. as well as other groups showed that $sPrP^{Sc}$ is clearly pathogenic [229]. These studies described the generation

of novel protease-sensitive synthetic prions [229]. Indeed, some findings established that $sPrP^{Sc}$ alone, in the absence of detectable $rPrP^{Sc}$, is sufficient to cause neurodegeneration [226][230][231][232]. The creation of these novel protease-sensitive prions challenges the accepted definition of what constitutes a prion. Although examples of natural prion diseases that feature $sPrP^{Sc}$ predominantly are rarely reported [230], mixtures composed of $rPrP^{Sc}$ and $sPrP^{Sc}$ appear in many prions observed in nature [231][224][232][233][234][225], though the relationship between them is unclear. These findings also suggest that $sPrP^{Sc}$ does not arise as an off-pathway product during the replication of $rPrP^{Sc}$ since it can be recruited infectious products by digestion.

Proteinase digestion is still being used as standard for the identification of infectious prions. In fact, limited proteolysis using, for example, proteinase K (PK) digestion is instrumental for the detection of prions. The readout is usually the partial resistance or sensitivity of prions to proteolitic digestion [21][225]. Fischer *et al.* identified plasminogen, a proprotease implicated in neuronal excitotoxicity, as a PrP^{Sc}-binding protein[235]. Binding is abolished if the conformation of PrP^{Sc} is disrupted by 6M urea or guanidine. Because plasminogen does not bind to PrP^{C}, the authors suggested it represents the first endogenous factor discriminating between normal and pathologic prion protein.

The pathological effects of PrP^{Sc} might include directly perturbed endocytosis, signaling, cell-to-cell contact, axonal transport, metal homeostasis, membrane trafficking, and membrane fluidity or potential [236][237][238][239]. Some evidence argues that PrP^{Sc} may not be the proximate cause of neuronal dysfunction and degeneration in prion diseases. In several kinds of transmission experiments, significant pathology and/or clinical dysfunction develop with little accumulation of PrP^{Sc} [240][241][242]. In addition, some familial prion diseases are not transmissible, and are not accompanied by the accumulation of protease resistant PrP [243][244][245][246][247]. On the other hand, there are sub-clinical infections with abundant PrP^{Sc} but little symptomatology, e.g., after inoculation of hamster prions into mice [248][249]. Because high levels of prions and PrP^{Sc} accumulate in the brains of clinically healthy animals, whether PrP^{Sc} itself is neurotoxic or not needs to be addressed. Several lines of evidence suggest that PrP^{Sc} itself may not be highly neurotoxic. Büeler *et al.* reported that by 20 weeks after inoculation with RML scrapie prions, mice carrying only one functional PrP allele accumulated levels of infectivity and PrP^{Sc} as high as wild-type animals, but remained healthy until almost a year after inoculation, while wild-type animals died by about 26 weeks [250]. In another experiment, PrP over-expressing brain tissue was grafted into PrP knockout mice, which were then inoculated with prions. While the grafted, PrP-overexpressing tissue developed hallmark signs of prion disease, such as spongiform change and accumulation of PrP^{Sc}, the surrounding tissue (in which PrP was not expressed) suffered no deleterious effects [251]. Also, in human fatal familial insomnia there are severe clinical symptoms, although the levels of PrP^{Sc} are low or undetectable[252]; some of these cases were transmitted to susceptible animals, confirming the presence of infectious prions [253]. Transmission of BSE to wild-type mice resulting in characteristic prion disease in the absence of detectable PrP^{Sc} has also been reported [241].

These observations suggest that PrP^{Sc}, as defined by its physicochemical properties of insolubility and partial resistance to protease treatment, while being an accurate marker of prion infection, may not be the neurotoxic molecule responsible for the pathogenesis of these diseases. The neurotoxic species may be a different form of PrP, possibly an intermediate formed in the conversion of PrP^{C} to PrP^{Sc}, which remains to be defined at the molecular level [248][254]. Perhaps PrP^{Sc} is a relatively inert end-product, with the rate of neurodegeneration governed by the rate at which the neurotoxic intermediate is formed [248]. Therefore, several alternative forms of PrP, distinct from both PrP^{C} and PrP^{Sc}, were hypothesized to be the primary neurotoxic species [159]

2.6 Prion infection

The molecular basis for prion infectivity is the ability of PrP^{Sc} to efficiently induce the transformation of PrP^{C} into PrP^{Sc} [255]. Despite the obvious differences between prions and conventional infectious micro-organisms (such as bacteria or viruses), prions exhibit the typical characteristics of *bona fide* infectious agents: exponential multiplication in an appropriate host; transmission between individuals by various routes (including food-borne and blood-borne); titration by infectivity bioassays; resistance to biological clearance mechanisms; penetration of biological membrane barriers; ‘‘mutation’’ by structural changes forming diverse strains; and transmission controlled by species barriers [256].

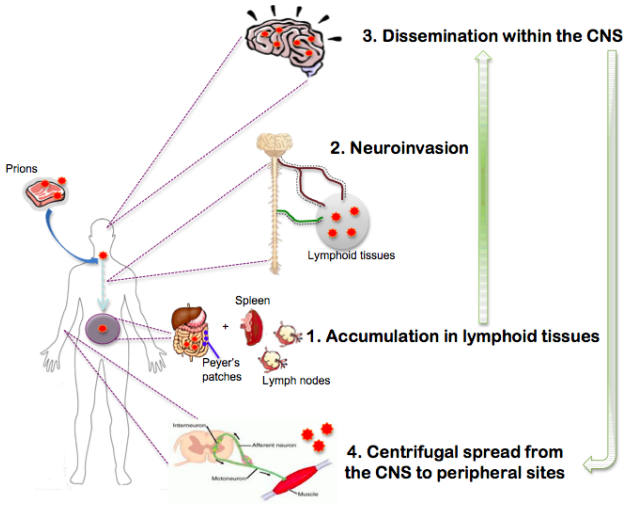

Figure 9. Different stages of prion infection. 1) Accumulation of prions in lymphoid tissues; (2) neuroinvasion, i.e. the spread from the lymphoid tissues to the peripheral nervous system (PNS); (3) dissemination within the brain and spinal cord (central nervous system, (CNS) and, (4) centrifugal spread from the CNS to further peripheral sites such as muscles. (PhD Thesis by Maddalena Costanzo, "Mechanism of spreading prion and poly glutamine aggregates and role of the cellular prion protein in Huntington’s disease").

2.6.1. Prion infection in nature

TSE infections in animals have arisen through feeding with PrP^{Sc}-contaminated animal food. It is not clear how prions pass through the intestinal mucosa after oral uptake. Microfold cells (M cells), which are portals for antigens and pathogens [257], may be involved in the transepithelial transport of prions [258] (Figure 10). Thus, the infectious agent may penetrate the mucosa

through M cells and reach the Peyer's patches. Although prion diseases are neurological disorders, critical events in their pathogenesis take place in restricted sites outside the nervous system, especially in peripheral lymph organs [259].

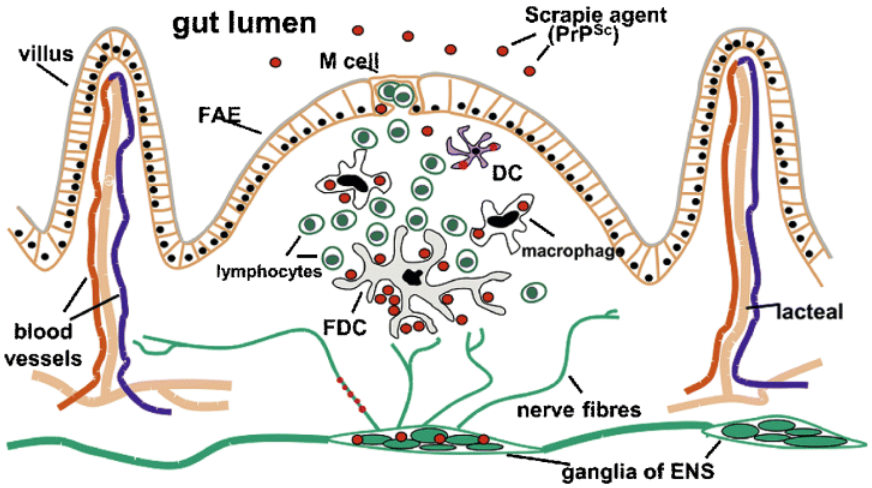

Figure 10. Intestinal cell types and tissue components showing deposition of disease-associated prion protein from transmissible spongiform encephalopathy-affected individuals (PrP_{TSE}) after exposure of the alimentary tract to transmissible spongiform encephalopathy agents. Microfold cells (M cells) in the follicle-associated epithelium (FAE), dendritic cells (DCs), macrophages, and follicular dendritic cells (FDCs) of the gut-associated lymphoid tissue (GALT), as well as fibers and ganglia of the enteric nervous system (ENS), may be involved in the uptake, replication and spread of prions [260].

PrP^{Sc} first accumulates in gut-associated lymphoid tissues (GALT) such as Peyer's patches in the intestine before neuroinvasion occurs [261][262]. The dendritic cells (DCs) of the suprafollicular dome in the Peyer's patches are thought to capture PrP^{Sc} [263]. Moreover, PrP^{Sc} is taken up by other immune cells such as macrophages in the Peyer's patches, and subsequently transmitted and concentrated in intestinal follicular dendritic cells (FDCs) [264][265][266]. PrP^{Sc} then migrates to the enteric nervous system (ENS) [264][267][268][269], passing asymptomatically through the peripheral nervous system (PNS) by axonal anterograde and retrograde transport mechanisms via the vagus and splanchnic nerves [270]. A number of studies suggest that macrophages, DCs and FDCs play an important role in the transmission of PrP^{Sc} from the gastrointestinal tract to the CNS [271][272][273]. However, the mechanism of PrP^{Sc} transmission from the immune system to the nervous system as well as from nerve to nerve is still unknown.

2.6.2. In vivo

In vivo studies with transgenic mice have examined the roles of the seed factors and templates to identify the characteristics that decide the nature of the final product [143]. In fact, a small amount of purified PrP^{Sc} can produce neurotoxicity and induce apoptosis, which demonstrate their neurodegenerative capability [274]. Certain kinds of seed factors or templates increase the titre of infectious prions in the inoculum [275]. Like the effect of infectious materials within cell models (described below in paragraph 2.6.3), dissociation and/or denaturation treatments by sonication have also been used to increase the titre of infectious PrP *in vivo* [276][277][278][279][280]. Understanding the nature of prions base on *in vivo* experiments has

been further complicated by the recent demonstration that infectious prions can arise spontaneously from normal brain [281]. The catalyst in this study was steel wire, which had been previously shown to effectively bind infectious prions. Surprisingly, even non-infected mouse brain homogenate attaching to the wires could induce a prion infection in cell cultures, which was transmissible to mice. This finding may emphasize that the emergence of a single or a few misfolded PrP proteins, not necessarily originating from mutational changes in the PrP gene, might be enough to initiate a cascade of misfolding events involving homologous proteins. Interestingly, prion infection of mice expressing PrP lacking a GPI anchor indicated that membrane association was necessary for maximal PrP^{Sc} toxicity. PrP^{Sc} amyloid built up in the brains of these mice, but they either showed no evidence of neurodegeneration or developed late-onset neurological dysfunction, depending on the PrP expression levels [282][283].

It has long been argued that the incubation period of a prion disease can exceed the natural life span of an animal studied *in vivo* [284]. After inoculation of mice with mouse-adapted scrapie prions, prion titres typically rise first in spleen and later in brain, and histopathological changes develop in the CNS during a long incubation period devoid of clinical symptoms. Early preclinical signs in brain are increased PrP^{Sc} levels and astrocytosis, accompanied by subtle behavioral changes and loss of synapses and synaptic proteins [285][286][287][288][113]. Under certain circumstances, the incubation period approaches the natural life span of the animal and, if it were to exceed it, the brain and other tissues could harbor significant levels of infectious prions even though clinical signs of infection never appear. Obviously, one cannot determine whether or not clinical symptoms would have appeared had the animals lived longer, underlining the difficulty in distinguishing between preclinical and subclinical disease. Thus, clinically, asymptomatic animals may have significant infectious titres in brain and other tissues. However, there may also be subclinical, as distinct from such preclinical, forms of prion infection, where animals become asymptomatic carriers of infectivity and would not develop clinical disease. The incubation periods are extremely prolonged; distinction between subclinical and preclinical states is difficult. It certainly can be argued that animals dying after a typical life span without clinical signs of prion disease but harboring high levels of infectivity represent the late preclinical stage of "transmissions" where the "incubation period" exceeds the normal life span. The term subclinical prion infection was operationally defined to refer to animals in which prion replication is occurring, but which have not developed clinical signs of prion disease during a normal life-span [248][289]. The subclinically infected animals harbored significant prion levels in their brain that in some cases exceeded those in terminally sick, wild-type, controls [290]. Subclinical prion infection has also been described in Tga20 mice (transgenic mice overexpressing mouse PrP) injected with low doses of RML or ME-7 prions [291]. The response of these animals oscillated between a healthy appearance and mild scrapie symptoms. However, animals that developed an ataxic syndrome always progressed to terminal stages of disease. Surprisingly, the subclinically infected animals that were sacrificed over 200 days after inoculation contained similar levels of infectivity as terminally sick animals. This again shows that prion titres may reach maximum levels without eliciting clinical disease. Therefore, in judging susceptibility to infection of an animal exposed to prions, it is not sufficient to monitor for clinical signs, but it is necessary to assay for PrP^{Sc} and/or prion infectivity. In some studies investigating the role of the lymphoreticular system in the pathogenesis of prion disease, B-cell-

deficient mice appeared resistant to peripheral prion infection as judged by their failure to develop clinical disease [292]. They were, however, susceptible to prion infection when inoculated intracerebrally, exhibiting incubation periods similar to those seen in wild-type control animals. Although peripherally challenged immunodeficient mice showed no clinical signs of scrapie, marked accumulation of PrP^{Sc} in their brains was observed.

2.6.3. In vitro

To date, cell culture models have been one of the most powerful and useful experimental tools to study at the molecular and cellular levels the biological properties of PrP in both forms, and to investigate the events controlling the conversion of PrP^{C} into PrP^{Sc}. Cell culture systems make it possible to determine the natural effect at single cell level of the infectious agents and the factors governing their propagation, screen drugs with potential therapeutic values, and also determine biological markers for the infectious materials with potential diagnostic and physiological interest. However, the use of these models in general is limited by the failure to generate mutated PrP^{Sc} [293]. Cell culture models are also useful for analyzing PrP^{Sc} transmission *in vitro*. Although mouse neuronal cell lines, N2a and GT-1 cells [294][295] are frequently used to propagate PrP^{Sc} in tissue culture models, whether PrP^{Sc} transmission from immune cells to neuronal cells occurs from cell-to-cell or is medium-mediated is still undetermined. Indeed, it has been reported that PrP^{Sc} can be transmitted to other cells in the supernatant of scrapie-infected GT-1 cells [295]. On the other hand, cell-to-cell contact is required for PrP^{Sc} transmission in the case of scrapie-infected neuronal SMB cells [296]. In cultured cells, PrP^{C} traffics to the plasma membrane before conversion to PrP^{Sc} takes place [297][298] but whether conversion occurs on the plasma membrane and/or in an endo-lysosomal compartment is unclear. After PrP^{C} to PrP^{Sc} conversion, N-terminal amino acids 23–89 of the mature protein are trimmed off in acidic late-endosomal compartments in cultured cells [299][300].

To be infectious, the prion protein must undergo a conformational change involving a decrease of α-helical content along with an increase of β-strand structure. In cellular models, the abnormal PrP is added to the cells media; even though they are prepared in different ways, they share common conformation features within the amyloid forms. The infectivity of individual cells infected with amyloid infectious materials depends on the dimensions of amyloid aggregates. This was showed on experimental results on amyloid assembly [301] and cellular biological responses. This factor is likely mediated by surface interactions, for example between fibrils and membranes and/or between fibrils themselves. In order to further the understanding of fundamental infectivity of prion disease, precise information is highly needed regarding the effect of the environmental factors on the formation and properties of amyloid fibrils [302] as well as the molecular determinants of fibril structure, stability and dynamics [303][304][305], how these properties alter the fragmentation rate, size and distribution of amyloid species and the effect on their infectious ability.

First, the changes in the physical dimensions of fibrils, without parallel changes in their composition or molecular conformation, could be sufficient to alter the biological responses to their presence in amyloid disease. Wei-Feng Xue *et al.* showed a striking relationship between reduced length of fibril (caused by fibril fragmentation) and enhanced ability of fibril samples to

disrupt membranes and to reduce cell viability. These conclusions hypothesize that the physical dimensions and surface interactions of fibrils play key roles in prion disease. The precise rates of fibril fragmentation for different amyloid systems or different amyloidogenic sequences represent the key parameter that must be characterized in this case. The rates of fragmentation (the division/replication of fibril particles), the rates of nucleation (the creation/infection of new fibril particles), and extension (the growth of existing fibril particles), represent the key triad of processes that together determine the size distributions of amyloid species, and may dictate the detailed infectious progress. The type and extent of cellular responses to the addition of amyloids are determined by fibril length and the length distribution of fibrils. Information regarding fibril length will also be vital to characterize the process of fibril fragmentation, as fragmentation rates are themselves fibril length-dependent [306]. Fibril fragmentation has recently been implicated as a key process in determining the kinetics of amyloid assembly [301][307]. As amyloid formation in disease, the concentration of nucleation is slow and the rate of fibril growth can be drastically accelerated by the process of fragmentation through the resulting creation of extension-competent surfaces when fibrils break. Fragmentation of fibril particles has also been shown to affect the phenotype strength of different yeast prion strains, as increased brittleness of fibrils increases the efficiency of prion infection [307]. Different types of aggregation species lead to different biological responses, but changes in the physical dimensions of aggregates alone, without parallel changes in their composition or molecular conformations, may also be sufficient to alter the biological responses to amyloids [308,309]. Fibrils (at least micrometers in length) [223] could interact with membranes either through their end surfaces or through their surface along the fibril axis. On the other hand, both types of surfaces may be able to interact co-occurrently with membranes for fibrils that are shorter than the size of cells or cellular compartments (in the order of hundred nanometres or shorter), possibly leading to enhance the interactions. Thus, in cell models used in infectivity assays of synthetic prion experiments, the differences in biological response may depend on differences in fibril length and the length distributions of fibrils that populate each amyloid preparation. In addition, inside the population of fibril samples, fibril-fibril interactions depend on the length of fibrils: long fibrils are likely to be more prone to entangle and form clusters or networks that are less biologically active than their unclustered counterparts.

Secondly, it has been shown that each prion strain is enciphered by a distinct conformation of PrP^{Sc}, therefore the conformational distinct amyloid states of amyloid/fibril preparation become crucial profiles to study. In this case, the biological response and infectivity not only depend on the physiological dimension structure, but also on the structural properties of each infectious material generated *in vitro* at molecular level. The PrP expression level of the cell lines that are used for infectious assays with amyloids is an important factor to detect a successful infection. Recent data on permissible cell lines revealed that cultures have the potential to accumulate as in the brain from affected animals with many infectious units per mg of protein [310]. In addition, the presence of infectivity has been also detected in the culture medium of infected cells [311][295], confirming that these extracellular infections are very efficient in propagating the infectious agent and represent a useful tool to study prion conversion and to produce prions for a variety of further studies in cell culture models. Although brain- and cell-derived PrPres are different, strain-specific banding pattern differences observed for brain PrPres were also

detected after serial propagation in cultured cells [312][313][314][315]. The available data also suggest that the biological properties of the strains are not modified after propagation in cultured cells. Importantly, strain-specific features of abnormal PrP are maintained upon multiplication in cultured cells, indicating that these models represent interesting cell biological systems to study how distinct abnormal PrP from various amyloid states is generated in a single cell type. On the other hand, there are some suggestions that the subcellular distribution of abnormal PrP may vary depending on the cell type in which a given infectious amyloid/strain is replicated [316].

Using these models can decrease the effectiveness of prion propagation mostly because of differences in primary amino sequences of PrP. Other neuroblastoma cell lines replicate prion agents with the same efficacy as N2a cells [317][318][311][295][319]. Also widely used, the hypothalamic cell line called GT1 represents a reliable support for prion replication *ex vivo* [295]. GT1 cells are well differentiated, neuronal cell lines originating from the central nervous system and were established from gonadotropin-releasing hormone neurons immortalized by genetically targeted tumourigenesis in transgenic mice. From the different studies published so far, using homologous models of cell lines, regarding the transmission of prions in general, only some strains can replicate in one particular cell line; only some cells from a culture become infected and subcloning could improve the susceptibility to prions. In some cases of infection with infectious materials, the propagation of prions induces subtle changes in the phenotype of the cultures. Another way for understanding the molecular strain determinants could be studying infected cells. For example, it has been shown that SMB cells could be infected with different strains of scrapie and that the biological properties and prion-protein profiles characteristic of each of the original strains were propagated in this mode [313]. In synthetic prion studies, experiments with fibril/amyloid-infected cell cultures models have given significant information concerning abnormal PrP propagation. It is clear that one cell line can be infected by several amyloid species. Conversely, it appears that one amyloid species can infect several different cell lines. In addition to the level and the type of PrP molecules expressed in cells, several other factors may also account for this phenomenon.

2.7 Prion conversion and propagation

The molecular detail of the process by which PrP^{Sc} is made from PrP^{C} is still an area of intense research. In crystal structural studies, some structures reveal two types of homo-dimeric interactions that can exist between PrP molecules, providing a glimpse into the structure repertoire of PrP and the interactions that may be relevant to the conversion into the pathogenic state [183][184][185][320][321]. The first type of interaction is the pairing of the two-stranded antiparallel β-sheet within a symmetry related PrP molecule in the crystal lattice to form an extended four-stranded β-sheet. This extended β-sheet is particularly notable because the interaction between molecules centers on residue 129, the site of a Met/Val polymorphism in the human population that affects the susceptibility to prion disease [322][323][324]. Therefore, it has been suggested that the interaction between PrP molecules may play a role (possibly as a nucleation site) in the PrP^{C}–PrP^{Sc} conversion [185][190][320]. The second type of interaction found in the majority of crystallized human PrP variants is the symmetrical exchange of helices 2 and 3 between the pair of PrP molecules in a phenomenon called “domain swapping” [325][183][184]. The formation of such dimers requires the breaking and reforming of two covalent disulfide bonds and implies an intermediate state of protein under which such an

exchange could happen. Domain swapping has also been proposed as a mechanism of ordered protein aggregation for some amyloidogenic protein [326][327][328]. However, at present it is not clear whether any domain swapped form of PrP exists *in vivo*. There are some other factors that are involved in the PrP^{Sc} conversion: for instance, a structural understanding of the coordination of copper to the octapeptide repeats was discussed above (paragraph 2.3.1). The binding sites of C-terminal with the octapeptide repeat are potentially significant as they are within the 90-230 region, a part of the protein critical for prion infectivity. Therefore this raises the possibility that the copper binding could modulate the conversion of PrP^{C} to PrP^{Sc} [166]

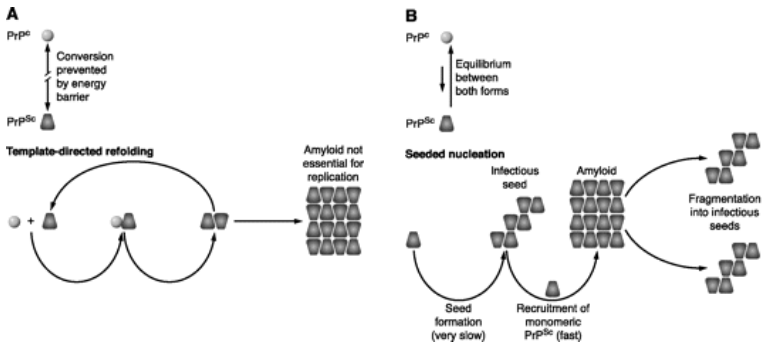

Figure 11. Models for the conformational conversion of PrP^{C} into PrP^{Sc}. A: the "refolding" or template assistance model postulates an interaction between exogenously introduced PrP^{Sc} and endogenous PrP^{C}, which is induced to transform itself into further PrP^{Sc}. A high-energy barrier may prevent spontaneous conversion of PrP^{C} into PrP^{Sc}. B: the "seeding" or nucleation-polymerization model proposes that PrP^{C} and PrP^{Sc} are in a reversible thermodynamic equilibrium. Only if several monomeric PrP^{Sc} molecules are mounted in a highly ordered seed, can further monomeric PrP^{Sc} be recruited and eventually aggregate to amyloid. Fragmentation of PrP^{Sc} aggregates increases the number of nuclei, which can recruit further PrP^{Sc} and thus results in apparent replication of the agent [89].

In biochemical studies, it is believed that this conversion occurs through PrP^{Sc} contact with PrP^{C}, thereby inducing it to change into PrP^{Sc} [50]. The conversion of normal PrP to the protease-resistant PrP in a cell-free system requires the presence of preexisting pathogenic PrP [329]. However, Ma et al showed in their studies that recPrP can be converted to $recPrP^{Sc}$ by PMCA without any added preexisting PrP^{Sc} [277]. .Many findings provided direct evidence that the pathogenic PrP can be formed from specific protein-protein interactions between it and the normal PrP. Prion protein retrogradely transported out of the endoplasmic reticulum produces both amorphous aggregates and a PrP^{Sc} in the cytosol. The distribution between these forms correlated with the rate of appearance in the cytosol. Once conversion to the PrP^{Sc} occurred, it was sustained. Thus, PrP has an inherent capacity to promote its own conformation conversion in mammalian cells [330]. Although it is clear that PrP^{C} is necessary for prion disease, there is still debate regarding whether other ancillary proteins or molecules are involved in the change of protein conformation *in vivo*[331][332]. The plasma membrane invaginations with PrP^{Sc} aggregates in the fold are an early sign of prion pathology [333]. A recent study of Peyer's patches in mice orally inoculated with prions also strongly suggested that prion formation occurs on plasma membranes of follicular dendritic cells [334]. Furthermore, epitope-tagged PrP^{C}

converts to PrP^{Sc} primarily on the plasma membrane of neuroblastoma cells exposed to exogenous PrP^{Sc} [335]. By contrast, studies using trafficking inhibitors in cultured cells provide evidence for PrP^{C}-PrP^{Sc} conversion in recycling vesicles [336]. Endocytosis of PrP^{C} is also relevant in prion disease pathology, since the endosomal compartment has been identified as a putative conversion site for prions [297][337].

After the infection process, the conversion process follows the seeding-nucleation model with infectious PrP^{Sc} acting as a seed to capture PrP^{C} into the polymer [338] (Figure 11). The molecules of PrP^{C} stay with PrP^{Sc} aggregates and acquire the same conformation of the PrP^{Sc} template to be able to incorporate stably into the polymer. In this way, PrP^{Sc} aggregates grow and at a certain stage polymers can be broken down into smaller pieces multiplying the number of oligomeric seeds to further propagate prion replication. Prion replication requires exposure to tiny quantities of PrP^{Sc}, present in the infectious material, to trigger the autocatalytic conversion of host PrP^{C} to PrP^{Sc}. This process follows a crystallization-like model in which the infectious particle (a small PrP^{Sc} aggregate) acts as a nucleus to recruit monomeric PrP^{C} into the growing PrP^{Sc} polymer [339]. A key step in prion replication is the breakage of large PrP^{Sc} aggregates into many smaller seeding-competent polymers that amplify the prion replication process, resulting in the exponential accumulation of PrP^{Sc} [279]. This seeding-nucleation mechanism of prion propagation has been reproduced *in vitro* to "cultivate" prions with infectious properties when inoculated into animals [278][280][277]. However, the precise mechanisms and cellular factors required for prion replication *in vivo,* as well as the detailed structure of the infectious folding of the prion protein are still unclear.

Prion propagation in brain proceeds via two distinct phases: a clinically silent exponential phase not rate-limited by prion protein concentration that rapidly reaches a maximal prion titer, followed by a distinct switch to a plateau phase. The latter determines time to clinical onset in a manner inversely proportional to prion protein concentration. Therefore, there is an uncoupling of infectivity and toxicity [340]. Production of neurotoxic species is triggered when prion propagation saturates, leading to a switch from autocatalytic production of infectivity (phase 1) to a toxic (phase 2) pathway [340]. Recent studies suggest that the rate of prion replication is controlled by the conformational stability of prion fibrils. The results are consistent with a view that failure in inducing clinical disease of non-transgenic animals was reported for the first time with synthetic prion mice [214]. It might be due to a slow rate of prion replication rather than lack of infectivity in preparations of synthetic prions. The slow replication rate seems to be a manifestation of the exceptionally high conformational stability of synthetic prions. Gaining insight into the molecular mechanisms that link the incubation time to disease and conformational stability of prion fibrils, Ying *et al.* proposed that conformational stability determines critical physical properties of fibrils, such as their intrinsic fragility, i.e. their ability to fragment into small pieces, and/or the size of the smallest possible fragments [341]. Fibril fragmentation is believed to be a key step in prion replication, as it is essential for multiplication of active centers [341][341]. The rate of multiplication of active centers is regulated by intrinsic fragility and the length of fibrillar fragments [342], parameters that could have a direct impact on prion infectivity. Variations in intrinsic fragility of prion amyloid structures or the length of the smallest possible fibrillar fragments could account for strain-specific differences in the incubation time to disease.

2.8 Prion spreading, transmission and strains

PrP^{Sc} at intercellular junctions may indicate cell-to-cell spread (Figure 13). Several mechanisms for intercellular prion spread have been proposed, including transfer via membrane-bound subcellular particles such as exosomes, or membrane bridges [343][344][345]. Other studies indicated that cells could become infected by contact with prion-infected cells, even if these were fixed [296][346][347]. As mentioned in some studies, transgenic animals expressing human misfolded protein transgene develop some clinical and neuropathological features of the human disease, whereas PrP knock-out mice are resistant to prion infection [348], showing that misfolded proteins are intimately implicated in the malady. Indeed, all inherited cases of prion diseases are linked with mutations in the prion protein gene, which usually have an earlier onset and more severe phenotype than the sporadic forms [89]. Moreover, some transgenic mice carrying mutation homologous to human prion disease also develop spontaneous disease which is transmissible [349][46][350,351][352]. Most TSEs are transmitted naturally by peripheral routes, either orally or transcutaneously. The mechanism of spread from the periphery to the central nervous system (CNS) is an important issue [353]. Experiments performed since the early 1960s have demonstrated that transmission of prion disease between mammalian species is limited, less efficient than within species, by a so-called "species" or "transmission barrier" [354]. Recognition of prion transmission usually relies on the appearance of clinical symptoms in inoculated animals and the interval between inoculation and appearance of clinical disease is designated incubation period. When, following transmission across a species barrier, brain homogenate from the sick recipient is passaged through the same species, the incubation period shortens and becomes much more consistent. This marked difference in transmission parameters between primary and second passage is diagnostic for the existence of a species barrier and the extent of the fall provides a guide to the size of the barrier. At some points during this clinically silent period, neuropathological and biochemical changes as well as accumulation of prions in the brain can be detected and this stage can be called preclinical prion disease. Recently, several lines of evidence have suggested that subclinical forms of prion disease exist, in which high levels of infectivity and PrP^{Sc} are found in animals that do not develop clinically apparent disease during a normal life-span. These asymptomatic prion "carrier" states [289] were found to be involved in the molecular basis of barriers to transmission.

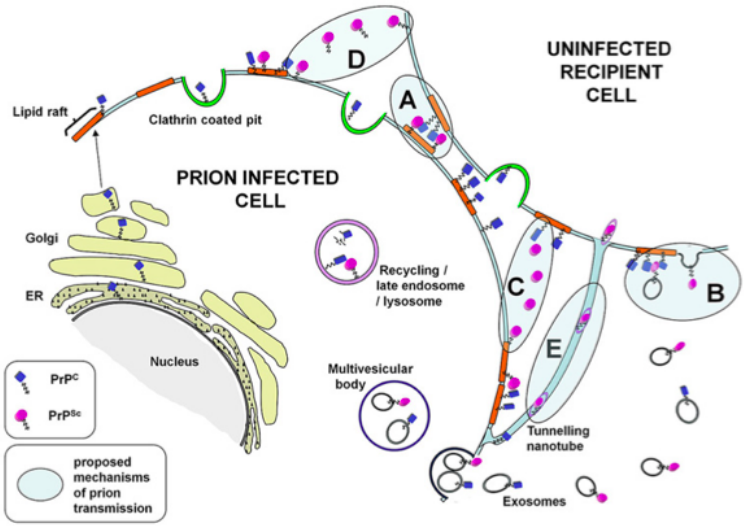

Figure 12. Proposed mechanisms of cell-to-cell spread of prion infectivity. (A) Prion transmission through direct cell-to-cell contact (conversion of recipient PrP^{C} without internalization of donor PrP^{Sc}). (B) Transmission of prions through exosomal PrP^{Sc} association; both a direct interaction of exosome-associated PrP^{Sc} with cell-associated PrP^{C} and incorporation of exosomal membrane with recipient cell membrane are represented. (C) C-terminal truncation of PrP^{Sc} allowing release from an infected cell and movement to an uninfected recipient cell. (D) "GPI-painting" mode of prion transfer. (E) PrP^{Sc} spread through tunneling nanotubes, in association with small vesicles of lysosomal origin. Mode (A) is represented by lipid raft associated PrP, but could involve non-raft associated PrP. Mode (D) is depicted by transfer of cell surface PrP^{Sc}, but could potentially occur with exosomal PrP^{Sc}. [355]

Different prion strains produce distinct phenotypes, as defined by the pattern of neuropathological lesions (so called lesion profile) and length of the incubation period when inoculated into susceptible animals. Several strains of naturally occurring sheep scrapie have been isolated by biological cloning in mice [356]. The finding that different prion strains can be propagated in in-bred mice expressing PrP with the same primary sequence suggests that strain variation is not necessarily dependent on the primary sequence of the host prion protein gene [357]. Several lines of evidence suggest that PrP^{Sc} itself encodes prion strain information. For example, the hyper (HY) and drowsy (DY) strains of transmissible mink encephalopathy (TME), which can be passaged in hamsters and distinguished by their disease phenotype, differ in the physicochemical properties of PrP^{Sc} deposited in the brains of the affected animals [358]. The different mobilities of PrP^{Sc} in immunoblots of brain extracts after digestion with proteinase K are due to cleavage at different amino-proximal sites, whose exposure to proteinase may reflect distinct conformations of PrP^{Sc} characteristic for each strain [350][46]. Differences in the banding pattern of protease-treated PrP^{Sc} are also observed in cases of CJD in humans that present with distinct phenotypes [46][53] (Figure 14). Crucially, these biochemical differences can be transmitted to PrP in transgenic mice expressing human PrP [46][359][360].

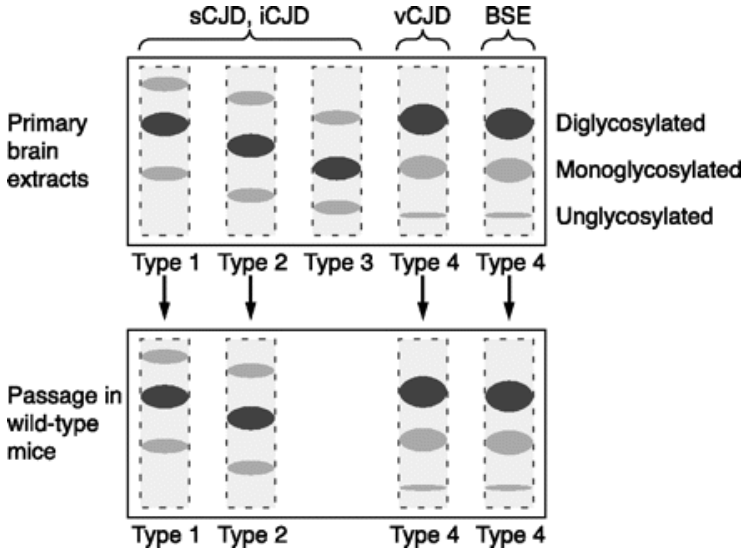

Figure 13. Representation of the three glycosylated PrP^{Sc} moieties (un-, mono-, and diglycosylated PrP^{Sc}) in immunoblots of brain extracts after digestion with proteinase K. Different inocula result in specific mobilities of the three PrP bands as well as different predominance of certain bands (top panel). These characteristic patterns can be retained, or changed to other predictable patterns after passage in wild-type mice (bottom panel). On the basis of the fragment size and the relative abundance of individual bands, three distinct patterns (PrP^{Sc} types 1–3) were defined for sCJD and iCJD cases. In contrast, all cases of vCJD and of BSE displayed a novel pattern, designated as type 4 pattern. [89]

Several parameters are known to influence the transmissibility of prions both across and within species. These include polymorphisms in the prion protein gene that give rise to differences in PrP^{C} primary structure between donor and host, prion strain type, the route of inoculation (e.g., peripheral versus intracerebral) and the dose. The effect of a very substantial species barrier is that few, if any, animals succumb to disease on primary passage, and if they do so, then only after incubation periods approaching the natural life span of the animal [289]. The PrP primary structure is the major determinant of species barriers [361]. Experiments with transgenic mice expressing a variety of mammalian PrP genes have been useful in assessing barriers to prion disease. For instance, transgenic mice devoid of mouse PrP but expressing human PrP lack a barrier to infection with human prions from sCJD, but not vCJD cases [46][253].

A strong barrier to the development of clinical disease has frequently been observed when prions are transferred from one mammalian species to another. In some cases of transmission, both natural and experimental, of cattle BSE prions, only a relatively low barrier to clinical disease is observed. In the transmission of cattle BSE into wild-type mice, they succumb to clinical disease with a low, but distinct, barrier to the development of clinical disease [359][362]. On the other hand, a barrier to transmission, as determined by appearance of clinical disease, may also be due to differences in the prion strain rather than to differences in the PrP^{C} of donor and recipient. Hence, it has been proposed that "transmission barriers" reflect the complex relationship between species, PrP primary structure and prion strain type, and the contribution these parameters make to the disease process [363].

3. Synthetic prions: *de novo* mammalian prion generation

The prion hypothesis states that the infectious agent in TSEs is composed exclusively of PrP^{Sc}, which replicates in infected individuals by transforming PrP^{C} into more of the misfolded isoform [50], but this hypothesis remained controversial for decades. Recent studies have settled all doubts by demonstrating that infectious material can be generated *in vitro*, in the absence of genetic material, by replication of the protein misfolding process [214,277,278,280]. Although lacking both glycosylation and the GPI anchor, secondary and tertiary structures of recPrP appear to be identical to those of brain-derived PrP^{C} [167],therefore they provided a useful tool for studying the physiochemical properties and conformational transitions of the prion protein.

One of the most important, recent advancements in prion biology has been the discovery of the *de novo* generation of prion infectivity from recombinant protein sources. Amyloid fibrils prepared *in vitro* from bacterially expressed PrP have confirmed that PrP^{Sc} is the principal, if not the sole, causative agent of TSEs, providing the definitive proof for the prion hypothesis. These PrP amyloid fibrils can be used as a synthetic surrogate of PrP^{Sc} to obtain a model for understanding the structural basis of prion conversion, for studying prion neurotoxicity, or for the development of drug leads able to halt the fibrilization process. However, the specific infectivity (i.e. titer per unit protein) of PrP amyloid fibrils is very low in Tg overexpressors (i.e. >100 million fold lower than brain derived prions) and undetectable in wild type hosts. In the past few years, considerable progress has been made in the understanding of prion diseases through the development of several protocols for producing amyloid fibrils from recombinant PrP (recPrP) [364]. This chapter recapitulates relevant studies and experimental data that have led to the generation of synthetic prions (Table 3).

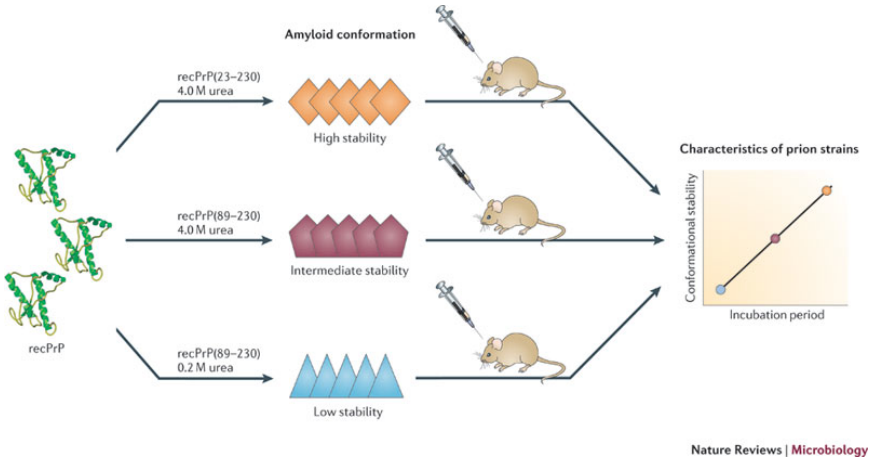

Figure 14. Diverse prion protein (PrP) conformations account for the phenotypes displayed by synthetic prion strains. PrP amyloids with high, intermediate and low stability can be formed by altering the length of the recombinant PrP (recPrP) construct and the conditions used for refolding. In mice, the incubation periods and conformational stabilities of the resulting prion strains seem to be dependent on the conformational stability of the recPrP amyloid from which they originated [143]

Table 3. The generation of synthetic prions

Strategy	Methods	Results	Infectivity	Reference

Cell-free assay	Incubation of PrP^{C} with PrP^{Sc}	PK-resistant PrP^{Sc}	Negative on wild-type mice	[365][366][329]
	Overexpression of PrP pathological mutants	*Bona fide* prion diseases	Negative on wild-type mice	[177][367][368][196]
Mouse transgenesis	Knock-in mice expressing FFI causing mutation	*Bona fide* FFI disease	Positive on WT mice carrying 3F4 epitope, and after passage in Tga20 mice	[369]
	Tg(1020) mice overexpressing mutations causing structural rigidity in the α_2-β_2 loop	*Bona fide* prion diseases	Positive in Tga20 mice; resistance to some prion strains.	[275][192]
	Amplification and conversion of Syrian hamster PrP^{C} into PrP^{Sc}	PK-resistant PrP^{Sc}	Positive in WT Syrian hamster	[370][278][129]
PMCA	Generation of prions starting from normal brain homogenates in the absence of any PrP^{Sc} seed	PK-resistant PrP^{Sc}	Positive in Syrian hamster	[276]
	De novo prions starting from recombinant MoPrP, POPG and RNA	*Bona fide* prion disease	Positive in WT mice	[371][277]
ASA	Incubation in partially denaturing condition of recMoPrP(89-230)	*Bona fide* prion disease	Positive in Tg9949 and after passage in WT FVB mice and Tg4053	[229][372][214][373][374]
Annealing	Incubation of recPrP with normal brain homogenate at different heating/cooling cycles	*Bona fide* prion disease	Positive in WT Syrian hamsters	[375][376]

recPrP-PMCA	Similar to PMCA, but recPrP as substrate for the conversion instead of normal brain homogenate	PK-resistant PrP^{Sc}	Not determined	[377]
QuIC	recPrP as a substrate and automated tube shaking rather than sonication	PK-resistant PrP^{Sc}	Not determined	[378]
qPMCA	The PrP^{Sc} content is estimated by the number of PMCA rounds necessary for a positive response	PK-resistant PrP^{Sc}	Not determined	[379]
RT-Quic	Similar to ASA, but the PrP^{Sc} content is estimated by serial dilution of the seed	PK-resistant PrP^{Sc}	Not determined	[380][381][382][383]

3.1. Cell-free assay using mammalian prions

The earliest efforts in defining the *in vitro* process of PrP^{C} conversion into PrP^{Sc} have been described in the 1990s by Caughey and collaborators. Radiolabeled, eucaryotically expressed, purified PrP^{C} was incubated with PrP^{Sc} derived from scrapie-diseased animals. The interaction with PrP^{Sc} resulted in the formation of a PK-resistant form of the radiolabeled progenitor [329]. The same method has been used for inter and intraspecies transmission studies of prion diseases. The incubation of radiolabeled PrP^{C} with two different strains of PrP^{Sc}, the hyper (HY) and drowsy (DY) strains of hamster transmissible mink encephalopathy (TME) generated two distinct sets of PK-resistant progenitor forms [365]. Additionally, the mouse PrP MH2M variant (expressing a Syrian hamster (SHa) PrP sequence in the central region), extracted from cell culture, has been converted in a PK-resistant form after incubation with the SHa263K scrapie strain. However, no infectivity was detected when the converted material was inoculated into wild-type CD1 mice [366]. These pioneering studies recapitulate many features associated with prion transmission *in vitro*, demonstrating that the direct interaction between PrP^{Sc} and PrP^{C} is one of the key events during the conformational transition. Nevertheless, the PK-resistant PrP isoforms in the above mentioned studies could not be properly considered synthetic prions as they lacked infectivity.

3.2. *De novo* generation of prions by mouse transgenesis

A different approach that was largely explored for the purpose of generating *de novo* infectious material consists in expressing PrP pathological mutants. These experiments were based on the hypothesis that PrP mutants should produce infectivity by increasing the likelihood of misfolding. This hypothesis is supported by evidence *in vitro* showing that some recPrP mutants (F198S and H187R) display an increased propensity to self-aggregate in amyloid PK-resistant fibrils reminiscent of natural prions [384,385]. Early efforts included the expression of two pathological mutants (six extra octapeptide insertions and the homologous human E200K) in stably transfected CHO cells, resulting in the formation of mutant proteins with biochemical properties similar to the scrapie isoform [386]. However, none of them was shown to be infectious.

Transgenic (Tg) mice expressing PrP containing pathological mutations develop a spectrum of neurological diseases that are comparable with TSEs [177][367][368][387][196]. However, none of the brain extracts from diseased Tg animals resulted able to reproduce the infectivity when inoculated in wild-type mice. Therefore, it has been argued that the neurological symptoms similar to those of prion diseases observed in these Tg mice could be merely an acceleration of pre-existing diseases in the recipient mice, rather than *bona fide* transmission [387]. One possible explanation for why these experiments failed to develop *de novo* prions is that these models employed randomly integrated transgenes. In all these cases, mutant PrP transgene integrates in a random position, often with a variable copy number and without the control of the PrP promoter complex. The integration of multiple PrP copies causes an unusual high level of PrP expression, which would increase the likelihood of pathological conversion. Indeed, sometime an uncoupling of messenger RNA transcription levels and variable, and usually lower proteins expression are described. This may represent the complexity of protein expression regulation that Tg mice often lack.

New insights in the generation of *de novo* prions were derived by experiments carried out in knock-in mice expressing a PrP mutation (D179N-M129 with the 3F4 epitope tag) associated with a human prion disease, FFI [369]. These mice developed biochemical, physiological, behavioral and neuropathological traits that were similar to FFI observed in humans. Interestingly, FFI knock-in mice display protease sensitive PrP as well as human FFI cases [388][389][68][390], and other type of prion diseases [391]. Moreover, this spontaneous disease is infectious when transmitted to mice carrying the same 3F4 epitope, and to other Tg mice, namely Tga20 [392], expressing high level of wild-type PrP. These knock-in mice were generated replacing the endogenous mouse *PRNP* gene with the construct carrying the FFI mutation, leaving the native regulatory elements unchanged. The implications of this work on the comprehension of prion diseases are remarkable. The presence of PK-sensitive PrP^{Sc} in FFI mice supports recent findings showing that novel synthetic prions become infectious yet the protein remains protease sensitive [229]. These results extend the notion about prions, which are not obligatorily protease resistant [393][394]. The observation that only knock-in mice developed *de novo* infectious materials suggests that PrP needs to be expressed and regulated in particular cell types in order to generate TSE. Changes in the PrP regulatory elements or the overexpression of PrP may play a role by altering the physiological pathways in which PrP is

involved. In any case, the observation that *de novo* prions were generated expressing a PrP mutant with endogenous expression level fulfills the prion hypothesis.

Recently, two papers reported the spontaneous appearance of infectivity from chimeric constructs of PrP inducing rigidity in the α_2-β_2 loop [275][192]. Sigurdson and coworkers [275] developed Tg mice (Tg1020), termed RL-PrP, overexpressing a PrP containing two artificial mutations, S170N and N174T, which confer a rigid structure to the α_2-β_2 loop in elk and horse PrP [191][395]. These RL-PrP mice developed spontaneous and progressive clinico-pathological features similar to prion diseases, suggesting that these two aminoacidic substitutions are pathogenic for mice. These RL-PrP mice exhibited a very prolonged incubation time when infected with wild-type RML strain, arguing that the structural variation imposed by the artificial mutations creates transmission barrier to prion disease. Interestingly, sick animals are able to transmit disease to Tga20 mice causing similar symptoms after a long incubation time. However, when brain homogenates of RL-PrP mice were inoculated in Tga20 recipient mice, they caused similar neurological signs, but with shorter incubation periods. Both PK resistance and conformational stability increased after each passage. These data indicated the presence of a transmission barrier that was gradually overcome by repeated passaging. Finally, after serial passages in Tga20 mice, the prion infected brain homogenates were transmissible to wild-type mice but not to PrP deficient mice. This work clearly confirms previous findings, demonstrating that *de novo* prions could be generated by altering PrP coding sequence. Moreover, it underlies the role of α_2-β_2 loop region in modulating prion susceptibility and infectivity.

3.3. *De novo* prions *in vitro* by PMCA

An invaluable contribution to the demonstration of the prion hypothesis is represented by an alternative conversion system, denoted as Protein Misfolding Cyclic Amplification (PMCA). This technique is based on the experience of the "cell-free conversion" developed by Caughey and collaborators, and it is widely used to generate *de novo* prions *in vitro*. This approach developed by Soto's group [396][279] mimics the PrP^{Sc} autocatalytic amplification. It consists in the incubation of a large excess of PrP^{C} from healthy brain homogenate with an extremely low titer (usually 10^{-10} dilution factor) of PrP^{Sc} derived from TSE-infected animals. Basically, the mixture is incubated to enlarge PrP^{Sc} conformers, and then subjected to multiple rounds of sonication in order to break down the aggregates and generate multiple smaller units of PrP^{Sc} conformers. The products are then diluted in new healthy brain homogenate for further amplification cycles allowing the elimination of the original PrP^{Sc} seed (10^{-20} dilution factor of the starting brain infectious material). The presence of newly generated PrP^{Sc} has been confirmed by different biochemical assays, such as the resistance to PK digestion, insolubility in non-ionic detergent or fourier transform infrared spectroscopy [278]. Importantly, it has been shown that PMCA-generated PrP^{Sc} is infectious when intracerebrally injected into wild-type SHa, leading to a disease with biochemical and clinico-pathological features identical to the illness caused by the natural prion strain. The only difference reported was the longer incubation time of the disease in the animals infected by PMCA-generated prion (177 ± 7.3 days) compared to those infected by 263K prion (106 ± 2.9 day), arguing a lower efficiency of infectivity [278]. Additionally, this method was used to amplify five different mouse strains, obtaining the same strain-specific features (incubation time, biochemical and neuropathological characteristics) in wild-type mice

infected by PMCA-generated PrP^{Sc}[397]. To rule out the possibility that other unknown agents in the TSE-infected brain homogenate may trigger in turn the conversion of PrP^{C} during the PMCA process, the same group demonstrated the *de novo* generation of prions starting from normal brain homogenates in the absence of any PrP^{Sc} seed [276], however the results were not reproducible and could have been due to cross-contamination. Importantly, another group demonstrated the feasibility of the *de novo* prion generation by PMCA, showing that PMCA of the DY and HY strains of TME recapitulates the strain specific properties of PrP^{Sc} when inoculated in wild-type SHa [370][129]. However, the presence of many unknown molecules in the brain homogenates used for the PMCA has brought on uncertainty about whether the infectivity is indeed derived from the prion agent only, or from other facilitating factors. The objective of inducing prion diseases in wild-type animals using only recPrP still represents a great challenge.

An important step forward in defining the chemical composition of mammalian prions derived from studies showing that polyanions, particularly RNA [398][280][331][399], and lipids [400][60] facilitate the PrP conversion *in vitro*, and thus might promote the *de novo* prion formation [280]. On the basis of these findings Wang *et al.* recently applied PMCA to produce *de novo* prions starting from recPrP (murine full-length PrP) in the presence of both lipid (the synthetic phospholipid POPG) and RNA (total RNA isolated from mouse liver) [371][277]. The infected brain homogenates were able to propagate the disease to recipient wild-type mice. These findings support the hypothesis that RNA and lipids are potentially important cofactors for the PrP conversion, and may represent a definitive answer to the question whether altered conformations of recPrP cause *bona fide* prion disease in wild-type mice. However, one of the major criticisms concerns the role of RNA for prion replication *in vivo*, since it is not clear whether nucleic acids are physiologically relevant or simply mimic other not well-characterized polyanionic molecules.

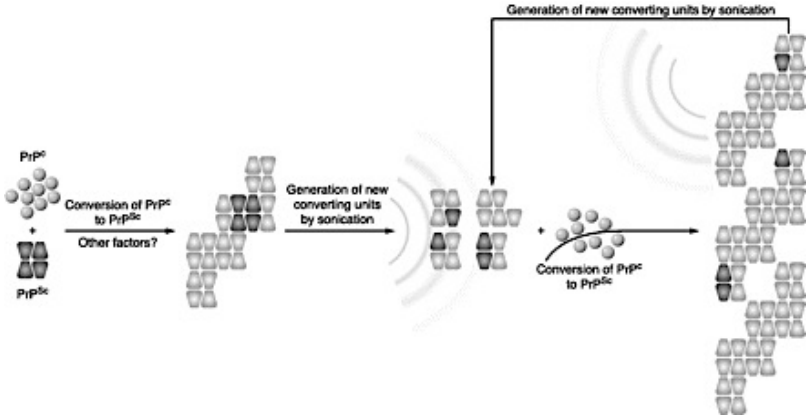

Figure 15. Schematic representation of the protein misfolding cyclic amplification (PMCA) reaction. PrP^{C} is recruited into growing aggregates of PrP^{Sc}; hence, it undergoes conformational conversion and becomes PrP^{Sc}. During PMCA, the growing PrP^{Sc} species are disrupted by repeated sonication in the presence of detergents. This treatment generates an expanded population of converting units for the continuous recruitment of PrP^{C}. The whole procedure is repeated several times. PrP^{C} is shown as light gray spheres. PrP^{Sc} is shown as trapezium. The original seed is in dark gray, and the newly formed PrP^{Sc} is in light gray. [89]

3.4. *De novo* prions by amyloid seeding assay

Another largely explored strategy consists of using several physico-chemical approaches to induce misfolding of the recPrP into β-strand rich states. Such investigations are relevant because they address the question whether PrP alone is sufficient for the spontaneous formation of prions without the presence of any exogenous agent or facilitator of the conversion. A plethora of studies have attempted to provide an answer to this question, but these experiments have largely failed in producing infectivity *in vivo* or the infectivity potential has not been tested so far [401][402][403][404][405][406][325][407]. However, in 2004 the production of synthetic prions via the *in vitro* conversion of bacterially expressed recPrP was reported [214]. In a previous work [401] the same authors had analyzed in detail the multiple misfolding pathways of recPrP (from residue 89 to 230) leading to β-sheet rich conformers. Depending on the reaction conditions, two misfolded forms were adopted: at acidic pH (3 to 5) and in the presence of partially denaturing urea concentration (4-5 M) a β-oligomer PrP^{Sc}-like is formed with no further aggregation, whereas under neutral or slightly acidic pH values and at low concentration of urea (1-2 M) recPrP aggregates in fibrillar structures which develop into amyloid. The polymerization process was monitored simply adding thioflavin T (ThT) to the reaction mixture. This dye shows strong increase of fluorescence upon binding to β-sheet rich structures like amyloid aggregates. Importantly, the authors discovered that the addition of a seed of pre-folded amyloid to the fresh reaction substantially reduces the time of the fibrilization (called lag phase) process, demonstrating that recPrP fibrils can be induced by seeding. Starting from these findings, Prusiner and collaborators [214] addressed the question of whether these synthetic fibrils were infectious when inoculated into mice. The pre-folded amyloid fibrils (denoted as “unseeded”) and the seeded ones composed of recMoPrP(89-230) were intracerebrally injected into Tg9949 mice, which overexpress MoPrP(89-230). Seeded amyloid fibrils exhibited shorter incubation time (382 days) and PK resistance than unseeded (473 days and PK sensitivity). Interestingly, also the neuropathological features associated with seeded and unseeded amyloids were different in terms, for instance, of vacuolation and gray matter PrP^{Sc} deposition. The authors argued that this result might be due to the creation of two new prion strains, denoted as MoSP1 (for Mouse Synthetic Prion strain 1, obtained from seeded PrP amyloids) and as MoSP2 (from unseeded amyloid). Moreover, MoSP1 prion exhibited infectivity and shortened incubation periods upon serial passages to both wild-type FVB mice and different Tg mice lines [214][373][374]. The conformational stability of MoSP1, as measured by the GndHCl concentration required to denature half of the sample, was very high (~4.5 M) compared to other natural prion strains, confirming that a novel synthetic prion has been obtained [373]. Subsequent serial passages of this strain led to shorter incubation periods and a decreased conformational stability of the resulting prions. Combining these data with those available for naturally occurring prion strains, it was demonstrated that the length of the incubation time in mice is directly proportional to the conformational stability of the prion strain [372,374] (Figure 15). These results suggest that decreasing PrP^{Sc} stability increases the fragmentation of PrP^{Sc}. This in turn causes the generation of multiple seeds that can increase the rate of the conversion and shorten the incubation period. Consistent with this hypothesis, studies examining other fibrillogenic proteins (Sup35, Tau, synuclein and β-amyloid) demonstrate that less stable fibrils have a higher propensity to undergo breakage, creating new seeds for the conversion [408][409][410][307][336][411][412]. It has been reported that partially

purified prion strains preparation may act as a seed for the polymerization of recPrP in amyloid fibrils. This conformational change can be monitored simply by a fluorescence shift in the dye ThT. When used in conjunction with multi-well plates and automated fluorescence plate readers, the ThT represents a feasible, highly sensitive, high-throughput approach for the detection of conformational changes of proteins. Authors denoted “amyloid seeding assay” (ASA) the method of amyloid fibrils formation seeded by preformed PrP^{Sc} and monitored by ThT fluorescence. ASA is able to detect PrP^{Sc} (both PK sensitive or resistant) from different human or animal infected brain samples [229][372]. Another feature of ASA is the possibility to shake the sample in order to enhance the interaction between recPrP and the seed (included preformed amyloid from recPrP or partially purified PrP^{Sc} from infected sample) and promote the generation of multiple seeds. Additionally, the partial unfolding of recPrP is enhanced by the presence of low denaturant concentration (usually Gnd-HCl).

Colby *et al.* recently also reported the generation of protease-sensitive, synthetic prions *in vitro* during the polymerization of recPrP into amyloid fibrils [229]. The inoculation of this amyloid preparation to Tg9949 mice resulted in novel, protease-sensitive, synthetic prions, which caused severe neuropathology and were transmissible both in Tg9949 mice and in Tg4053 mice, which moderately overexpress the full-length MoPrP. These results demonstrate that also PK-sensitive synthetic prions are able to transmit prion disease and change our notion that the protease resistance is not an obligatory feature of PrP^{Sc}, as it has been reported in some sporadic [391] and genetic [388][389][68][390] cases of prion disease. The finding that different synthetic prions are able to generate TSE *de novo* provided the strongest evidence that PrP^{Sc} is the main and crucial element needed for infectivity. The main criticism about these findings is the observation that transgenic animals overexpressing PrP develop prion-like disease spontaneously [413][178][414].

Therefore, it could not be ruled out that the effects observed might be just an acceleration of a disease process. However, it is important to note that the authors clearly answered to these criticisms demonstrating by means of different assays (ASA, PK digestion and histopathology) that the spontaneous neurological dysfunctions observed in Tg9949 control mice are not related to spontaneous generation of prions, but rather to aging of the animals [229].

3.5. *De novo* prions by annealing technique

Additional evidence has shown that synthetic prions can be generated when amyloid fibrils from full length SHaPrP are intracerebrally inoculated in wild-type hamster [376]. Makarava *et al*. converted recPrP into cross-β-sheet amyloids and subjected them to "annealing". Basically, this procedure consisted in the incubation of recPrP with normal brain homogenate, and then in subjecting the mixture to different heating and cooling cycles [375]. The result was then verified by PK-treatment. No disease was produced in the first passage although PrP^{Sc} was detected in the brain. However, serial transmission gave rise to a TSE disease phenotype with highly unique clinical and neuropathological features and a very long incubation time.

4. The prion principle in other protein misfolding disorders

Despite the fact that all protein misfolding and aggregation processes have the intrinsic possibility for transmissibility, it is likely that biological and pharmacokinetic barriers may prevent

some amyloid aggregates from acting like prions [338]. For example, the so-called infectious seeds may not be able to reach the correct place of the tissue and the right subcellular compartment to propagate the misfolding. This is likely to be a problem especially for some of the intracellular aggregates, such as LBs in PD or intranuclear aggregates in Huntington disease. There could also be a problem of biological stability, determining that the clearance may be faster than the rate of polymer elongation. The high resistance of PrP^{Sc} to proteases and extreme conditions may be key in the efficiency of prions as infectious agents [415]. Finally, some misfolded proteins form hyperstable aggregates may be poor at propagating misfolding [416]. Indeed, from findings with the *in vitro* amplification of mammalian prions [279] and from studies of the replication of yeast prions[408], it seems clear that fragmentation of aggregates is essential for effective propagation.

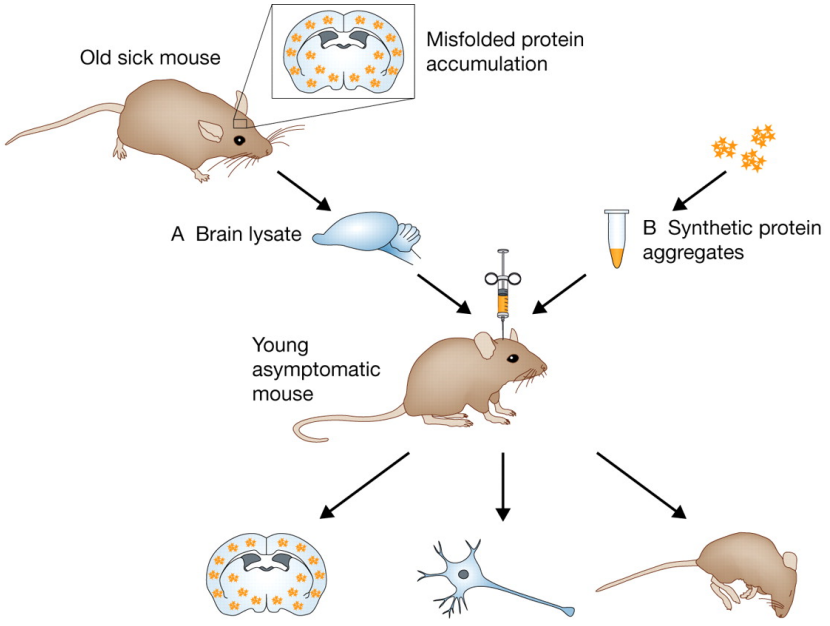

	Induction of aggregation		Neuronal loss		Fatal disease	
	Lysate	Synthetic	Lysate	Synthetic	Lysate	Synthetic
PrP^{Sc}	Yes[1]	Yes[2]	Yes[1]	Yes[2]	Yes[1]	Yes[2]
Aβ	Yes[3]	No[3]	Yes[3]	No[3]	No[3]	No[3]
α-synuclein	Yes[4,5]	Yes[5]	Yes[4,5]	Yes[5]	Yes[4,5]	Yes[5]
Tau	Yes[6]	n.d.	Yes[6]	n.d.	No[6]	n.d.

[1]Initially by Chandler 1961 and replicated by many; [2]Wang *et al*. 2010; [3]Meyer-Luehmann *et al*. 2006; [4]Mougenot *et al*. 2011; [5]Luk *et al*. 2012; [6]Clavaguera *et al*. 2009

Figure 16. Scheme summarizing evidence for seeded aggregation and cell-to-cell spreading in animal models of neurodegeneration. The figure depicts the experimental paradigm originally used to replicate infectious prions in mice, which is now used to replicate spreading of misfolded Aβ, α-syn, and tau. Protein aggregates containing brain lysates from old sick mice (A) or pure recombinant fibrils aggregated *in vitro* (B) are introduced in the brains of young asymptomatic mice by injection. It is important to note that some prion-containing lysates (Chandler *et al.* 1961) or synthetic prion aggregates (Wang *et al.*, 2010) can transmit disease to wild-type nontransgenic mice, whereas all other aggregates have thus far

only been shown to induce aggregation and neuronal dysfunction in transgenic mice expressing the human versions of the respective proteins [417]

The putative transmissibility of protein misfolding diseases has not been analyzed in detail, but the lack of epidemiological data supporting disease transmission is often used to rule out an infectious origin for these diseases. However, it is likely that, without the fortuitous transmission of sheep scrapie in 1937 or Gajdusek's milestone discovery of kuru transmission by cannibalism [418], an infectious origin for TSEs might have never been suspected. Indeed, epidemiological studies of relatives and people in contact with Creutzfeldt-Jakob disease (CJD) patients consistently produce negative results. Epidemiological tracking of an infectious origin for these diseases can be complicated by variable and extended time between exposure to the infectious agent and the onset of clinical symptoms, especially when this interval can be decades, as is typical for human TSEs.

A series of recent studies has provided experimental evidence for prion-like mechanisms of pathological transmission in various common neurodegenerative diseases (Figure 17 and Table 4). For example, Alzheimer's disease (AD) is associated with the misfolding and aggregation of two proteins: amyloid-β (Aβ) accumulation in extracellular amyloid plaques and hyperphosphorylated tau, which forms neurofibrillary tangles inside of neurons. To assess the possibility that AD pathology might be transmissible by a prion-like mechanism, transgenic mice expressing the human amyloid protein were injected intracerebrally with diluted brain homogenates derived from AD patients [419,420]. The results clearly showed accelerated Aβ-deposition in the brain of inoculated animals and preformed Aβ aggregates are required to seed amyloid plaque deposition *in vivo* [420]. Reminiscent of prions, seeding-competent Aβ aggregates are partially resistant to proteolysis and consist of a continuum of various sizes, with the most efficient seeds being smaller Aβ oligomers [421]. Oligomerization may be enhanced by posttranslational modifications, such as pyroglutamylation, promoting the formation of the first seeds that then propagate in a prion-like manner [422]. However, unlike prion disease, which can be induced *de novo* in animals that do not spontaneously develop the pathology, the induction of Aβ deposition observed in these studies only represents an acceleration by a few months of the spontaneous process that is set to occur by introduction of the mutant gene. Recent experiments performed in transgenic animals expressing low levels of wild-type human amyloid precursor protein found that disease alterations can be induced in animals that, without exposure to this material, will never develop the pathology during their entire life span [423,424]. Another important step forward in the similarities between Aβ and prion transmission has been the demonstration that AD brain abnormalities can be induced by intraperitoneal inoculation of transgenic mice with Alzheimer's brain extracts [425]. This finding suggests that seeds acquired by peripheral routes of exposure may induce disease in the brain. However, because the source of misfolded Aβ used in these experiments is sick brain homogenates, the relevance of these findings for AD transmissibility is uncertain. Various studies have been performed to analyze the transmission by seeding of tau aggregates, the other typical feature of AD, which is also found in other neurodegenerative diseases, collectively called tauopathies (e.g., fronto-temporal dementia, chronic traumatic encephalopathy, etc.). Intracerebral injection of brain extract containing tau aggregates into transgenic mice expressing human wild-type tau that do not form aggregates spontaneously induced the assembly of native tau into misfolded aggregates in

recipient mice [426]. Interestingly, the pathology spreads over time beyond the site of injection to anatomically connected neighboring brain regions [426]. Unlike Aβ and PrP^{Sc}, tau aggregates are located in the cytoplasm, suggesting that, in this case, protein misfolding is transmitted between cells. This hypothesis is further supported by *in vitro* studies of cultured cells in which extracellular tau aggregates were taken up and induced the misfolding and aggregation of intracellular tau [427][428][429]. These intracellular tau aggregates spread among cells to extend the pathology to the entire culture. Moreover, recent studies using a transgenic mice overexpressing human mutant tau only in a restricted area of the entorhinal cortex showed that the pathology initiated in this region spread throughout the brain even to areas without detectable human tau expression [430][431]. The progressive accumulation of tau aggregates in these animals leads to synaptic degeneration and later to axonal damage and neuronal death.

Neuropathological studies by Braak *et al.* and other groups have shown that neurofibrillary tangles in AD and LBs in PD initiate very early in the disease in a circumscribed area of the brain, and pathology progresses in a topographically predictable manner through anatomical connections [432] [433][434]. The defined spatiotemporal progression of the lesions may well be explained by spreading of misfolded proteins between cells and by axonal transport between different brain regions to propagate the pathology by transmission of protein misfolding.

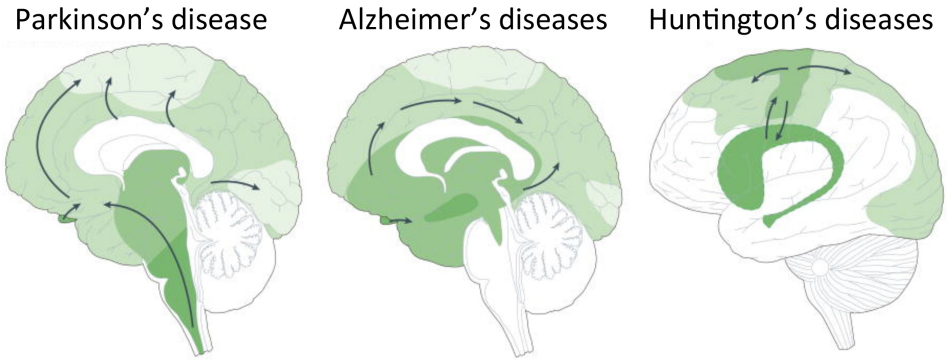

Figure 17. Principles for progression of neuropathological changes. Three drawings propose principles for how neuropathological changes in Parkinson's, Alzheimer's and Huntington's diseases spread spatiotemporally during disease progression. The earlier the neuropathology develops in a given brain region, the darker the shading in the diagram. As only one view (mid-sagittal for Parkinson's and Alzheimer's diseases; lateral for Huntington's disease) of the brain is depicted for each disorder, not all relevant anatomical structures and details of the spreading patterns (indicated by arrows) are presented. [435]

Table 4. Potential candidate disease-associated transmissible proteins

Disease	Protein (Location)	Experimental Transmission	Natural Transmission	References
Prion disease	PrP^{Sc} (extracellular)	Infectious in diverse animal species by various	Infectious in diverse species by	[50,89]

		routes	various routes	
Alzheimer's disease	Alzheimer's disease Aβ (extracellular)	Induction of pathology in transgenic mice by intracerebral and intraperitoneal inoculation	Not shown	[419][420][425][423]
Parkinson's disease	α-synuclein (cytoplasmatic)	Cell-to-cell and host-to-grafts spreading in animal models and transmission by intracerebral inoculation	Host-to-graft spreading in humans	[436][437][438][439][440][441]
Huntington's disease	Huntingtin (nuclear)	Cell-to-cell spreading in culture	Not shown	[442]
Tauopathies	Tau (cytoplasmatic)	Cell-to-cell spreading in culture and transmission in transgenic mice by intracerebral inoculation	Not shown	[426][427][428][429][430][431]
Secondary amyloidosis	Amyloid-A (extracellular)	Acceleration of pathology in mice by various routes of administration	Possible transmission to captive cheetah	[443][444]
Mouse senile amyloidosis	Apolipo protein A (extracellular)	Acceleration of pathology in mice by various routes of administration	Transmission to mice in the same cage by feces consumption	[445][446]

5. Synucleinopathies

Synucleinopathies are a subset of neurodegenerative disorders that have in common a pathological lesion composed of fibrillary aggregates of insoluble α-synuclein protein (α-syn) in selective populations of neurons and glia. The discovery of a point mutation in the α-syn gene

as a rare cause of familial PD has led scientists to the finding that α-syn is the major component of Lewy bodies (LB) and Lewy neurites (LN) in idiopathic PD and dementia with LB (DLB)[447][18][448]. The LB pathology that is sometimes associated with other neurodegenerative diseases, such as sporadic and familial AD, Down's syndrome, and neurodegeneration with brain iron accumulation type 1 (Hallervorden-Spatz syndrome), has also been shown to be α-syn-positive [448][449][450][451][452][453][454]. Moreover, the filamentous glial and neuronal inclusions of multiple system atrophy (MSA) are made of α-syn [452][455][456][457][458]. Taken together, these works have shown that PD, DLB, and MSA are α-synucleinopathies. The abnormal α-syn is a major component of the tubulofilamentous inclusions found in oligodendrocytes, known as glial cytoplasmic inclusions (GCIs). Clinically, they are characterized by a chronic and progressive decline in motor, cognitive, behavioral, and autonomic functions, depending on the distribution of the lesions. [459].

5.1. Parkinson’s disease

5.1.1. Symptoms and neuropathology

Parkinson's disease (PD) was first described by James Parkinson in 1817 [460][461]. This disease approximately affects 1% of the population over age 50 with a higher prevalence in men [462]. PD is characterized clinically by severe motor symptoms including uncontrollable resting tremor, muscular rigidity, impaired postural reflexes, and bradykinesia, which vary among patients [463][464]. These abnormalities can be accompanied by other symptoms, such as autonomic dysfunction, depression, and a general slowing of intellectual processes [465]. Pathologically, the marked degeneration of dopaminergic neurons in the substantia nigra pars compacta leads to the depletion of dopamine (DA) in its striatal projections, and of other brainstem neurons, with consequent disruption of the cerebral neuronal systems responsible for motor functions [463][464]. This neurodegeneration is accompanied by the presence of cytoplasmic (LBs) and neuritic (LNs) inclusions [466] in the surviving dopaminergic neurons and other affected regions of the central nervous system (CNS), but the mechanism underlying their formation is unclear, as is their pathogenic relevance. The substantia nigra, located in the midbrain or mesencephalon, has been the main focus of PD research. The motor symptoms are thought to result from the loss of dopamine-producing brain cells in this region and subsequent lack of transmitter input into the striatum, an important motor control area. Despite the focus on the substantia nigra, most PD patients have additional, non-motor symptoms, and PD is coming to be understood as a much broader disease. Chronic constipation, loss of smell, and REM sleep disorders often occur before the motor problems [467]. One of the attractive features of Braak’s staging scheme [468] is that the areas of the nervous system littered with LBs at the earliest stages of disease could account for these non-motor symptoms. Muqit *et al.* provided a review of the role of mitochondrial dysfunction, including oxidative damage and apoptosis, in the pathogenesis of PD [469]. Current thinking is that mitochondrial dysfunction, oxidative stress, and protein mishandling have a central role in PD pathogenesis [470].

5.1.2. Parkinson's disease genes

There is a growing list of mutations linked to PD. They account for 2–3% of the late-onset cases and ~50% of early-onset forms [471][472]. Typically, late-onset PD with LB pathology is linked to mutations in three genes: *SNCA* (encoding α-syn), *LRRK2* (encoding leucine-rich repeat kinase 2) and *EIF4G1* (elongation initiation factor 4G1). A pathogenic role for α-syn in these disorders is supported by various genetic data. Missense mutations in *SNCA* were first linked to familial Parkinsonism with late onset [447], and subsequent *SNCA* duplications were found in kindred in which age of onset, progression and associated comorbidities relate to gene dosage [473][474]. Multiplications of *SNCA* [475] and various point mutations in this gene (A53T, A30P and E46K) [476][447][477][478] result in rare autosomal dominant forms of familial PD and DLB. Moreover, certain polymorphisms in *SNCA* are major risk factors for sporadic PD [479]. In particular, the development of non-motor features correlates with α-syn gene copy number as well as gene and protein expression [480]. These studies suggest that increased neuronal α-syn protein levels are a primary factor in the disease. The causes and consequences of α-syn aggregation in neurons are not yet fully understood, despite a large number of molecular studies [481].

In addition, polymorphisms in the promoter region [482][483] and the un-translated region [484] of α-syn gene are also reported as risk of PD or DLB, and recent genome-wide association studies also identified the α-syn gene as one of the major risk loci for sporadic PD [485][479]. Recessive forms of Parkinsonism have been recognized that are caused by mutations in the genes for parkin [486][487], DJ-1 [488], ubiquitin carboxy-terminal hydrolase L-1 [489] and PINK1 [42]. Additional loci have been mapped on chromosomes 2p13 [490], 12cen [491], 1q [492], and 2q [493]. The main proteins that cause genetic forms of PD are summarized in Table 5. Proteins that play a significant role in sporadic disease have come to the forefront mostly from non-genetic research avenues [494].

Table 5**.** The main proteins that cause genetic forms of PD

Form	Pattern of inheritance	Chromosome region	Name of gene	Gene identified	Name of protein	Function of protein
Familial PD	AD	4q21-q22	*PARK 1*	yes	α-syn	Synaptic protein
Young-onset PD	AR/AD	6q25.2-q27	*PARK 2*	yes	parkin	Ubiquitin protein ligase
Familial PD	AD	4q region	*PARK 4*	yes	Multiplication of α-syn chromosome	Excess α-syn protein

					region	
Young-onset PD	AR	1p35-p36	*PARK 6*	yes	PINK1	Mitochondrial stress induced degeneration
Young-onset PD	AR	1p36	*PARK 7*	yes	DJ-1	Oxidative stress protection
Familial PD	AD	12p11.2-q13.1	*PARK 8*	yes	LRRK2 Dardrin	Protein phosphorylation
Familial PD	AR	1p36	*PARK 9*	yes	ATP13A2	Lysosomal protein

***AD = autosomal dominant, AR = autosomal recessive* [494]**

5.2. Dementia with Lewy bodies

Dementia with Lewy bodies (DLB) is a type of dementia closely associated with both Alzheimer's and Parkinson's diseases. It is characterized anatomically by the presence of LB, clumps of α-syn and ubiquitin protein in neurons, detectable in post mortem brain histology. Age at onset ranges from 50 to 80 years, with a slight male predominance, and disease duration is from 1 to 20 years. Clinically, DLB is characterized by dementia, fluctuating cognitive impairment, persistent visual hallucinations, and parkinsonism. Although dementia is the most frequent presenting feature, psychiatric symptoms or transient alterations of consciousness are other early features [495].

5.3. Multiple system atrophy

Multiple system atrophy (MSA) is a progressive sporadic neurodegenerative disorder, clinically characterized by parkinsonism, autonomic failure, cerebellar and pyramidal dysfunction, in any combination [496]. The historical terms striatonigral degeneration (SND), olivopontocerebellar atrophy (OPCA), and Shy-Drager syndrome (SDS) refer to neuropathological descriptions of patients with a combination of symptoms with predominant parkinsonism in SND, cerebellar dysfunction in OPCA, or autonomic failure in SDS, which have been embraced under the term MSA [497]. The age of onset can range from 33 to 78 years, and disease duration is from 0.3 to 24 years from the onset of symptoms [498]. Neuropathologically, MSA is characterized by a high density of ubiquitin-, tau-, and α-syn–positive GCIs, associated with neuronal loss and gliosis, in some or all of the following structures: inferior olives, pontine nuclei, cerebellar Purkinje cells, putamen, caudate nucleus, globus pallidus, substantia nigra, locus coeruleus, autonomic nuclei of brainstem, intermediolateral cell columns of the spinal cord, and Onuf's nucleus [498][499]. Although highly specific, GCIs are not exclusive of MSA, as they have been found in a minority of brains with progressive supranuclear palsy or corticobasal degeneration

[459]. The clinical presentation is variable. Parkinsonism is the predominant symptom in more than 80% of cases (MSA-P). A cerebellar syndrome predominates in less than 20% of patients (MSA-C) but develops in approximately half of the patients. Autonomic dysfunction is present in almost every patient to a certain extent. In addition to these key features, a variety of accompanying symptoms may also develop [459].

5.4. Pure autonomic failure

Pure autonomic failure (PAF) is a rare clinical manifestation of Lewy body disorders. It is an idiopathic, sporadic, neurodegenerative disorder characterized by primary orthostatic hypotension as the cardinal symptom, usually with evidence of more widespread autonomic failure [500]. No other neurological symptoms are present. Nevertheless, some patients who initially present features of PAF may later develop additional symptomatology that prompts reclassification of the diagnosis to PD, MSA, or DLB [501]. Neuropathological findings have shown severe compromise of both central and peripheral autonomic structures. Postmortem studies disclosed prominent LBs, LNs, and neuronal loss both in preganglionic and postganglionic sympathetic and parasympathetic systems [502][503][504]. Additionally, varying amounts of LBs and neuronal loss have been found in substantia nigra and locus coeruleus, and one study documented the presence of LBs in the dorsal raphe nucleus and pedunculopontine nucleus [503]. Since the first time the presence of anti–α-syn antibody immunoreactivity was found in a case of PAF, this disease belongs to the spectrum of α-synucleinopathies [503].

5.5. Proteins in synucleinopathies

5.5.1.The synuclein family

The first synuclein nucleotide and amino acid sequences were reported in 1988 from the electric organ of the Pacific electric ray (*Torpedo californica*) [505]. The protein was named synuclein because of its apparent localization in presynaptic nerve terminals and portions of the nuclear envelope. In 1991, cDNA sequences from rat brain were found homologous to the synuclein sequence from *T. californica* [506]. The amino acid sequence of an abundant protein from rat brain was called phosphoneuro protein-14 [507]. In 1993, the amino acid sequence of a protein from human brain was named non-amyloid-β component precursor (NACP), because of the apparent localization of a portion of this protein in some amyloid plaques from AD brain [508]. However, more recent studies using new antibodies have been unable to reproduce the original finding that may have resulted from antibody cross-reactivity with the β-amyloid protein [509][510]. The amino acid sequences of two homologous proteins from human brain were identified because they reacted with an antibody raised against paired helical filament preparations from AD brain [511]. The first protein was identical to NACP, whereas the second protein was the human homologue of rat phosphoneuroprotein-14. The authors noticed that the proteins were similar to each other and to synuclein from *T. californica* and consequently named them α-syn and β-synuclein, respectively. Human α-syn is 140 amino acids in length, whereas β-synuclein is 134 amino acids long. The amino acid sequence of a protein from zebra finch brain, synelfin, is the zebra finch homologue of α-syn [512]. Human α- and β-synucleins are

62% identical in amino acid sequence and share a similar domain organization. The amino-terminal half of each protein is taken up by imperfect amino acid repeats, with the consensus sequence KTKEGV. Individual repeats are separated by an inter-repeat region of 5–8 amino acids. Depending on the alignment, α-syn has 5–7 repeats, whereas β-synuclein has five repeats. The repeats are followed by a hydrophobic middle region and a negatively charged carboxy-terminal region, although both proteins have an identical carboxy-terminus. The human α-syn gene maps to chromosome 4q21, whereas the β-synuclein gene maps to chromosome 5q35 [513][514][515][516][517]. Their genes are composed of five coding exons of similar sizes, with the overall organization of these genes being well conserved. Alternative mRNA splicing has been observed for exons 4 and 6 of the human α-syn gene [518]. Similarly, the rat cDNAs SYN1, SYN2, and SYN3 appear to be splice variants of the same synuclein gene [506]. However, at the protein level, there is no evidence to suggest the existence of multiple α-syn isoforms. So far, no splice variants have been described for β-synuclein. The α- and β-synuclein sequences from several vertebrate species are very similar. No synuclein homologues have been identified in *Saccharomyces cerevisiae* and *Caenorhabditis elegans*, suggesting that the presence of synucleins may be limited to vertebrates [519]. α-Syn and β-syn mRNAs are expressed at highest levels in the nervous system, with lower transcript levels in other tissues [508] [511]. Both proteins are concentrated in nerve terminals, with little staining of nerve cell bodies and dendrites. Ultrastructurally, they are found in nerve terminals, in close proximity to synaptic vesicles [506][507][508][509][510][511]. In 1997, Ji *et al.* reported the amino acid sequence of a 127 amino acid protein that they named breast cancer-specific gene-1 (BCSG1) protein, because of its presence in large amounts in human breast cancer tissue [520]. BCSG1 shares 55% sequence identity with human α-syn and has therefore been renamed γ-synuclein [521]. It was independently discovered by Buchman *et al.* who named it persyn [522]. The synuclein that was originally identified in *T. californica* [505] was probably a γ-synuclein homologue. γ-Synuclein has the same general domain organization as α-syn and β-synuclein and is also encoded by five exons [523][524]. The human γ-synuclein gene maps to chromosome 10q23. γ-Synuclein mRNA is expressed at highest levels in the nervous system and the heart, with lower transcript levels in other tissues. It appears to be present throughout nerve cells, unlike α-syn and β-syn which are concentrated in presynaptic nerve terminals. In 1999, Surguchov *et al.* reported the sequence of a 127 amino acid protein that they named synoretin because of its expression in the retina [525]. Synoretin is 87% identical to γ-synuclein at amino acid level and shows the same tissue distribution as γ-synuclein mRNA. γ-Syn is highly expressed in various areas of the brain, particularly in the *substantia nigra*, and has been found to be overexpressed in some breast and ovarian tumors [526]. The sequences of all synucleins are similar [527], although only α-syn is implicated in disease.

5.5.2. Alpha synuclein

Alpha synuclein (α-syn), as mention above, was originally identified in the electric organ of the Pacific electric eel *Torpedo Californica* [505]. α-Syn is a thermo stable protein [508][511]. Hundreds of well-conserved α-syn protein homologues exist in human, bird, mouse, bovine, and rat, but no homologues have been reported in lower organisms such as *Escherichia coli*, yeast, *C. elegans*, or *Drosophila*. Its localization is concentrated at presynaptic nerve terminals [528][511][529]. This is a major component of the fibrillar aggregates in LBs and LNs in sporadic

PD and in dementia with Lewy bodies (DLB) [18]. The process of α-syn aggregation, eventually leading to the formation of LBs and LNs, appears to be a major contributor to neurodegeneration in PD [478][530]. Proteasomes [531][532][533] and lysosomes [534] are responsible for the cellular metabolism of α-syn. Recent studies have suggested that soluble oligomeric forms of amyloidogenic proteins, including α-syn, are pathogenic and lead to neuronal cell death [535]. It has also been shown that soluble α-syn oligomers are elevated not only in post mortem parkinsonian brain [536] but also in PD patient CSF [537]. Moreover, in altered conditions *in vitro* and *in vivo*, α-syn may self-assemble to form ordered fibrils [538] characterized by cross β-sheet structures similar to Lewy body aggregates [539]. Recent studies provide a sequential explanation for the process of α-syn oligomerization in the membrane, and support the role of generated pore-like structures in the molecular mechanisms of the PD neurodegenerative process [540][541]. α-Syn monomers might also have a role in synucleinopathies by their displacement from their physiological location, resulting in a loss of cellular function, or by disrupting the activity of other molecular or signaling pathways [542].

5.5.2.1. α-Syn structures

α-Syn is a 14 kDa protein (140 amino acids; pKa of 4.7) [508] characterized by an amphipathic lysine-rich amino terminus, which has a crucial role in modulating its interactions with membranes, and a disordered, acidic carboxy-terminal tail, which has been implicated in regulating its nuclear localization and interactions with metals, small molecules and proteins [543][544] (Figure 19). The highly conserved amino-terminal domain of α-syn (residues 1-65) includes six copies of an unusual 11 aa imperfect repeat that displays variations of a KTKEGV consensus sequence and is unordered in solution, but can shift to an α-helical conformation [527] [545] that appears to consist of two distinct α-helixes interrupted by a short break [546]. The amphipathic α-helixes [547] are reminiscent of the lipid binding domains of class A2 apolipo proteins [548]. α-Syn can bind to negatively charged phospholipids and becomes α-helical upon binding [544][549][548], suggesting that the protein may normally be membrane associated [548]. Several recent studies [550][551][552] have shown that lipidic environments promoting α-syn folding also accelerate α-syn aggregation, suggesting that the lipid-associated conformation of α-syn may be relevant to α-syn misfolding in neurodegenerative diseases. α-Syn is a soluble, natively unfolded protein with an extended structure primarily composed of random coils [544], but it may acquire secondary structural elements upon interaction with a number of ligands and proteins [549] that likely alter its native state conformation and lead to α-syn adopting partially folded conformations.

The central hydrophobic domain of α-syn (residues 66-95) is known as the non-Aβ component of plaque (NAC) [508][553], the second major component of brain amyloid plaques in AD. [508][554]. It comprises the highly amyloidogenic part of the molecule that is responsible for the ability of α-syn to undergo a conformational change from random coil to β-sheet structure [555] and to form Aβ-like protofibrils and fibrils [554][555]. These features distinguish α-syn from β-syn and γ-syn, which fail to form copolymers with α-syn [554]. The NAC region carries a phosphorylation site on Ser 87 [556]. It contains a highly hydrophobic motif that comprises amino acid residues 65–90 [508][18][557] (Figure 17). The NAC region is indispensable for α-

syn aggregation; the deletion of large segments within this motif greatly diminished α-syn oligomerization and fibrilization *in vitro* [558][554] and in a cell-based assay[437].

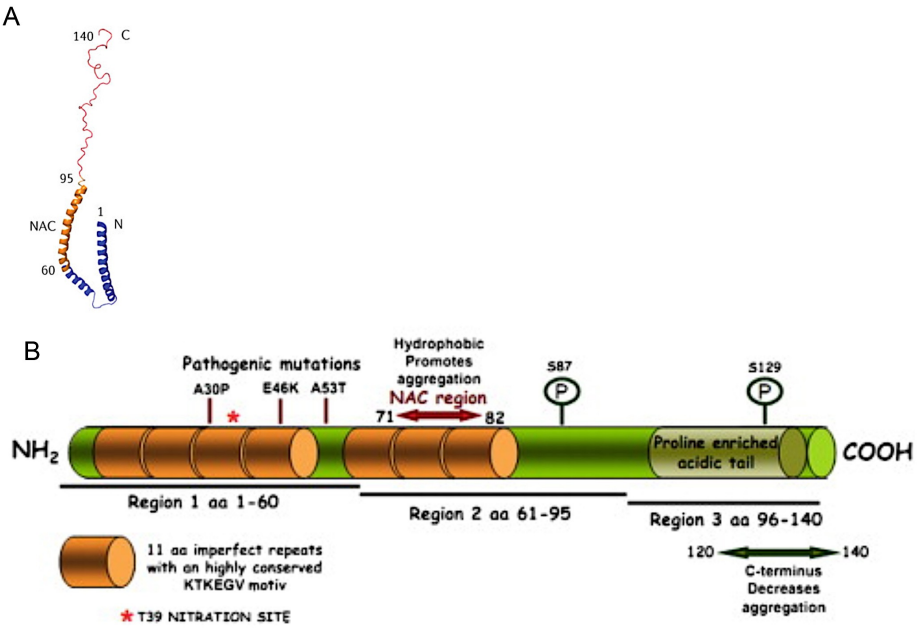

Figure 18. Schematic representation of micelle-bound α-syn (α-syn; Protein Data Bank ID: 1XQ8) (A) [559]. The N-terminal region, the non-amyloid-β component of Alzheimer's disease amyloid plaques (NAC) region and the C-terminal part are colored blue, orange and red, respectively. Numbers refer to amino acid residues flanking the different regions. Schematic representation of the full length 140 amino acid α-syn transcript (B). Pathogenic mutations as well as phosphorylation and nitration sites are indicated [560]

The acidic carboxyl-terminal domain (residues 96-140) of α-syn has no recognized structural elements but has a strong negative charge composed primarily of acidic amino acids [527]. Different from the amphipathic amino-terminal and the hydrophobic NAC regions, which are highly conserved between species, the carboxyl-terminal region is highly variable in size and in sequence [526]. It hosts an acidic domain (residues 125-140) that appears critical for the chaperone-like activity of α-syn [561], as demonstrated by deletion mutants of the carboxyl-terminal region in which the α-syn chaperone activity is lost [562][563]. Several phosphorylation sites have been detected in the carboxyl-terminal region on Tyr-125, -133, and -136, and on Ser-129 [564]. Considering that the carboxyl-terminal domain of α-syn is required for its chaperone-like activity [561], it is conceivable that phosphorylation of these Tyr residues in this region would also affect this property of α-syn. The residue Ser-129 is also phosphorylated by G-protein-coupled receptor protein kinases [565]. Studies *in vitro* suggest that phosphorylation at Ser-129 promotes formation of α-syn filaments as well as oligomers [566] as a consequence of a change in charge distribution and hydrophobicity of α-syn carboxyl-terminal region [567]. Extensive and selective phosphorylation of α-syn at Ser-129 is evident in synucleinopathy lesions, including LBs [566]. Other post-translational modifications in the carboxyl-terminal, including glycosylation on Ser-129 [567] and nitration on Tyr-125, -133, and -136 [568], may affect aggregation of α-syn. An *O*-glycosylated form of α-syn (α-Sp22), a specific substrate for ubiquitination by parkin, has been identified [487]. Although it has not been determined where α-

syn is glycosylated, a potential target for glycosylation is the carboxyl-terminal Ser-129, hosting *O*-linked sugars [487]. Truncation of the carboxyl-terminal region by proteolysis has been reported to play a role in α-syn fibrillogenesis in various neurodegenerative diseases [569]. Full-length as well as partially truncated and insoluble aggregates of α-syn have been detected in highly purified LBs [570].

Studies by several groups using different biophysical methods (for example, NMR, light scattering and circular dichroism) consistently showed that α-syn purified from *Escherichia coli* under native or denaturing conditions exists predominantly as stable unfolded monomers [544] [571]. When α-syn was extracted from patients diagnosed with LBD and age-matched controls and evaluated by non-denaturing gels or size exclusion chromatography (SEC) columns, α-syn monomers migrated as 57–60 kDa proteins, but in denaturing gels they migrated as 14 kDa proteins [558][437]. Two recent studies reported that native α-syn exists as a folded tetramer [572][371]. The first study showed that α-syn purified from mammalian cell lines or red blood cells exists as a stable α-helical tetramer with an apparent size of 58–60 kDa, as was discerned by size exclusion chromatography (SEC), native PAGE and sedimentation equilibrium studies [572]. The second study used NMR, chemical crosslinking and SEC, and indicated that α-syn produced in *Escherichia coli* exists as a dynamic tetramer that is rich in α-helical structure [573]. Both studies suggested that the tetrameric helical form of α-syn is resistant to aggregation and fibril formation. Initially, the apparent size of α-syn in native gels and SEC led many researchers to propose that this protein exists as a stable oligomer, but subsequent detailed biophysical studies demonstrated that the larger than expected size is mainly due to the fact that monomeric α-syn adopts an unfolded, extended conformation [571][559] which results in a larger than expected hydrodynamic radius (nature a-syn structure). These findings are in agreement with most studies on the oligomeric state of native α-syn, which have consistently shown that α-syn behaves as an unfolded monomer [574][571][559]. The migration of α-syn with an apparent molecular weight slightly above 66 kDa in native gels and SEC is probably the result of its tendency to adopt extended conformations, and not because it exists in an oligomeric form (for example, as a tetramer), as the addition of denaturants or boiling of α-syn samples from various sources did not change α-syn migration [559]. On the other hand, the apparently multifunctional properties of α-syn may lie in its conformational flexibility, which may allow the protein to adopt different conformations upon interacting with biological membranes of different compositions, other proteins or protein complexes [575][576]. It is well established that α-syn adopts an α-helical conformation upon binding to synthetic or biological membranes *in vitro* [544]. Several factors, including oxidative stress [577], post-translational modifications [578][579], proteolysis [580][581] and the concentrations of fatty acids [582][583][584], phospholipids and metal ions [585][577] were shown to induce and/or modulate α-syn structure and oligomerization *in vitro*, and these factors may influence this equilibrium between the monomer and oligomer state *in vivo*.

Mutations on α-syn may make it easier to be in the random coil state so that aggregation is more likely to occur. It has been suggested that this may be due to acquisition of a β-sheet configuration by the protein, which renders it more prone to aggregation and filament formation. The A30P and A53T mutations increase the rate of α-syn oligomerization, whereas the rate of mature fibril formation is increased and decreased by A53T and A30P mutations, respectively

[569]. α-Syn is one of the composers of filamentous inclusions in nerve cells or glial cells which are the defining neuropathological feature of a group of neurodegenerative diseases including PD, DLB and MSA [521]. In these so-called synucleinopathies, α-syn is deposited in a hyperphosphorylated form with β-sheet rich, fibrillar structure [18][457][586][455][566]. Since soluble α-syn never induced such pathology [587], the structural difference between soluble and filamentous forms of α-syn, for example cross-β structure in α-syn fibrils [588] is critical for pathogenesis.

5.5.2.2. α-Syn functions

Transgenic mice evidence, studies on α-syn knockout mice [589] and primary neurons [590] suggested that α-syn is involved in DA neurotransmission. α-Syn appears to be associated with synaptic vesicles, and there is evidence that it regulates the size of the synaptic vesicular pool [590]. α-Syn is also involved in synaptic plasticity by augmenting transmitter release from the presynaptic terminal [591]. Furthermore, α-syn can interact with presynaptic membranes, indicating that one of its functions may be in the regulation of DA release and reuptake [592][593][594]. There is also evidence that α-syn can modulate expression of genes involved in DA synthesis [595] and can affect enzymes involved in chromatin remodeling [596] and signal transduction [597]. Several cellular targets of α-syn have been found. The protein is thought to be an important component of the presynaptic protein scaffold that regulates dopamine release. In fact, inhibiting α-syn or proteins that interact with it at the synapse alters dopaminergic transmission and synaptic function [589,598][599]. Furthermore, aggregated α-syn impacts on various membrane structures of the cell. It can form pore-like complexes in the plasma membrane that alter membrane excitability and calcium permeability [600,601], affect the integrity of lysosomal and endosomal compartments, and inhibit vesicular trafficking from the endoplasmic reticulum to the Golgi apparatus in a Rab-dependent manner [602].

Transgenic mice overexpressing human α-syn exhibit impairment in synaptic vesicle exocytosis and a reduction in neurotransmitter release [594][603][604]. Similar effects have been observed after α-syn overexpression in genetic rodent models of PD [605][606] and in the PC12 stable cell line [607]. At the ultra structural level, overexpression of α-syn induces a decrease in readily releasable vesicles [605] and affects the recycling of synaptic vesicles following endocytosis, inducing a reduction in the size of the synaptic vesicle recycling pool [604]. Moreover, excess α-syn induces a reduction in dopamine reuptake in dopaminergic terminals [606] and inhibits intersynaptic trafficking of vesicles, leading to a smaller reserve pool of vesicles [608]. α-Syn associates with the distal reserve pool of synaptic vesicles [609][610][444] and the deficiencies in synaptic transmissions observed in response to knockdown or overexpression of α-syn. Therefore α-syn has a role in the regulation of neurotransmitter release, synaptic function and plasticity.

The possible role of α-syn in regulating synaptic homeostasis is not exclusively related to its direct interaction with synaptic vesicles. α-Syn interacts with synaptic proteins controlling vesicle exocytosis [611][612]. It also functions as a chaperone to maintain the integrity of the presynaptic terminal because α-syn overexpression rescues the neurodegenerative phenotype

of cysteine-string protein knockout mice [593]. Recent studies reported that α-syn can act as a chaperone protein for the presynaptic SNARE protein complex by controlling the degradation and affecting the assembly, maintenance and distribution of this complex, which is directly implicated in the release of neurotransmitters, including dopamine [613]. Thus, authors concluded that α-syn might function to sustain normal SNARE complex assembly in a presynaptic terminal during aging. Together, these observations indicate that α-syn has an important role in the trafficking of synaptic vesicles and in the regulation of vesicle exocytosis, and may contribute to more subtle regulatory phenomena by controlling synaptic homeostasis-associated proteins. The fact that the individual synuclein knockouts (α-, β- and γ-syn) are viable suggests that synucleins are not essential components of the neurotransmitter release machinery but may contribute to the long-term regulation and maintenance of nerve terminal function [614]. The neuroprotective effects of α-syn against progressive neurodegeneration in mice deficient in cysteine-string protein-α (CSPα; also known as DNAJC5) [593] strongly suggest that its functional properties become more prominent or essential under conditions of stress. The neuroprotective function of α-syn appears to be mediated by its ability to bind to membranes and vesicles, as the A30P α-syn mutant, which is deficient in membrane binding, failed to show protection in CSPα gene-knockout mice.

6. Is Parkinson's disease a prion disorder?

In recent years, evidence has grown to suggest that toxic amyloidogenic proteins, such as Aβ and tau, pass between neurons along functionally connected pathways, corrupting their normal counterparts [615][430]. The concept became clearer when aggregate migration was discovered in neurodegenerative diseases involving these amyloidogenic proteins. Aβ [616], tau [426][617], and polyglutamine peptides [442] all spread across the brain (Figure 18). In addition, a growing body of evidence indicates that self-propagating protein aggregates play central roles in many neurodegenerative diseases, including PD and AD [426][439][441,618].

Since PD is characterized by the accumulation of intracytoplasmic aggregates, made of a-syn and primarily located in the substantia nigra, an increasing body of evidence from animal models as well as data from genetic, biochemical and biophysical studies support the hypothesis that the processes of α-syn oligomerization [574][620] and fibril growth [585,621] have central roles in the pathogenesis of PD and other synucleinopathies [622]. Neuropathologically, α-syn lesions are believed to spread progressively throughout the brain, and their spread seems to be correlated to the staging of clinical symptoms [623]. Supporting the potential relevance of this concept in the pathogenesis of α-synucleinopathies, postmortem studies on patients with advanced PD who received grafts from healthy embryonic neurons many years before showed that some transplanted neurons contained a-syn aggregates [627][628][632][633]. In a few cases, the transplanted cells showed phenotypic alterations, such as loss of dopamine transporters.

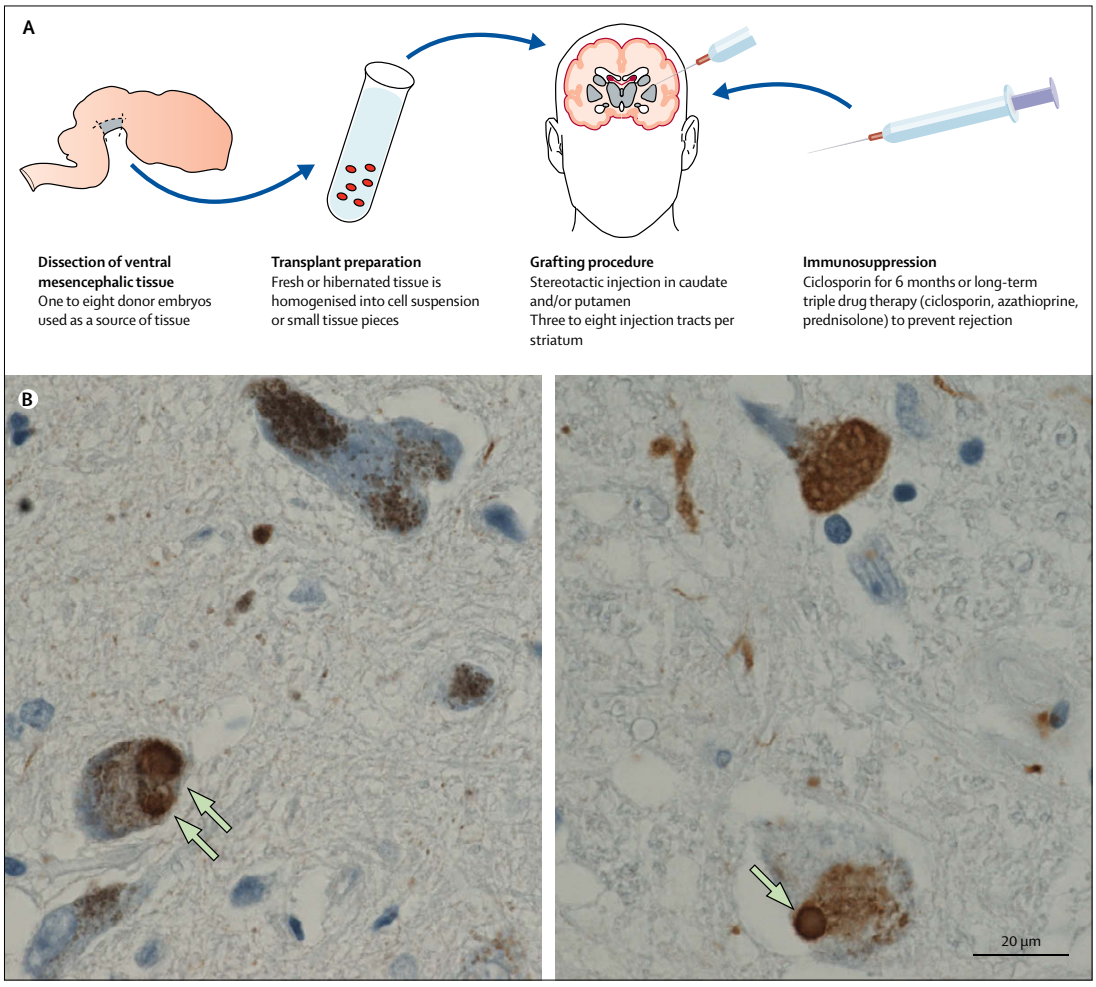

Figure 19. Grafting of neurons into brains of patients with Parkinson's disease (A) Summary of the procedure used to prepare long-term grafts. (B) Immunostaining with α-syn antibodies of sections from a 16-year-old graft (left panel). Lewy bodies (arrows) in the graft are similar to those seen in the substantia nigra of the host (right panel). [619]

Interestingly, α-syn has also been shown to ectopically accumulate in oligodendroglial cells in multiple system atrophy [624] and in astroglial cells in PD [625][626]. Some patients died 13–16 years after transplantation of fetal nigral cells into the striatum. The inclusion bodies appear identical in morphology and staining to the LBs found in host dopamine neurons in the SNc [627][628][629][630][631]. These LBs occurred in about 5–8% of the grafted neurons similar to the proportion found in SNc neurons in cases of PD and stained for α-syn, ubiquitin and thioflavin S. Some other previous studies have shown accumulation of α-syn in fetal grafted neurons in patients with PD [632][633], as well as in grafted neuronal precursor cells in the hippocampus [436] and basal ganglia [634] in mouse models. In human α-syn-expressing mice that received stem cell grafts, the transplanted cells also picked up the protein, similar to what may have happened to cell grafts in human clinical trials for PD [628][627]. Moreover, the ascending distribution of the LB pathology in LBD, as described by Braak [625], has been interpreted to support the dissemination of α-syn from subcortical to cortical brain regions. Most interestingly, in support for this possibility that α-syn may be transmissible from diseased

neurons to healthy neurons, recent studies showed that exogenous α-syn fibrils induced LB pathology in cultured neurons [436][635][428][438], transgenic mouse brains [439][636] and wild-type mouse brains [636] [587]

6.1. Mechanism of LB presence or paths to increased expression and accumulation of α-syn in disorders

PD, DLB and other LBDs show accumulation and redistribution of α-syn in various brain regions and cellular populations. These changes in the natural structure and localization of α-syn may have pathogenic roles in these disorders and can be reproduced in α-syn transgenic animals [637][638][639][640][641] and wild-type mice [441] [587]. The levels of α-syn in the CNS depend on the balance between the rates of α-syn synthesis, aggregation and clearance [642] (Figure 21). An imbalance between these mechanisms, caused by dysfunction of one or more of these pathways (Figure 21), can result in abnormal levels of α-syn that might favor the formation and/or accumulation of oligomeric and fibrillar species, which may be toxic. Indeed, in some familial forms of parkinsonism, multiplication of *SNCA* results in increased accumulation of α-syn because of increased protein expression [475], whereas in others, *SNCA* mutations enhance the propensity of α-syn to aggregate [574]. A genome-wide association study (GWAS) showed that individuals with certain variations in the *SNCA* gene had a higher risk of PD [643]. One such polymorphism is known as Rep1, which occurs in the promoter region of *SNCA* and might increase the susceptibility to PD by increasing the expression of α-syn [483]. Clearance of α-syn monomers and aggregates occurs via direct proteolysis [644], binding to molecular chaperones [645], the proteasome [646][647][533] and autophagy (involving the activity of the lysosome) [642][648][436][649]. In sporadic forms of PD and DLB, failure of the autophagy pathways to eliminate oligomers might enhance α-syn-mediated toxicity [436] and may contribute to the pathological release of α-syn [610]. Chaperone-mediated autophagy [648] has been shown to be disrupted by oligomeric forms of wild-type and disease-associated mutant α-syn. In PD and DLB, the levels of key autophagy molecules such as ATG7, a ubiquitin-like modifier-activating enzyme, and mammalian target of rapamycin (mTOR), a serine/threonine protein kinase, are deregulated [650]. Other mechanisms have been considered for the presence of LB in transplanted cells involved in inflammation, oxidative stress, excitoxicity and loss of neurotropic support [434]. Interestingly, the secretion of both monomeric and aggregated α-syn is elevated in response to proteasomal and mitochondrial dysfunction and cellular defects found in PD [651][617][652].

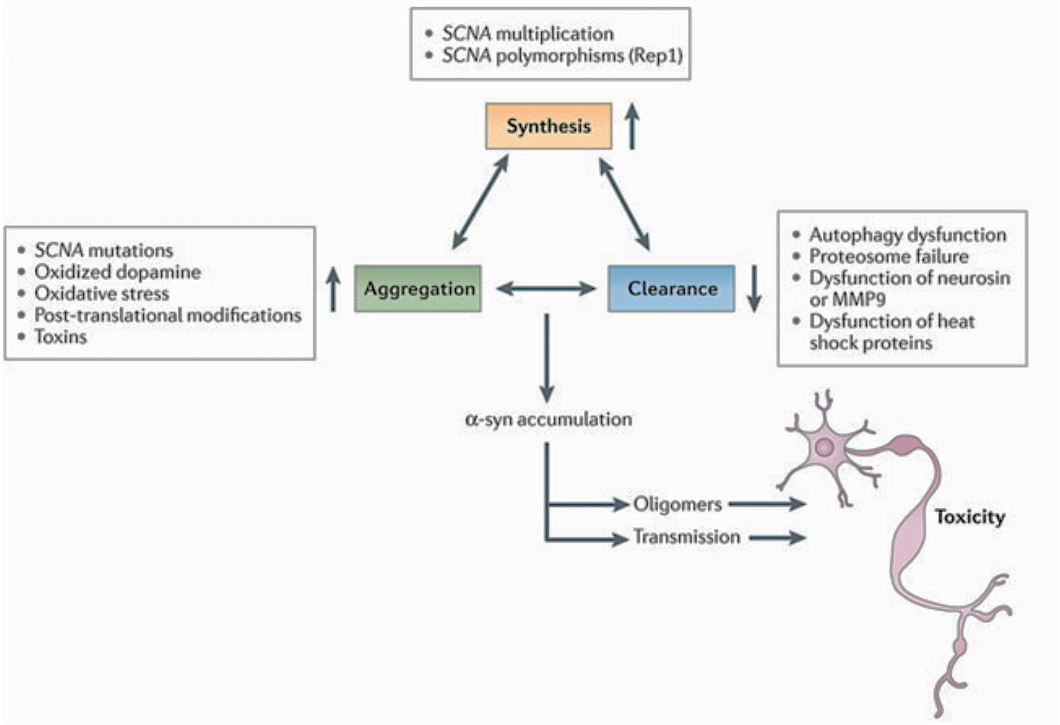

Figure 20. Cellular events controlling intracellular α-syn levels. Intracellular α-syn levels are tightly regulated by the balance between the rates of α-syn synthesis, clearance and aggregation. Abnormalities affecting α-syn synthesis, including *SNCA* multiplication and polymorphisms (such as Rep1), may increase intracellular α-syn levels and induce its accumulation. Accumulation may also be caused by a failure to degrade α-syn. Clearance deficits might arise from failure of the ubiquitin–proteasome system, chaperone-mediated autophagy dysfunction (induced by Parkinson's disease-linked mutations) or dysfunction of proteases (neurosin or matrix metalloproteinase 9 -MMP9). Finally, certain *SNCA* mutations, post-translational modifications, oxidative stress, toxins and interaction with oxidized dopamine increase the propensity of α-syn to aggregate and accumulate [653]

The presence of toxic aggregates of α-syn along these paths can act as seeding phenomenon in prions concept. "Seeding" is synonymous with the addition of preformed aggregates to a solution of monomers. This process can eliminate the lag phase of aggregate growth that is associated with the formation of soluble assembly-competent oligomers (known as the "nuclei") and can accelerate fibril formation, therefore increasing the accumulation of proteins. Since seeding is the theoretical basis for prion infectivity, or the conveyance of prion proteins from animal to animal [653], this has been used as a strong approach for researchers in the field of prion-like diseases to study especially the possible transmission and infectivity of PD.

6.2. α-Syn spreading and transmission mechanisms

6.2.1. Braak's hypothesis

The discovery of LBs in the intestine of patients led to a new theory on the origin and progression of PD. This theory suggests that PD starts outside the CNS, induced by a virus or other pathogen, and then spreads to different areas of the brain in stages. Epidemiological research suggests that in human patients, constipation might be one of the early signs of PD, preceding motor symptoms by decades [654][655]. Animal studies provide some support for this

conclusion as well [656]. A transgenic mouse expressing a mutated human α-syn gene was developed. This strain develops α-syn aggregation in the gut at three months of age. These mice have signs of constipation and reduced defecation similar to what is seen in PD patients. Because this mutation causes some familial forms of PD, the results provide a link between PD and a disease process in the gut. These studies concluded this mouse model mimics the early stages of PD. In the model, the pathology does not, however, progress to the CNS [656].

The ability of wild-type α-syn to convert to a pathological form and then spread in brain has gained support recently. This hypothesis is developed by Heiko Braak and considered by some to be far-fetched initially. In patients, the enteric nervous system (ENS) is riddled with LBs long before they are found in the brain or before motor symptoms emerge [657]. This hypothesis focuses on the localization of LBs throughout the nervous system. In this hypothesis, disease pathology shows a predictable distribution pattern, in which they suggest that the pathology starts in the gut and not the substantia nigra and the pathology might spread across synapses from one neuron to the next [658]. Based on painstaking observations of hundreds of tissue samples, Braak and colleagues proposed that the pathology associated with PD advances systematically through the nervous system in six stages, sequentially moving from the vagus nerve up the brainstem to the substantia nigra in the midbrain and eventually reaching the forebrain and cerebral cortical areas [659] (Figure 22). They based this staging scheme on the assumption that disease pathology would not occur in an area of lower vulnerability without also being present in areas of higher vulnerability. In stage 1, while samples show mild pathology, the LBs are typically confined to the olfactory bulb and the dorsal motor nucleus of the vagus nerve. Because the vagus nerve connects the brain to the enteric nervous system (ENS), the authors proposed that the disease could start in the gut and move along the vagus nerve in an upstream or retrograde direction toward the brain. In stage 2, LBs continue to ascend into the brainstem, reaching the medulla oblongata and pontine tegmentum, parts of the brainstem that control swallowing, sleep, and other autonomic functions sometimes affected in PD. By Stage 3, pathology starts to affect the amygdala (an almond-shaped mass of neurons involved in processing fear and other emotions, but also the sense of smell) and in the substantia nigra; this is the stage when the motor phase of the disorder begins. In Stage 4, pathology in areas affected in earlier stages worsens, and LBs progress to the forebrain and encroach on a portion of the cerebral cortex (the temporal mesocortex), whereas the neocortex, the part of the brain involved in higher functions, remains unaffected. In Stages 5 and 6, the pathology is full-blown, appearing initially in the anterior association and prefrontal areas of the neocortex and then spreading to the posterior association areas, which are involved with memory, learning, and planning movement.

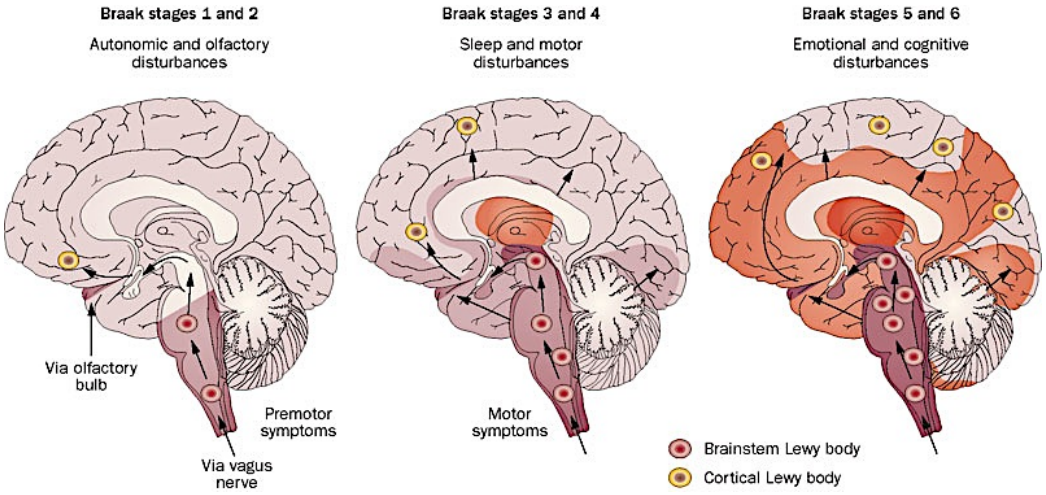

Figure 21. The Braak staging system of Parkinson's disease, showing the initiation sites in the olfactory bulb and the medulla oblongata, through to the later infiltration of LB pathology into cortical regions. α-Syn-related pathology is possibly initiated in the periphery via input from the olfactory epithelium or vagal inputs from the stomach, perhaps involving xenobiotic factors. The red shading represents the pattern of pathology. [468]

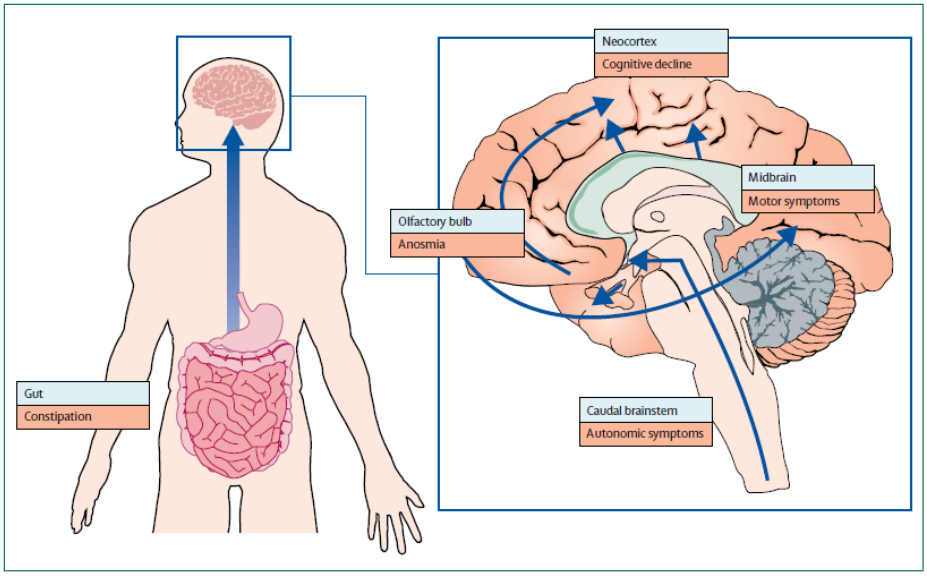

Figure 22. Dual-hit hypothesis of propagation of synucleinopathy during Parkinson's disease. Parkinson's disease-associated neuropathology originates in the gut (first hit) or the nose (olfactory bulb; second hit) and then propagates to the caudal brainstem and the temporal lobe. LB pathology then ascends to midbrain structures and cortical areas. Blue arrows depict the proposed ascending progression of Parkinson's disease pathology. Boxes indicate affected systems and main associated symptoms. [619]

In a subsequent study, Braak *et al.* focused on the ENS. The two sites where PD pathology begins are the gut and the olfactory bulb. The sPD-associated involvement of the ENS initially reported found relatively little resonance in comparison to the literature devoted to lesions in the CNS [657]. In autopsies of patients who had positive LB in the CNS, they found LB in both the Meissner's and Auerbach's plexus, the two layers that make up the ENS. Because the ENS lesions were found both in PD cases and in asymptomatic individuals who only had LBs in the

lower brainstem, the results confirmed that the disease could start off in the ENS. But a further postulate was that the disease could be set off by a yet-unidentified pathogen in the gut [660]. Moreover, another publication [661] found no evidence that PD starts in the gut, such as aggregates of phosphorylated α-syn. The phosphorylated α-syn aggregates appear in the spinal cord or any peripheral site without also being present in the brain [661]. Then, this hypothesis was revised to suggest that the pathogen could simultaneously enter the nose, by inhalation, and the gut, by swallowing nasal secretions, and then progress to the brain from two directions, providing a "dual-hit" [662] (Figure 23).

6.2.2. From cell to cell *in vitro*

Cells normally keep their α-syn problems to themselves, but when they accumulate more than they can handle, they may release the protein into the extracellular space [436] and the nearby cells can pick up α-syn jetsam, helping the toxic protein spread from cell to cell across the brain. Indeed, there are discoveries that neurons can exocytose [651] and endocytose [610] α-syn. One suggestion to account for these results is that α-syn pathology spreads by a prion-like process [663]. The toxic forms of the protein move from cell to cell, seeding new aggregates as they go. Accordingly, extracellular α-syn is taken up by neighboring neurons through endocytosis, leading to aggregation and intracellular inclusions [651]. Cell-to-cell transmission of α-syn was found in neuronal cultures [436][664][438]. Researchers have not quite worked out how the malformed proteins jump from cell to cell, perhaps across synapses; some reports have suggested endocytosis is involved [436][440]. It is also possible that cell-to-cell transmission occurs through direct cellular contact, involving nanotubes, or is mediated by exosomes or microvesicles [346] as similar findings have been also reported with other misfolded proteins, such as huntingtin, superoxide dismutase, and TDP-43, associated to Huntington's disease and ALS [442][665][666][667]. Cell biology studies are obtained in characterizing the endocytosis of α-syn fibrils and oligomers [610], and the release of α-syn by neurons [651][668], while prior research has shown smaller species of α-syn, namely soluble oligomers and monomers, getting released by neurons and wreaking havoc on neighboring cells [669][670][436][635]. The α-syn inclusion, which is seeded by recombinant fibrils and oligomers, recruits normal α-syn in cultured primary neurons [669]. More recently, a cell model system that uses preformed α-syn fibrils to induce LB pathology, synaptic dysfunction, and death in wild-type mouse neurons was developed [438]. The authors showed that pre-formed material of α-syn could jumpstart the aggregation process in cells since it is templated recruitment. In this case, these preformed α-syn fibrils work like seeds in recruiting normal protein to adopt an abnormal conformation. The pre-formed fibrils can drive formation of LB-like aggregates in cells [437], but the system was extremely artificial in which the host was a non-neuronal cell line engineered to express humongous levels of α-syn.

The inclusions and functional deficits failed to develop in neurons from α-syn knockout mice, indicating that endogenous α-syn forms the insoluble intracellular deposits. This study on α-syn knockout neurons is a primary work in α-syn transmission by the description of the temporal progression of aggregates from the axons to the somato dendrites, and the association of aggregate formation with impaired neural activity and connectivity. However, because artificial

fibrils were used but not neuron-released α-syn, the physiological relevance of the results and the release of α-syn by neurons [651] [668] remains to be determined [610]. Again, the mechanisms through which extracellular α-syn oligomers transfer to other cells include endocytosis [671], direct penetration [672], trans-synaptic dissemination [670] and membrane-receptor-mediated access [610]. Once inside the acceptor cell, α-syn oligomers could act as a focal point for further intracellular aggregation or the protein could be targeted for degradation.

6.2.3. From cell to cell *in vivo*

A few micrograms of pure, synthetic, aggregated α-syn is all it takes to corrupt normal protein in the brain, according to the successful seeding in cell cultures. While injecting brain extracts from one diseased rodent into another could seed α-syn pathology, a study was similarly performed with synthetic seeds. In PD model mice, a single injection of this synthetic aggregate was sufficient to speed up age-related pathology in still-healthy animals, killing them within a few months. This is a direct demonstration that the fibril alone is sufficient to cause this pathology and spreading [441]. More recently, studies in intracerebral injection of brain and spinal cord lysates from sick, aged (more than a year old) mice into the striatum or neocortex of young (two to five months) asymptomatic animals showed that the α-syn pathology quickly extended throughout both sides of the brain, and triggered an early onset of the disease with motor alteration and accumulation of aggregates [439]. Similar tainted-tissue injections can transmit amyloid-β inclusions [425][420] and tau aggregates [426]. These studies came to the same conclusion that amyloidogenic proteins from the donor animals seed new aggregates in the recipients. However, with brain extracts there is always "an element of doubt" because the lysate might contain some secondary factor that promotes disease along with the misfolded protein. After injection of recombinant α-syn fibrils in Tg mice, they showed responses similar to PD [439][636]. In fact, the pathology was more robust. The inclusions reached more parts of the brain of injected mice than they normally inhabit in these model mice when they age. The injected young mice had more inclusions than did naturally aging sick mice [636]. In addition, the progression of pathological inclusions was faster than normal and they died more quickly than the aged animals. An explanation for this unnaturally quickly pathology is the expression of higher-than-normal concentrations of α-syn. Animals heterogeneous for the mutant gene had a slower rate of progression following aggregate injection. While the disease does not move so quickly in people, familial PD which is due to extra copies of α-syn do have earlier onset and fast progression. This is a so-called prion-like seeding phenomenon: the pathology can spread through the brain in a manner that is highly reminiscent of the actual disease. It seem that it was more difficult to seed amyloid-β aggregation with recombinant protein, and only recently this succeeded with the prions that are the prototype for this kind of malformed protein transmission [276][673][674]. The overall picture thus far indicates that, while amyloid-β and prions require very specific, hard-to-make conformations to convert their normal structures into pathological forms, α-syn may readily adopt an infectious form. Indeed, intracerebral injections of insoluble α-syn from brains of patients with dementia with LB induced hyperphosphorylated α-syn pathology in wild-type mice [587].

Moreover, infection of fibrils of recombinant human and mouse α-syn efficiently induced similar α-syn pathologies in wild-type mice [587][441]. In non-transgenic mice, after a single intrastriatal inoculation of a small amount of synthetic α-syn into the dorsal striatum [441] or substantia nigra

of wild-type C57BL6/C3H mice [587], the aggregates and hyperphosphorylated α-syn spread to areas of the brain at the injection site and showed up around this site. The induction of phosphorylated α-syn pathology in wild-type mice is time- and brain region-dependent [587]. Luk *et al.* reported dopaminergic neuronal loss and motor dysfunction in wild-type mice injected with mouse α-syn fibrils in striatum. In contrast, human α-syn or mouse α-syn fibril-injected mice, which were performed in substantia nigra, did not show any motor and cognitive deficits, and a dramatic reduction of enkephalin was observed in the amygdala central nucleus and globus pallidus [587]. The different phenotypes of these mice might be explained by differences in the injection sites. Nonetheless, the spreading pattern of the pathological α-syn is different between these studies. Differential vulnerability of neurons to these abnormal proteins may also affect phenotypes of these mice. As LBs in these areas multiplied over a longer period, inclusions also began turning up in additional connected areas—the neocortex, ventral striatum, thalamus, and occipital cortex. Pathology also spread the same way after injection of two other wild-type mice CD1 and C57BL6/SJL [675]. Synthetic alpha-syn fibrils led to the cell-to-cell transmission of pathologic α-syn and Parkinson-like LB pathology in anatomically interconnected regions. LB pathology accumulation resulted in progressive loss of dopamine neurons in the substantia nigra pars compacta, but not in the adjacent ventral tegmental area, and was accompanied by reduced dopamine levels culminating in motor deficits. However, the spreading pattern of the pathological α-syn was found different in different sites of injection, for example striatum [441] and substantia nigra [587]. This recapitulation of a neurodegenerative cascade thus established a mechanistic link between transmission of pathologic α-syn and the cardinal features of PD. These findings suggest that α-syn pathology is spreading in the brain by a prion-like transmission process in which intracellular aggregates gain access to the extracellular space either by secretion or by damage of the host cell and then get internalized into neighboring cells — most likely through endocytosis — where they bind the normally folded, soluble protein and template the misfolding process.

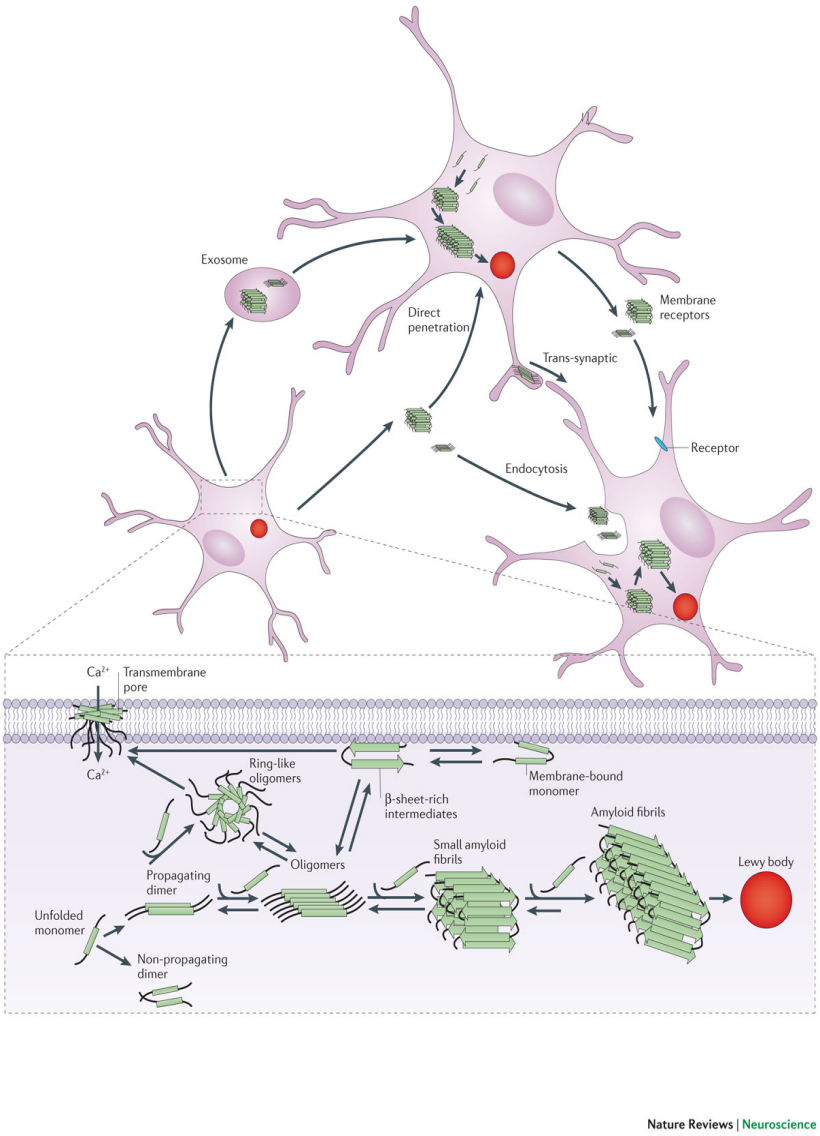

Figure 23. Mechanisms of α-syn aggregation and propagation. α-Syn aggregation can take place either in the cytoplasm or in association with the cellular membrane. In the cytosol, unfolded monomers interact to form initially unstable dimers, which grow slowly to generate oligomers of varying morphologies — including transient spherical and ring-like oligomers — that eventually convert to fibrils. The α-syn oligomers are in equilibrium with monomers and convert to fibrils by monomer addition via a nucleated polymerization mechanism. The accumulation of these amyloid fibrils leads to the formation of intracellular inclusions called LBs. Membrane-bound monomeric α-syn adopts a predominantly α-helical conformation, but at high concentrations the protein undergoes a conformational change either before or coincident with its oligomerization to form membrane-bound β-sheet-rich structures that self-associate to form oligomers, including trans-membrane amyloid pores (the formation of which may involve several intermediates) and fibrils. Note that the ring-like cytosolic oligomers may also associate with the membrane and form trans-membrane pores. During α-syn fibrillogenesis and aggregation, the intermediate species (oligomers and amyloid fibrils) are highly toxic, affecting mitochondrial function, endoplasmic reticulum–Golgi trafficking, protein degradation and/or synaptic transmission, and these intracellular effects are thought to induce neurodegeneration. The transmembrane pores disrupt membrane integrity as well as intracellular calcium homeostasis and signaling, and may also contribute to neuronal toxicity. Interestingly, α-syn oligomers and fibrils, as well as the monomers, can be transferred between cells and induce disease spreading to other brain regions. Spreading mechanisms are multiple

and can occur via endocytosis, direct penetration, trans-synaptic transmission or membrane receptors. Once inside the host cells, α-syn aggregates can nucleate aggregation and propagate via the mechanisms described above[653].

6.2.4. α-Syn propagation in recipient cells

The pattern of spreading observed in *in vivo* studies suggested that the injected fibrils acted as seeds that converted native α-syn to a pathogenic form, which then aggregated, crept through functionally linked areas, and converted more native protein. Indeed, evidence from *in vitro* biophysical studies has consistently shown that fibrilization of α-syn follows a nucleated polymerization mechanism [676] although the exact process of intracellular oligomer and fibril propagation remains unclear. A definition for the terms of propagation, dissemination and infectivity is provided by key terminology in the field of prion-like disease. This mechanism is characterized by a nucleation phase that initially involves the formation of assembly-competent oligomers (nuclei), which is followed by cooperative oligomer growth and fibril formation by monomer addition [428] (Figure 24). This process can be seeded (initiated) and accelerated by the addition of preformed fibrils (the seed) and is thought to serve as the underlying mechanism for the spreading of α-syn pathology in the brain. This phenomenon has been observed in a cell-based assay in which the introduction of recombinant α-syn fibrils results in seeding, the recruitment of endogenous α-syn and the formation of LB-like inclusions [441]. As mentioned above, a recent *in vivo* study on the inoculation of α-syn transgenic mice [636] with homogenates containing α-syn protofibrils and fibrils and non-transgenic mice with synthetic mouse a-syn fibrils [441][587] resulted in considerable enhancement of the α-syn pathology and propagation. As reported, one tiny injection of misfolded, fibrillar, synthetic mouse α-syn recruits native protein and converts it to a pathogenic form. Although the setting off a neurodegenerative cascade was established, there is still no evidence was showed for a real infection by the following passages in mice. Since the mouse expresses only wild-type α-syn of its own species, as do most humans with the disease, this injection model could be the closest yet to simulate pathogenic protein templating in sporadic forms of PD. Similar works showed that not only fibrils made of recombinant mouse α-syn, but also ones from human α-syn fibrils can efficiently induce α-syn pathology. Endogenous mouse α-syn is converted into the abnormal form and deposited in neurons of the brain through a prion-like mechanism or by seed-dependent aggregation by crossing the species barrier [587]. Propagation patterns of pathology in the inoculated mice were basically identical regardless of the species of injected seeds (i.e. recombinant human, mouse α-syn fibrils or dementia with Lewy bodies brain extracts), but extracts of brains with DLB showed lower propagation efficiency than recombinant fibrils [587]. This relatively low efficiency may be explained by the lesser amount of abnormal α-syn contained in the DLB brain extracts. Comparison of human α-syn fibrils and mouse α-syn fibrils indicated that mouse α-syn fibrils showed slightly higher efficiency [587]. *In vitro* experiments also indicated that mouse α-syn fibrils promote fibrilization of the soluble mouse α-syn monomer faster than human α-syn fibrils [587]. It is well known that prion propagation can cross the species barrier [677] and the efficiency of propagation depends on the amino acid sequences of prion proteins. α-Syn, mouse α-syn and human α-syn share 95% amino acid sequence homology, and this may be the reason why endogenous mouse α-syn can aggregate by inoculation of human α-syn fibrils. Another factor may be that mouse α-syn protein has a threonine residue at amino acid position 53, which is known as an aggregation-prone mutation in familial PD in humans [447].

6.3. Is there strain-specificity for prionic α-syn?

Since the fibrillar forms of α-syn are detected mostly in LB [678][679] that are localized in the neuronal cell body, these intracellular structures are the neuropathological hallmark of PD and DLB. There are a number of different α-syn conformers, including oligomers, protofibrils and fibrils that have been associated with the pathogenesis of these diseases [653].

In vivo, strong indirect evidence supports the existence of various oligomeric α-syn species under pathophysiological conditions. SDS-resistant dimers as well as low- and high-molecular-weight oligomeric forms of α-syn have been detected in diseased human brains [620] [680][586] and in brains of transgenic animal models of synucleinopathies [620][609][681] that express wild-type or PD-associated mutant variants of α-syn [540]. In contrast to fibrillar α-syn, oligomeric aggregates are most likely located in axons and presynaptic terminals, where they might damage synapses and dendrites [603][604][606][560][682][683].

In vitro, several oligomeric species of different morphologies, including spherical, chain-like and annular oligomers, have been observed before α-syn fibril formation [684]. The various oligomeric species seem to exist in equilibrium with monomeric α-syn and undergo a very slow conversion to fibrils in the absence of a high molar ratio of monomers to other species of α-syn. However, the relationships between the various α-syn oligomeric species and mechanisms of the inter-conversion between these different oligomers remain poorly understood, although some studies suggest that the formation of ring-like oligomers is not on the pathway to amyloid formation.

Both *in vitro* and animal model studies show that three PD-linked *SNCA* mutations (A30P, E46K and A53T) accelerate α-syn oligomerization, but only two of these (E46K and A53T) enhance fibrilization *in vitro* and *in vivo* [574][558][685]. Although the A30P mutation has been shown to result in enhanced α-syn fibrilization *in vivo*, as illustrated by an autopsy case of a patient with this mutation who had extensive LB pathology [643], *in vitro* it exhibits reduced fibrilization compared with the wild-type protein and other mutants.

Biophysical and SEC studies suggest that α-syn SDS-resistant oligomers from post-mortem human and transgenic animal brains can be in general divided into small (~2–5-mers), medium (~5–15-mers), and large (~15–150-mers) oligomers [686][687]. Spherical oligomers 2–6 nm in diameter may be the toxic forms of α-syn, as they promote neuronal degeneration and abnormal calcium currents in cultured primary cortical neurons [687]. The detection of oligomeric forms of α-syn was solely based on indirect evidence and the use of native and/or denaturing gel electrophoresis techniques [559]. Thus, it remains unknown to what extent the oligomers formed *in vitro* share similar characteristics and size with those formed *in vivo* or isolated from human brains or brains of transgenic animal models of synucleinopathies.

AIMS OF STUDY

The infectious prion protein can induce a self-perpetuating process that leads to amplification and spreading of pathological protein assemblies in prion diseases. The possibility that proteins causing neurodegeneration are all prions, and in particular that the β-sheet rich pathological α-synuclein may cross from the transplanted patients' own neurons into the grafted cells and induce a change in the structure of α-synuclein in Parkinson's disease has sparked great interest. On the other hand, studies on synthetic prions showed that recombinant (rec) prion protein (PrP) is refolded into infectious conformation *in vitro*; these synthetic PrP^{Sc} stimulate the conversion of PrP^{C} into nascent PrP^{Sc} and induces the accumulation of PrP^{Sc} that causes neurodegeneration *in vivo*.

My PhD work, by using defined biophysical and biochemical conditions *in vitro*, has focused on (i) developing methods for the pathological conversion of recPrP into PrP^{Sc} and (ii) establishing whether synthetic pathological agents of rec human α-syn amyloids are able to infect mouse and human normal neuronal cell lines *in vitro*, and wild-type mice *in vivo*. The pathological conversion process required only purified recombinant proteins and common chemicals. We generated putative infectious materials with different conformational structures. Moreover, we designed a novel build-in methodology for screening amyloid preparations to achieve putative infectious materials using amyloid-infected-cell culture assay. The two parts of the investigation are detailed as follows:

Part 1: *De novo* synthetic prion infection of neuronal cell lines and generation of diverse infectious prions

Prions are infectious proteins that possess multiple self-propagating structures. The information for strains and structural specific barriers appears to be contained exclusively in the folding of the pathological isoform, PrP^{Sc}. Many recent studies determined that *de novo* prion strains could be generated *in vitro* from the structural conversion of recPrP into amyloid structures. The aim was to elucidate the conformational diversity of pathological recPrP amyloids and their biological activities, as well as to gain novel insights in characterizing molecular events involved in mammalian prion conversion and propagation. To this end I generated putative infectious materials with different conformational structures. My methods for the prion-like conversion of recPrP required only purified recombinant full-length mouse (Mo) PrP and common chemicals. Neither infected brain extracts nor amplified PrP^{Sc} were used.

Part 2: Horizontal transmission of synthetic human α-synuclein prions in mice

Synucleinopathies are a group of neurodegenerative disorders characterized by fibrillary aggregates of α-syn in the cytoplasm of selective populations of neurons and glia. Using cellular and animal models for this class of maladies, recent studies have focused on the mechanism whereby fibrillary aggregates of α-syn form and spread among cells. In fact, it has been proposed that α-syn fibrillary aggregates may share peculiar molecular analogies with well-established proteinaceous infectious agents such as prions. Given the striking similarities between the pathological mechanisms of TSEs and synucleinopathies, a critical question is whether Parkinson's disease is transmissible and whether the synthetic α-syn amyloid forms

implicated may also behave as infectious agents. Based on these premises, I considered the possibility that recombinant human α-syn could acquire prion properties *in vitro* and *in vivo* after being infected in cell lines and wild-type mice, respectively, during passaging.

MATERIALS AND METHODS

Part 1: *De novo* synthetic prion infection of neuronal cell lines and the generation of diverse infectious prions

Expression and purification of recPrP

RecMoPrP(23-231) was expressed in *E. coli* Rosetta2(DE3) with pET11a(MoPrP23-231)-without His-tag. The transformed bacteria were grown in LB media using a Biostat B plus fermenter 2L vessel. Expression was induced with IPTG at a final concentration of 1mM. The cultures were harvested after 24 hours of induction, centrifuged (1500 x g, 30min, 4ºC) and resuspended in buffer A (25mMTris-HCl pH 8.0, 5mM EDTA, 1mM PMFS). After centrifugation, pellets were resuspended in buffer B (25mMTris-HCl, 5mM EDTA, 1mM phenylmethylsulphonylfluoride (PMSF), 0.5% Triton X-100). To disrupt bacterial cells, the solution was passed three times through the microfluidizer at 15000-18000 psi. The solution was centrifuged for 30min at 3400 x g and inclusion bodies were washed twice with buffer C (25mMTris-HCl, 5mM EDTA, 0.8% Triton X-100) and buffer D (25mMTris-HCl pH 8.0) and twice with double-distilled H_2O. Pellets containing MoPrP(23-231) protein were solubilized in 8M Gdn-HCl, shaken overnight at 37ºC and centrifuged (3400 x g, 30min). The solution was then brought to a buffer containing 6M Gdn-HCl, 20mMTris-HCl pH8.0, 500mM NaCl and loaded onto HisTrap FF crude column (GE Healthcare). The column was washed with buffer A (20mM Tris-HCl pH 8.0, 10mM Imidazole, 2M Gdn-HCl) and protein was eluted with linear imidazole gradient (20-500 mM imidazole in buffer A). Fractions containing MoPrP(23-231) protein were then loaded onto reverse phase column (Jupiter C4, 250x21.2mm, 300 A, Phenomenex). The column was washed with buffer A (0.1%TFA) and protein was eluted with a linear gradient from 0 to 95% acetonitrile in 0.1% TFA (buffer B). Fractions containing PrP protein were then lyophilized.

Amyloid preparations

RecMoPrP(23-231) was expressed and purified as described. All stock solutions for fibrilization were sterile, filtered through a 0.22µm filter prior to each assay in order to avoid the presence of contaminants. Lyophilized protein was dissolved in 6M Gdn-HCl at 10mg/mL or 8M Urea at 10mg/mL, aliquoted, and frozen at -80^{o}C. To form fibrils in the non-REDOX process, a solution of Gdn-HCl (concentrations are indicated in Table 7), 50mM buffer acetate pH 5.5 or PBS pH 7.5, NaCl (concentrations are indicated in Table 8) and 10 µm ThT was mixed before adding recPrP, which has a final concentration of 100 µg/mL or 200 µg/mL (indicated in Table 1). To form fibrils in the REDOX process as described (Fig. 24), after dissolving in 6M Gdn-HCl, the lyophilized protein was reduced by adding 100mM DTT at 37ºC for 1 hour. In case of conditions containing NaCl (as indicated in Table S2) this was added to the protein stock solution saturated level. The next steps were the same as those of the non-REDOX process described above. For fibrilization, a 3-mm glass bead (Sigma) was added to each well of a 96-well black plate with clear bottom (BD Falcon). The final volume fibrillization mixture was 200 µL in each well. The

plate was covered with sealing tape (Fisher Scientific) and shaken continuously at 37ºC using M5 fluorescence plate reader with auto mix capability (Spectramax M5 Molecular Devices). ThT fluorescence was measured with the same plate reader at 444/485 nm excitation/emission spectra every 5 min after 72 hours or 52 hours continuous shaking by bottom fluorescence reading. Each sample was measured in six independent replicate wells. Fibrils were collected by ultracentrifugation at 100,000 x g for 30 min to remove other soluble components before further characterizations.

Atomic Force Microscopy (AFM)

This method was employed in accordance with that described above [407,688]. Specimens were imaged with a Nanowizard-II BioAFM (JPK Instruments AG, Berlin, Germany, www.jpk.com) operating in dynamic mode and using non-contact Si cantilevers (NSG11, NT-MDT – Moscow, Russia, www.ntmdt.com or ARROW-NCR, Nano World-Neuchâtel, Switzerland, www.nanoworld.com) with tip radii of <7-10 nm, spring constants of 20-40 N/m, and resonance frequencies of 285-325 kHz. After fibrilization, 5-10µL samples were spread onto a freshly cleaved mica sheet and left to adhere for 10-20min. Samples were then washed with distilled H_2O and dried naturally. The images were acquired at line scan rates of 0.5-1 Hz at room temperature (RT). The AFM free oscillation amplitudes ranged from 25nm to 40nm, with characteristic set points ranging from 75% to 90%. AFM data were analyzed with Gwyddion (www.gwyddion.net).

Testing for disulfide bond interchain of fibrils from REDOX process

After fibrilizations, 1µg of protein samples was precipitated by ultracentrifugation at 100,000 x g for 30min, dissolved in non-reducing sample buffer (125 mM TrisHCl, pH 6.8, 4% SDS, 0.2% bromophenol blue, 20% glycerol) and separated in 10% non-reducing SDS-PAGE gels. For disulfide bond interchain test, 1µg of protein after precipitation by ultracentrifugation was treated with 2-β-mercaptoethanol at the last concentration of 150mM or incubated in 1mL 6M Gnd-HCl for 3 days, then treated with 150 mM 2-β-mercaptoethanol. These samples were centrifuged at 100,000 x g for 1 hour, resuspended in reducing loading buffer, boiled for 10min at 100°C and separated in 10% polyacrylamide gels. Western blotting was carried out and gels were subsequently transferred overnight onto Immobilon P PVDF membranes (Millipore). Membranes were blocked by 5% non-fat milk, incubated first with 1 µg/mL anti-PrPFab D18 and then with goat anti-human IgG F(ab)2 fragment conjugated with horseradish peroxidase (HRP). Blots were developed with the enhanced chemiluminescent system (ECL, Amersham Biosciences) and visualized on Hyperfilm (Amersham Biosciences).

Preparations of prion amyloid fibrils for cellular assays

Collection of amyloid fibrils from 96-well plates into 1.5 mL tubes was performed under sterile conditions. Samples were transfered first to eppendorf tubes then centrifuged at 100,000 x g for 30 min at 4°C in an ultracentrifuge (Beckman Coulter). The pellets were resuspended in sterile 1X PBS and then sonicated for 5 min prior to being added to cultured cell media.

Cell cultures

Mouse neuroblastoma N2a cells were cultured in minimal essential medium with Earle's salt (EMEM) supplemented with 10% FBS, 1% non-essential amino acids, 1% L-glutamax, 100 units/mL penicillin and 100 µg/mL streptomycin. Mouse hypothalamic GT1 cells and mouse hippocampal PrP-deficient HpL3-4 were cultured in Dulbecco's modified Eagle's medium (DMEM) supplemented with 10% fetal bovine serum (FBS), 100 units/mL penicillin and 100 µg/mL streptomycin. Cell cultures were cultivated in 10-cm plates and incubated at 37ºC in humidified 5% CO_2. Cells were split at ratio 1:10 for further cultivation when the confluence reached 95%.

Infecting N2a, GT1 and HpL 3-4 cell lines with amyloid fibrils

At the end of the fibrilization, after collection as describe above, 200µL of fibril solutions were resuspended in sterile 1X PBS and sonicated in a water-cooled cup-horn sonicator for 5min for preparation of fibrillar infections. Cells were seeded in tissue culture plates 1 day prior to infection and around 5% confluent on the day of the infection. After removing the media, cells were washed and changed once with fresh media. After adding fibrils into the media, cells were incubated for 6-7 days. Once confluence was reached, cells in the plate were washed with 1X PBS, trypsinized and transferred to another tissue culture plate. Cells were subjected to 1:10 split, which was counted as passage 1. Subsequently, cells were subjected to routine cell culture procedures for further passages. Cell lysates were collected at every passage. After the cell plates reached the confluence, they were washed with 1X PBS and lysed in 500 µL cell lysis buffer (10mMTris-HCl pH 8.0, 150mMNaCl, 5.0% NP40, 5.0% DOC). Total protein content of cell lysates was measured using bicinchoninic acid protein quantification kit (Pierce) and stored at -20^{o}C until analysis.

PK-resistant PrP detection by Western blotting in amyloid fibril-infected cell lysates

Fibril-infected cell lysates were collected at each passage. The accumulation of PK-resistant PrP was detected by proteinase K (PK) digestion followed by immunoblotting of lysated cells. Five hundred µL of lysis buffer (10 mM Tris-HCl pH 8.0, 150 mM NaCl, 0.5% nonidet P-40, 0.5% deoxycholic acid sodium salt) was added to each 10-cm cell plate and cell lysates were collected after centrifugation at 400 x g for 5 min in a bench microfuge (Eppendorf). The total protein content of samples was measured by means of bicinchoninic acid assay (BCA) (Pierce). Lysated cell samples were adjusted to 1mg/mL total protein; 2µg/mL PK (Invitrogen) was added

to reach the final volume of 0.5 mL. Following 1 hour incubation at 37ºC, digestion was stopped by adding PMSF at 2mM final concentration. Digestion products were precipitated by centrifugation at 100,000 x g for 1 hour at 4°C in an ultracentrifuge (Beckman Coulter), and resuspended in 2X SDS-PAGE loading buffer (125 mM Tris-HCl, pH 6.8, 10% 2-mercapethanol, 4% SDS, 0.2% bromophenol blue, 20% glycerol). For non-PK digested samples, 50 µg of cell lysates were used and 2X SDS-PAGE loading buffer was added in a 1:1 ratio. The samples were boiled for 10 min at 100°C, loaded onto a 12% Tris-Glycine SDS-PAGE gel, and transferred overnight onto Immobilon P PVDF membranes (Millipore). Membranes were blocked by 5% non-fat milk, incubated first with 1 µg/mL anti-PrPFab D18 or Clone P and then with goat anti-human IgG F(ab)2 fragment HRP-conjugated. Blots were developed with the enhanced chemiluminescent system (ECL, Amersham Biosciences) and visualized on Hyperfilm (Amersham Biosciences).

PK-resistant PrP detection by Western blotting in different amyloid preparations

One hundred microliters and 7 µL of samples after fibrilization were centrifuged at 100,000 x g for 30 min at 4°C (Beckman Coulter ultracentrifuge). Pellets were resuspended in the same volume of 1X PBS. One hundred microliters of samples were digested by 2 µg/mL or 20 µg/mL of PK in 500 µL total volume of 1X PBS for 1 hour at 37°C. The reaction was stopped with 2 mM PMSF and the PK-digested samples were centrifuged at 100,000 x g for 1 hour at 4°C (Beckman Coulter ultracentrifuge). Pellets were resuspended in 1X SDS-PAGE loading buffer. As non-PK digestion samples, 7 µL of fibril solutions in 1X PBS were added into 2X SDS-PAGE loading buffer in a 1:1 ratio. The samples were boiled for 10 min at 100°C, loaded onto a 12% Tris-Glycine SDS- PAGE gel, and transferred overnight onto Immobilon P PVDF membranes (Millipore). Membranes were blocked by 5% non-fat milk, incubated first with 1 µg/mL anti-PrPFab D18 and then with goat anti-human IgG F(ab)2 fragment HRP-conjugated. Blots were developed with the enhanced chemiluminescent system (ECL, Amersham Biosciences) and visualized on Hyperfilm (Amersham Biosciences).

Fluorescence immunostaining of prion amyloid fibril-infected cells

One million cells/mL of each cell line were cultured for 1 day in each well of a 24-well plate containing a 1.2 cm coverslip and appropriate culture medium. Medium was removed and cells were washed with 1X PBS. Cells were fixed for 30 min in 4% PFA (paraformaldehyde in 1X PBS) at RT then washed twice for 15 min with 1X PBS. Fixed cells were blocked in blocking buffer (5% normal rabbit serum (NRS) in 1X PBS + 0.3% Triton), exposed to anti-PrP monoclonal antibody D18 or clone P (10 µg/mL final concentration) for 2 hours. Primary antibodies were made up in 1% blocking solution and PBS. Cells were washed once with 1X PBS for 15 min. The secondary antibody used is goat anti-human Alexa 488 at 1:500 dilution in 1% blocking buffer and 1X PBS. Secondary antibodies were incubated for 1 hour at RT. Finally, cells were washed twice for 15min with 1X PBS. The coverslips were taken out and dried

naturally. Coverslips were mounted in DAPI and subsequently placed on glass slides and stored at 4ºC for confocal fluorescence microscopy.

Fluorescence immunostaining of prions in cells

PrP^{Sc} was revealed specifically by PK digestion and Gdn-HCl treatment to remove PrP^{C} and expose PrP^{Sc} as described [305][335]. Briefly, GT1, amyloid-infected GT1 and ScGT1, N2a, amyloid-infected N2a and ScN2a cells were seeded to semi-confluence on glass coverslips for 24h. The cells were fixed with 4% paraformaldehyde, freshly prepared, and simultaneously permeabilized with 0.1% of Triton-X 100 for 1h at RT. Denaturation with 6M Gnd-HCl for 10 minutes followed. After blocking with 1% bovine serum albumin (BSA) for 30 min at RT, the cells were incubated with 0.025% of thioflavin S. After washing several times with 80% ethanol and water, the primary antibody incubation followed (monoclonal antibody mAb SAF 61, 1:500) diluted in 1% of blocking buffer. After appropriate washing with PBS, fluorescently labeled secondary antibody incubation followed (Goat anti-mouse – Alexa 594) for 1h at RT. For proteinase K digestion, ScGT1, GT1, amyloid-infected GT1, ScN2a, amyloid-infected N2a and N2a cells were grown on coverslips pretreated with poly-L-lysine (0.2mg/ml) for 1h at RT. Twenty-four hours later cells were fixed and permeabilized with 8% paraformaldehyde and 0.1% of Triton-X 100 for 45 min at RT. Cells were incubated with PK (20 µg/ml) for 15 min at 37°C. Digestion was stopped with 2mM phenylmethylsulphonylfluoride (PMSF, Sigma) for 15 min at RT. Cells were denatured with 6M GndHCl for 10 min. After blocking with 1% BSA for 30 min at RT, cells were incubated with primary and secondary Abs which were diluted in 1% BSA for 30 min at 37°C.

PMCA - In collaboration with Dr. Olivier Andréoletti's group, INRA-ENVT, Interactions Hôtes Agents Pathogènes, Toulouse, France

- PMCA Substrate

Transgenic mice lines that express murine PrP (Tga20) were used to prepare the substrate [689]. Mice were euthanized by CO_2 inhalation and perfused (intra-cardiac) with PBS pH 7.4/EDTA 5mM (40-60 mL per mouse). The brains were then harvested and snap frozen in liquid nitrogen. Ten percent brain homogenate was prepared (disposable UltraTurax – 3 min) in 4°C PBS pH 7-7.65 + 0.1% Triton X100+ 150 mM NaCl (10% w/v). Substrate was then aliquoted and stored at -80°C.

- PMCA reaction and controls

Desired amount of cell pellets were resuspended in 200µL of 4°C PBS pH 7.4 + 150mM NaCl+ 0.1 TRITON X100 and homogenized at high speed (Precess 48, Bertin, France). Samples were then spun down 15,000g for 20 seconds and then stored at -80°C or used fresh. Seven µL of the seed were mixed with 63µL of substrate in 0.2mL ultrathin wall PCR tube that contained eight to fourteen 1mm diameter silica/zirconium beads (Biospec Cat. No.11079110z).

Amplification was performed in a modified Misonix 4000 cup horn (see below), using water recirculation system (39.5°C). The reactions tubes were then submitted to 96 cycles of 30 seconds sonication (power 70%) followed by 29 minutes 30 seconds incubation period. After the PMCA round, 7µL of the reaction product was added to a new tube containing fresh substrate and new round (96 cycles) was performed. In order to limit cross contamination risks that are linked to serial PMCA, the procedures employed are similar to those in place for nested PCR. In particular, PMCA substrates, amplification and handling of amplified products were performed in different rooms using dedicated material. On each PMCA run, a standard 1/10 dilution series (ovine BSE, 10% brain homogenate, 10-5 to 10-9 diluted) was included to check the amplification performance. A large batch of these controls was prepared and stored at -80°C as single use aliquots. Similarly unseeded controls (1 unseeded control for 5 seeded reactions) were included on each run. Over a total of 62 PMCA runs were performed in the framework of this study. A contamination of some negative controls reactions (false positive) was observed in 4 runs. In two of these runs, contamination was a likely consequence of a fault in the tube caps (obvious loss of reaction mixture in the tube). In two other cases the source of the contamination remained undetermined. When a false positive was observed, the complete PMCA runs were discarded and restarted from the first amplification round.

- Misonix 4000 x Sonicator modifications

Modifications consisted in the enlargement (5mm inner diameter) of existing holes and creation of new holes for water recirculation in crown surrounding the plate horn. These holes allowed a closed water circulation system in the horn delivering over 1.5 liter of water per minute. Permanent water re-circulation was ensured by a peristaltic pump (Watson Marlow 520U) and deflectors were added to the horn to avoid water projection. The water circuit consisted of a 10 meters flexible tygon tube (diameter 9.2 mm) placed in a water bath. This system allowed the temperature of the water in the horn to return to its nominal value (39.5°C) within 20-40 seconds following the sonication burst and also maintained the water level in the horn at a constant level. The reaction tubes were positioned at a height of 2mm above the horn plate and the water level in the horn was adjusted (before each PMCA round) to be at the same level as the reaction mixture in the tubes. Finally the acoustic protection box containing the sonicator horn was placed in an environment (temperature regulated room or incubator) maintaining the air temperature between 35°C and 40°C (limitation of condensation).

- Abnormal PrP Western blotting

PK resistant abnormal PrP extraction (PrPres) and Western blot were performed as previously described [690], using a commercial extraction kit (Biorad, France). For PMCA products the equivalent of 20µL of reactions were loaded onto each lane. PrP immunodetection was performed using either Sha31 monoclonal antibody (0,06 µg per mL, epitope: YEDRYYRE, amino acid 145-152) or 12B2 (4 µg/mL) (epitope WGQGG, amino acid sequences 89-93). Both Sha31 and 12B2 antibodies have been described in previous studies to bind the mouse, ovine, bovine, porcine and human PrP^{C} and PrPres in WB [691][692][693][694][695].

Measurement of cell viability

Cell viability was examined based on mitochondrial activity, measured by MTT assay. GT1 and N2a cells were maintained in DMEM and EMEM, respectively, and supplemented with FBS and antibiotics. After 1 day of incubation, media were aspirated from a confluent 10-cm plate, and cells were detached by adding 1 mL of 1X trypsin-EDTA solution. Media were added, and cell density determined using a haemacytometer. Cell density was adjusted to 2.5×10^5 cells/mL with media. A 96-well, tissue culture-treated, clear bottom, black plate (Costar) wetted with 96 µL of media was incubated at 37°C, prior to use. One hundred microliters of cell suspension was added to each well and cells were allowed to settle for 2 hours, before adding prion amyloid fibrils. Four microliters of prion fibril solutions from different amyloid preparations in 1X PBS was added to each well (final concentration 2µg/mL of PrP), and plates were incubated at 37°C in 5% CO_2. After incubating for 5 days, media were aspirated and cells were washed twice with 200 µL of 1X PBS. After treatment with different amyloid samples, cells were further incubated for 3 hours in fresh media with a final concentration of 0.5 mg/mL MTT. DMSO was added to release the insoluble purple substrates converted by the active mitochondrial dehydrogenases in the surviving cells. After shaking 30min for solubilization, the fluorescence emission intensity was measured using a SpectraMax M5 fluorescence plate reader, with 570/690 nm excitation/emission ratio. [696].

Part 2: Horizontal transmission of synthetic human α-synuclein prions in mice

Cell lines

Mouse hippocampal neuronal cell line, Hpl 3-4 [697][698], mouse astroglial GpL3 cell line [699], and mouse neuronal NpL2 immortalized cell line [700] were all established from the brain of ZrchI*Prnp*$^{0/0}$mice kindly provided by Dr. T. Onodera (Department of Molecular Immunology, School of Agricultural and Life Sciences, University of Tokyo, Japan). Mouse hypothalamic GT1 cell line established from gonadotropin hormone releasing-hormone neurons immortalized by genetically targeted tumorigenesis in transgenic mice [701] and mouse neuroblastoma N2a cell line derived from the spontaneous mouse C1300 neuroblastoma by Klebe and Ruddle (1969) [702] are often used in prion biology and were kindly provided by Dr. Stanley B. Prusiner. The SH-SY5Y cell line is a thrice-cloned sub-line of SK-N-SH cells, which were originally established from a bone marrow biopsy of a neuroblastoma patient with sympathetic adrenergic ganglial origin [703]. HpL3-4, GpL3, NpL2 and GT1 cells were seeded in 10-cm plates containing 10 mL of Dulbecco's modified Eagle's medium (DMEM) culture media, supplemented with 10% fetal bovine serum (FBS) and 1% penicillin-streptomycin. N2a cells were cultivated in 10-cm plates, containing 10 mL of minimal essential medium with Earle's salt (EMEM) culture media, supplemented with 10% FBS, 1% non-essential amino acids, 1% L-glutamax, 1% penicillin-streptomycin. SH-SY5Y normal cells were cultivated in 10-cm plates, containing 10 mL of minimal EMEM: Ham F12 (1:1) culture media, supplemented with 15% FBS, 1% non-essential

amino acids, 0.5% L-glutamax, 1% penicillin-streptomycin and 1% G-418 (only for SH-SY5Y wild-type cells transfected for over-expressing α-syn). The cells were grown at 37°C in 5% CO_2 to 95% confluence for 1 week before splitting at 1:10 for further cultivation.

Expression and purification of recombinant human α-syn

Expression and purification of recombinant human α-syn were performed in accordance with the method previously described [704]. Briefly, cloning and expression of human α-syn gene were performed in pET11a vector using BL21 (DE3) *E. coli* strain. Expression of α-syn was obtained by growing cells in Luria-Bertani broth medium with 100 mg/mL ampicillin at 37°C until an $O.D._{600}$ of about 0.6, followed by induction with 0.6 mM isopropyl β-D-thiogalactoside (IPTG) for 5 hours. The protein was purified according to the method of Huang *et al.* [705].

α-Syn amyloid preparations

All solutions were sterilized by filtration through a 0.22 μm filter prior to each assay run. Reactions were prepared in a 96-well black plate (BD Falcon), and each well contained 200 μL of reaction solution (1.5 mg/mL recombinant human α-syn, 100 mM NaCl, 10 μM thioflavin T (ThT) in 20 mM Tris-HCl pH 7.4). Each sample analysis was performed in fifteen replicates. Each well contained one 3-mm glass bead (Sigma). The plate was covered with sealing tape (Fisher Scientific) and incubated at 37°C under continuous shaking, and read on SpectraMax M5 fluorescence plate reader (Molecular Devices) by top fluorescence reading every 5 min at excitation of 444 nm and emission of 485 nm.

AFM analysis

AFM analysis was performed in accordance with the method previously described [704]. Three to five μL of fibril solution was deposited onto a freshly cleaved piece of mica and left to adhere for 30 min. Samples were then washed with distilled water and blow-dried under a flow of nitrogen. Images were collected at a line scan rate of 0.5-2 Hz in ambient conditions. The AFM free oscillation amplitudes were ranging from 25 nm to 40 nm, with characteristic set points ranging from 75% to 90% of these free oscillation amplitudes. AFM data were analyzed with Gwyddion (gwyddion.net) and SPIPTM (www.imagemet.com).

α-Syn amyloid solution for cell Infection

α-Syn amyloid solution from 96-well plate into 1.5 mL Eppendorf tube was collected under sterile conditions. The solution was centrifuged at 100,000 g for 30 min at 4°C in an ultracentrifuge (Beckman Coulter). Pellets were resuspended in 1X PBS and then sonicated (Branson 2510) for 5 min prior to adding to cultured cell plate.

α-Syn fibril infection into cell lines

Three hundred μg of α-syn amyloids was added to HpL3-4, NpL2, GpL3, GT1, N2a and SH-SY5Y cell plates (10 cm-plate) and exposed in the cell culture media for 7 days before the next splitting and media change. Cells were split and maintained for six additional passages. Cell lysates were collected at each passage for Western blotting and immunofluorescence studies.

For immunofluorescence of amyloids internalization, cells were cultured in 12 wells plate with coverslips, 30 µg of α-syn amyloids was added into cell culture media and incubated for 7 days.

α-Syn aggregates detection and analysis in infected cells by Western blot

The total protein content of samples was measured by bicinchoninic acid assay (BCA) (Pierce). Fifty µg of Cell lysates was used and 5X loading buffer was added in a 1:5 ratio. The samples were boiled for 5 min at 100°C, loaded onto a 10% Tris-Glycine SDS-PAGE gel, and transferred overnight onto Immobilon P PVDF membranes (Millipore). Membranes were blocked by 5% nonfat milk, incubated with 0.4 µg/mL rabbit polyclonal anti-α-syn antibody (Santa Cruz) followed by incubation with goat anti-rabbit IgG F(ab)2 fragment conjugated with horseradish peroxidase. Blots were developed with the enhanced chemiluminescent system (ECL, Amersham Biosciences) and visualized on Hyperfilm (Amersham Biosciences). For analysis of α-syn aggregation in cell samples, cells were scraped in TBS buffer containing 1% Triton X100, protease cocktail inhibitors and phosphatase inhibitor. After sonication (Sonicrep 150) with 10 amplitude microns for 3 times (30 seconds of sonication and 30 seconds intermediate stop) cells were centrifuged at 2000 RPM for 5 min then the protein was quantified. Fifty µg cellular protein of samples was centrifuged at 100,000 g for 30 min. Supernatant (in term S-TX) was collected and the pellets were resuspended in 2% SDS. Samples in SDS 2% were centrifuged, supernatant (in term S) and pellet (in term P). All the fractions were added to loading buffer 5X in ratio 1:5 and prepared similarly for Western blotting.

Immunocytochemistry and ThS staining of α-syn fibril-infected cells

Cells on coverslips were washed with PBS and fixed with 4% paraformaldehyde, then washed twice, 15 min/time with PBS and blocked in blocking buffer (5% normal goat serum in PBS + 0.3% Triton) for 1 hour. For Thioflavin S (ThS) staining, fixed cells were incubated with 0.025% of the fluorophore (Sigma) for 8 min and washed three times with 80% ethanol for 5 min each time, before the antibody incubations. Fluorescence immunocytochemistry was performed using primary antibodies and secondary antibodies listed in Table 6. Primary antibodies were made up in 1% blocking buffer and PBS. After incubation, the cells were washed 5 times for 5 min/time with PBS then secondary antibodies were incubated in 1% blocking buffer and PBS for 45 min. Finally, cells were washed 5 times, 5 min/time with PBS, and counterstained with DAPI to reveal nuclei, then mounted in Vectashield Mounting Medium. Cell coverslips were stored at 4°C for confocal fluorescence microscopy. Images were obtained with a Leica SP5 confocal laser-scanning microscope.

Table 6. Antibodies used in this study

Antibody	Source	Host	Dilution (IF)	Dilution (WB)	Dilution ICC)	Exposed time
α-synuclein (C-20)-R	Santa Cruz	Rabbit	1:500	1:500		4 hours
α-synuclein {LB 509}	Abcam	Mouse	1:1,000	1:1,000		2 hours
α-synuclein (D37A6)	Cell Signaling Technology	Rabbit	1:100	1:500		Overnight
α-synuclein (clone 4D6)	Signet	Mouse			1:1,000 (o/n)	
α-synuclein (phospho S129)	Abcam	Rabbit	1:500	1:500	1:300 (o/n)	4 hours
Glial fibrillary acidic protein (GFAP)	DakoCytomation	Rabbit			1:800 (o/n)	
Iba1	Abcam	Goat			1:2,000 (o/n)	
Tyrosine Hydroxylase	Santa Cruz	Rabbit			1:800 (o/n)	
Monoclonal ANTI-FLAG® M2	Sigma	Mouse	1:1,000	1:10,000	1:300 (o/n)	2 hours
Alexa 488 anti-mouse		Goat	1:500		1:800 (o/n)	45 min
Alexa 488 anti-rabbit		Goat	1:500		1:2,000 (o/n)	45 min
Alexa 594 anti-mouse		Goat	1:500		1:800 (o/n)	45 min
Alexa 594 anti-rabbit		Goat	1:500			45 min

Immunofluorescence

All dopaminergic neuroblastoma SH-SY5Y cells were grown on ibidi dishes (Biovalley) for microscopy. After washing in PBS, cells were fixed using 4% (w/v) paraformaldehyde (Sigma) in PBS for 15 min and permeabilized with 0.01% Triton X-100 (Sigma) in PBS for 3 min, washed and blocked in 2% Bovine serum albumin (Sigma) in PBS for 20 minutes. Cells were immunostained using anti-α-syn (Santa Cruz Biotechnology, INC) and anti-phospho S129 α-syn (Abcam) followed by secondary antibody coupled to Alexa 488 (Invitrogen). Cells were mounted in Aqua Poly/Mount (Polysciences) and pictures were acquired using white field Axiovision microscope (Zeiss) with a 63 x objective. Quantification experiments were carried out independently at least three times; more than 150 cells were counted for each condition. Individual differences were assessed using individual student's t-tests. Data are shown as mean + standard error of the mean (SEM).

Animal inoculations - In collaboration with Prof. Fabrizio Tagliavini's group, NeuroPrion - Istituto Nazionale Neurologico Carlo Besta, Milan, Italy

- First passage

All surgical procedures were performed under sterile conditions. Six week-old CD1 mice (n=7) were anesthetized with tribromoethanol (100 µL/10 g) and placed in a stereotaxic instrument on a mouse and neonatal rat adaptor. Ten µL of (i) synthetic human α-syn monomers, (ii) synthetic human α-syn oligomers, (iii) synthetic human α-syn short fibers, (iv) synthetic human α-syn long fibers and (v) PBS was inoculated in the right *substantia nigra pars compacta* (SNpc) following these stereotaxical coordinates (- 3.28 caudal; + 1.5 lateral; 4.5 depth). Uninjected animals were used as negative controls.

- Second passage

Thirty µL of (i) α-syn brain homogenate, (ii) mock brain homogenate and (iii) PBS was inoculated in the right *striatum* following these stereotaxical coordinates (- 1 caudal; + 2 lateral; 3.5 depth). Uninjected animals were used as negative controls.

Brain homogenization

Ten percent brain homogenate (w/v) was prepared from a symptomatic animal previously injected with short fibers of synthetic human α-syn. Ten percent mock homogenate (w/v) was obtained from healthy CD1 mouse brain. Each homogenate was prepared using saline solution (NaCl, B. Braun 0.9%) with the addition of protease inhibitors (Roche).

Behavior test

Animal behavior analysis was performed in all groups from 7 dpi (passage 1) and 63 dpi (passage 2) until mice were sacrificed. All tests were performed at the same time point between 15:00 and 17:00 CET. The general aspect and behavioral indicators of PD-mimetic symptoms (hypokinesia, muscle rigidity and equilibrium) were evaluated. First, general aspect and normal

behavior of mice were assessed by scoring based on the following scoring scale: General aspect, (0)=normal; (1)=medium; (2)=bad, (point out symptoms); (3)=pathognomonic. Normal behavior, (0)=curiosity; (1)=faint alterations, less curiosity; (2)=less movement but alert, isolated, no curiosity; (3)=vocalization, abnormal behaviors. Secondly, motor deficits were assessed using "open field" spontaneous locomotion activity by scoring animals in walking on the open field, orientation and curiosity: (0)=normal walking; (1)=faint problems in walking; (2)=severe problems in walking; (3)=ataxia. Thirdly, muscle rigidity and weakness, and equilibrium were evaluated and scored using a "grid" test based on the animal's ability to hang on the grid: walking on a grid, (0)=good hand-grip and agile; (1)=good hand-grip but uncertain; (2)=good hand-grip but motionless; (3)=bad hand-grip but walk; (4)=bad hand-grip and motionless; (5)=no hand-grip. Equilibrium: (0)=agile, (1)=good hand-grip, faint uncertain; (2)=problems in moving; (3)=clinging but motionless; (4)=clinging but falling down with posterior limbs; (5)=falling down from inclined or inverted grid.

Histological analysis

Brains were fixed in Alcolin (Diapath), dehydrated and embedded in paraplast. Seven-μm thick serial sections were stained with haematoxylin-eosin (H&E) or immunostained with antibodies against: α-syn (monoclonal, clone 4D6, Signet), phosphorylated α-syn (rabbit polyclonal, Abcam), glial fibrillary acidic protein (rabbit polyclonal, GFAP, DakoCytomation) as marker of astrocytes, Iba1 (goat polyclonal, Abcam) as marker of activated microglial cells, tyrosine hydroxylase (rabbit polyclonal, Santa Cruz Biotechnology) as marker of dopaminergic neurons. To test for the presence of protease-resistant α-syn, some sections were post-fixed in formalin and treated for 5 min with proteinase K at different concentrations (5-30 μg/ml in 0.3% Brij-35). Immunoreactions were visualized using anti-rabbit or anti-goat biotinylated secondary antibody (1:100, Vector) and streptavidin-peroxidase complex (1:200, Vector). For mouse monoclonal antibodies, a specific streptavidin-biotin system (Animal Research Kit and Peroxidase, DakoCytomation) was applied. 3-3'-diaminobenzidine (DAB, DakoCytomation) was the chromogen used.

Preparation of brain homogenates (BH) for biochemical analysis

To prepare 10% (w/v) brain homogenates, nine volumes of ice-cold PBS were added to brain tissue in a 15-ml tube. Brain tissue was homogenized on ice using micro homogenizer (Ultra-Turrax T8, Ika Labortechnik). The sample was centrifuged at 500 x g for 5 min at room temperature to clarify the samples. The supernatant was collected, the pellet was discarded and aliquots were frozen at -80°C until use.

Amyloid seeding assay (ASA) with brain homogenates

Based on similar monitoring of the kinetics of *in vitro* amyloid formation in human α-syn amyloid preparations (shown above), ASA was performed with BH containing mouse α-syn prions as seeding factors in amyloid formation of recombinant mouse α-syn (recMo-α-syn). 0.17% of BH was added to each well. As control, we used buffer only, buffer plus seeds without recMo-α-syn; also BH of non-injected mice and PBS-infected mice were added similarly. Each sample analysis was performed in five replicates.

RESULTS AND DISCUSSION

Part 1: *De novo* synthetic prion infection of neuronal cell lines and the generation of diverse infectious prions

1.1. Objectives

- Generating variant structural conformations of infectious synthetic prions from recombinant prion protein.

- Creating a novel cell culture assay for screening infectivity of amyloid preparations.

- Elucidating the conformational diversity of pathological recPrP amyloids and their biological activities, as well as gaining novel insights in characterizing molecular events involved in mammalian prions conversion and propagation.

1.2. Specific background

For most proteins, if not all, the same amino acid sequence can encipher numerous conformationally different amyloid states [707][708]. The ability of PrP to acquire multiple self-propagating structures can thus explain the formation of multiple prion strains within the same host [50]. The information for prions is enciphered in these structures by a distinct conformation of the pathological isoform [350,351,373].

Recently, synthetic prions were produced via *in vitro* induction of misfolding and aggregation of bacterially expressed recPrP [214]. This work clearly indicates that PrP^{Sc} is the sole component of the infectious agent, which propagates by converting PrP into various misfolded forms [214][373][228]. These first synthetic prions were produced injecting amyloid fibrils of recMoPrP residues 89-230 (MoPrP(89-230)) in transgenic (Tg) mice carrying the homologous sequence. This endeavor has opened new avenues in the structural characterization of infectious prions [214]. An array of recPrP amyloids with varying conformation stability was produced, showing a direct relationship between stability and incubation times of prion strains. The conformational stabilities of the new synthetic prion strains and their incubation periods seem to be dictated by the properties of the amyloid preparations from which they were generated [228]. Although lacking both glycolsylation and the GPI anchor, secondary and tertiary structures of refolded recPrP appear to be identical to those of brain-derived PrP^{C} [167]. Remarkably, using recPrP to generate different amyloid preparations can induce the production of prions within the brains of the Tg mice harboring new strains with novel neuropathological and biochemical features [214][373][228]. This approach provided a useful tool to further investigate the functional/structural relationships of mammalian prions.

The crystal structure of rec human PrP has revealed a possible mechanism for oligomerization in which the three-dimensional swapping of the C-terminus helix 3 and the re-arrangement of the disulfide bond result in the formation of a dimer [184][183]. These data have suggested a possible role for a sulfhydryl-disulfide exchange reaction during the conversion of PrP^{C} to PrP^{Sc}. Moreover, this mechanism has been recapitulated *in vitro* by seeded conversion of rec hamster

PrP(90-231) truncated form with His-tag to a disulfide-bonded oligomer by a reduction-oxidation (REDOX) process [325].

We therefore established two different experimental procedures for amyloid preparations: (i) REDOX process, and (ii) non-REDOX process, using rec full-length MoPrP residue 23 to 231 (MoPrP(23-231)). Our methods for the prion-like conversion of PrP required only purified rec full-length MoPrP and common chemicals. Neither prion-infected brain extracts, nor amplified exogenous PrP^{Sc} were used. In both processes, recMoPrP(23-231) converted to conformational structures of fibrils without any seeded factor. The fibrils generated by the REDOX process most likely contained intermolecular disulfide bridge structures. In addition, the recMoPrP(23-231) amyloid preparations subjected to the REDOX and non-REDOX *in vitro* processes exhibited different morphological and biochemical prion-like characteristics.

Bioassay in animals has been the most commonly used method for assessing prion infectivity *in vivo*. However, employing animal models in synthetic prion studies has been known as an expensive and time-consuming method for initial screening of putative infectious materials. As an alternative procedure, cell-culture models are among the most powerful and useful experimental tools to study the biological properties of PrP at the molecular and cellular levels, as well as to investigate the events controlling the conversion of PrP^{C} to PrP abnormal forms. Furthermore, cell-culture systems may contribute to determine the cellular factors governing prion propagation. Two cellular models have been widely employed in prion biology for *in vitro* studies of infectivity*:* (i) the murine neuroblastoma Neuro2a (N2a) and (ii) hypothalamic-derived GT1 cell lines [709].

1.3. Results

To generate recPrP amyloids with different conformations, we systematically altered the conditions for their formation, including denaturant concentrations, pH and buffer composition (Table 8 and Table 9). The mechanism of amyloid formation determines significantly the amyloid structure of recPrP. The protein has been known to convert to different types of amyloid and some may be induced with the formation of intermolecular disulfide bonds leading to domain-swapping [710][711]. These alternative structures showed the coexistence of different molecular forms of PrP with the capacity of self-propagating prions [325]. In our experiments, we started from different states of recMoPrP(23-231) using either REDOX or non-REDOX processes. This resulted in different amyloid preparations in which the monomeric recMoPrP(23-231) followed different pathways for more stable free energy states. We induced the REDOX process by reducing disulfide bonds of recMoPrP(23-231) at high concentration of reducing agent in the presence of 6M Gdn-HCl and with or without the addition of NaCl. The concentration of all these components and of the protein was subsequently decreased by means of direct dilution to reach the final concentrations for fibrilization reactions (Fig. 24). This process differs from the earlier protocol reported to convert PrP *in vitro* [325], although sharing the same mechanism [710][711]. In order to study the converted ability and folding behaviors of recMoPrP(23-231), we analyzed the kinetics of purified recMoPrP(23-231) conversion into β-sheet-rich forms under different defined biophysical and biochemical conditions (Table 8 and Table 9). To monitor the amyloid formations, we used a thioflavin T (ThT)-binding assay [712,713]. Kinetic curves presented a sigmoidal shape, typically denoting an increased content

of β-sheet structures, as well as enhanced aggregation of monomeric recPrP (Fig. 25A). These sigmoidal curves highlighted a lag phase followed by rapid accumulation of fibrils (Fig. 25B and Fig. 33). The quantitative analysis of the lag phase was carried out by estimating the increase in ThT fluorescence intensity [407]. The end of the lag phase coincides with the point when ThT fluorescence intensity started to increase. The four main amyloids described in this part (amyloids #4, #19, #28, #32) were prepared under different conditions, including denaturant concentrations ranging from 1M to 4M of Gdn-HCl, and buffers at various pH values (see "Materials and Methods").

The maximum ThT fluorescence intensities exhibited a wide range between the two amyloid preparation processes. In the non-REDOX process, the maximum intensities are higher than those of the REDOX process (Fig. 25A). At neutral pH, the lag phases for aggregation processes of recMoPrP(23-231) are shorter in comparison with acidic pH 5 (Fig. 33). The shortest lag phase and most rapid production of amyloid were observed at pH 7.4 (Fig. 33) ($p<0.05$, $n=12$). No fibrils were found at pH 3.5 after at least 72 hours of fibrilization (data not shown). Interestingly, the fibrilization showed that lag phases vary in the presence of 2M Gdn-HCl between different conditions (amyloids #6, #14, #19 in non-REDOX process and amyloids #25, #26, #33, #34 in REDOX process) and also under the same conditions, which were indicated with high error bar values (Fig. 33). These data suggest that at different concentrations of Gdn-HCl, which is used as chaotropic agent for improving the yields and shorten the lag phase of aggregation [410], monomeric recMoPrP(23-231) explores many states of accessible free energies. However, based on the positive increase of ThT intensities, no further conversion was detected for up to 72 hours of fibrilization of amyloid preparations #1, #2, #3, #13, #21, #22, #35, #36, #37, #38 (data not shown). At denaturant concentration less than 1M, production of amyloids was observed only at pH 7.5 in the REDOX process, whereas no amyloid form was found after fibrilizations at pH 5.0. Full-length PrP tends to generate most amyloidal structures at neutral pH.

Differences in kinetic traces and maximum intensity values (Fig. 25 and Fig. 33) were also highlighted in terms of morphology, as revealed by atomic force microscopy (AFM) (Fig. 26 and Fig. 34A).

Therefore, to gain further insights into the aggregated morphology of the end products, we studied the aggregated topology of all recMoPrP(23-231) amyloid preparations by AFM. The recMoPrP(23-231) aggregation products were imaged at two end point times of fibrilization, i.e. 52 hours (Fig. 31B) and 72 hours (Fig. 26 and Fig. 34A). AFM scans of mica surfaces treated with different amyloid preparations showed that recMoPrP(23-231) aggregated after 72 hours and clearly revealed marked morphological differences. The morphology-dependence of the fibrilizations was observed at different concentrations of denaturant (Fig. 34B). At 1M Gdn-HCl (amyloids #20, #32), 3M Gdn-HCl with NaCl (amyloid #27), 4M Gdn-HCl (amyloids #4, #30) and 4M Gdn-HCl with NaCl (amyloid #29) in both REDOX and non-REDOX processes, the AFM analyses displayed a relatively homogenous population of spherical particles (β-oligomers) [403] and very short fibrils (approximately less than 0.5 μm) (Fig. 26 and Fig. 34A). In both processes, at 2M Gdn-HCl (amyloids #6, #14, #19, #26, #34), 2M Gdn-HCl with NaCl (amyloids #25, #33), and 3M Gdn-HCl (amyloids #5, #18, #28) of denaturant concentrations, recMoPrP(23-231) was

converted to amyloid forms. These were visualized by AFM as fibrils, ranging from very short to longer and more mature fibrils. The major fibrillar subtypes were straight (amyloids #18, #34), slightly curvy ribbons (amyloids #5, #25, #28, #33) or rod-shaped fibrils (amyloids #6, #11, #14, #19, #26) (Fig. 26 and Fig. 34A). These results are all in agreement with earlier studies [341]. In some instances amyloid morphology was not clear (amyloid #12, #31). In order to ascertain whether these were true amyloids, further experiments were carried out to test their capability of seeding amyloid formation.

In our amyloid morphology analyses, different amyloid preparations of recMoPrP(23-231) showed aggregate clusters of different heights (Table 7 and Table 10), which in turn were comprised of unit steps of varying heights (Fig. 26B). These were revealed by aggregated feature height profiles data. Indeed, 3-D views and height distribution (Fig. 26C) revealed structures with different topologies from different amyloid preparations.

The analyses of both AFM and kinetics data showed that different amyloid preparations in which pH, denaturing conditions, ionic strength and REDOX processes were defined, reflect differences in aggregation pathways and morphology of recMoPrP(23-231) end products.

Our methods for the conversion of PrP required only purified recPrP and common chemicals. Neither prion-infected brain extracts nor PrP^{Sc} were used. As spontaneous air re-oxidation occurs in the REDOX amyloid preparation process, the disulfide bonds rearrange, changing from monomeric intramolecular PrP form to intermolecular multimeric PrP. In order to prove that the converted amyloid forms under different amyloid preparations from the REDOX process were oligomerized through intermolecular disulfide bonds, we checked for the presence of these structures. In comparison with non-reducing experiments, we used a high concentration of reducing agent and reduced electrophoresis. Western blottings showed that converted amyloid forms from both processes had apparent monomeric, dimeric molecular masses and higher, more complex multimeric forms under non-reducing treatments (Fig. 4A). After treatment with the reducing agents to disrupt all disulfide bridges, the REDOX-converted PrP forms showed a significant decrease in dimeric and trimeric structures. Higher molecular weight forms were also observed (Fig. 4B, REDOX amyloids). In amyloid preparations established following the REDOX process — which includes the swapping of domains and the rearrangement of intra and intermolecular disulfide bridges in PrP molecules — the conversions require both non-covalent and covalent bonds to break up. Moreover, induced reduction occurs optimally in denaturing condition. Therefore, after incubating the REDOX-converted forms with high concentration of denaturant (Gdn-HCl 6M) for three days, and subsequently treating them with reducing agent, the amyloid forms were disassembled. This was indicated by the disappearance of PrP complexes with structures other than the monomeric form (Fig. 27C, REDOX amyloids). In contrast, recMoPrP(23-231) converted into the amyloid forms in the non-REDOX process — in which the oxidized PrP was diluted to reach the final concentrations in fibrilization buffer — showed greater stability of dimeric and higher structures after treatment with reducing agent. A high concentration of denaturant was also observed (Fig. 27B and Fig. 27C, non-REDOX amyloids). Besides the differences in morphology and kinetics formation, our intermolecular disulfide bridge tests showed that REDOX amyloids are most likely to contain intermolecular disulfide bridge conformation structures [325,710,711].

So far, PK-resistance has been used to distinguish PrP^{C} from PrP^{Sc}, although many studies showed the existence of PK-sensitive PrP^{Sc}. We treated amyloid fibrils at PK/recMoPrP(23-231) ratios of 1:10 and under standard conditions used for detecting PrP^{Sc} in brain homogenates (20 µg/mL PK, at 37°C for 1 hour) at the ratio of 1:1. This process aimed at determining whether: (i) our abnormal isoforms of PrP generated *in vitro* are resistant to PK digestion, and (ii) they have a PK-resistant core resembling that of PrP^{Sc} subjected to PK treatment. Both the β-oligomers and the amyloid fibrils in some amyloid preparations showed PK-resistance. Interestingly, in both processes, most amyloid preparations in PBS pH 7.4 appeared more sensitive to PK digestion than those in acidic conditions, although digestion patterns were undistinguishable (Fig. 28 and Fig. 35). At ratio 1:10, the PK-resistant bands of non-REDOX amyloid digestion displayed several resistant fragments with molecular masses in the range of ~19-17 KDa. Only in the case of amyloid preparations in acidic pH and amyloid #14, molecular masses were less than 15 KDa. Contrastingly, REDOX amyloid fibrils exhibited PK-resistant bands of molecular masses in the range of ~19-17 KDa (Fig. 28, Fig. 35). In particular, after treatment with PK at ratio 1:1, amyloid fibril #28 showed bands with molecular mass of ~16 KDa (Fig. 28). Notably, amyloid preparations subjected to the REDOX process in neutral buffers (Fig. 35, #31-34) showed most PK-sensitive structures. Upon treatment with high concentration of PK, nearly all of these amyloid preparations were almost entirely digested, showing only trace amounts of similar KDa bands.

The biochemical analyses of our amyloid preparations showed that in different biochemical and biophysical environments, recMoPrP(23-231) converted to distinct amyloidal forms. These different structures exhibited distinct stability in the presence of high concentration of denaturant (Fig. 27C), PK treatment (Fig. 28 and Fig. 35) and molecular masses patterning of PK-resistant cores. Kinetic studies of fibrilization (Fig. 33) showed that at neutral pH, the lag phase of recMoPrP(23-231) was short, and the protein was more prone to generate amyloids different from those formed at different pH. Interestingly, the stability of amyloid forms under neutral pH condition was lower.

The molecular basis of prion infectivity is the ability of PrP^{Sc} to efficiently induce the conversion of PrP^{C} into PrP^{Sc}. This process follows the seeding-nucleation model, with infectious PrP^{Sc} acting as a seed to capture PrP^{C} into a prion polymer [338]. Using cell-cultured models for the screening of several amyloid preparations, we seeded our amyloid fibrils in media of cultured mouse hypothalamic GT1, mouse neuroblastoma N2a cells and mouse hippocampal knock-out PrP HpL3-4 cells. After six cell passages, PK-resistant PrP (Fig. 29A, Fig. 36) and aggregated forms of PrP were found in amyloid fibril-infected GT1 as well as in N2a cells (Fig. 29B, Fig. 37 and Fig. 38), whereas HpL3-4 knockout PrP cells did not harbor any detectable, aggregated PrP (data not shown). Throughout serial passages, endogenous PrP^{C} was induced to change its conformation to PK-resistant PrP forms. This change was indicated by the increase in PK-resistant PrP from seeding passage (P1) to further passages (Fig. 30). After digestion with PK, PK-resistant bands showed molecular weights of 30-27 and ~19 KDa. The aggregation and PK resistance of PrP in amyloid-infected cells were also confirmed by immunofluorescence microscopy experiments including constraining PrP and ThS, with or without PK digestion (detail in “Materials and Methods”) (Fig. 30 and Fig. 39).

PMCA is able to detect the equivalent of a single molecule of infectious PrP^{Sc} and propagate prions that maintain high infectivity, strain properties and species specificity. PMCA assay can answer fundamental questions about infectivity of infectious agent *in vitro* [423]. We applied the PMCA method in order to test the replication ability of the materials from amyloid infected cells. After the third amplification, with 1/10 (Fig. 32A) or 1/100 (Fig. 32B) dilution of cell pellet (homogenized in 200µl) as seed, these materials led to accelerated prion replication. Although we used a smaller amount of PK than PMCA standards, the resistant bands were similar to the ScGT1 as positive control. Indeed, in PK digestion assay with cell lysate, PK was used at low concentration to obtain the resistant bands. Therefore, the infectious materials after replication in PMCA still maintain their partial PK resistance property.

Some preparations induced aggregation only in one cell line. Amyloids #27 and #30 promoted PK-resistant PrP forms in amyloid fibril-infected N2a cells but not in GT1 cells (Fig. 36, Fig. 37 and Fig. 38). Cell lines used in this work derived from different sources, which may account for the diverse susceptibility to various conformations of putatively infectious PrP. Interestingly, incubation with amyloid preparations #5, #6, #18, #19 did not promote PK-resistant PrP formation in either GT1 or N2a cells (Fig. 29A, Fig. 36).

The immunofluorescence analyses of amyloid fibril-infected cell lines (Fig. 29B) showed different staining and stronger PrP immunoreactivity detection than those of uninfected cells in both GT1 (Fig. 38) and N2a (Fig. 37) cell lines. Some cells showed accumulation, indicated by punctate and clusters of immune signal. Detected PrP accumulation in amyloid fibril-infected cells was found at the cell membrane and in the cytosolic compartments.

These data suggested that amyloid preparations, in both REDOX and non-REDOX conditions, can act as seeds, like natural prions do, in propagating within cultured neuronal cells, leading to accumulation and promotion of PK-resistant PrP forms from endogenous PrP.

The lack of PK-resistant PrP bands in PK digestion assay (Fig. 29A and Fig. 36) excluded any seeded ability for amyloid preparations #6 and #19. Neither did they show any change of PrP detection level in immunofluorescence experiments compared with non-infected cells (Fig. 29B, Fig. 37 and Fig. 38). The amyloid state, starting from a different amyloidogenic precursor, oligomeric state, protofibril/filament or mature fibril, is one of the possible elements that might affect the bioactivity of amyloid fibrils *in vitro* [714]. We collected our samples after 72 hours of fibrilization. In the case of amyloid #19, which did not lead to PK-resistant PrP formation in infected-cell culture assay, the end point of fibrilization was stable (Fig. 25A). In the various other preparations, the lag phases ranged from 6 to 40 hours over the final 72 hours of fibirilization (Fig. 25B), thus indicating a different kinetics in the maturation of fibrils (Fig. 26). On the other hand, in the presence of 2M Gdn-HCl, the kinetics of amyloid formation showed a non-homogeneous lag phase (Fig. 25B and Fig. 33) accounting for the large range of standard deviation. In order to elucidate the relationship between the amyloid state of recMoPrP(23-231) and its seeding ability, the timing of fibrilization processes for amyloid #19 was reduced to 55 hours. The sample was then separated at different stages of the lag phases. The long, medium and short lag phases were numbered as 1, 2 and 3, respectively (Fig. 31A). After 55 hours of fibrilization, amyloid #19 showed seeded ability in infected-cell cultured assays. This was

indicated by the presence of PK-resistant PrP (Fig. 31B) and accumulation of PrP (Fig. 31D) in amyloid-infected cells. For the same amyloid fibrils, after 72 hours of fibrilization neither PK-resistant PrP nor accumulation of PrP was observed in cell lines (Fig. 29). Moreover, amyloid forms obtained with different lag phases of amyloid #19 showed differences in promoting PK-resistant PrP (Fig. 31). These data suggested that the seeding ability of amyloid formations in cultured cells may depend on their states at the end of fibrilization.

In several recent independent studies on different proteins, both synthetic and natural amyloid forms have been shown to induce apoptosis in cell cultures [715,716,717]. To check for possible toxic effects on neuronal cell lines, we measured cell viability after treatment with amyloid preparations in a similar procedure with amyloid fibril-infected cell assay using MTT assay. Indeed, some amyloid preparations showed toxicity in cell culture while most did not (Fig. 40).

Discussion

The production of synthetic prions was introduced in 2004, via a simple *in vitro* induction of misfolding and aggregation of bacterially expressed recPrP [214]. PrP amyloids possessing different conformation stability were generated by altering the conditions for their formation, including urea concentration, pH and temperature. After passaging in mice, a large ensemble of synthetic prions showed a direct relationship between stability and incubation time of novel prion strains [229]. The recent, impressive progress in this technique has spurred the renewed investigation of prion structural biology [718][719][720][721][182].

The aggregation pathway plays an important role in prion disease as it is commonly accepted that both species barrier and strain phenomenon are due to different conversion pathways [722]. However, the molecular basis of prion conversion remains unclear, especially the varied structural landscape of PrP^{Sc}, which forms the basis of the strain phenomenon [723]. Therefore, the differences in conformational amyloid states of putative infectious materials — which can be generated *in vitro* under defined biophysical and biochemical conditions using recPrP — are the key elements to determine the biological activities of functional, pathological amyloid fibrils. In our studies, we created amyloid fibers under an array of different chaotropic conditions at two pH values: either mimicking the extracellular environment (neutral pH) or the endocytic compartment (acidic pH at 5). Although the high concentrations of chaotropic agent are not close to physiological conditions, in these cases the kinetics of full-length PrP demonstrated the tendency of the protein to adopt different folding states, which may encipher alternative pathogenic states (so-called prion states). In the presence of Gdn-HCl, our data showed a direct correlation between protein concentration and the final morphologies in fibrilizations (Fig. 34B).

Although most fibrilizations were obtained in 72 hours and the stable kinetics of some amyloid preparations was long, the final samples of some fibrilizations visualized under AFM showed oligomeric morphologies (Fig. 26 and Fig. 34A). Indeed, several oligomerization pathways of PrP may coexist, underlying that some oligomeric types may eventually assemble into fibrils, whereas others may just lead to a dead-end pathway [724][401].

Earlier works reported that, in infected brains, PrP^{Sc} accumulates at the plasma membrane and occasionally in late endosome/lysosome-like structures [725]. More recent studies show that prion conversion occurs in the endosomal recycling compartment where it transits after being internalized from the cell surface [336]. In addition, in both REDOX and non-REDOX processes, under similar concentration of denaturant and ionic strength, at either neutral pH or acidic pH, a shorter lag phase (Fig. 33) indicated that recMoPrP(23-231) is prone to convert to amyloid forms under neutral pH. On the other hand, amyloid fibrils converted in neutral pH showed low stability when treated with protease and denaturant. In fact, studies have shown that, in mice, less stable amyloids produced less stable prion strains, exhibiting short incubation time [229]. Generally, they replicate faster because of the lower stability. These data suggested that the very first step for PrP conversion and spreading may occur at extracellular sites. Tanaka *et al.* showed that infection of yeast with different amyloid conformations composed of a recombinant Sup35 fragment leads to different {*PSI*$^{+}$} strains. This evidence indicates that this prion-like protein adopts an infectious conformation before entering the cells [708].

In general, prion diseases are known to be triggered by PrP conformational conversion and subsequent aggregation [726]. These aggregates may be determined by non-covalent hydrophobic interactions and/or intermolecular disulfide bond formation. The oxidized and reduced states are two basic states of PrP, which are responsible for the formation of disulfide bonds. Starting from these two states, our amyloid preparation processes revealed different formation mechanisms. In the non-REDOX process, the oxidized recMoPrP at high concentration of denaturant was diluted directly into the fibrilization buffer in order to reach the final concentrations. During this procedure, protein particles seem to take a random pathway and aggregate. In this case the size of the clustered aggregation sometimes can be larger than those ones held together by regular, weaker forces, and may thus cause precipitation [727]. The underlying kinetic mechanism is likely to be a diffusion-limited aggregation process [728]. Indeed, at 3M Gdn-HCl of amyloid preparation #18 (non-REDOX) after 72 hours of 15-minutes interval shaking (Fig. 41), we achieved a classical form of diffusion-limited aggregation, whereas this was not obtained for condition #28 (REDOX) (data not shown).

Despite sharing the same conversion mechanism based on domain swapping and rearrangement of disulfide bridge, our REDOX amyloid preparation process differs from one previously described [325] in which His-tag hamster PrP(90-231) was converted into oligomeric forms and showed seed conversion properties in cell-free conversion systems. Indeed, in some cases our REDOX amyloid preparations exhibited a PK-resistant PrP band with a molecular mass of ~19 KDa, as well as characteristics similar to amyloid preparations obtained using a non-REDOX process. These results depart from data reported in [325].

Here we demonstrate that seeds derived from our recMoPrP(23-231) amyloid fibrils, which were generated by an array of recMoPrP(23-231) amyloid preparations, exhibited different structural properties due to different mechanisms of prion aggregation. When directly added to neuronal cell lines, endogenous PrP^{C} was induced to change its conformation to PK-resistant PrP forms, which are well-known diagnostic markers for prions. We used immunofluorescence with confocal microscopy to demonstrate location and level of PrP within the neuronal amyloid fibril-infected cells at sixth passage. This observation suggested that small amounts of amyloid fibrils,

which were added only in the beginning passage (P1), could seed endogenous misfolded PrP and lead it to accumulate at membrane and cytosolic compartments. Therefore, our amyloid-infected cell culture assay using recMoPrP(23-231) to produce synthetic prions may facilitate investigation aimed at unraveling mechanistic steps in prion formation. This method is indeed a useful and time-efficient tool for screening putative infectious materials. The data we gathered lead to three important conclusions. First, putative infectious materials can be generated *in vitro,* under controlled and well-defined biophysical and biochemical conditions using solely rec protein and some simple chemicals, without employing prion-infected brain homogenate or purified PrP^{Sc}. Secondly, the PK-resistant ability of amyloid fibril-infected cells increases during cellular passages. Thirdly, different structural properties of putative infectious materials may account for different prion-like characteristics.

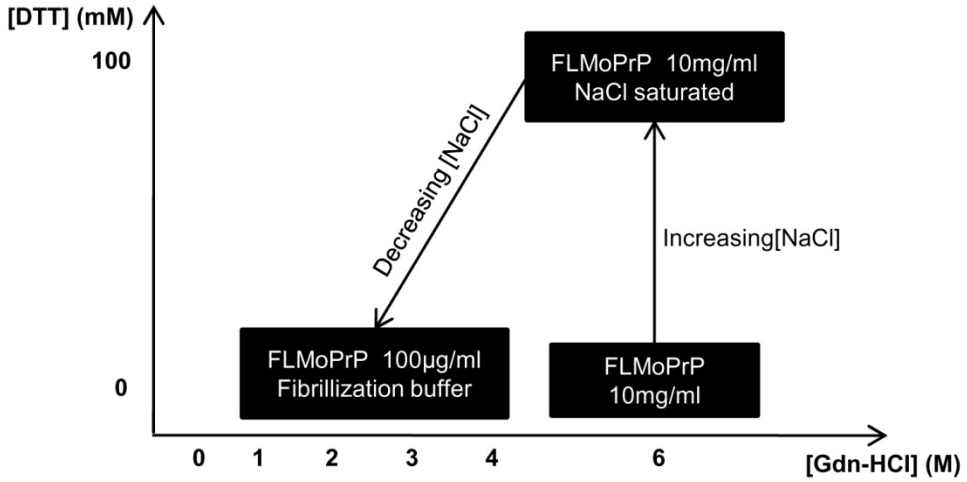

Figure 24. Schematic diagram for the conversion of the monomeric recMoPrP(23-231) to an amyloid form by REDOX process.

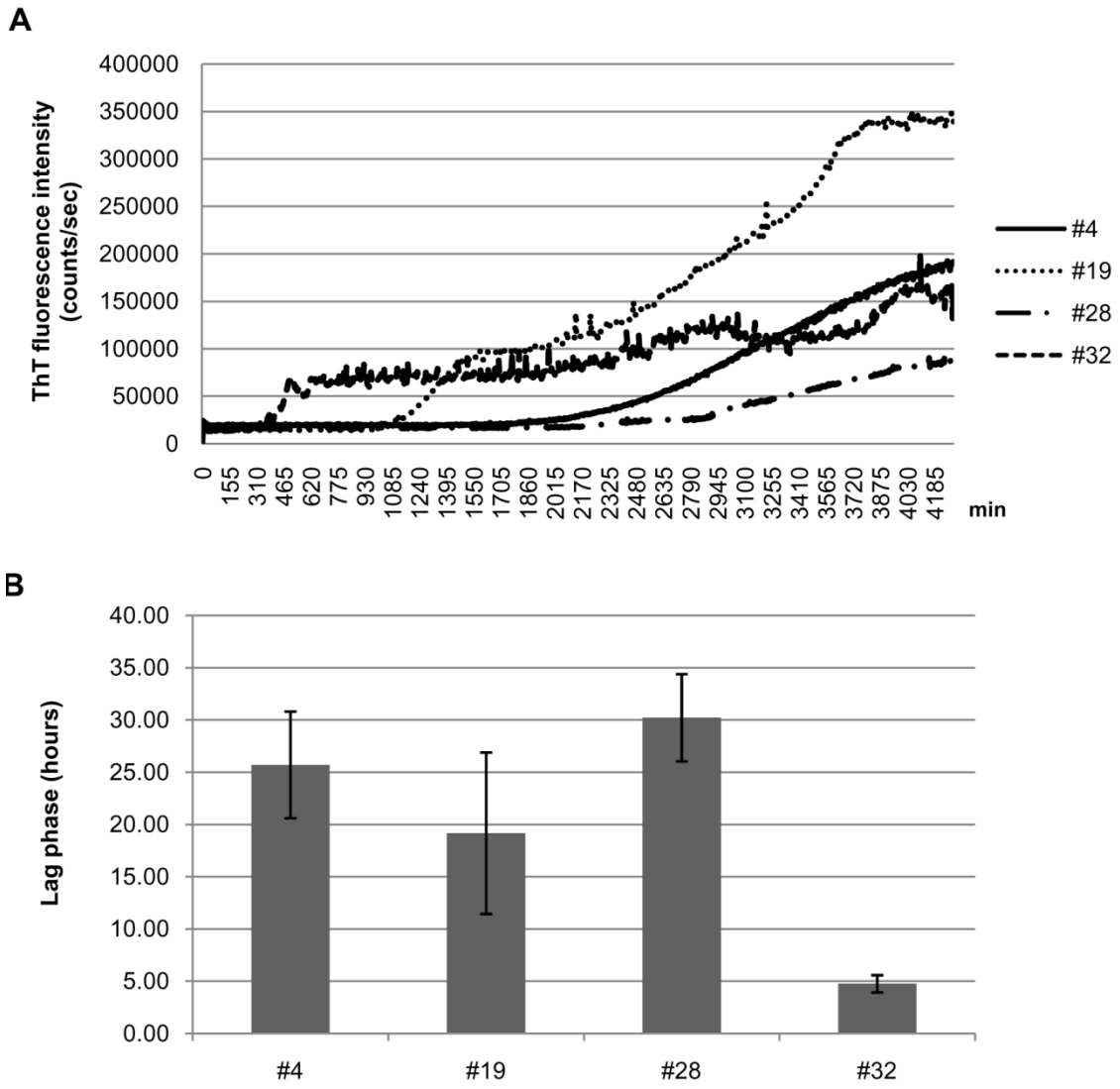

Figure 25. RecMoPrP(23-231) was converted *in vitro* into different amyloid forms (amyloids #4, #19, #28, #32). The amyloid preparations shown (A) exhibited different kinetics for the formation of recMoPrP(23-231) aggregates. Lag phase distribution of amyloid preparations (B).

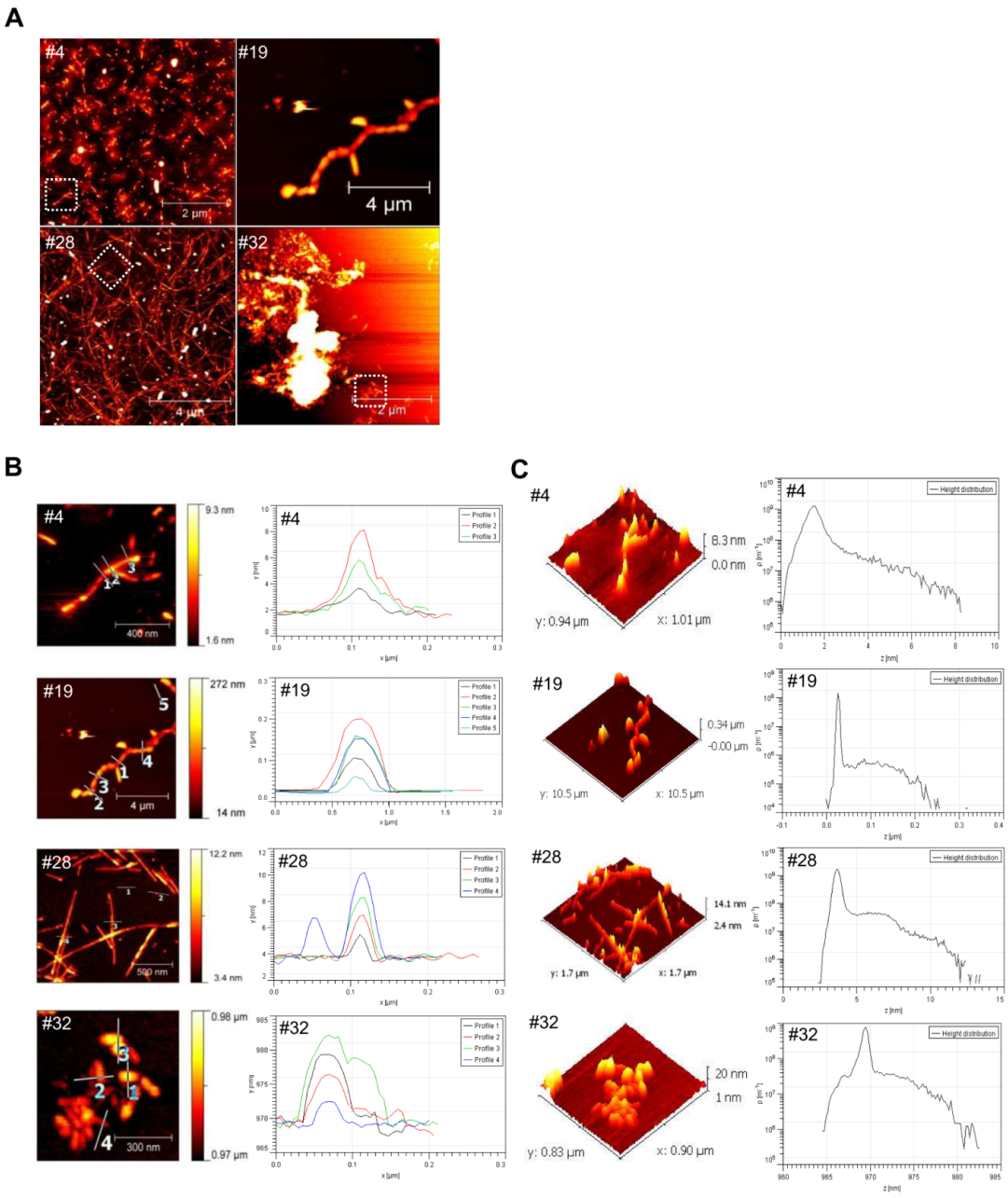

Figure 26. AFM imaging analysis was performed at the end of the fibrilization reactions after 72 hours (amyloids #4, #19, #28, #32). AFM scan topographical images of PrP deposited on mica surface, large-scale images (A). AFM height profiles along the numbered lines in topographical images. The profile reflects the lines as numbered in the images. Higher resolution scan images belonging to the area are marked by a white dashed square in part A (B). Three-dimensional representation of AFM topography images and height distribution data obtained from the AFM images in part B (C).

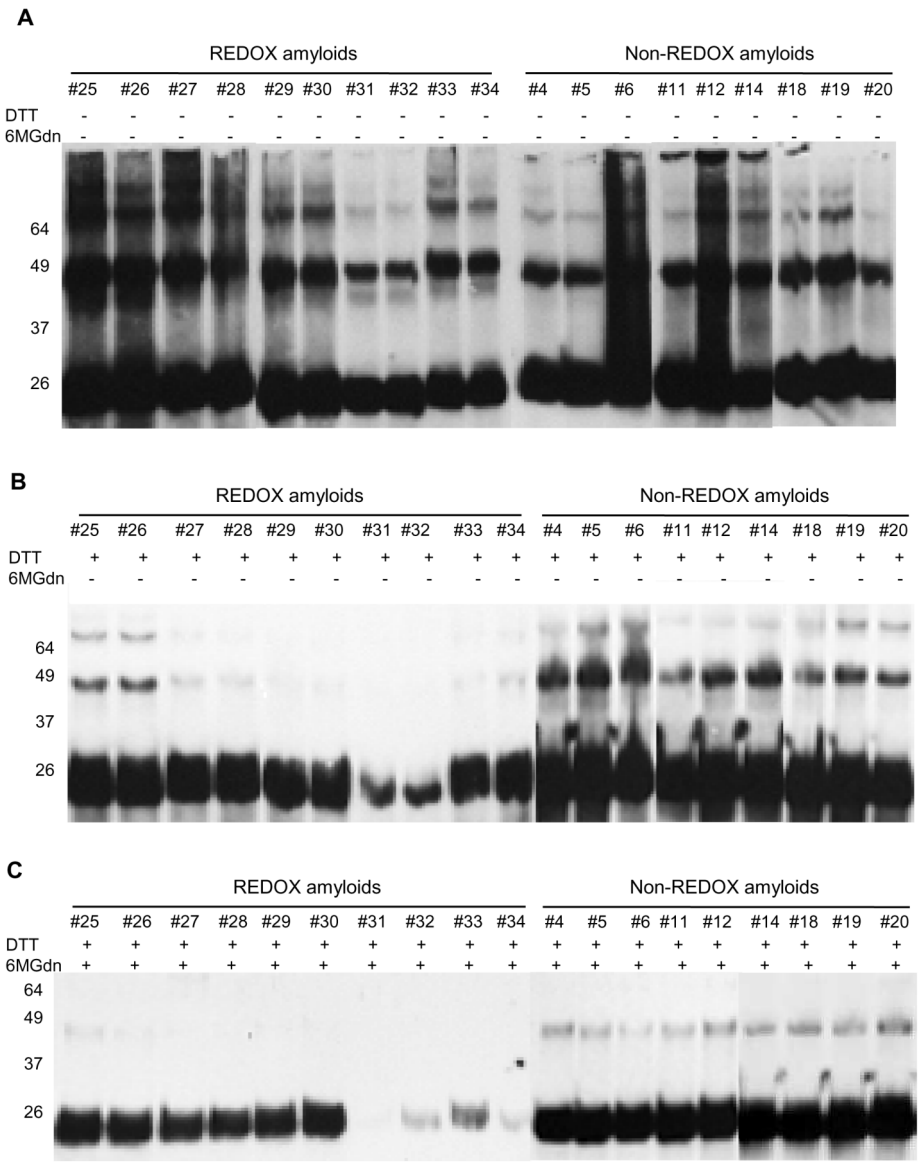

Figure 27. Monomeric recMoPrP(23-231) was converted into amyloid forms by intermolecular disulfide linkage following the REDOX process. Western blotting of non-reducing SDS-PAGE showing the conversion of recMoPrP(23-231) to amyloids is indicated by dimer, trimer, and more complex structures in both processes (A). Western blotting of reducing SDS-PAGE after treatment of amyloid with reducing agent (β-mercaptoethanol) shows the decrease in signals of dimer, trimer and more complicated structures in all lanes of amyloid samples from REDOX-process (B). Western blotting of reducing SDS-PAGE of amyloid after a 3-day treatment with denaturant (6M Gdn-HCl), and subsequently with reducing agent (β-mercaptoethanol) shows only monomeric recMoPrP(23-231) bands and the disappearance of more complicated structures in all lanes of amyloid samples in REDOX process (C).

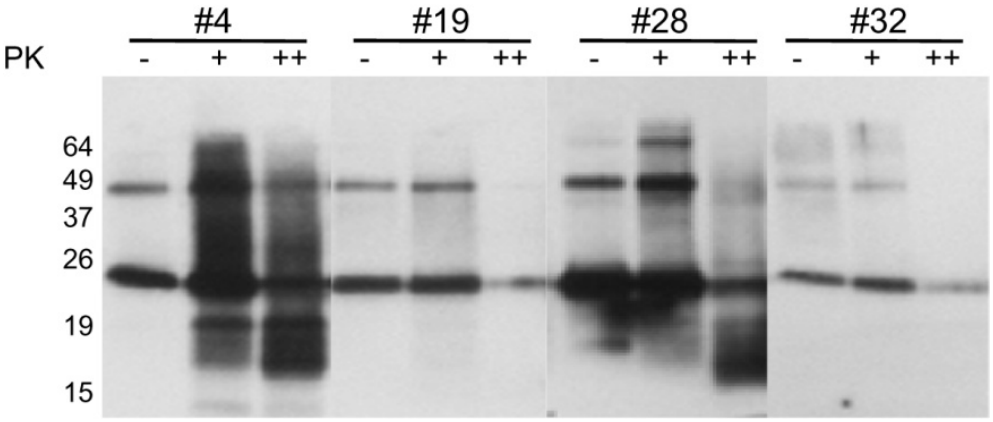

Figure 28. Western blotting of PK digestion assay (amyloids #4, #19, #28, #32) showed partial protease K (PK) resistance of recMoPrP(23-231) (amyloids #4 and #28). RecMoPrP(23-231) amyloids (PK- lanes) were digested with PK at ratio 1:10 (w/w) (PK+ lanes) and 1:1 (w/w) (PK++ lanes).

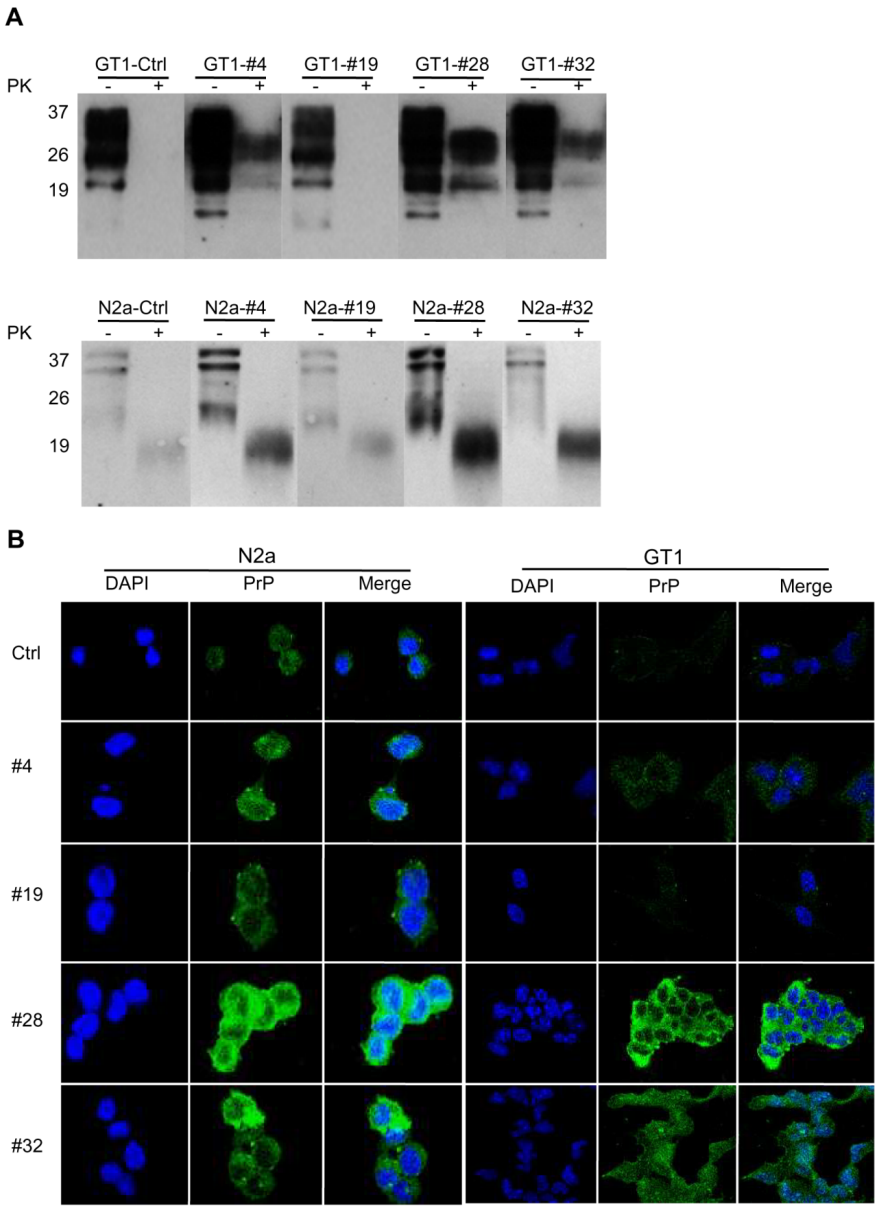

Figure 29. Seeding of recMoPrP(23-231) amyloid preparations induced the conversion of endogenous PrP^{C} to PK-res forms (A) and accumulation (B) in mouse neuroblastoma N2a and mouse hypothalamic GT1 amyloid-infected cell lines. Western blotting shows the partial protease K (PK) resistance of N2a and GT1 amyloid fibril-infected cell lysates. Fibril-infected cell lysates (PK-lanes) were digested with PK at ratio 1:500 (w/w) (PK+ lanes) (A). Immunofluorescence imaging shows the accumulations of PrP in N2a and GT1 amyloid fibril-infected cell lines. Cells were infected with different amyloid preparations. The deposition and level of PrP (green) in amyloid fibril-infected cell lines after six passages were detected by D18 anti PrP antibody. The nuclei (blue) were stained with DAPI (B).

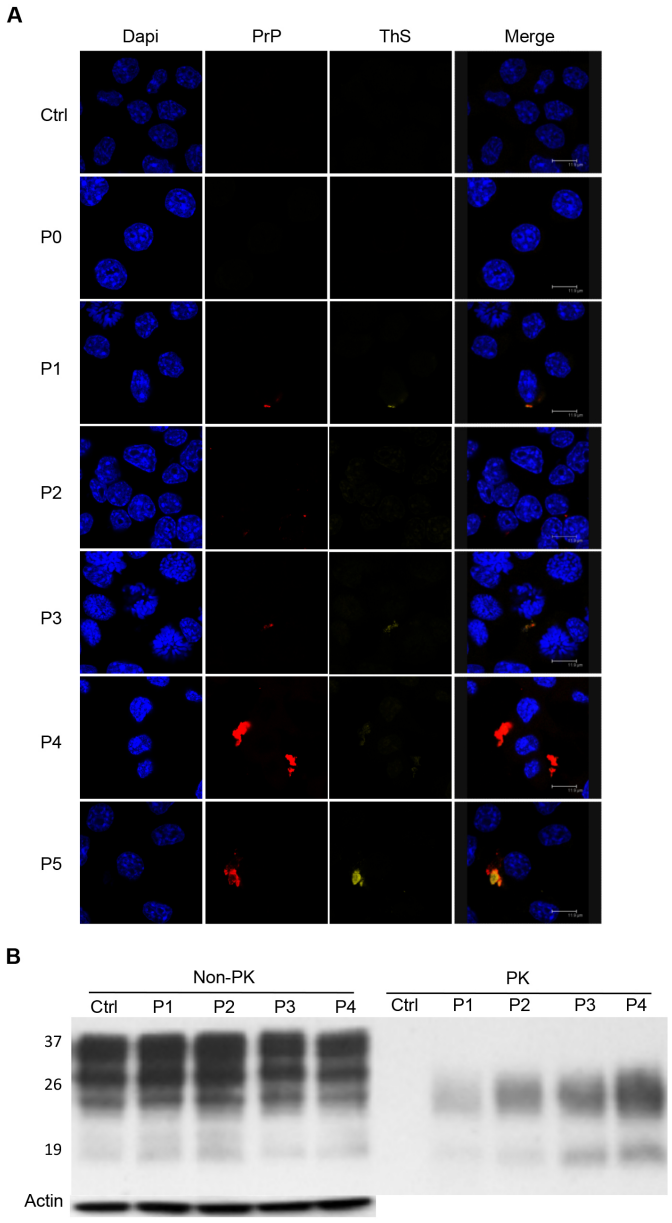

Figure 30. Induction of PrPres form and aggregation in amyloid infected cells. Immunofluorescence images of amyloid infected cells after PK treatment are positive with double staining PrP and ThS (A). Western blotting of N2a cell lines infected with PrP amyloid preparations was observed throughout, from first passage (P1) to fifth passage (P5) and after treatment with proteinase K at ratio 1:500 (w/w) (B).

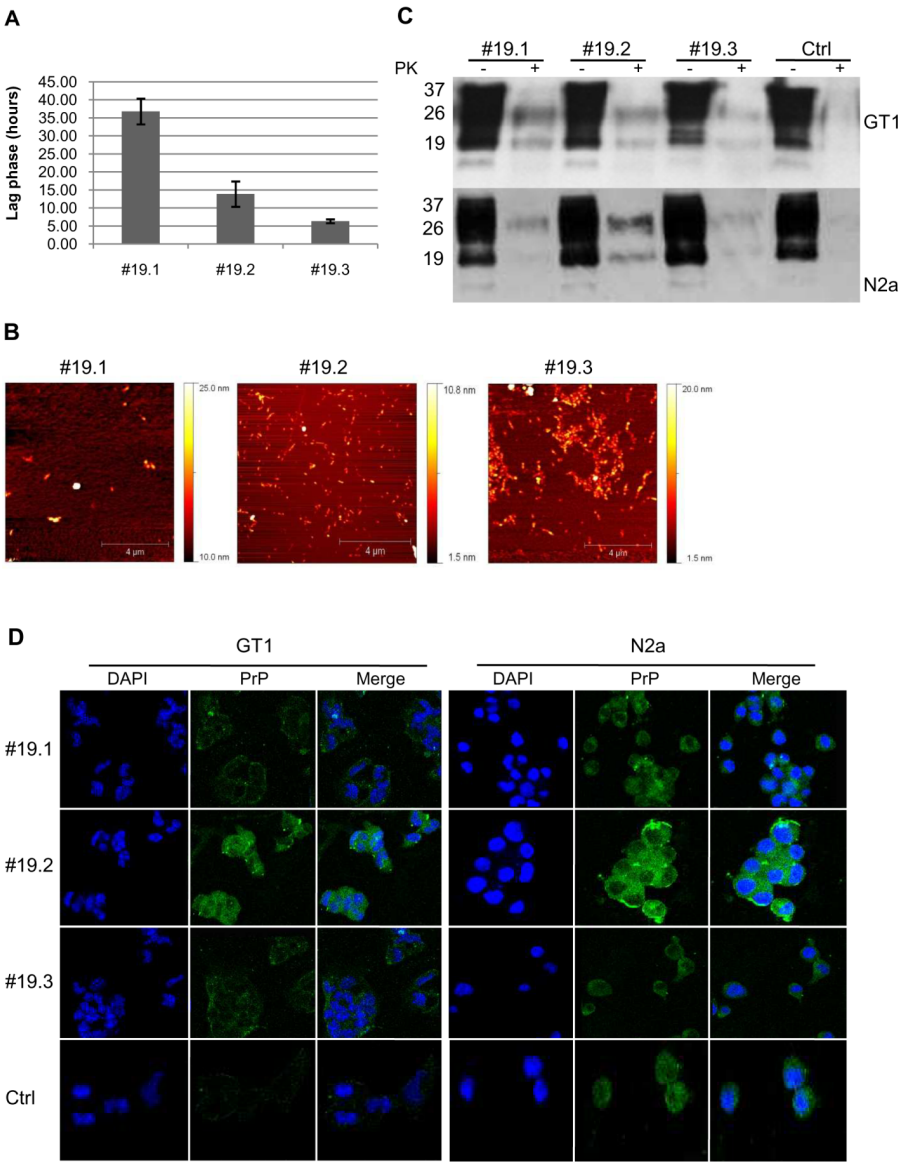

Figure 31. Seeding ability of amyloid formations in cultured cells depends on their state in fibrilization. Lag phase distribution of separated amyloid samples of preparation #19 (termed #19.1, #19.2, #19.3) after 55 hours of fibrilization (A). AFM imaging at the end of the fibrilization reactions shows morphologies of separated amyloid samples after 55 hours of fibrilization (B). Western blotting shows the partial protease K (PK) resistance of N2a and GT1 cells after infection with amyloids #19.1, #19.2, #19.3. Fibril-infected cell lysates (PK- lanes) were digested with PK at ratio 1:500 (w/w) (PK+ lanes) (C). Mouse neuroblastoma N2a and mouse hypothalamic GT1 cells were infected with separated amyloid samples #19.1, #19.2, #19.3. The deposition and level of PrP (green) in amyloid fibril-infected cell lines after six passages were detected by D18 anti PrP antibody, using immunofluorescence. The nuclei (blue) were stained with DAPI (D).

A

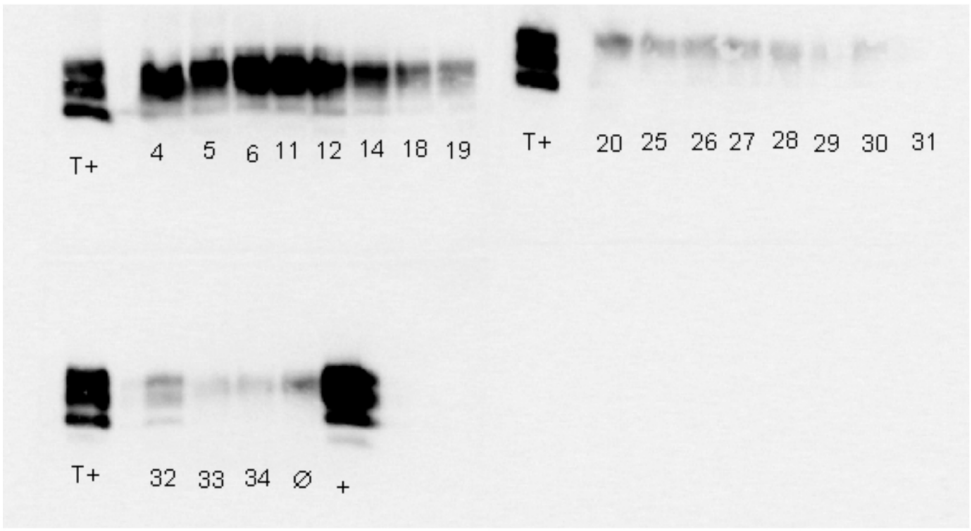

B

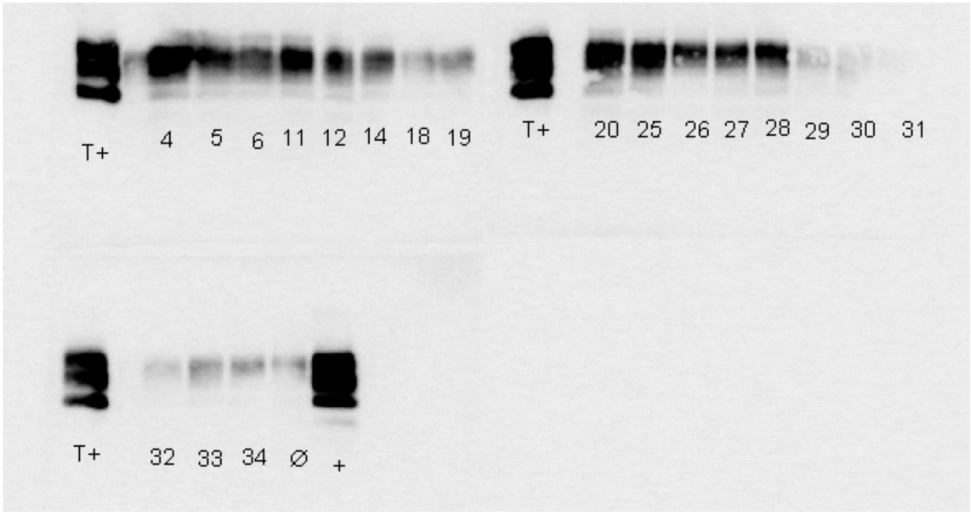

Figure 32. Detection and replication of synthetic PrP^{Sc} form from GT cell line infected with different amyloid preparations after 3 cycles of PMCA, with dilution 1/10 (A) and 1/100 (B) of cell pellets (homogenized in 200µl buffer). Western blots demonstrate amplification of protease-resistant prion protein (PrP) after serial PMCA. x is normal GT1 as negative control. T+ (RML) and + (ScGT1), both are positive controls. The samples were numbered based on the name of each amyloid preparation that was used to infect cells.

Supporting Figures

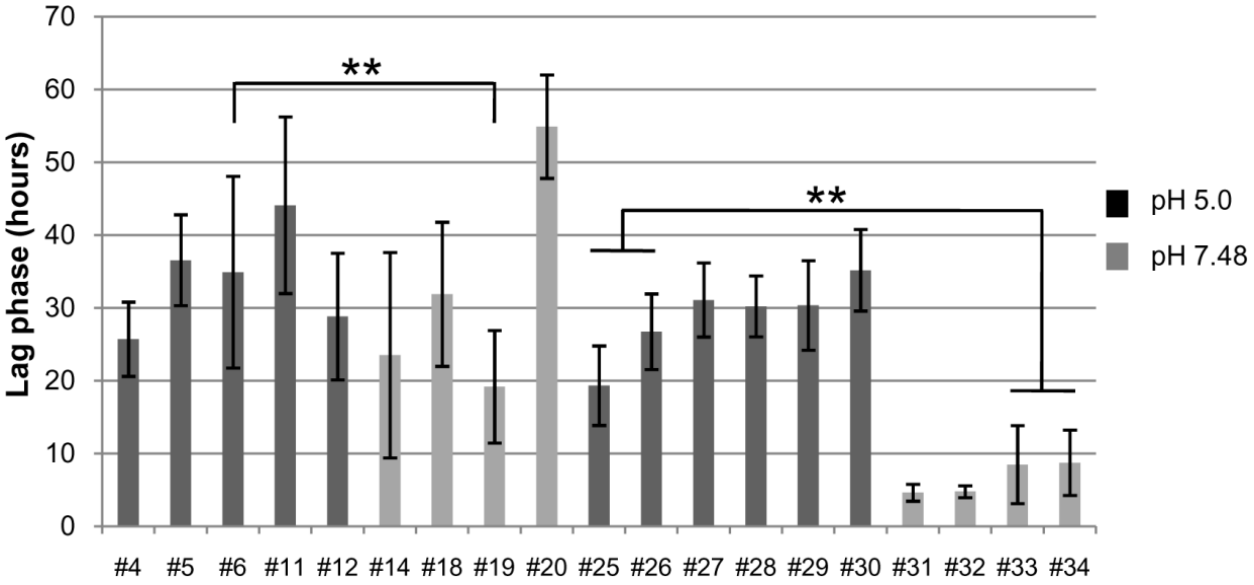

Figure 33. Lag phase distribution of amyloid preparations following non-REDOX and REDOX processes compared to pH 5.0 and pH 7.5. (**, P<0.01, n=12)

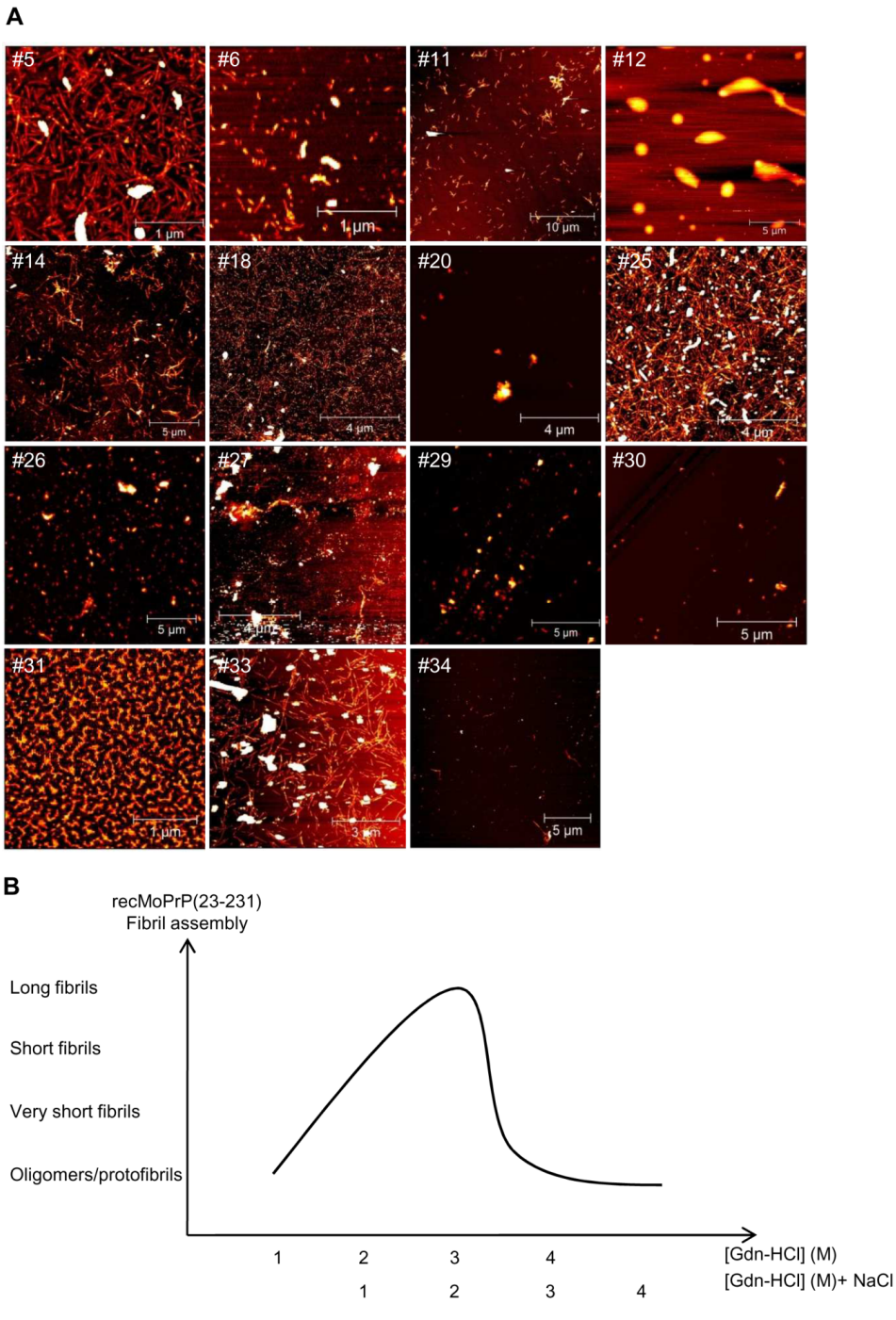

Figure 34. The morphology-dependence of the fibrilizations was observed at different denaturant concentrations. AFM imaging at the end of the fibrilization reactions shows morphologies of amyloid preparations after 72 hours of fibrilization (A). Correlation of amyloidal morphologies and Gdn-HCl concentrations in fibrilizations (B).

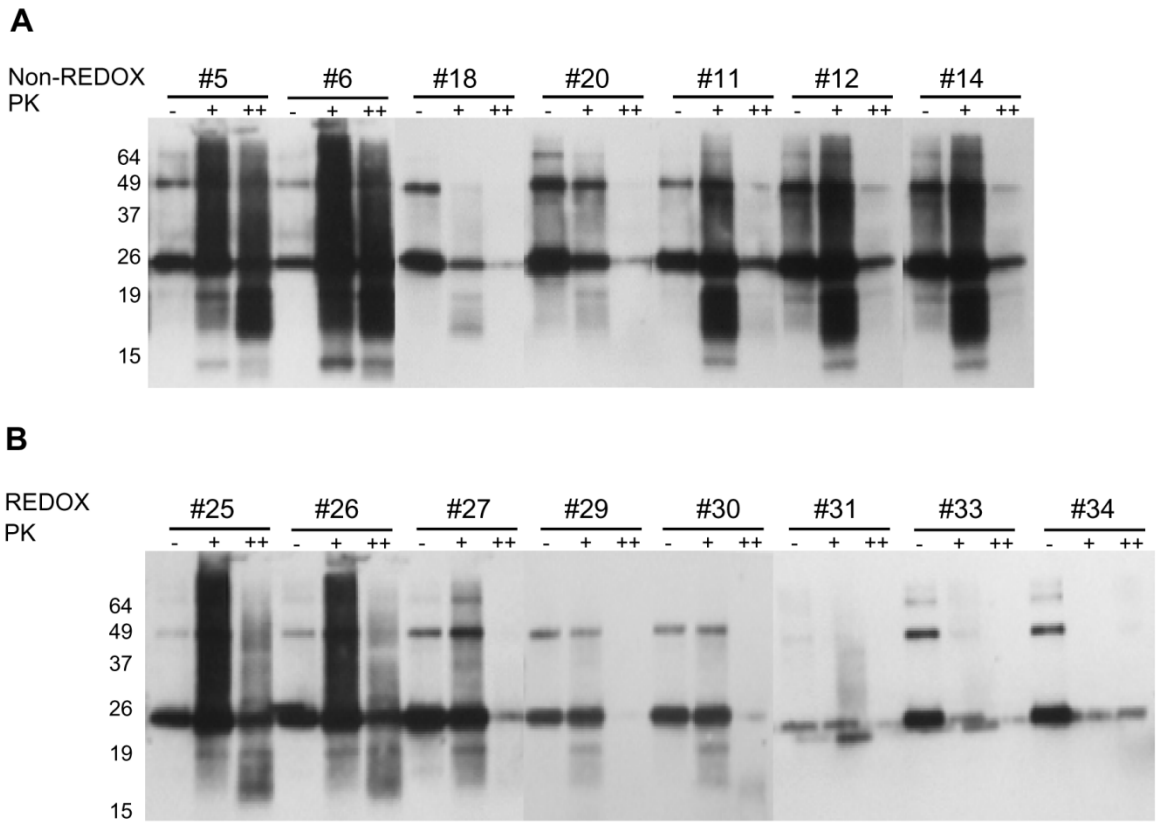

Figure 35. Western blotting of PK digestion assay showed partial protease K (PK) resistance of recMoPrP(23-231) amyloid preparations. RecMoPrP(23-231) amyloids (PK-lanes) were digested with PK at ratio 1:10 (w/w) (PK+ lanes) and 1:1 (w/w) (PK++ lanes).

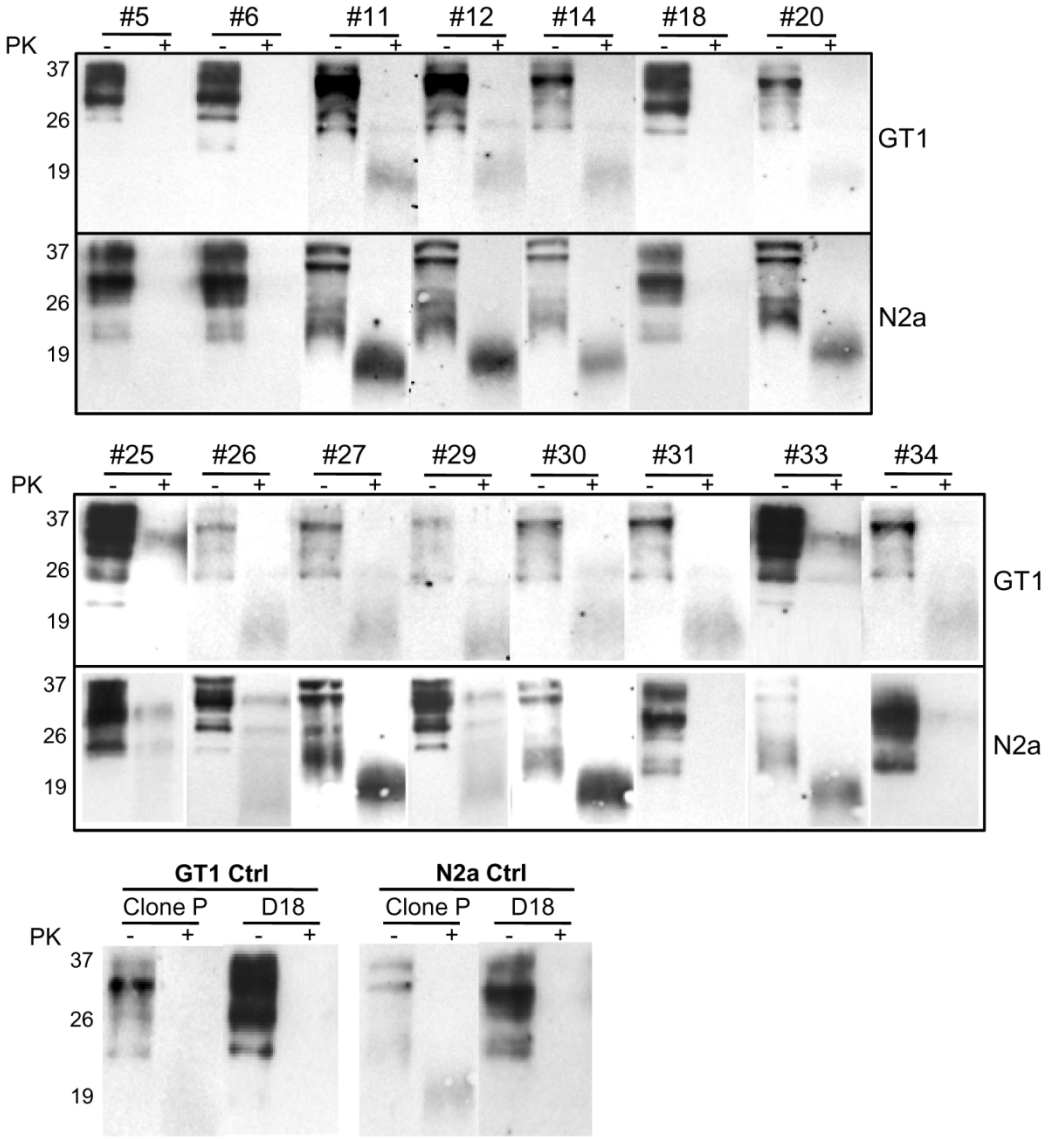

Figure 36. Seeding of recMoPrP(23-231) amyloid preparations induced the conversion of endogenous PrP^C into protease K (PK) resistant forms. Western blotting shows the partial PK-resistance of neuroblastoma N2a and mouse hypothalamic GT1 amyloid fibril-infected cell lysates. Fibril-infected cell lysates (PK- lanes) were digested with PK at ratio 1:500 (w/w) (PK+ lanes).

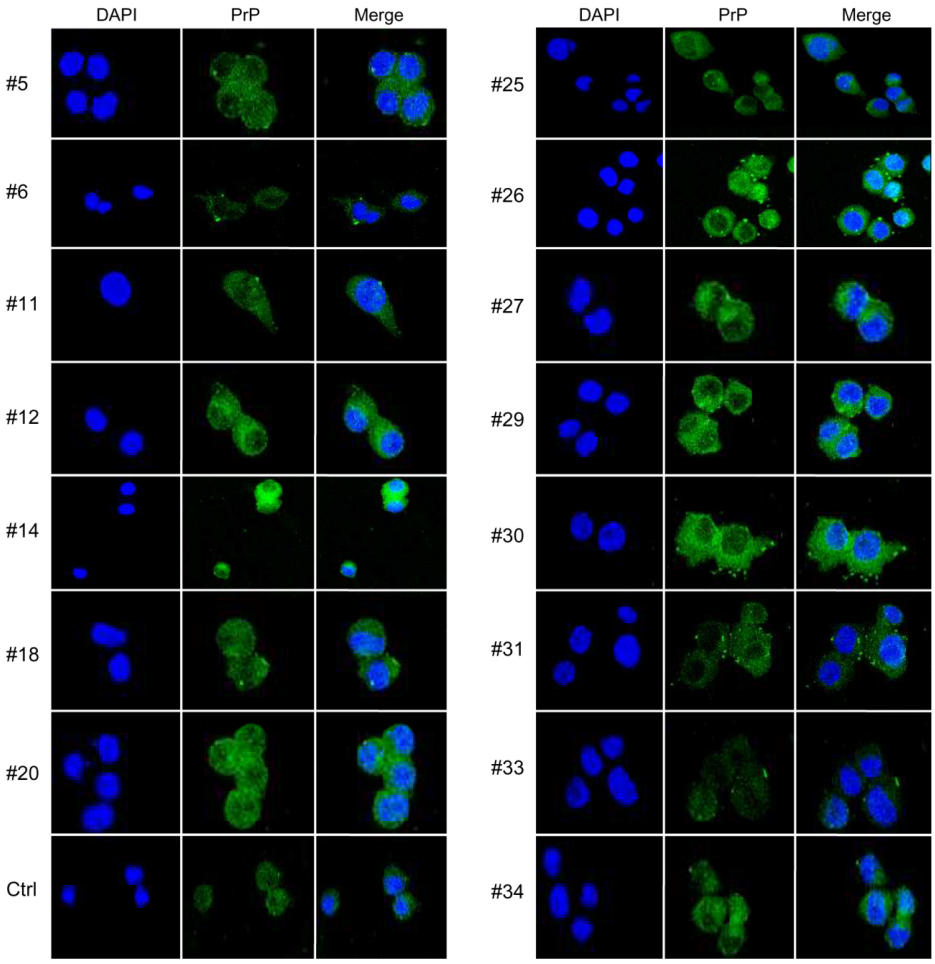

Figure 37. Accumulation of PrP was observed in neuroblastoma N2a amyloid fibril-infected cell lines infected with different amyloid preparations. The depositions and level of PrP (green) after six passages were detected by D18 anti PrP antibody, using immunofluorescence. The nuclei (blue) were stained with DAPI.

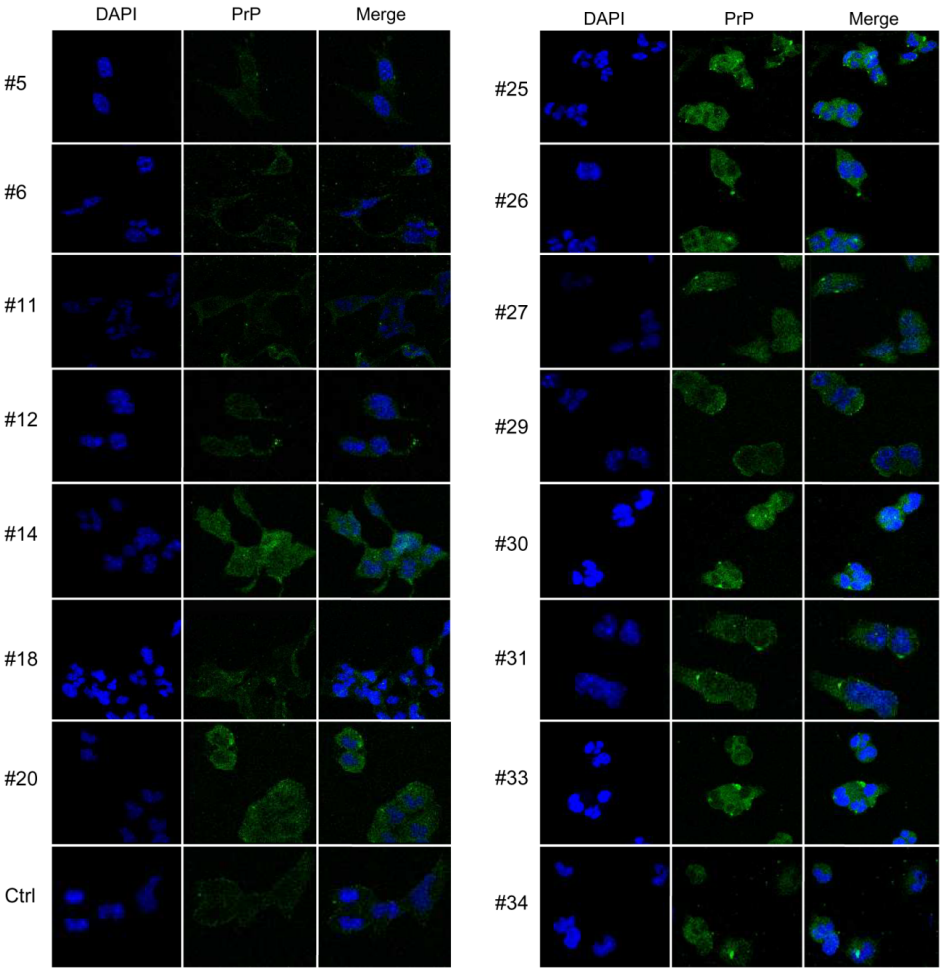

Figure 38. Accumulation of PrP was observed in mouse hypothalamic GT1 amyloid fibril-infected cell lines infected with different amyloid preparations. The depositions and level of PrP (green) after six passages were detected by D18 anti PrP antibody, using immunofluorescence. The nuclei (blue) were stained with DAPI.

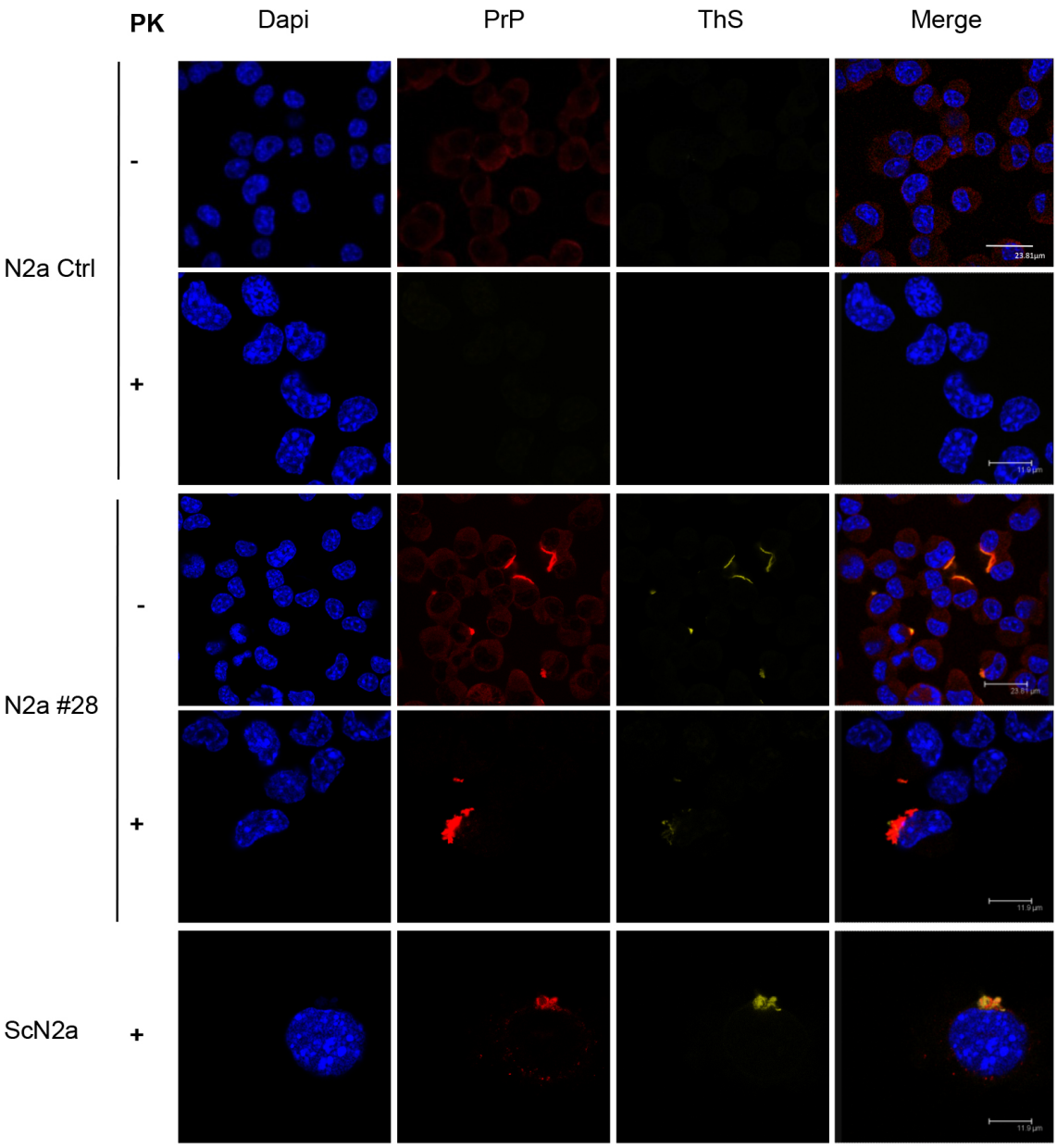

Figure 39. PrPres form and aggregation in amyloid infected cells. Immunofluorescence images of amyloid infected cell with/without PK treatment are positive with double staining PrP and ThS.

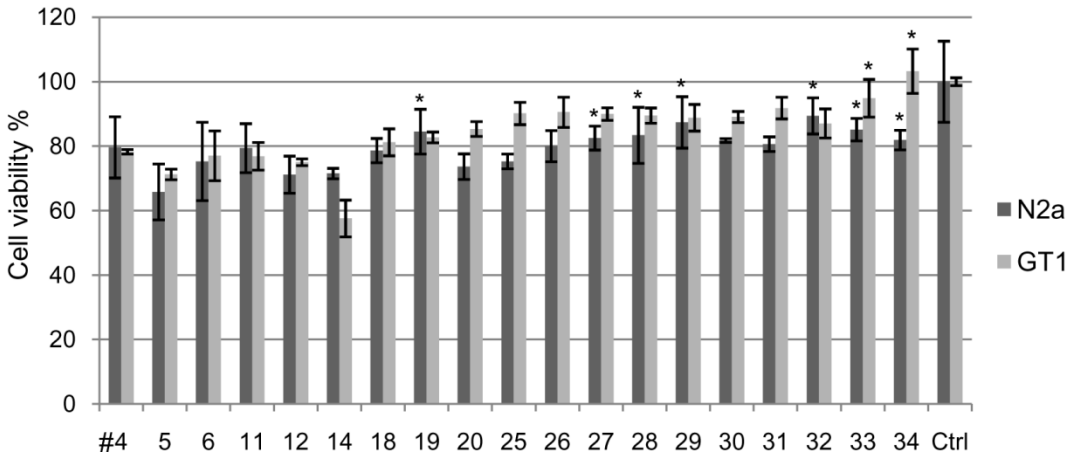

Figure 40. Amyloid fibrils recMoPrP(23-231) induced cell death in infected-cell cultures. Cell viability based on mitochondrial activity was measured by MTT assay. Control cells without treatment were counted as 100%. (*, P>0.05, n=6)

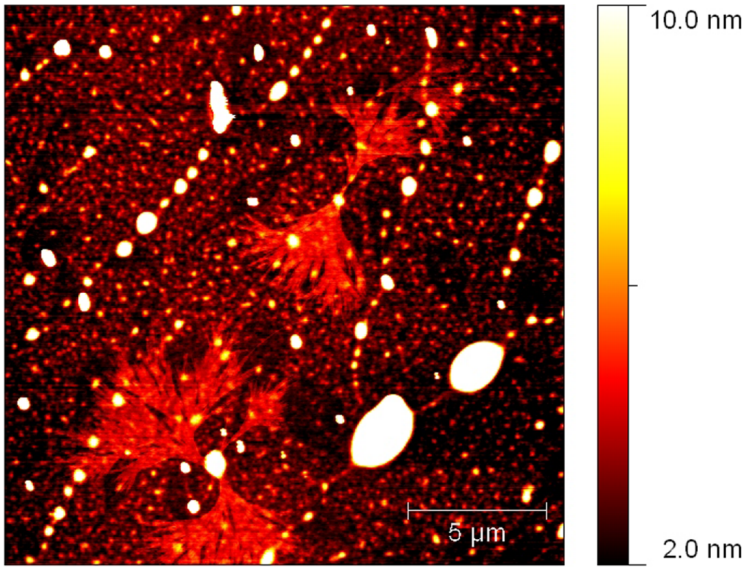

Figure 41. AFM imaging analyses were carried out at the end of the fibrilization reaction of amyloid preparation #18 (non-REDOX) after 72 hours with 15 minutes of interval-shaking time. AFM scan topographical image of PrP amyloid #18 deposited on mica surface showed classical forms of diffusion-limited aggregation.

Table 7. Different height of clusters of recMoPrP (23-231) aggregates

Amyloid preparation (#)	[Gdn-HCl] (M)	Buffer	pH	Unit height steps (nm)	Top height distribution (nm)
4	4	50mM Acetate	5.0	1.8-2.2	1.8
19	2	PBS	7.4	25-50	25
28	3	50mM Acetate	5.0	1.2-2.5	2.5
32	1	PBS	7.4	2.5-4.5	4.5

Table 8. Conditions used for the formation of diverse amyloid preparations in non-REDOX process

Amyloid preparation (#)	[Denaturant]	Buffer	pH	[MoPrP] µg/mL	[NaCl] (M)
1	4M Urea	50mM Acetate	6.0	100	-
2	4M Urea	50mM Acetate	5.0	100	-
3	4M Urea	50mM Acetate	3.5	100	-
4	4M Gdn-HCl	50mM Acetate	5.0	100	-
5	3M Gdn-HCl	50mM Acetate	5.0	100	-
6	2M Gdn-HCl	50mM Acetate	5.0	100	-
7	1M Gdn-HCl	50mM Acetate	5.0	100	-
8	0.5M Gdn-HCl	50mM Acetate	5.0	100	-
9	0.25M Gdn-HCl	50mM Acetate	5.0	100	-
11	4M Urea	50mM Acetate	5.0	100	0.4
12	4M Urea	50mM Acetate	5.0	200	0.4
13	1M Gdn-HCl	50mM Acetate	5.0	200	0.4
14	2M Gdn-HCl	PBS	7.5	200	-
17	4M Gdn-HCl	PBS	7.5	100	-
18	3M Gdn-HCl	PBS	7.5	100	-
19	2M Gdn-HCl	PBS	7.5	100	-
20	1M Gdn-HCl	PBS	7.5	100	-
21	0.5M Gdn-HCl	PBS	7.5	100	-
22	0.25M Gdn-HCl	PBS	7.5	100	-

Table 9. Conditions used for the formation of diverse amyloid preparations in REDOX process

Amyloid preparation(#)	[Denaturant]	Buffer	pH	[MoPrP] µg/mL	[NaCl]
23	1M Gdn-HCl	50mM Acetate	5.0	100	+
24	1M Gdn-HCl	50mM Acetate	5.0	100	-
25	2M Gdn-HCl	50mM Acetate	5.0	100	+
26	2M Gdn-HCl	50mM Acetate	5.0	100	-
27	3M Gdn-HCl	50mM Acetate	5.0	100	+
28	3M Gdn-HCl	50mM Acetate	5.0	100	-
29	4M Gdn-HCl	50mM Acetate	5.0	100	+
30	4M Gdn-HCl	50mM Acetate	5.0	100	-
31	1M Gdn-HCl	PBS	7.4	100	+
32	1M Gdn-HCl	PBS	7.4	100	-
33	2M Gdn-HCl	PBS	7.4	100	+
34	2M Gdn-HCl	PBS	7.4	100	-
35	3M Gdn-HCl	PBS	7.4	100	+
36	3M Gdn-HCl	PBS	7.4	100	-
37	4M Gdn-HCl	PBS	7.4	100	+
38	4M Gdn-HCl	PBS	7.4	100	-

Table 10. Different height of clusters of recMoPrP (23-231) aggregates

Amyloid preparation (#)	Unit height steps (nm)	Top height distribution (nm)
5	0.8-1.2	1.6
6	0.5-0.8	0.5
11	4	4
14	3-4.5	4.5
18	1.6-1.8	1.6
20	5-7	5
25	1.8-2	1.6-1.8
26	4-18	4
27	1.6-5	1.6-1.8
29	40-43	40
30	30-35	60
31	-	0.35
33	1.5-2.5	1.5
34	1.6-2.2	1.6

Table 11. The morphology-dependence of the fibrilizations observed at different concentrations of denaturant

[Gdn-HCl] (M)	1	2	3	4	-
[Gdn-HCl] (M) + NaCl	-	1	2	3	4
Morphologies	Oligomer, very short fibrils	Very short and short fibrils	Long and mature fibrils	Oligomer, very short fibrils	Oligomer, very short fibrils
Amyloid preparations (#)	20, 32	6, 14, 19, 26, 34	5, 18, 25,28, 33	4, 30, 27	29

Oligomer: homogenous population of spherical particles, <0.1 μm

Very short fibrils: <0.5 μm

Short fibrils: <1 μm

Long fibrils: >1 μm

Part 2: Horizontal transmission of synthetic human α-synuclein prions in mice

2.1. Objectives:

- To evaluate the possibility that recombinant human α-syn could acquire prion properties, once it is converted into a β-sheet-rich structure, and thus determine the fate of endogenous α-syn of either human or murine immortalized cell lines.

- To investigate whether there are striking similarities between the pathological mechanisms of TSEs and synucleinopathies *in vitro* and *in vivo*.

- To answer critical questions: is Parkinson's disease transmissible? May the synthetic α-syn amyloid forms implicated also behave as infectious agents during the passaging?

2.2. Specific background

Synucleinopathies are a group of neurodegenerative disorders characterized by fibrillary aggregates of α-syn in the cytoplasm of selective populations of neurons and glia. These pathologies include Parkinson's disease (PD), dementia with Lewy Bodies (LBs), multiple system atrophy and pure autonomic failure. Depending on the distribution of the lesions, these disorders are characterized by a chronic and progressive decline in motor, cognitive, autonomic functions and behavior. Because of clinicopathologic overlap, differential diagnosis may be difficult [459].

Using cellular and animal models for this class of maladies, recent studies have focused on the mechanism whereby fibrillary aggregates of α-syn form and spread among cells. In fact, it has been proposed that α-syn fibrillary aggregates may share peculiar molecular analogies with well-established proteinaceous infectious agents such as prions [729]. The observation that LBs are present in grafted fetal brain cells in PD patients who underwent transplantation is suggestive that α-syn may turn into prion-like elements [730] produced in the grafted cells [627]. Another important analogy with prions is the conversion from either a monomeric and unfolded [544] or α-helical structured α-syn [572] to a β-sheet-rich structure, orderly organized into oligomers or amyloid fibrils [731]. Most importantly, it has been shown that recombinant α-syn in a β-sheet-rich structure can recruit endogenous soluble α-syn protein to form pathological species in primary cell cultures [437] and induce homologous α-syn prion formation in transgenic and non-transgenic mice [439][636][441].

Based on these premises, we considered the possibility that recombinant human α-syn could acquire prion properties, once it is converted into a β-sheet-rich structure, and thus determine the fate of endogenous α-syn of either human or murine immortalized cell lines.

Human α-syn differs from mouse α-syn in seven positions: A53T, S87N, L100M, N103G, A107Y, D121G e N122S. Interestingly, in humans the A53T substitution is a pathological mutation leading to rare autosomal dominant genetic cases of PD [732].

2.3. Results and discussion

We produced highly pure recombinant human α-syn protein (Fig. 46) either as wild-type sequence or tagged with a FLAG epitope, and established a protocol to induce the acquisition of structured amyloid fibers as previously shown for the production of mammalian synthetic prions [214] (Fig. 47). For the purpose of this work, we decided to collect β-sheet-rich structures at different time points during the fibrilization assay: (i) at the early inflection of the sigmoid curve, as measured by fluorescence detection; (ii) at the middle portion of the curve; and (iii) at plateau. We reasoned that these diverse β-sheet-rich structures might differ from the quaternary structure of the assembled recombinant human α-syn protein. Indeed, as predicted, atomic force microscopy measurements showed diverse assemblies: oligomers, short and long amyloid fibers (Fig. 42).

The human sympathetic adrenergic ganglial neuroblastoma SH-SY5Y cell line was then exposed to these diverse molecular assemblies in an attempt to establish whether these β-sheet-rich structures were able to induce endogenous human α-syn protein to aggregate. To this end, we followed different strategies. Either recombinant human α-syn or FLAG-tagged recombinant human α-syn proteins were used. The latter would allow the exogenous protein assembly to be readily detectable. A single exposure to β-sheet-rich structures of recombinant human α-syn was sufficient to induce aggregation of endogenous α-syn in untransfected human neuroblastoma SH-SY5Y cells. Remarkably, only short fibrils of α-syn efficiently induced the endogenous α-syn to aggregate after seven days in culture (Fig. 43A). The SH-SY5Y cells exposed to short fibrils of recombinant human FLAG-tagged α-syn were stained with either an anti-human α-syn antibody or an anti-FLAG immunoglobulin. The immunoreactivity was mostly cytosolic, with substantial co-localization of anti-FLAG and anti-human α-syn antibodies.

We next addressed the question whether infection with short fibrils of α-syn was sustained over time. We exposed SH-SY5Y cells to FLAG-tagged recombinant human α-syn short fibrils, and at each passage we measured the aggregation of endogenous α-syn. Figure 2B shows a typical experiment where the aggregation of α-syn was assessed in serial cellular passages. While exogenous aggregated α-syn was readily seen after seven-day incubation, corresponding to a single passage (P0), only a residual staining of endogenous α-syn could still be observed in the subsequent passage (P1) and no staining was detectable in the ensuing two passages (P2 and P3). Surprisingly, aggregates of endogenous α-syn reappeared at passages four to six (P4-P6). We performed additional passages (up to passage 12) and in each one a sustained aggregation of endogenous α-syn was still present (data not shown). In agreement with immunohistochemistry, biochemical analysis showed that aggregated α-syn extracted from SH-SY5Y cells was mostly present in cultures incubated with short fibrils, and it had the same electrophoretic mobility as pure recombinant human FLAG-tagged α-syn oligomers or short fibrils (Fig. 48).

We performed similar experiments using a human neuroblastoma SH-SY5Y cell line stably over-expressing human α-syn (Fig. 49). Immunostaining of α-syn in this cell line is predominantly nuclear. Upon infection with short fibrils of α-syn and after ten passages in cell culture, we observed a stronger nuclear staining and, most importantly, the presence of several

spots of α-syn throughout the cytosol (Fig. 43C, white arrows). This suggests that α-syn short fibrils are able to seed aggregation of over-expressed α-syn in this cellular model.

To further characterize α-syn aggregates, the different cell lines were probed with an antibody to α-syn phosphorylated at position 129. All cells showed nuclear staining, regardless of over-expression of α-syn or infection with α-syn short fibrils (Fig. 43C, P-S129 α-syn panel). In addition, the cytoplasm of several α-syn infected SH-SY5Y cells contained α-syn aggregates. Quantitative analysis showed that the number of cells with these cytoplasmic inclusions was remarkably higher in α-syn infected cells compared to non-infected cells (54.8% vs. 7.7%, $p<0.001$) (Fig. 43C, bottom left). We thus concluded that although over-expression of α-syn induces aggregation, this occurs to a much greater extent when combined with infection (Fig. 43C, bottom left). Interestingly, the bar graphs in Fig. 43C show a comparative number of cells containing aggregates upon staining with α-syn and phosphorylated α-syn, suggesting that most α-syn aggregates are phosphorylated. We found the same increase in phosphorylated aggregates in α-syn infected cells compared to α-syn cells (44.7% vs. 9.2%, $p<0.001$) (Fig. 43C, bottom right) indicating that most α-syn aggregates induced by short fibrils are phosphorylated.

The increment in endogenous α-syn aggregates in human neuroblastoma SH-SY5Y cell line stably over-expressing human α-syn was measured over passages (Fig. 50). We noticed that the immunofluorescent signal becomes brighter over passages (Fig. 50, P1 to P6). The corrected total cell fluorescence measurements revealed a steady increase in the signal of immuno-positive α-syn in either untransfected SH-SY5Y cell line (Fig. 43B) or SH-SY5Y cell line stably over-expressing human α-syn, whereas the signal derived from FLAG-tagged recombinant human α-syn short fibrils abruptly decreased over the first two passages (Fig. 43B and Fig. 50, P0 to P1).

Having studied the aggregation properties of recombinant human FLAG-tagged α-syn and its ability to infect human neuroblastoma SH-SY5Y cell line *in vitro*, we questioned whether this material would be suitable to induce aggregation of endogenous α-syn in murine cell lines. We employed several murine cell lines (see Materials and Methods) and for each one we performed the same analysis carried out with SH-SY5Y cells. In particular, we infected mouse hypothalamic GT1 cell lines. As shown in Fig. 51, GT1 cells were exposed to human α-syn short fibrils following the same procedure applied to SH-SY5Y cell line. In GT1 cell line, expression of endogenous mouse α-syn was low and, as expected, human α-syn was missing (Fig. 51). A signal derived from immuno-positive human α-syn short fibrils was visible at early passages (P0 to P1, Fig. 51, in red) but it was absent in subsequent passages (P2 to P4, Fig. 51). At later passages, there was a marked increase in granular immuno-positive mouse α-syn signal (P3 to P4, Fig. 51, in green). Again, the corrected total cell fluorescence measurements showed a steady increase in the signal of immuno-positive mouse α-syn, whereas that derived from FLAG-tagged recombinant human α-syn short fibrils abruptly decreased over the first two passages (Fig. 51, graph).

The presence of aggregated endogenous mouse α-syn in infected GT1 cell line was evaluated using ThS to assess the extent of binding to β-sheet-rich structures such as amyloids (Fig. 52B).

Based on these premises, we attempted *in vivo* inoculation of human α-syn short fibrils in wild-type CD-1 mice. One-hundred-twenty-six days after the injection, most animals in group (iii) (n=5) injected with human α-syn short fibrils exhibited some behavioral abnormalities, including reduced growth rates, which mostly led to less mobility and curiosity though mainly related to olfactory tasks. After the treatment, the general condition of mice injected with α-syn short fibrils was worse than that of all other mouse groups ($p<0.05$, Fig. 53). The most striking difference was observed between general condition score of α-syn short fibrils and the control group ($p<0.05$). Indeed, as shown in Fig. 53, compared to the control group, mice injected with α-syn short fibrils exhibited significant physiological and behavioral differences, detailed as follows: lower ponderal growth ($p<0.01$), worse general condition ($p<0.05$), altered spontaneous behavior ($p<0.02$), partially impaired auditory sensory responses ($p<0.05$), poorer performance in vertical and upside-down grid tests ($p<0.05$). We also evaluated the general pathological condition of these animals. Fig. 53 shows the clear pathogenetic effect and characteristics of α-syn short fibrils compared to the control group, and all other molecular assembly and PBS control injected animals ($p<0.001$). The pathological score is significantly worse not only in the comparison between α-syn short fibrils and control group ($p<0.001$) but also between α-syn short fibrils and α-syn oligomers ($p<0.001$), as well as between α-syn short fibrils and α-syn long fibrils ($p<0.02$).

Even though none of the animals belonging to groups (i), (ii), (iv) and (v) showed any behavioral alteration, all mice were sacrificed and the brains were analyzed neuropathologically and immunohistochemically.

Paralleling the behavioral abnormalities in α-syn short fibrils injected mice, immunohistochemically we detected focal intraneuronal accumulation of α-syn (LB-like pathology) in neurons of specific brain regions, in particular in amygdala and cerebral cortex. These pathological inclusions were localized both in the perikarion and in the neurites, and were more clearly identifiable by immunostaining for phosphorylated α-syn (Fig. 44A-C). No immunodecoration for phosphorylated α-syn was detected in mice inoculated with monomers, oligomers, or long fibers of α-syn (Fig. 44D-F).

After establishing that α-syn short fibrils were able to induce behavioral changes and consequently LB-like pathology in injected mice, we attempted a second passage using total brain homogenates. Again we used CD-1 wild-type mice and followed the same inoculation procedures as in the first passage. In this experiment, the incubation period in CD-1 mice inoculated with brain homogenate of mice with α-syn short fibrils was 402±106 days post inoculation (dpi) (Fig. 45, panel A). Therefore, at this passage, this isolate exhibited a significantly different incubation time from mice inoculated with human α-syn short fibrils. This extension in incubation time may be due to the amount of α-syn prions formed at the first passage. Control mice were sacrificed at 502 dpi, which correspond to the end of the experiment. We assessed the behavioral changes over the whole duration of the experiments. The inoculated mice showed significantly altered behavior and motor function (Fig. 45, panel B). We performed all tests up to 502 dpi, when all mice, including controls, showed no significant differences in the grid tests. In these tests, impairment is a phenomenon mostly related to aging problems. All behavior and motor tests were carried out following the standard scoring

evaluations of the animals' health with particular focus on neurological symptoms. In terms of general health conditions, similarly to short fibril-inoculated mice on first passage, the brain homogenate-inoculated mice showed decreased mobility and curiosity after 131 dpi, sometimes even no curiosity at all, and paralysis in some cases. Significant changes were found first by tail-suspension tests. After 118 dpi, inoculated mice showed hind-leg clasping reflex (Fig. 54). This is a marker of disease progression in a number of mouse models of neurodegeneration [733]. Moreover, infected mice clearly showed body and tail rigidity, and kyphosis (Fig. 54). Kyphosis is a characteristic dorsal curvature of the spine regarded as a common sign of neurodegenerative disease in mouse models [734]. Kyphosis is caused by a loss of muscle tone in the spinal muscles as a consequence of neurodegeneration. Most likely symptoms resembling PD are related to open-field activity. Inoculated mice were less curious and exhibited an awkward and shuffling gait, barely lifting their feet off the ground, with short steps and slow movement. Gait is a measure of coordination and muscle function. These infected mice showed tremor, lowered pelvis, or feet pointing away from the body during locomotion (duck feet) (Fig. 54). During the tests with the grid, aimed at evaluating the levels of impaired motor coordination and balance, injected mice performed poorly on wire-hang test, a complementary measure of motor strength and coordination. Impairment was confirmed by significant higher scores in walking on the grid and equilibrium tasks (Fig. 45, panel B) in comparison with controls. All these changes in normal behavior indicate that mice infected with human α-syn mouse passaged prions maintained the behavioral abnormalities from first passage. During aging, infected mice showed symptoms resembling those of PD.

The level of α-syn in the CNS depends on the balance between the rates of α-syn synthesis, aggregation and clearance [642]. We noticed that the level of α-syn increased in infected mice, in comparison with the controls, at both first and second passages (Fig. 45, panel C). A single inoculation with small amounts of synthetic human α-syn short fibrils in the *subtantia nigra pars compacta* of wild-type CD1 mice led to aggregation of monomers. In prion diseases the seeding effect is the conveyance of prions from animal to animal [653]. By using an amyloid seeding assay analogous to that developed for prions [372], α-syn prions containing brain homogenate were detected in both passages (Fig. 45, panel D, left) by elimination of the lag phase of aggregate growth. The accelerated fibril formation (1.99 +/- 0.3 compared to 0.86 +/- 0.25 hours, Fig. 45, panel D, right) indicated the presence of mouse-passaged synthetic human α-syn prion isolates.

In the mice of the second passage, immunohistochemistry for phosphorylated α-syn was negative. However, marked and diffuse microglial activations were detected. Cells labeled by the microglial marker Iba1 were numerous in the cerebral cortex and hippocampus, and their activation was revealed by cytoplasmic enlargement and increased number of labeled ramified processes (Fig. 44H). Mild astrogliosis was also present.

In the brain of mice of the first and second passages, pretreatment with proteinase K abolished α-synuclein immunoreactivity as in normal control mice (Fig S10).

Similarly, the comparison of the different mice groups by histology and immunostaining for tirosine hydroxylase (TH) did not reveal neuronal loss or reduction of TH immunoreactivity (Fig. 56).

In conclusion, in this work we show that recombinant human α-syn can adopt a conformation that is able to recruit cellular α-syn in either human or mouse cell lines and convert the endogenous α-syn protein, regardless of the species, into molecular assemblies that replicate and accumulate *in vitro*. This event is paralleled by the introduction of post-translation modifications such as phosphorylation at position S129, a hallmark of pathological α-syn.

A single inoculation of these molecular species, such as α-syn short fibrils in the *substantia nigra pars compacta* of wild-type CD-1 mice, can induce α-syn aggregation, accumulation and phopshorylation *in vivo*. This event has been described as a prion-like spreading in the CNS of mice [587] a mechanism similar to that occurring in humans [627]. Based on the results presented in this work, we propose that the mechanism of α-syn aggregation, replication and accumulation is *bona fide* that effected by prions, since second passage experiments in mice show behavioral changes, microglial activation in CNS, α-syn accumulation and seeding properties analogous to prion disorders. As for synthetic prions, inoculation of recombinant prion protein amyloid fibrils into wild-type mice will eventually lead to new prion strains only after several passages [376]. It is therefore conceivable that, in our studies, subsequent passages in wild-type CD-1 mice may also lead to the isolation of the first biologically cloned α-syn prions.

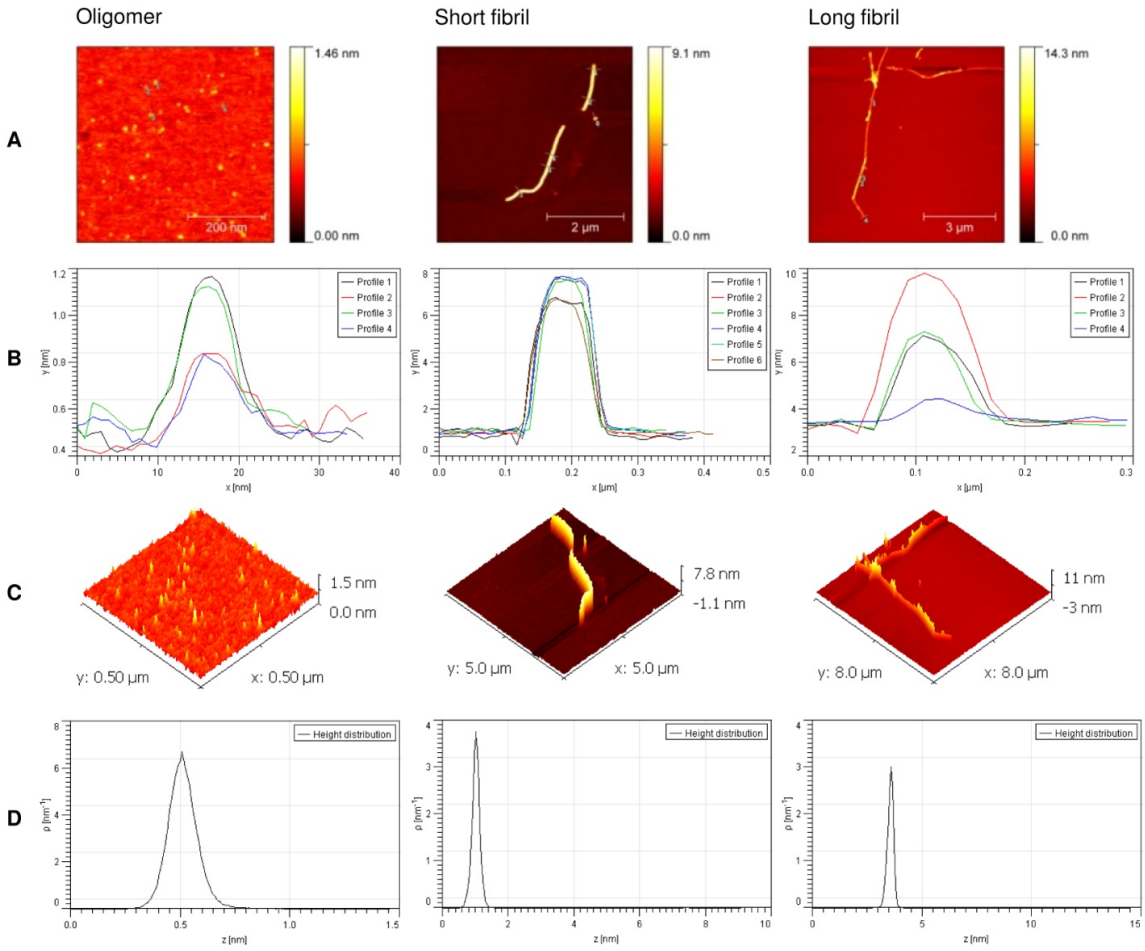

Figure 42. Recombinant human α-syn was converted *in vitro* into different β-sheet-rich structures (oligomer, short and long fibrils). AFM imaging analysis was performed at the end of the fibrilization reactions. AFM scan topographical images of α-syn deposited on mica surface (A). AFM height profiles along the numbered lines in topographical images (B). The profile reflects the lines as numbered in the images. Three-dimensional representation of AFM topography images (C) and height distribution data obtained from the AFM images (D).

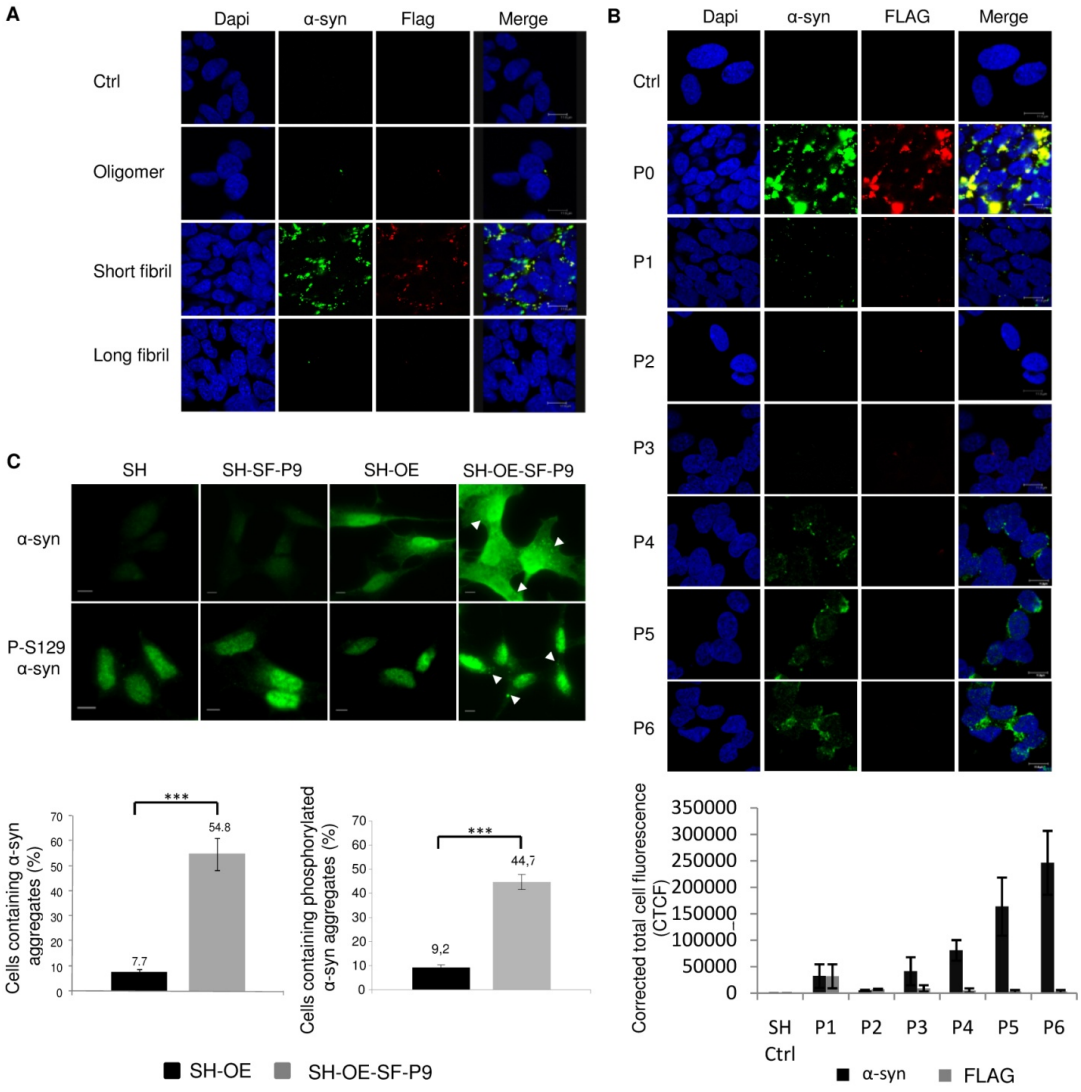

Figure 43. Internalization of FLAG-α-syn amyloids into neuroblastoma cells SH-SY5Y (A). α-Syn deposition (green) was detected by anti human α-syn antibody. Immunofluorescence was performed on cells exposed to FLAG-α-syn amyloids (oligomer, short fibril and long fibril) for 7 days. Bar, 11.9 μm. Immunofluorescence images showing induction of aggregation of endogenous human α-syn neuroblastoma cell line SH-SY5Y exposed to human FLAG-α-syn (B). Cells were infected with recombinant human FLAG-α-syn short fibril preparations. Cells were cultured over coverslips for each passage (P0 to P6). The deposition of exogenous short fibrils FLAG-α-syn (red) was detected by anti FLAG antibody. Human endogenous a-syn detected by anti human α-syn antibody (green). The nuclei were stained with DAPI (blue). Bar, 12 μm. Corrected total cell fluorescence (CTCF) from immunofluorescence imaging shows the induction of endogenous α-syn in neuroblastoma cell line SH-SY5Y infected human α-syn short fibrils during the passages (Bottom panel). Infection with human α-syn short fibrils induces aggregation of α-syn in stably transfected SH-SY5Y cells over-expressing human α-syn (C). (Top panel) Presence of phosphorylated α-syn aggregates in α-syn short fibrils infected SH-SY5Y cells over-expressing α-syn passage 9. From left to right: neuroblastoma SH-SY5Y (SH), SH-SY5Y infected with human α-syn short fibrils passage 9 (SH-SF-P9), SH-SY5Y over-expressing α-syn (SH-OE) and SH-SY5Y over-expressing α-syn infected with human α-syn short fibrils (SH-OE-SF-P9). Cells were immunolabeled with α-syn (green, upper panel) or phospho S129 α-syn (green, lower panel). Scale bars, 5 μm. Arrows point at α-syn aggregates. Images are representative of at least three independent experiments. (Bottom panel) High percentage of phosphorylated α-syn aggregates in SH-OE-SF-P9. Bar

diagram showing quantification of α-syn aggregates (left) and phospho S129 α-syn aggregates (right) in SH-OE cells and SH-OE-SF-P9 cells. ***, $p<0.001$ (Student *t* test, $n>150$ cells counted for each condition per experiment). Error bars represent the SEM.

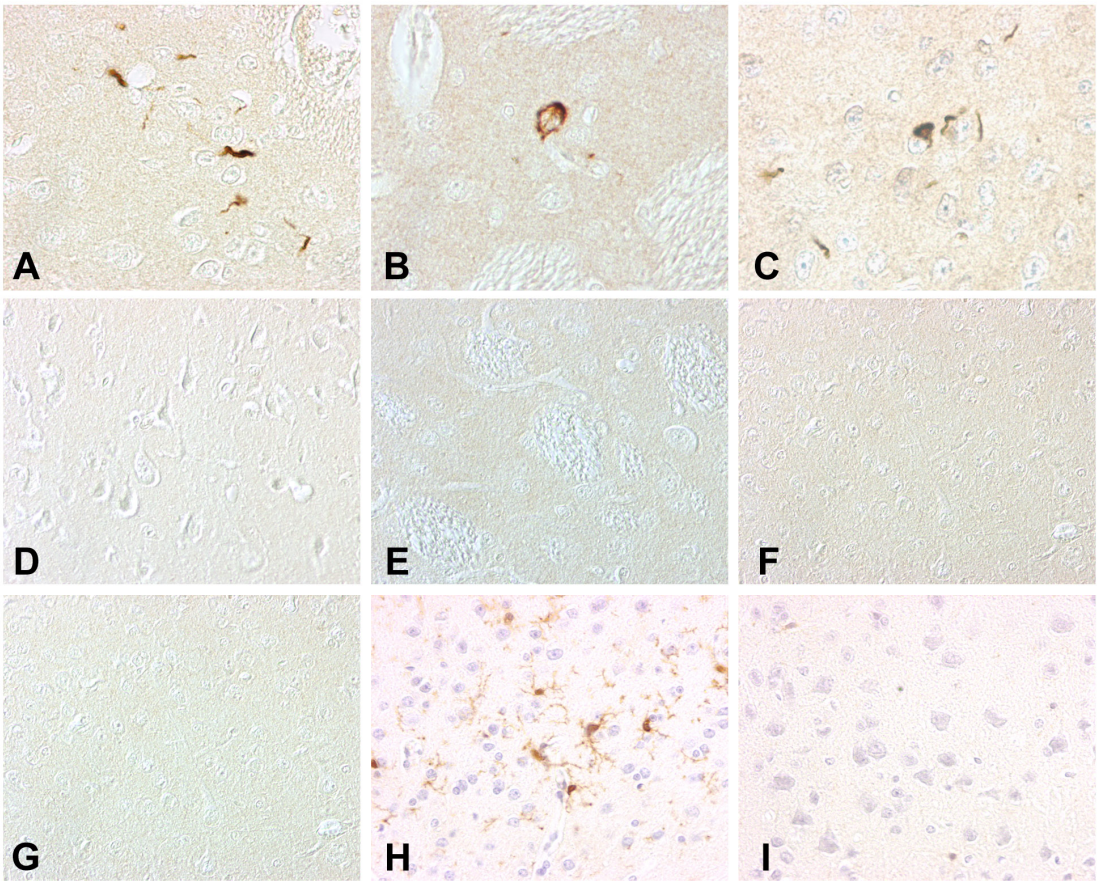

Figure 44. Immunostaining for phosphorylated α-syn (A, D, G: cerebral cortex; B, E: striatum; C-G: amygdala) and for Iba1 as marker of microglia activation (cerebral cortex: H, I). In the first passage (A-F), inclusions of phosphorylated α-synuclein are present in neuronal perykaria and neurites in the brain of mice inoculated with α-syn short fibrils (A-C), whereas they are absent in mice inoculated with other types of fibrils or PBS (the brain of a mouse that received α-syn long fibers is shown in D-F). In the second passage (G-I), inclusions of phosphorylated α-syn are not present in mice inoculated with the brain homogenate that received α-syn short fibrils (G) but marked and diffuse microglial activation was detected (H) whereas this was absent in the control mice (I). Magnification: 40x in all panels.

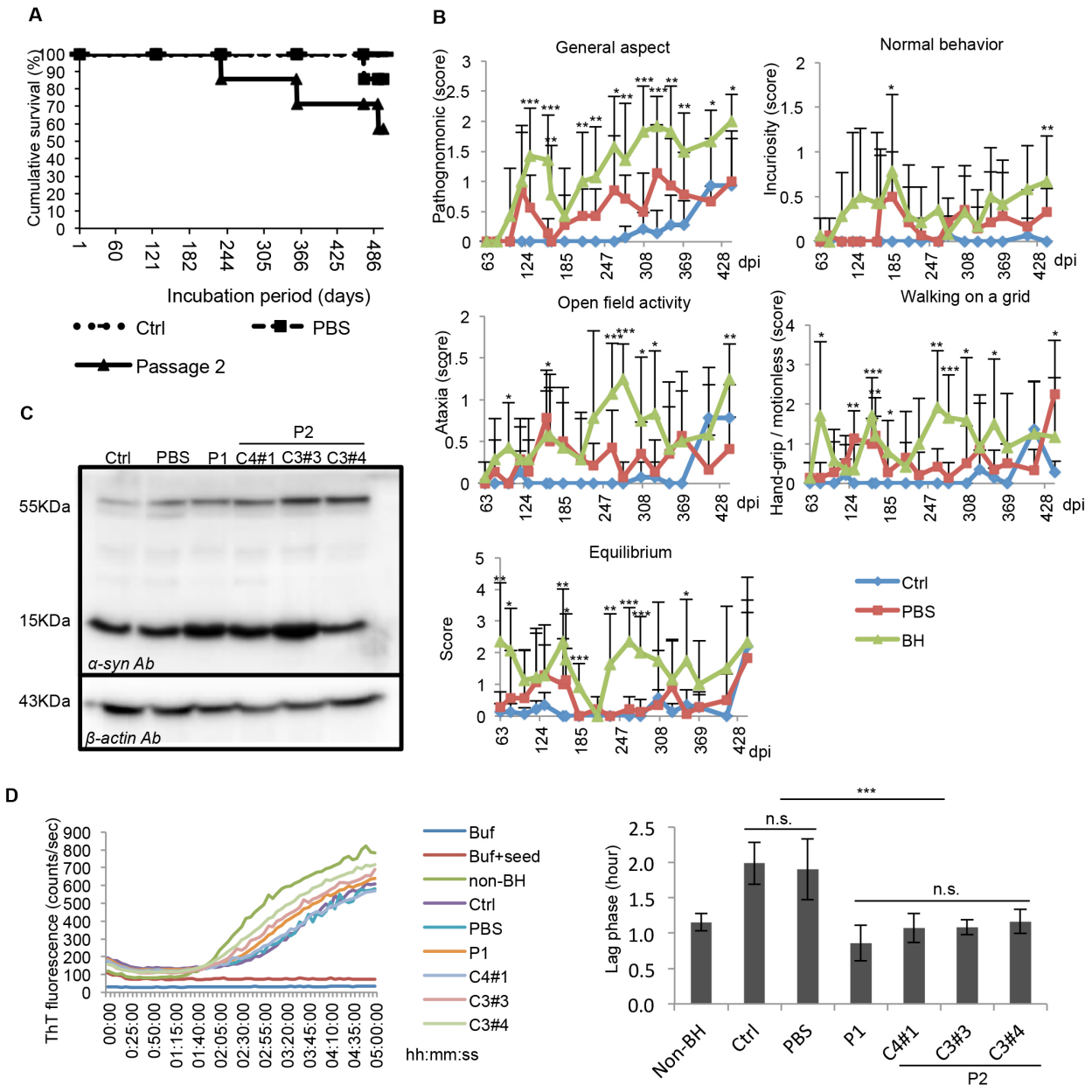

Figure 45. Survival curve of wild-type CD1 mice inoculated with short fibril-injected brain homogenate from passage 1 (A). Behavioral assessment of CD1 WT mice (*N* = 7 mice per group) after a single unilateral inoculation of brain homogenate (BH) from short fibril-inoculated mice at first passage into the *substantia nigra pars compacta* (B). BH-injected mice, as well as age-matched non-injected and PBS-injected CD1 mice are also shown. Data are mean values ±SD; (*), p<0.05; (**), p<0.01; (***), p<0.001. Western blotting of brain homogenate of CD1 mice from first (P1) and second passages (P2) shows increasing α-syn levels in comparison with the controls, exposed by anti α-syn antibody staining (C). Brain homogenate (BH) containing mouse α-syn prions from first passage (P1, short fibril-injected mice) and second passage (P2, P1 BH-injected mice) can seed and facilitate amyloid formation of recombinant mouse α-syn (recMo-α-syn), (D). As control, buffer only (buf), buffer plus BH of P1 without recMo-α-syn (buf+seed), BH of non-injected mice (Ctrl) and PBS-infected mice (PBS) were added similarly. Seeding reactions with infected BH (n=5; ***, p<0.001) significantly shorten the mean lag phase (right panel) or period before ThT fluorescence rises above background (left panel).

Supplementary Figures

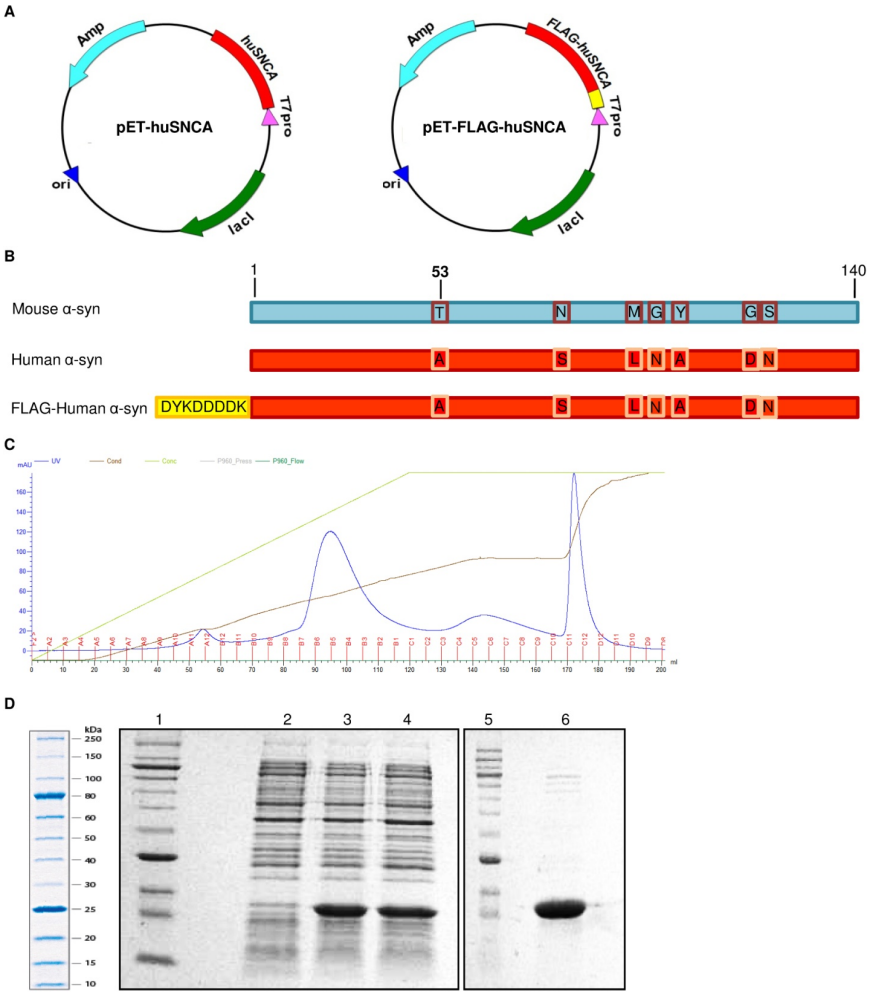

Figure 46. Plasmids used for expressing human α-syn and FLAG-human α-syn in *E. coli* BL21(DE)3 (A). Homology comparison between mouse α-syn and human α-syn, highlighting amino acid substitutions (B). Typical chromatogram obtained from human α-syn protein purification by anion-exchange chromatography with HiTrap Q Sepharose Fast Flow column (C). The protein was eluted with a 0-0.5 M NaCl gradient in 20 mM Tris pH8.0. Fractions B7-B2 correspond to purified protein. Expression of recombinant human α-syn protein (D), 15% SDS-PAGE. Lane 1 and 5, molecular mass marker; lane 2, whole cell extract before IPTG induction; lanes 3 and 4, cell extract after IPTG induction: 5 hours (lane 3), overnight induction (lane 4); lane 6, purified α-syn protein.

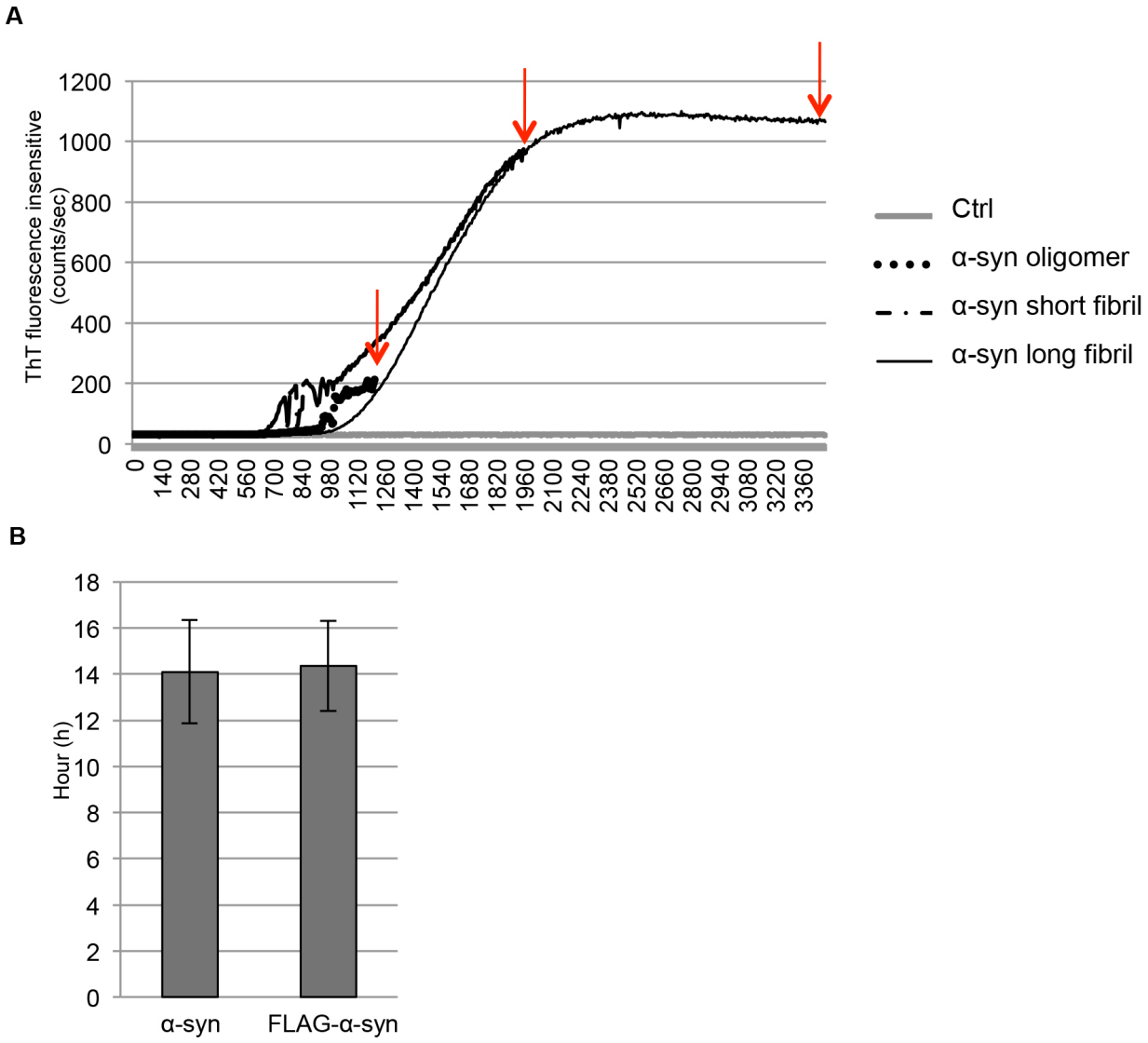

Figure 47. *In vitro* conversion of recombinant human α-syn into different β-sheet-rich structures (oligomers, short and long amyloid fibrils). The kinetics for the formation of β-sheet-rich structure: human α-syn oligomer (dotted line), human α-syn short fibrils (dashed line) and human α-syn long fibrils (solid line) (A). Lag phase, in hours, of all β-sheet structure preparations (B) was measured by thioflavin T assay. Lag phase distribution of α-syn and FLAG-α-syn amyloid preparations showed no difference (P>0.5).

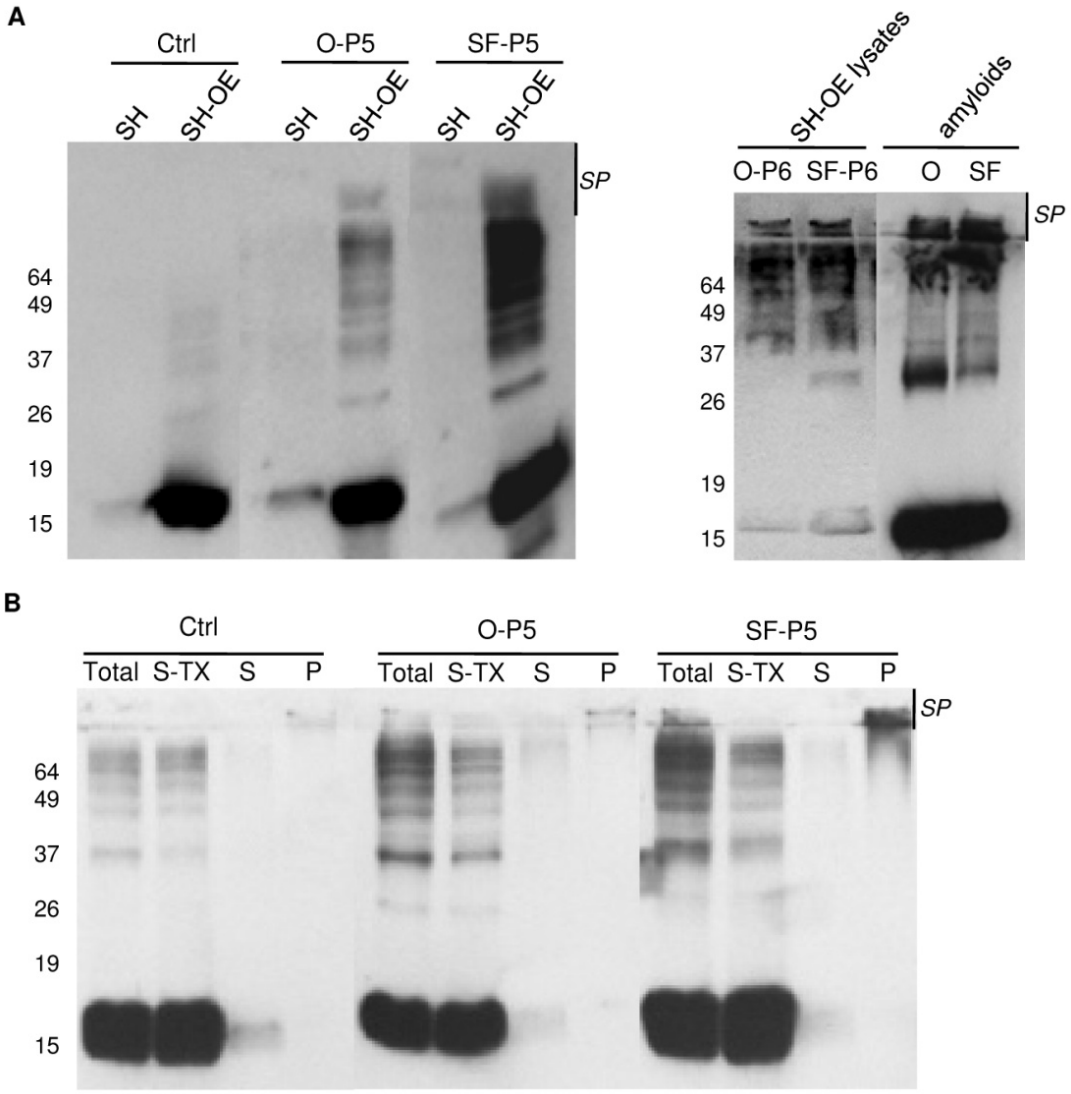

Figure 48. Aggregation of α-syn in dopaminergic human cell lines (SH: neuroblastoma cell line SH-SY5Y, SH-OE: neuroblastoma cell line SH-SY5Y overexpressing human α-syn) infected with recombinant human α-syn amyloid preparations (O: oligomeric α-syn, SF: short fibril α-syn) at fifth passage (P5). Western blotting of cell lysates; OP5: α-syn oligomer infected-cells at fifth passage, SFP5: α-syn short fibril infected-cells at fifth passage (A, left panel). Western blotting of aggregated analysis of treated and non-treated SH-OE cell lysates with α-syn amyloid; total: cell lysates, S-TX: supernatant fractions after treatment with 1% TritonX100, S: supernatant fractions after pellet was treated with S-TX with 2% SDS, P: pellet fractions after pellet was treated with S-TX with 2% SDS (B). Aggregation profiles of α-syn in SH-OE infected with recombinant human α-syn amyloid preparations at sixth passage in comparison with original amyloids that were used for the infections. Western blotting exposed by anti α-syn antibody; OP6: α-syn oligomer infected-cells at sixth passage, SFP6: α-syn short fibril infected-cells at sixth passage, OA: oligomeric α-syn, SFA: short fibril α-syn. Anti α-syn antibody was used (A, right panel).

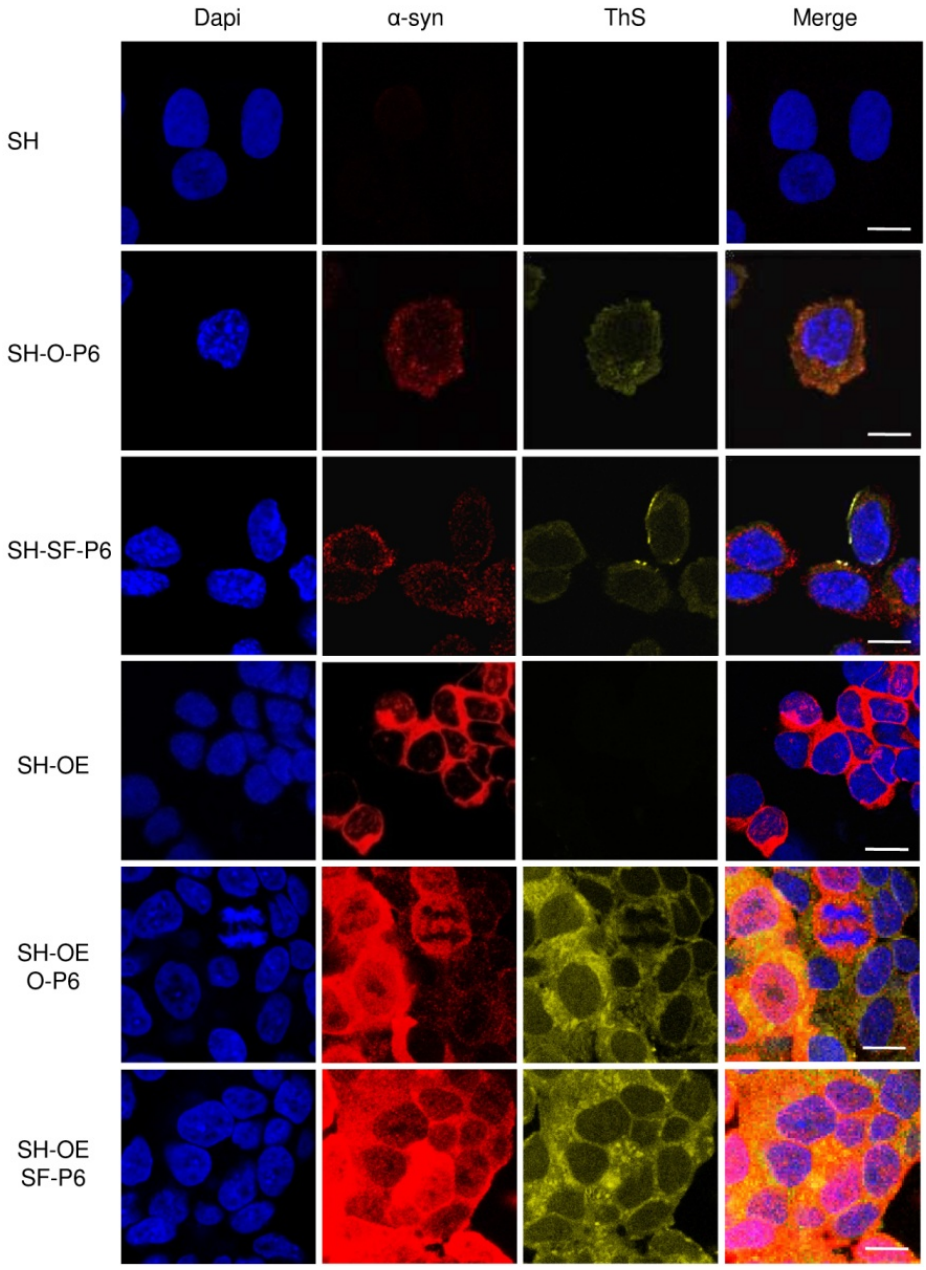

Figure 49. Immunofluorescence imaging of endogenous α-syn aggregation in neuroblastoma cell line SH-SY5Y(SH) and in SH-SY5Y over-expressing α-syn (SH-OE) incubated with α-syn oligomers and short fibril amyloid. Cells were infected with recombinant human α-syn amyloid preparations (O: oligomeric α-syn, SF: short fibril α-syn) at sixth passage (P6). The deposition and level of α-syn (red) in amyloid α-syn-infected cell lines after six passages were detected by anti α-syn antibody. The aggregation of a-syn was found by colocalization of immunoreactive α-syn and ThS binding costaining (yellow). The nuclei (blue) were stained with DAPI.

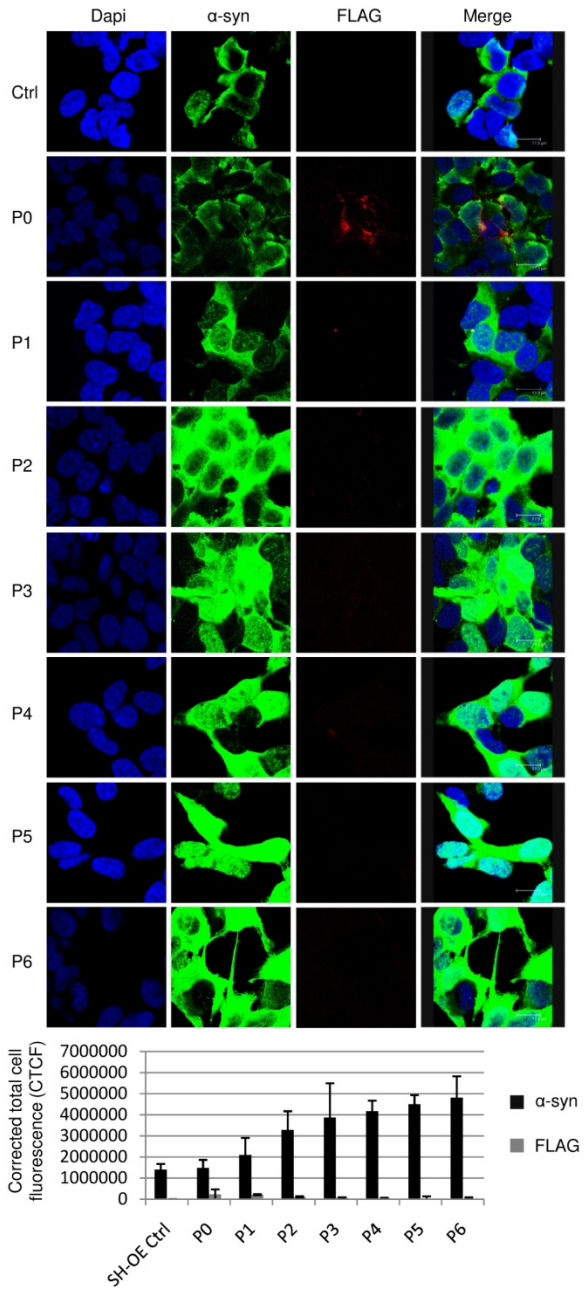

Figure 50. Immunofluorescence images showing induction of aggregation of endogenous human α-syn neuroblastoma cell line SH-SY5Y overexpressing human α-syn exposed to human FLAG-α-syn. Cells were infected with recombinant human FLAG-α-syn short fibril preparations. Cells were cultured over coverslips for each passage (P0 to P6). The deposition of exogenous short fibrils FLAG-α-syn (red) was detected by anti FLAG antibody. Human endogenous α-syn detected by anti human α-syn antibody (green). The nuclei were stained with DAPI (blue). Corrected total cell fluorescence (CTCF) from immunofluorescence imaging shows the induction of endogenous α-syn in SH-OE (neuroblastoma cell line SH-SY5Y overexpressing human α-syn) infected human α-syn short fibril during the passages.

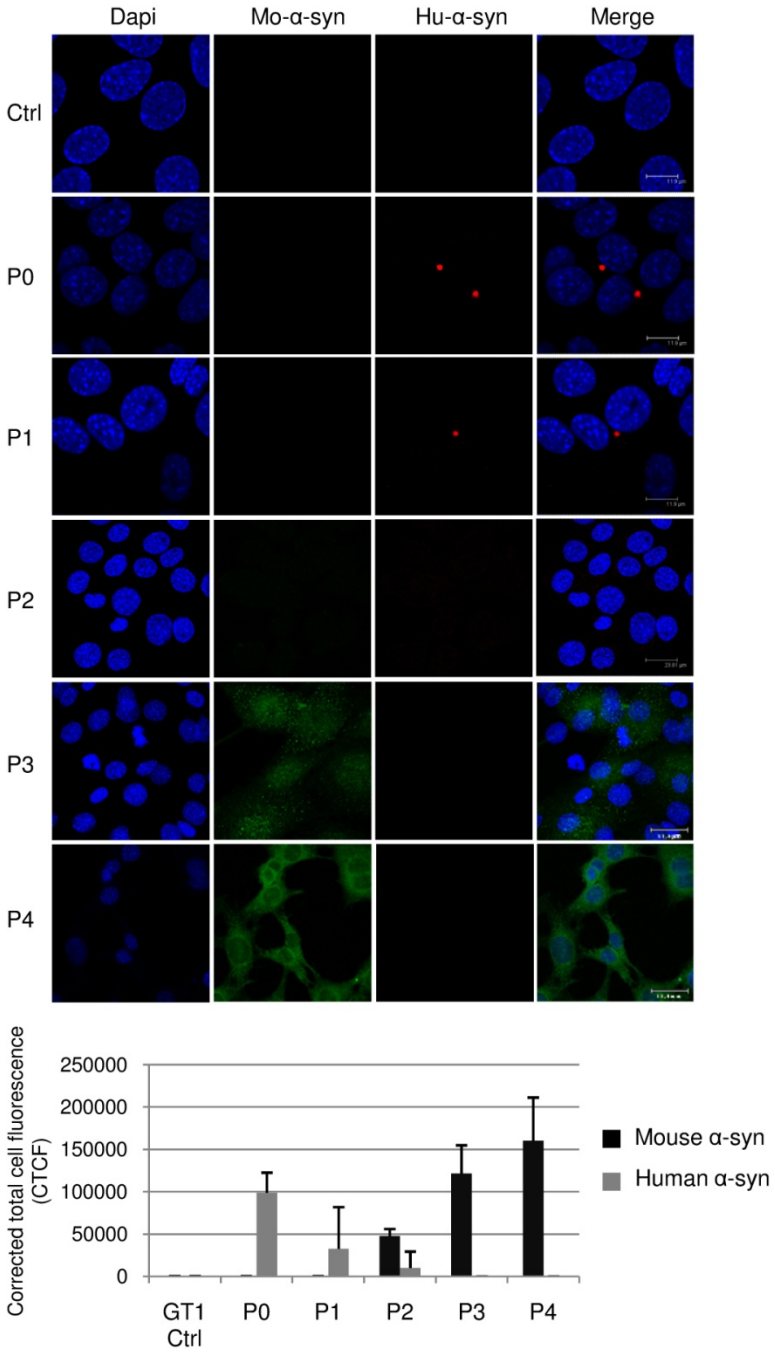

Figure 51. Immunofluorescence imaging shows the induction of endogenous mouse α-syn in GT1 infected human α-syn short fibrils during the passages. Cells were infected with recombinant human α-syn short fibril preparations that were cultured in coverslips for each passage (P). The deposition of exogenous short fibril human α-syn (red) in cells was detected by anti human α-syn antibody. Mouse endogenous α-syn was detected by anti mouse α-syn antibody (green). The nuclei were stained with DAPI (blue). Control bars, P0 and P1 are 12 μm; P2, P3, P4 are 24 μm.

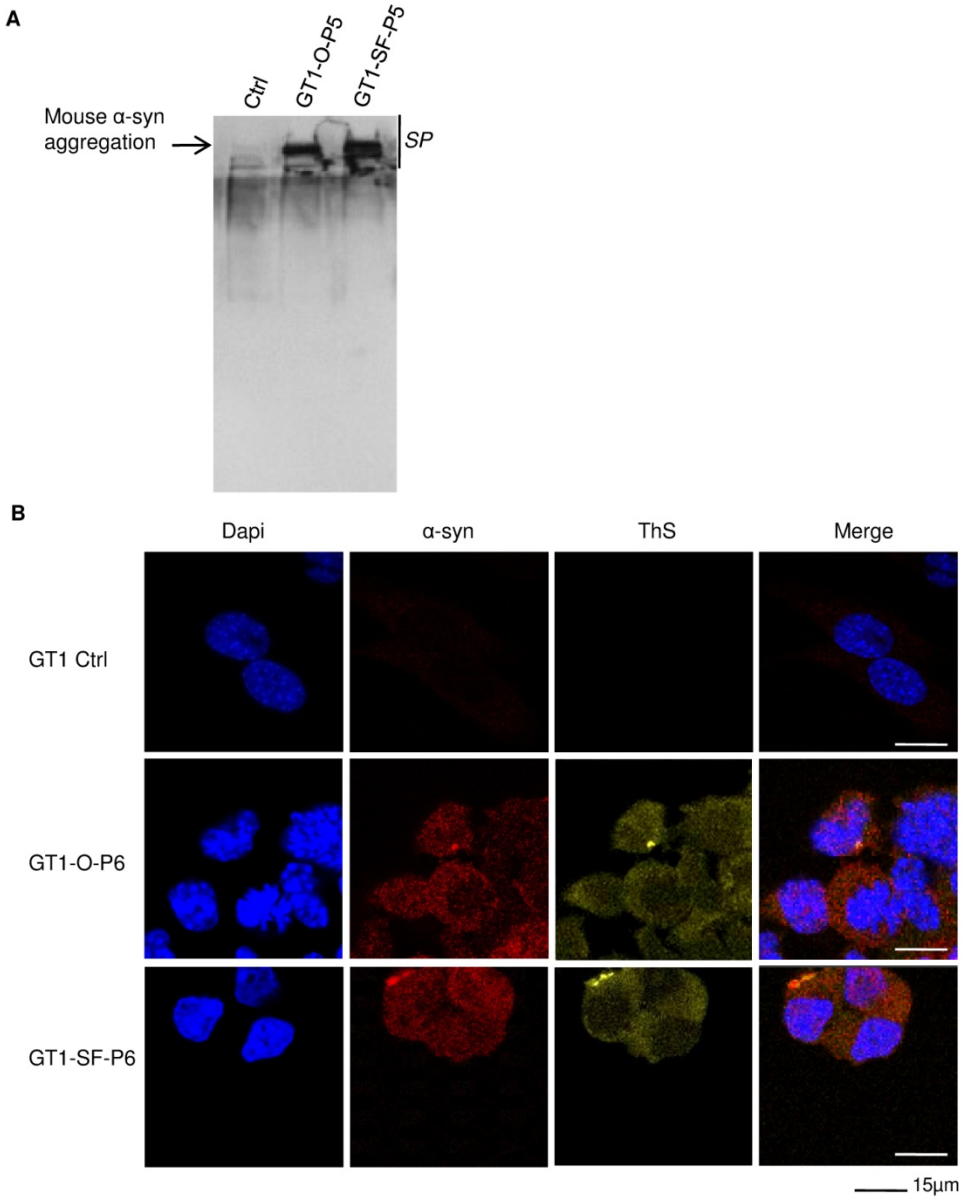

Figure 52. Aggregation of α-syn mouse cell lines, GT1 (mouse hypothalamic GT1) infected with recombinant human α-syn amyloid preparations (O: oligomeric α-syn, SF: short fibril α-syn) at fifth passage (P5). Western blotting of cell lysates exposed to anti α-syn antibody; OP5: human α-syn oligomer infected-cells at fifth passage, SFP5: human α-syn short fibril infected-cells at fifth passage (A). Immunofluorescence imaging shows the aggregation of mouse α-syn in GT1 α-syn amyloid-infected cell lines. Cells were infected with recombinant human α-syn amyloid preparations (O: oligomeric α-syn, SF: short fibril α-syn) at sixth passage (P6). The deposition and level of α-syn (red) in amyloid α-syn-infected cell lines after six passages were detected by anti mouse α-syn antibody. The aggregation of a-syn was found by colocalization of immunoreactive α-syn and ThS binding costaining (yellow). The nuclei were stained with DAPI (blue) (B).

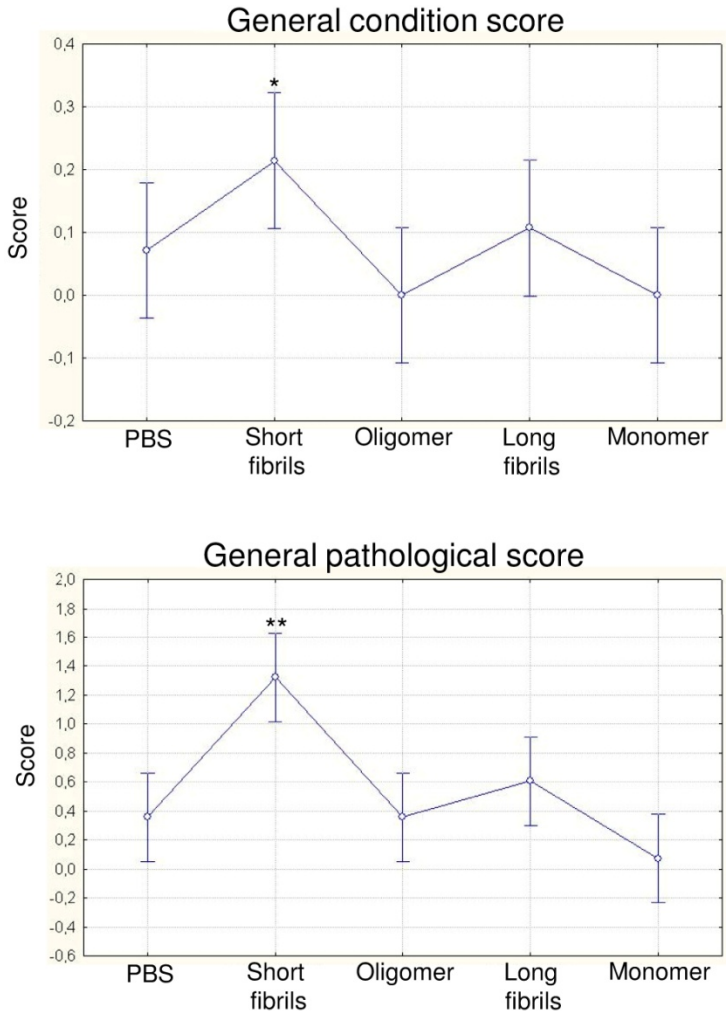

Figure 53. Behavioral assessment of CD1 WT mice (*N* = 7 mice per group) after a single unilateral inoculation of α-syn amyloid preparations (monomer, oligomer, short fibrils and long fibrils) into the *substantia nigra pars compacta*. Results of animals on the general health condition (top panel) and general pathological score (bottom panel) show significant change in behavior of short fibril-injected but not of other amyloid-injected or control mice. Data are mean values ±SD; (*), $p<0.05$; (**), $p<0.01$.

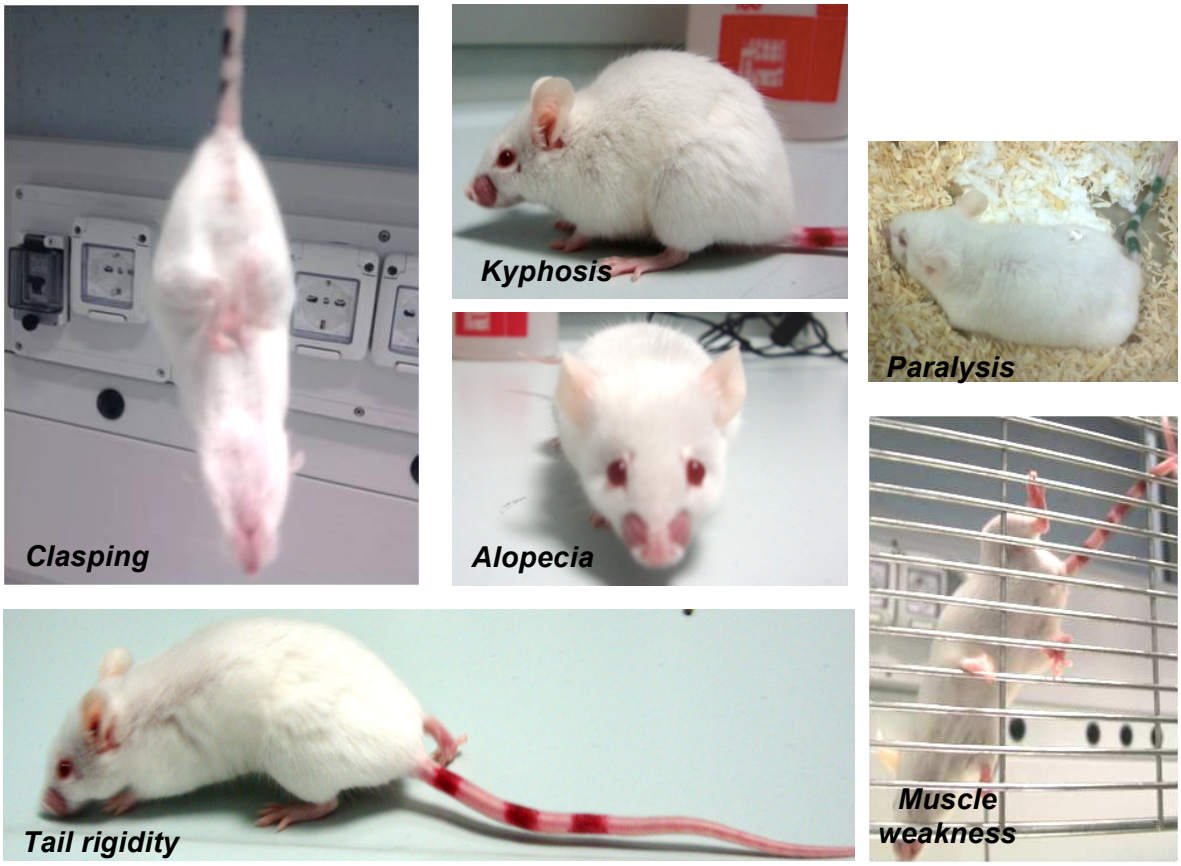

Figure 54. Behavioral changes of second passage mice after 89 dpi (clasping, alopecia), 152 dpi (tail rigidity), 257 dpi (muscle weakness and kyphosis) and 2 days before death (paralysis).

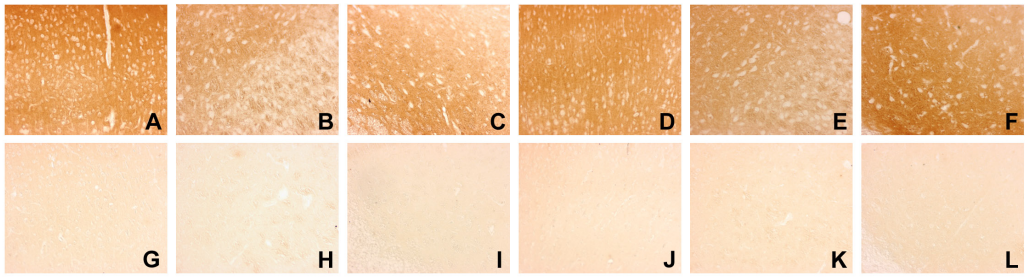

Figure 55. Protease digestion and immunostaining for α-syn (4D6 antibody) of the brains of control mice inoculated with buffer (A, B, C, G, H, I) and of second passage mice inoculated with the brain homogenate that received α-syn short fibrils (D, E, F, J, K, L). Immunostaining of sections including the frontal cortex (A, D, G, J), striatum (B, E, H, K) and *substantia nigra* (C, F, I, L) was carried out without (A-F) or after proteinase K digestion (G-L). No difference in the pattern of diffuse, finely granular immunolabeling was observed between control mice injected with buffer (A-C) and second passage mice inoculated with the brain homogenate that received α-syn short fibrils (D-F). Pretreatment with proteinase K abolished α-syn immunoreactivity in the two groups of mice. Magnification: 20x in all panels.

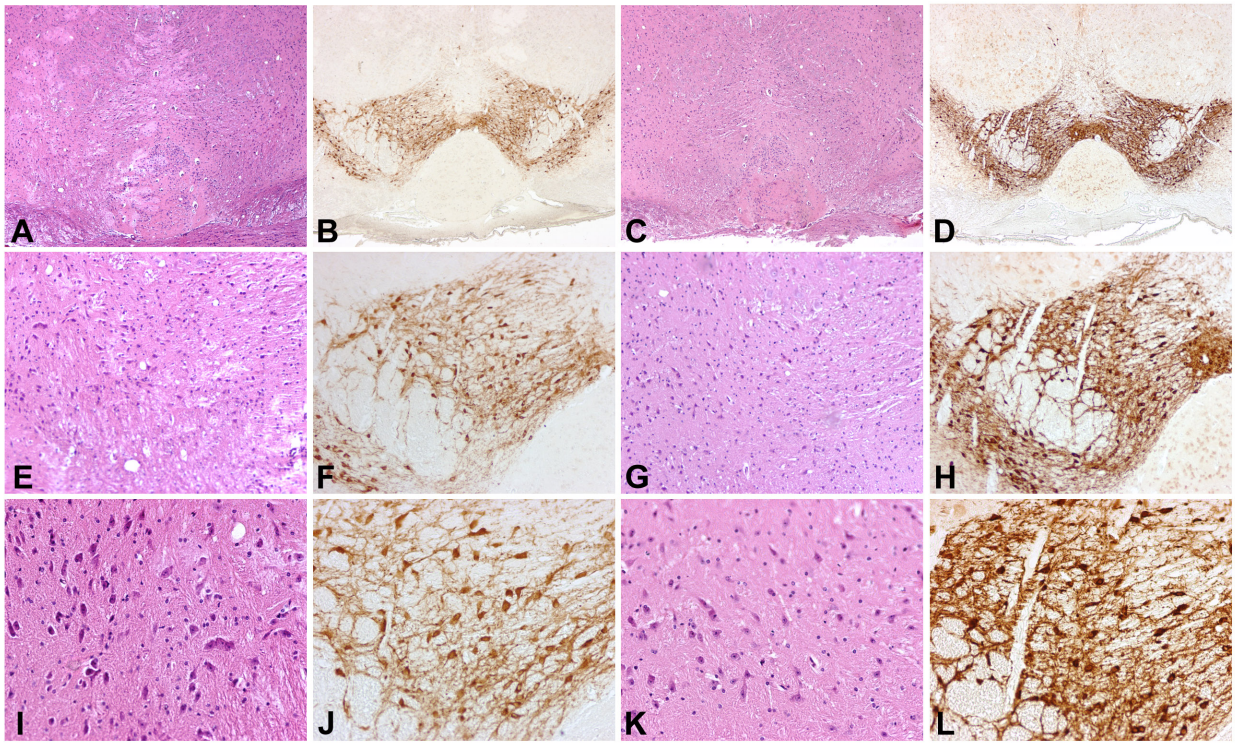

Figure 56. Hematoxylin and eosin stain and immunostaining for tirosine hydroxylase of the *substantia nigra* of the brains of control mice inoculated with buffer (A, B, C, G, H, I) and of second passage mice inoculated with the brain homogenate that received α-synuclein short fibrils (D, E, F, J, K, L). No difference is detectable between the two groups of mice, ruling out neuronal loss or reduction of TH immunoreactivity in the *substantia nigra* of second passage mice inoculated with the brain homogenate that received α-syn short fibrils. Magnification: A-D 4x; E-H 10x; I-L 20x.

CONCLUSION AND PERSPECTIVES

- The first part of my thesis reports the generation of variant putative infectious prion amyloids with different structural conformations using only purified recombinant prion protein. Two conversion processes, with different amyloid formation mechanisms, were applied. Amyloid preparations were infected in GT1 and N2a cell lines in order to elucidate the conformational diversity of pathological recPrP amyloids and their biological activities, as well as to gain novel insights in characterizing molecular events involved in mammalian prion conversion and propagation. This study employed a novel cell culture assay as a fast screening methodology to characterize putative infectious materials.

The experimental results we obtained led us to the following conclusions:

- Following two different *in vitro* protocols, one under reduction-oxidation (REDOX) and the other under non-REDOX conditions, recMoPrP converted to amyloid fibrils without any seeding factor. In different biochemical and biophysical environments, recMoPrP(23-231) converted to distinct amyloidal forms. Notably, the amyloid fibrils obtained using the REDOX process were organized in intermolecular structures.

- A large number of amyloid preparations are able to induce the conformational change of endogenous PrP^{C} to harbor several distinctive proteinase-resistant PrP forms and aggregation in neuronal cell lines.

- The seeding ability of amyloid formations in cultured cells may also depend on their states at the end of fibrilization.

- *De novo* PrP^{Sc} from amyloid infected cell lines can be detected and replicated in PMCA.

Our synthetic materials have different conformational structures and prionic properties such as PK resistance, infectivity in cell line and propagation, however they need to be further investigated *in vivo*. A recent study in synthetic prions shows that synthetic prions can assume multiple intermediate conformations before converging into one conformation optimized for *in vivo* propagation [735]. We are currently carrying on *in vivo* experiments on transgenic and wild-type mice in order to study the functional/structural relationship of mammalian prions, and test whether preparations that are structurally distinct from the initial amyloid preparations can encipher different biochemical and biological properties of the adapting strains.

- In the second part of my thesis, I focused on α-syn protein, which is involved in synucleinopathies, especially Parkinson's disease. Through a methodology used to obtain synthetic mammalian prions, we tested whether recombinant human α-syn amyloids can infect neuronal cell lines *in vitro*, and wild-type mice *in vivo*.

In these experiments we established that:

- A single exposure to β-sheet-rich structures of recombinant human α-syn was sufficient to induce aggregation of endogenous α-syn in untransfected human neuroblastoma SH-SY5Y cells.

- Only short fibrils of α-syn efficiently induced the endogenous α-syn to aggregate. After seven days in culture, α-syn short fibrils are able to seed aggregation of over-expressed α-syn in transfected SHSY5Y. Moreover, most α-syn aggregates induced by short fibrils are phosphorylated.

- Human α-syn short fibrils can induce aggregation of endogenous mouse α-syn in mouse hypothalamic GT1 cell line.

- A single inoculation of these molecular species, such as α-syn short fibrils in the *substantia nigra pars compacta* of wild-type CD-1 mice, can induce α-syn aggregation, accumulation and phosphorylation *in vivo.*

- Second passage experiments in mice show behavioral changes, microglial activation in CNS, α-syn accumulation and seeding properties analogous to prion disorders. The mechanism of α-syn aggregation, replication and accumulation is *bona fide* that effected by α-syn prions.

REFERENCES

1. Eanes ED, Glenner GG (1968) X-ray diffraction studies on amyloid filaments. J Histochem Cytochem 16: 673-677.
2. Geddes AJ, Parker KD, Atkins ED, Beighton E (1968) "Cross-beta" conformation in proteins. J Mol Biol 32: 343-358.
3. Dopson M, Baker-Austin C, Bond PL (2005) Analysis of differential protein expression during growth states of Ferroplasma strains and insights into electron transport for iron oxidation. Microbiology 151: 4127-4137.
4. Collinson SK, Parker JM, Hodges RS, Kay WW (1999) Structural predictions of AgfA, the insoluble fimbrial subunit of Salmonella thin aggregative fimbriae. J Mol Biol 290: 741-756.
5. Shewmaker F, McGlinchey RP, Thurber KR, McPhie P, Dyda F, et al. (2009) The functional curli amyloid is not based on in-register parallel beta-sheet structure. J Biol Chem 284: 25065-25076.
6. Hirota-Nakaoka N, Hasegawa K, Naiki H, Goto Y (2003) Dissolution of beta2-microglobulin amyloid fibrils by dimethylsulfoxide. J Biochem 134: 159-164.
7. Nilsson MR (2004) Techniques to study amyloid fibril formation in vitro. Methods 34: 151-160.
8. Zogaj X, Bokranz W, Nimtz M, Romling U (2003) Production of cellulose and curli fimbriae by members of the family Enterobacteriaceae isolated from the human gastrointestinal tract. Infect Immun 71: 4151-4158.
9. Dueholm MS, Nielsen SB, Hein KL, Nissen P, Chapman M, et al. (2011) Fibrillation of the major curli subunit CsgA under a wide range of conditions implies a robust design of aggregation. Biochemistry 50: 8281-8290.
10. McLaurin J, Yang D, Yip CM, Fraser PE (2000) Review: modulating factors in amyloid-beta fibril formation. J Struct Biol 130: 259-270.
11. Maji SK, Wang L, Greenwald J, Riek R (2009) Structure-activity relationship of amyloid fibrils. FEBS Lett 583: 2610-2617.
12. Kumar S, Walter J (2011) Phosphorylation of amyloid beta (Abeta) peptides - a trigger for formation of toxic aggregates in Alzheimer's disease. Aging (Albany NY) 3: 803-812.
13. Soto C (2003) Unfolding the role of protein misfolding in neurodegenerative diseases. Nat Rev Neurosci 4: 49-60.
14. Xue WF, Homans SW, Radford SE (2008) Systematic analysis of nucleation-dependent polymerization reveals new insights into the mechanism of amyloid self-assembly. Proc Natl Acad Sci U S A 105: 8926-8931.
15. Chiti F, Dobson CM (2006) Protein misfolding, functional amyloid, and human disease. Annu Rev Biochem 75: 333-366.
16. Glenner GG, Wong CW (1984) Alzheimer's disease: initial report of the purification and characterization of a novel cerebrovascular amyloid protein. Biochem Biophys Res Commun 120: 885-890.
17. Grundke-Iqbal I, Iqbal K, Quinlan M, Tung YC, Zaidi MS, et al. (1986) Microtubule-associated protein tau. A component of Alzheimer paired helical filaments. J Biol Chem 261: 6084-6089.

18. Spillantini MG, Schmidt ML, Lee VM, Trojanowski JQ, Jakes R, et al. (1997) Alpha-synuclein in Lewy bodies. Nature 388: 839-840.
19. DiFiglia M, Sapp E, Chase KO, Davies SW, Bates GP, et al. (1997) Aggregation of huntingtin in neuronal intranuclear inclusions and dystrophic neurites in brain. Science 277: 1990-1993.
20. Bruijn LI, Houseweart MK, Kato S, Anderson KL, Anderson SD, et al. (1998) Aggregation and motor neuron toxicity of an ALS-linked SOD1 mutant independent from wild-type SOD1. Science 281: 1851-1854.
21. Bolton DC, McKinley MP, Prusiner SB (1982) Identification of a protein that purifies with the scrapie prion. Science 218: 1309-1311.
22. Kayed R, Head E, Thompson JL, McIntire TM, Milton SC, et al. (2003) Common structure of soluble amyloid oligomers implies common mechanism of pathogenesis. Science 300: 486-489.
23. Thies W, Bleiler L (2011) 2011 Alzheimer's disease facts and figures. Alzheimers Dement 7: 208-244.
24. Wenk GL (2003) Neuropathologic changes in Alzheimer's disease. J Clin Psychiatry 64 Suppl 9: 7-10.
25. Tiraboschi P, Sabbagh MN, Hansen LA, Salmon DP, Merdes A, et al. (2004) Alzheimer disease without neocortical neurofibrillary tangles: "a second look". Neurology 62: 1141-1147.
26. Nelson PT, Braak H, Markesbery WR (2009) Neuropathology and cognitive impairment in Alzheimer disease: a complex but coherent relationship. J Neuropathol Exp Neurol 68: 1-14.
27. Duyckaerts C, Delatour B, Potier MC (2009) Classification and basic pathology of Alzheimer disease. Acta Neuropathol 118: 5-36.
28. Hashimoto M, Rockenstein E, Crews L, Masliah E (2003) Role of protein aggregation in mitochondrial dysfunction and neurodegeneration in Alzheimer's and Parkinson's diseases. Neuromolecular Med 4: 21-36.
29. Priller C, Bauer T, Mitteregger G, Krebs B, Kretzschmar HA, et al. (2006) Synapse formation and function is modulated by the amyloid precursor protein. J Neurosci 26: 7212-7221.
30. Turner PR, O'Connor K, Tate WP, Abraham WC (2003) Roles of amyloid precursor protein and its fragments in regulating neural activity, plasticity and memory. Prog Neurobiol 70: 1-32.
31. Hernandez F, Avila J (2007) Tauopathies. Cell Mol Life Sci 64: 2219-2233.
32. Selkoe DJ (2001) Alzheimer's disease: genes, proteins, and therapy. Physiol Rev 81: 741-766.
33. Goate AM (1997) Molecular genetics of Alzheimer's disease. Geriatrics 52 Suppl 2: S9-12.
34. Cummings CJ, Zoghbi HY (2000) Fourteen and counting: unraveling trinucleotide repeat diseases. Hum Mol Genet 9: 909-916.
35. Cattaneo E, Zuccato C, Tartari M (2005) Normal huntingtin function: an alternative approach to Huntington's disease. Nat Rev Neurosci 6: 919-930.
36. Davies SW, Turmaine M, Cozens BA, DiFiglia M, Sharp AH, et al. (1997) Formation of neuronal intranuclear inclusions underlies the neurological dysfunction in mice transgenic for the HD mutation. Cell 90: 537-548.

37. Abdel-Dayem HM, Radin AI, Luo JQ, Marans HY, Wong S, et al. (1998) Fluorine-18-fluorodeoxyglucose dual-head gamma camera coincidence imaging of recurrent colorectal carcinoma. J Nucl Med 39: 654-656.
38. Duyao M, Ambrose C, Myers R, Novelletto A, Persichetti F, et al. (1993) Trinucleotide repeat length instability and age of onset in Huntington's disease. Nat Genet 4: 387-392.
39. Scherzinger E, Lurz R, Turmaine M, Mangiarini L, Hollenbach B, et al. (1997) Huntingtin-encoded polyglutamine expansions form amyloid-like protein aggregates in vitro and in vivo. Cell 90: 549-558.
40. Uversky VN (2007) Neuropathology, biochemistry, and biophysics of alpha-synuclein aggregation. J Neurochem 103: 17-37.
41. Mohajeri MH, Kuehnle K, Li H, Poirier R, Tracy J, et al. (2004) Anti-amyloid activity of neprilysin in plaque-bearing mouse models of Alzheimer's disease. FEBS Lett 562: 16-21.
42. Valente EM, Abou-Sleiman PM, Caputo V, Muqit MM, Harvey K, et al. (2004) Hereditary early-onset Parkinson's disease caused by mutations in PINK1. Science 304: 1158-1160.
43. Aguzzi A (2003) Prions and the immune system: a journey through gut, spleen, and nerves. Adv Immunol 81: 123-171.
44. Haik S, Faucheux BA, Hauw JJ (2004) Brain targeting through the autonomous nervous system: lessons from prion diseases. Trends Mol Med 10: 107-112.
45. Collinge J (2001) Prion diseases of humans and animals: their causes and molecular basis. Annu Rev Neurosci 24: 519-550.
46. Collinge J, Sidle KC, Meads J, Ironside J, Hill AF (1996) Molecular analysis of prion strain variation and the aetiology of 'new variant' CJD. Nature 383: 685-690.
47. Parchi P, Zou W, Wang W, Brown P, Capellari S, et al. (2000) Genetic influence on the structural variations of the abnormal prion protein. Proc Natl Acad Sci U S A 97: 10168-10172.
48. Hill AF, Joiner S, Wadsworth JD, Sidle KC, Bell JE, et al. (2003) Molecular classification of sporadic Creutzfeldt-Jakob disease. Brain 126: 1333-1346.
49. Beck RW, Savino PJ, Schatz NJ, Smith CH, Sergott RC (1982) Plaque causing homonymous hemianopsia in multiple sclerosis identified by computed tomography. Am J Ophthalmol 94: 229-234.
50. Prusiner SB (1998) Prions. Proc Natl Acad Sci U S A 95: 13363-13383.
51. Geissen M, Krasemann S, Matschke J, Glatzel M (2007) Understanding the natural variability of prion diseases. Vaccine 25: 5631-5636.
52. Gambetti P, Kong Q, Zou W, Parchi P, Chen SG (2003) Sporadic and familial CJD: classification and characterisation. Br Med Bull 66: 213-239.
53. Parchi P, Giese A, Capellari S, Brown P, Schulz-Schaeffer W, et al. (1999) Classification of sporadic Creutzfeldt-Jakob disease based on molecular and phenotypic analysis of 300 subjects. Ann Neurol 46: 224-233.
54. Will RG (2003) Acquired prion disease: iatrogenic CJD, variant CJD, kuru. Br Med Bull 66: 255-265.
55. Ironside JW, Head MW (2004) Variant Creutzfeldt-Jakob disease: risk of transmission by blood and blood products. Haemophilia 10 Suppl 4: 64-69.

56. Brown P, Preece M, Brandel JP, Sato T, McShane L, et al. (2000) Iatrogenic Creutzfeldt-Jakob disease at the millennium. Neurology 55: 1075-1081.
57. Gajdusek DC, Zigas V (1957) Degenerative disease of the central nervous system in New Guinea; the endemic occurrence of kuru in the native population. N Engl J Med 257: 974-978.
58. Wadsworth TL, Bishop JA, Pappu AS, Woltjer RL, Quinn JF (2008) Evaluation of coenzyme Q as an antioxidant strategy for Alzheimer's disease. J Alzheimers Dis 14: 225-234.
59. Masters CL, Gajdusek DC, Gibbs CJ, Jr. (1981) Creutzfeldt-Jakob disease virus isolations from the Gerstmann-Straussler syndrome with an analysis of the various forms of amyloid plaque deposition in the virus-induced spongiform encephalopathies. Brain 104: 559-588.
60. Stewart LR, White AR, Jobling MF, Needham BE, Maher F, et al. (2001) Involvement of the 5-lipoxygenase pathway in the neurotoxicity of the prion peptide PrP106-126. J Neurosci Res 65: 565-572.
61. Hsiao K, Baker HF, Crow TJ, Poulter M, Owen F, et al. (1989) Linkage of a prion protein missense variant to Gerstmann-Straussler syndrome. Nature 338: 342-345.
62. Doh-ura K, Tateishi J, Sasaki H, Kitamoto T, Sakaki Y (1989) Pro----leu change at position 102 of prion protein is the most common but not the sole mutation related to Gerstmann-Straussler syndrome. Biochem Biophys Res Commun 163: 974-979.
63. Goldgaber D, Goldfarb LG, Brown P, Asher DM, Brown WT, et al. (1989) Mutations in familial Creutzfeldt-Jakob disease and Gerstmann-Straussler-Scheinker's syndrome. Exp Neurol 106: 204-206.
64. Brown P, Gibbs CJ, Jr., Rodgers-Johnson P, Asher DM, Sulima MP, et al. (1994) Human spongiform encephalopathy: the National Institutes of Health series of 300 cases of experimentally transmitted disease. Ann Neurol 35: 513-529.
65. Tateishi J, Kitamoto T, Hoque MZ, Furukawa H (1996) Experimental transmission of Creutzfeldt-Jakob disease and related diseases to rodents. Neurology 46: 532-537.
66. Parchi P, Chen SG, Brown P, Zou W, Capellari S, et al. (1998) Different patterns of truncated prion protein fragments correlate with distinct phenotypes in P102L Gerstmann-Straussler-Scheinker disease. Proc Natl Acad Sci U S A 95: 8322-8327.
67. Lugaresi E, Medori R, Montagna P, Baruzzi A, Cortelli P, et al. (1986) Fatal familial insomnia and dysautonomia with selective degeneration of thalamic nuclei. N Engl J Med 315: 997-1003.
68. Medori R, Tritschler HJ, LeBlanc A, Villare F, Manetto V, et al. (1992) Fatal familial insomnia, a prion disease with a mutation at codon 178 of the prion protein gene. N Engl J Med 326: 444-449.
69. Tateishi J, Brown P, Kitamoto T, Hoque ZM, Roos R, et al. (1995) First experimental transmission of fatal familial insomnia. Nature 376: 434-435.
70. McLean CA, Storey E, Gardner RJ, Tannenberg AE, Cervenakova L, et al. (1997) The D178N (cis-129M) "fatal familial insomnia" mutation associated with diverse clinicopathologic phenotypes in an Australian kindred. Neurology 49: 552-558.
71. Reder AT, Mednick AS, Brown P, Spire JP, Van Cauter E, et al. (1995) Clinical and genetic studies of fatal familial insomnia. Neurology 45: 1068-1075.

72. Silburn P, Cervenakova L, Varghese P, Tannenberg A, Brown P, et al. (1996) Fatal familial insomnia: a seventh family. Neurology 47: 1326-1328.
73. Almer G, Hainfellner JA, Brucke T, Jellinger K, Kleinert R, et al. (1999) Fatal familial insomnia: a new Austrian family. Brain 122 (Pt 1): 5-16.
74. Tabernero C, Polo JM, Sevillano MD, Munoz R, Berciano J, et al. (2000) Fatal familial insomnia: clinical, neuropathological, and genetic description of a Spanish family. J Neurol Neurosurg Psychiatry 68: 774-777.
75. Goldfarb LG, Haltia M, Brown P, Nieto A, Kovanen J, et al. (1991) New mutation in scrapie amyloid precursor gene (at codon 178) in Finnish Creutzfeldt-Jakob kindred. Lancet 337: 425.
76. Nieto A, Goldfarb LG, Brown P, McCombie WR, Trapp S, et al. (1991) Codon 178 mutation in ethnically diverse Creutzfeldt-Jakob disease families. Lancet 337: 622-623.
77. Goldfarb LG, Petersen RB, Tabaton M, Brown P, LeBlanc AC, et al. (1992) Fatal familial insomnia and familial Creutzfeldt-Jakob disease: disease phenotype determined by a DNA polymorphism. Science 258: 806-808.
78. Mead S, Mahal SP, Beck J, Campbell T, Farrall M, et al. (2001) Sporadic--but not variant--Creutzfeldt-Jakob disease is associated with polymorphisms upstream of PRNP exon 1. Am J Hum Genet 69: 1225-1235.
79. Williams ES, Young S (1980) Chronic wasting disease of captive mule deer: a spongiform encephalopathy. J Wildl Dis 16: 89-98.
80. Wyatt JM, Pearson GR, Smerdon TN, Gruffydd-Jones TJ, Wells GA, et al. (1991) Naturally occurring scrapie-like spongiform encephalopathy in five domestic cats. Vet Rec 129: 233-236.
81. Gordon RM (1946) Some entomological aspects of typhus. Public Health 59: 65.
82. Chandler RL (1961) Encephalopathy in mice produced by inoculation with scrapie brain material. Lancet 1: 1378-1379.
83. Brown P, Bradley R (1998) 1755 and all that: a historical primer of transmissible spongiform encephalopathy. BMJ 317: 1688-1692.
84. Anderson RM, Donnelly CA, Ferguson NM, Woolhouse ME, Watt CJ, et al. (1996) Transmission dynamics and epidemiology of BSE in British cattle. Nature 382: 779-788.
85. Sigurdson CJ, Miller MW (2003) Other animal prion diseases. Br Med Bull 66: 199-212.
86. Novakofski J, Brewer MS, Mateus-Pinilla N, Killefer J, McCusker RH (2005) Prion biology relevant to bovine spongiform encephalopathy. J Anim Sci 83: 1455-1476.
87. Dawson M, Wells GA, Parker BN (1990) Preliminary evidence of the experimental transmissibility of bovine spongiform encephalopathy to cattle. Vet Rec 126: 112-113.
88. Fraser H, McConnell I, Wells GA, Dawson M (1988) Transmission of bovine spongiform encephalopathy to mice. Vet Rec 123: 472.
89. Aguzzi A, Calella AM (2009) Prions: protein aggregation and infectious diseases. Physiol Rev 89: 1105-1152.
90. Ducrot C, Arnold M, de Koeijer A, Heim D, Calavas D (2008) Review on the epidemiology and dynamics of BSE epidemics. Vet Res 39: 15.
91. Saegerman C, Speybroeck N, Roels S, Vanopdenbosch E, Thiry E, et al. (2004) Decision support tools for clinical diagnosis of disease in cows with suspected bovine spongiform encephalopathy. J Clin Microbiol 42: 172-178.

92. Will RG, Ironside JW, Zeidler M, Cousens SN, Estibeiro K, et al. (1996) A new variant of Creutzfeldt-Jakob disease in the UK. Lancet 347: 921-925.
93. Chazot G, Broussolle E, Lapras C, Blattler T, Aguzzi A, et al. (1996) New variant of Creutzfeldt-Jakob disease in a 26-year-old French man. Lancet 347: 1181.
94. Houston F, Foster JD, Chong A, Hunter N, Bostock CJ (2000) Transmission of BSE by blood transfusion in sheep. Lancet 356: 999-1000.
95. Vulin J, Biacabe AG, Cazeau G, Calavas D, Baron T (2011) Molecular typing of protease-resistant prion protein in transmissible spongiform encephalopathies of small ruminants, France, 2002-2009. Emerg Infect Dis 17: 55-63.
96. Plinston C, Hart P, Chong A, Hunter N, Foster J, et al. (2011) Increased susceptibility of human-PrP transgenic mice to bovine spongiform encephalopathy infection following passage in sheep. J Virol 85: 1174-1181.
97. Seabury CM, Honeycutt RL, Rooney AP, Halbert ND, Derr JN (2004) Prion protein gene (PRNP) variants and evidence for strong purifying selection in functionally important regions of bovine exon 3. Proc Natl Acad Sci U S A 101: 15142-15147.
98. Sander P, Hamann H, Pfeiffer I, Wemheuer W, Brenig B, et al. (2004) Analysis of sequence variability of the bovine prion protein gene (PRNP) in German cattle breeds. Neurogenetics 5: 19-25.
99. Nicholson EM, Brunelle BW, Richt JA, Kehrli ME, Jr., Greenlee JJ (2008) Identification of a heritable polymorphism in bovine PRNP associated with genetic transmissible spongiform encephalopathy: evidence of heritable BSE. PLoS One 3: e2912.
100. Richt JA, Hall SM (2008) BSE case associated with prion protein gene mutation. PLoS Pathog 4: e1000156.
101. Juling K, Schwarzenbacher H, Williams JL, Fries R (2006) A major genetic component of BSE susceptibility. BMC Biol 4: 33.
102. Angers RC, Kang HE, Napier D, Browning S, Seward T, et al. (2010) Prion strain mutation determined by prion protein conformational compatibility and primary structure. Science 328: 1154-1158.
103. Tamguney G, Miller MW, Giles K, Lemus A, Glidden DV, et al. (2009) Transmission of scrapie and sheep-passaged bovine spongiform encephalopathy prions to transgenic mice expressing elk prion protein. J Gen Virol 90: 1035-1047.
104. Sigurdson CJ (2008) A prion disease of cervids: chronic wasting disease. Vet Res 39: 41.
105. Mathiason CK, Hays SA, Powers J, Hayes-Klug J, Langenberg J, et al. (2009) Infectious prions in pre-clinical deer and transmission of chronic wasting disease solely by environmental exposure. PLoS One 4: e5916.
106. Tamguney G, Giles K, Bouzamondo-Bernstein E, Bosque PJ, Miller MW, et al. (2006) Transmission of elk and deer prions to transgenic mice. J Virol 80: 9104-9114.
107. Balachandran A, Harrington NP, Algire J, Soutyrine A, Spraker TR, et al. (2010) Experimental oral transmission of chronic wasting disease to red deer (Cervus elaphus elaphus): early detection and late stage distribution of protease-resistant prion protein. Can Vet J 51: 169-178.
108. Martin S, Jeffrey M, Gonzalez L, Siso S, Reid HW, et al. (2009) Immunohistochemical and biochemical characteristics of BSE and CWD in experimentally infected European red deer (Cervus elaphus elaphus). BMC Vet Res 5: 26.

109. Seelig DM, Mason GL, Telling GC, Hoover EA (2010) Pathogenesis of chronic wasting disease in cervidized transgenic mice. Am J Pathol 176: 2785-2797.
110. Race B, Meade-White K, Race R, Chesebro B (2009) Prion infectivity in fat of deer with chronic wasting disease. J Virol 83: 9608-9610.
111. Spraker TR, O'Rourke KI, Gidlewski T, Powers JG, Greenlee JJ, et al. (2010) Detection of the abnormal isoform of the prion protein associated with chronic wasting disease in the optic pathways of the brain and retina of Rocky Mountain elk (Cervus elaphus nelsoni). Vet Pathol 47: 536-546.
112. Nichols TA, Pulford B, Wyckoff AC, Meyerett C, Michel B, et al. (2009) Detection of protease-resistant cervid prion protein in water from a CWD-endemic area. Prion 3: 171-183.
113. Tamguney G, Miller MW, Wolfe LL, Sirochman TM, Glidden DV, et al. (2009) Asymptomatic deer excrete infectious prions in faeces. Nature 461: 529-532.
114. Denkers ND, Seelig DM, Telling GC, Hoover EA (2010) Aerosol and nasal transmission of chronic wasting disease in cervidized mice. J Gen Virol 91: 1651-1658.
115. Denkers ND, Telling GC, Hoover EA (2011) Minor oral lesions facilitate transmission of chronic wasting disease. J Virol 85: 1396-1399.
116. Johnson CJ, Phillips KE, Schramm PT, McKenzie D, Aiken JM, et al. (2006) Prions adhere to soil minerals and remain infectious. PLoS Pathog 2: e32.
117. Seidel B, Thomzig A, Buschmann A, Groschup MH, Peters R, et al. (2007) Scrapie Agent (Strain 263K) can transmit disease via the oral route after persistence in soil over years. PLoS One 2: e435.
118. Green KM, Castilla J, Seward TS, Napier DL, Jewell JE, et al. (2008) Accelerated high fidelity prion amplification within and across prion species barriers. PLoS Pathog 4: e1000139.
119. White SN, O'Rourke KI, Gidlewski T, VerCauteren KC, Mousel MR, et al. (2010) Increased risk of chronic wasting disease in Rocky Mountain elk associated with decreased magnesium and increased manganese in brain tissue. Can J Vet Res 74: 50-53.
120. Kirkwood JK, Cunningham AA (1994) Epidemiological observations on spongiform encephalopathies in captive wild animals in the British Isles. Vet Rec 135: 296-303.
121. Poidinger M, Kirkwood J, Almond W (1993) Sequence analysis of the PrP protein from two species of antelope susceptible to transmissible spongiform encephalopathy. Arch Virol 131: 193-199.
122. Bencsik A, Debeer S, Petit T, Baron T (2009) Possible case of maternal transmission of feline spongiform encephalopathy in a captive cheetah. PLoS One 4: e6929.
123. Eiden M, Hoffmann C, Balkema-Buschmann A, Muller M, Baumgartner K, et al. (2010) Biochemical and immunohistochemical characterization of feline spongiform encephalopathy in a German captive cheetah. J Gen Virol 91: 2874-2883.
124. Zanusso G, Nardelli E, Rosati A, Fabrizi G, Ferrari S, et al. (1998) Simultaneous occurrence of spongiform encephalopathy in a man and his cat in Italy. Lancet 352: 1116-1117.
125. Marsh RF, Hadlow WJ (1992) Transmissible mink encephalopathy. Rev Sci Tech 11: 539-550.

126. Baron T, Bencsik A, Biacabe AG, Morignat E, Bessen RA (2007) Phenotypic similarity of transmissible mink encephalopathy in cattle and L-type bovine spongiform encephalopathy in a mouse model. Emerg Infect Dis 13: 1887-1894.
127. Marsh RF, Bessen RA, Lehmann S, Hartsough GR (1991) Epidemiological and experimental studies on a new incident of transmissible mink encephalopathy. J Gen Virol 72 (Pt 3): 589-594.
128. Bessen RA, Marsh RF (1992) Identification of two biologically distinct strains of transmissible mink encephalopathy in hamsters. J Gen Virol 73 (Pt 2): 329-334.
129. Shikiya RA, Ayers JI, Schutt CR, Kincaid AE, Bartz JC (2010) Coinfecting prion strains compete for a limiting cellular resource. J Virol 84: 5706-5714.
130. Bons N, Mestre-Frances N, Belli P, Cathala F, Gajdusek DC, et al. (1999) Natural and experimental oral infection of nonhuman primates by bovine spongiform encephalopathy agents. Proc Natl Acad Sci U S A 96: 4046-4051.
131. Moore RC, Lee IY, Silverman GL, Harrison PM, Strome R, et al. (1999) Ataxia in prion protein (PrP)-deficient mice is associated with upregulation of the novel PrP-like protein doppel. J Mol Biol 292: 797-817.
132. Watts JC, Drisaldi B, Ng V, Yang J, Strome B, et al. (2007) The CNS glycoprotein Shadoo has PrP(C)-like protective properties and displays reduced levels in prion infections. EMBO J 26: 4038-4050.
133. Oesch B, Westaway D, Walchli M, McKinley MP, Kent SB, et al. (1985) A cellular gene encodes scrapie PrP 27-30 protein. Cell 40: 735-746.
134. Kretzschmar HA, Stowring LE, Westaway D, Stubblebine WH, Prusiner SB, et al. (1986) Molecular cloning of a human prion protein cDNA. DNA 5: 315-324.
135. Basler K, Oesch B, Scott M, Westaway D, Walchli M, et al. (1986) Scrapie and cellular PrP isoforms are encoded by the same chromosomal gene. Cell 46: 417-428.
136. Liao YC, Lebo RV, Clawson GA, Smuckler EA (1986) Human prion protein cDNA: molecular cloning, chromosomal mapping, and biological implications. Science 233: 364-367.
137. Westaway D, Goodman PA, Mirenda CA, McKinley MP, Carlson GA, et al. (1987) Distinct prion proteins in short and long scrapie incubation period mice. Cell 51: 651-662.
138. Puckett C, Concannon P, Casey C, Hood L (1991) Genomic structure of the human prion protein gene. Am J Hum Genet 49: 320-329.
139. Gabriel JM, Oesch B, Kretzschmar H, Scott M, Prusiner SB (1992) Molecular cloning of a candidate chicken prion protein. Proc Natl Acad Sci U S A 89: 9097-9101.
140. Mahal SP, Asante EA, Antoniou M, Collinge J (2001) Isolation and functional characterisation of the promoter region of the human prion protein gene. Gene 268: 105-114.
141. McKnight S, Tjian R (1986) Transcriptional selectivity of viral genes in mammalian cells. Cell 46: 795-805.
142. Chesebro B, Race R, Wehrly K, Nishio J, Bloom M, et al. (1985) Identification of scrapie prion protein-specific mRNA in scrapie-infected and uninfected brain. Nature 315: 331-333.
143. Colby DW, Prusiner SB (2011) Prions. Cold Spring Harb Perspect Biol 3: a006833.

144. Manson J, West JD, Thomson V, McBride P, Kaufman MH, et al. (1992) The prion protein gene: a role in mouse embryogenesis? Development 115: 117-122.
145. Harris DA, Lele P, Snider WD (1993) Localization of the mRNA for a chicken prion protein by in situ hybridization. Proc Natl Acad Sci U S A 90: 4309-4313.
146. Moser M, Colello RJ, Pott U, Oesch B (1995) Developmental expression of the prion protein gene in glial cells. Neuron 14: 509-517.
147. Ford MJ, Burton LJ, Morris RJ, Hall SM (2002) Selective expression of prion protein in peripheral tissues of the adult mouse. Neuroscience 113: 177-192.
148. Mironov A, Jr., Latawiec D, Wille H, Bouzamondo-Bernstein E, Legname G, et al. (2003) Cytosolic prion protein in neurons. J Neurosci 23: 7183-7193.
149. Fournier JG, Escaig-Haye F, Billette de Villemeur T, Robain O (1995) Ultrastructural localization of cellular prion protein (PrPc) in synaptic boutons of normal hamster hippocampus. C R Acad Sci III 318: 339-344.
150. Laine J, Axelrad H (2002) Extending the cerebellar Lugaro cell class. Neuroscience 115: 363-374.
151. Vassallo N, Herms J (2003) Cellular prion protein function in copper homeostasis and redox signalling at the synapse. J Neurochem 86: 538-544.
152. Godsave SF, Wille H, Kujala P, Latawiec D, DeArmond SJ, et al. (2008) Cryo-immunogold electron microscopy for prions: toward identification of a conversion site. J Neurosci 28: 12489-12499.
153. Isaacs JD, Jackson GS, Altmann DM (2006) The role of the cellular prion protein in the immune system. Clin Exp Immunol 146: 1-8.
154. Chakrabarti O, Ashok A, Hegde RS (2009) Prion protein biosynthesis and its emerging role in neurodegeneration. Trends Biochem Sci 34: 287-295.
155. Drisaldi B, Stewart RS, Adles C, Stewart LR, Quaglio E, et al. (2003) Mutant PrP is delayed in its exit from the endoplasmic reticulum, but neither wild-type nor mutant PrP undergoes retrotranslocation prior to proteasomal degradation. J Biol Chem 278: 21732-21743.
156. Kang SW, Rane NS, Kim SJ, Garrison JL, Taunton J, et al. (2006) Substrate-specific translocational attenuation during ER stress defines a pre-emptive quality control pathway. Cell 127: 999-1013.
157. Ma J, Wollmann R, Lindquist S (2002) Neurotoxicity and neurodegeneration when PrP accumulates in the cytosol. Science 298: 1781-1785.
158. Rane NS, Kang SW, Chakrabarti O, Feigenbaum L, Hegde RS (2008) Reduced translocation of nascent prion protein during ER stress contributes to neurodegeneration. Dev Cell 15: 359-370.
159. Solomon IH, Schepker JA, Harris DA (2010) Prion neurotoxicity: insights from prion protein mutants. Curr Issues Mol Biol 12: 51-61.
160. Nicolas O, Gavin R, del Rio JA (2009) New insights into cellular prion protein (PrPc) functions: the "ying and yang" of a relevant protein. Brain Res Rev 61: 170-184.
161. Haraguchi T, Fisher S, Olofsson S, Endo T, Groth D, et al. (1989) Asparagine-linked glycosylation of the scrapie and cellular prion proteins. Arch Biochem Biophys 274: 1-13.

162. Pan T, Li R, Wong BS, Liu T, Gambetti P, et al. (2002) Heterogeneity of normal prion protein in two- dimensional immunoblot: presence of various glycosylated and truncated forms. J Neurochem 81: 1092-1101.
163. Rudd PM, Endo T, Colominas C, Groth D, Wheeler SF, et al. (1999) Glycosylation differences between the normal and pathogenic prion protein isoforms. Proc Natl Acad Sci U S A 96: 13044-13049.
164. Beringue V, Mallinson G, Kaisar M, Tayebi M, Sattar Z, et al. (2003) Regional heterogeneity of cellular prion protein isoforms in the mouse brain. Brain 126: 2065-2073.
165. DeArmond SJ, Qiu Y, Sanchez H, Spilman PR, Ninchak-Casey A, et al. (1999) PrPc glycoform heterogeneity as a function of brain region: implications for selective targeting of neurons by prion strains. J Neuropathol Exp Neurol 58: 1000-1009.
166. Surewicz WK, Apostol MI (2011) Prion protein and its conformational conversion: a structural perspective. Top Curr Chem 305: 135-167.
167. Hornemann S, Schorn C, Wuthrich K (2004) NMR structure of the bovine prion protein isolated from healthy calf brains. EMBO Rep 5: 1159-1164.
168. Riek R, Hornemann S, Wider G, Glockshuber R, Wuthrich K (1997) NMR characterization of the full-length recombinant murine prion protein, mPrP(23-231). FEBS Lett 413: 282-288.
169. Donne DG, Viles JH, Groth D, Mehlhorn I, James TL, et al. (1997) Structure of the recombinant full-length hamster prion protein PrP(29-231): the N terminus is highly flexible. Proc Natl Acad Sci U S A 94: 13452-13457.
170. Caughey B, Baron GS (2006) Prions and their partners in crime. Nature 443: 803-810.
171. Linden R, Martins VR, Prado MA, Cammarota M, Izquierdo I, et al. (2008) Physiology of the prion protein. Physiol Rev 88: 673-728.
172. Zahn R (2003) The octapeptide repeats in mammalian prion protein constitute a pH-dependent folding and aggregation site. J Mol Biol 334: 477-488.
173. Taubner LM, Bienkiewicz EA, Copie V, Caughey B (2010) Structure of the flexible amino-terminal domain of prion protein bound to a sulfated glycan. J Mol Biol 395: 475-490.
174. Prusiner SB, Groth DF, Bolton DC, Kent SB, Hood LE (1984) Purification and structural studies of a major scrapie prion protein. Cell 38: 127-134.
175. Hundt C, Gauczynski S, Leucht C, Riley ML, Weiss S (2003) Intra- and interspecies interactions between prion proteins and effects of mutations and polymorphisms. Biol Chem 384: 791-803.
176. Goldfarb LG, Brown P, McCombie WR, Goldgaber D, Swergold GD, et al. (1991) Transmissible familial Creutzfeldt-Jakob disease associated with five, seven, and eight extra octapeptide coding repeats in the PRNP gene. Proc Natl Acad Sci U S A 88: 10926-10930.
177. Chiesa R, Piccardo P, Ghetti B, Harris DA (1998) Neurological illness in transgenic mice expressing a prion protein with an insertional mutation. Neuron 21: 1339-1351.
178. Chiesa R, Drisaldi B, Quaglio E, Migheli A, Piccardo P, et al. (2000) Accumulation of protease-resistant prion protein (PrP) and apoptosis of cerebellar granule cells in transgenic mice expressing a PrP insertional mutation. Proc Natl Acad Sci U S A 97: 5574-5579.

179. Chiesa R, Harris DA (2001) Prion diseases: what is the neurotoxic molecule? Neurobiol Dis 8: 743-763.
180. Burns CS, Aronoff-Spencer E, Legname G, Prusiner SB, Antholine WE, et al. (2003) Copper coordination in the full-length, recombinant prion protein. Biochemistry 42: 6794-6803.
181. Zhang Y, Swietnicki W, Zagorski MG, Surewicz WK, Sonnichsen FD (2000) Solution structure of the E200K variant of human prion protein. Implications for the mechanism of pathogenesis in familial prion diseases. J Biol Chem 275: 33650-33654.
182. Ilc G, Giachin G, Jaremko M, Jaremko L, Benetti F, et al. (2010) NMR structure of the human prion protein with the pathological Q212P mutation reveals unique structural features. PLoS One 5: e11715.
183. Lee S, Antony L, Hartmann R, Knaus KJ, Surewicz K, et al. (2010) Conformational diversity in prion protein variants influences intermolecular beta-sheet formation. EMBO J 29: 251-262.
184. Knaus KJ, Morillas M, Swietnicki W, Malone M, Surewicz WK, et al. (2001) Crystal structure of the human prion protein reveals a mechanism for oligomerization. Nat Struct Biol 8: 770-774.
185. Antonyuk SV, Trevitt CR, Strange RW, Jackson GS, Sangar D, et al. (2009) Crystal structure of human prion protein bound to a therapeutic antibody. Proc Natl Acad Sci U S A 106: 2554-2558.
186. Zahn R, Liu A, Luhrs T, Riek R, von Schroetter C, et al. (2000) NMR solution structure of the human prion protein. Proc Natl Acad Sci U S A 97: 145-150.
187. Calzolai L, Zahn R (2003) Influence of pH on NMR structure and stability of the human prion protein globular domain. J Biol Chem 278: 35592-35596.
188. Wuthrich K, Riek R (2001) Three-dimensional structures of prion proteins. Adv Protein Chem 57: 55-82.
189. Hornemann S, Christen B, von Schroetter C, Perez DR, Wuthrich K (2009) Prion protein library of recombinant constructs for structural biology. FEBS J 276: 2359-2367.
190. Riek R, Hornemann S, Wider G, Billeter M, Glockshuber R, et al. (1996) NMR structure of the mouse prion protein domain PrP(121-231). Nature 382: 180-182.
191. Gossert AD, Bonjour S, Lysek DA, Fiorito F, Wuthrich K (2005) Prion protein NMR structures of elk and of mouse/elk hybrids. Proc Natl Acad Sci U S A 102: 646-650.
192. Sigurdson CJ, Nilsson KP, Hornemann S, Manco G, Fernandez-Borges N, et al. (2010) A molecular switch controls interspecies prion disease transmission in mice. J Clin Invest 120: 2590-2599.
193. Mead S (2006) Prion disease genetics. Eur J Hum Genet 14: 273-281.
194. Collinge J, Whittington MA, Sidle KC, Smith CJ, Palmer MS, et al. (1994) Prion protein is necessary for normal synaptic function. Nature 370: 295-297.
195. Mouillet-Richard S, Ermonval M, Chebassier C, Laplanche JL, Lehmann S, et al. (2000) Signal transduction through prion protein. Science 289: 1925-1928.
196. Shmerling D, Hegyi I, Fischer M, Blattler T, Brandner S, et al. (1998) Expression of amino-terminally truncated PrP in the mouse leading to ataxia and specific cerebellar lesions. Cell 93: 203-214.

197. Simons K, Toomre D (2000) Lipid rafts and signal transduction. Nat Rev Mol Cell Biol 1: 31-39.
198. Mange A, Milhavet O, Umlauf D, Harris D, Lehmann S (2002) PrP-dependent cell adhesion in N2a neuroblastoma cells. FEBS Lett 514: 159-162.
199. Malaga-Trillo E, Solis GP, Schrock Y, Geiss C, Luncz L, et al. (2009) Regulation of embryonic cell adhesion by the prion protein. PLoS Biol 7: e55.
200. Bounhar Y, Zhang Y, Goodyer CG, LeBlanc A (2001) Prion protein protects human neurons against Bax-mediated apoptosis. J Biol Chem 276: 39145-39149.
201. Kanaani J, Prusiner SB, Diacovo J, Baekkeskov S, Legname G (2005) Recombinant prion protein induces rapid polarization and development of synapses in embryonic rat hippocampal neurons in vitro. J Neurochem 95: 1373-1386.
202. Roucou X, Gains M, LeBlanc AC (2004) Neuroprotective functions of prion protein. J Neurosci Res 75: 153-161.
203. Roucou X, LeBlanc AC (2005) Cellular prion protein neuroprotective function: implications in prion diseases. J Mol Med (Berl) 83: 3-11.
204. Rambold AS, Muller V, Ron U, Ben-Tal N, Winklhofer KF, et al. (2008) Stress-protective signalling of prion protein is corrupted by scrapie prions. EMBO J 27: 1974-1984.
205. Zhang CC, Steele AD, Lindquist S, Lodish HF (2006) Prion protein is expressed on long-term repopulating hematopoietic stem cells and is important for their self-renewal. Proc Natl Acad Sci U S A 103: 2184-2189.
206. Zafar S, von Ahsen N, Oellerich M, Zerr I, Schulz-Schaeffer WJ, et al. (2011) Proteomics approach to identify the interacting partners of cellular prion protein and characterization of Rab7a interaction in neuronal cells. J Proteome Res 10: 3123-3135.
207. Viles JH, Klewpatinond M, Nadal RC (2008) Copper and the structural biology of the prion protein. Biochem Soc Trans 36: 1288-1292.
208. Davies P, Brown DR (2008) The chemistry of copper binding to PrP: is there sufficient evidence to elucidate a role for copper in protein function? Biochem J 410: 237-244.
209. Aguzzi A, Baumann F, Bremer J (2008) The prion's elusive reason for being. Annu Rev Neurosci 31: 439-477.
210. Lauren J, Gimbel DA, Nygaard HB, Gilbert JW, Strittmatter SM (2009) Cellular prion protein mediates impairment of synaptic plasticity by amyloid-beta oligomers. Nature 457: 1128-1132.
211. Kessels HW, Nguyen LN, Nabavi S, Malinow R (2010) The prion protein as a receptor for amyloid-beta. Nature 466: E3-4; discussion E4-5.
212. Bremer J, Baumann F, Tiberi C, Wessig C, Fischer H, et al. (2010) Axonal prion protein is required for peripheral myelin maintenance. Nat Neurosci 13: 310-318.
213. Prusiner SB (1982) Novel proteinaceous infectious particles cause scrapie. Science 216: 136-144.
214. Legname G, Baskakov IV, Nguyen HO, Riesner D, Cohen FE, et al. (2004) Synthetic mammalian prions. Science 305: 673-676.
215. Griffith JS (1967) Self-replication and scrapie. Nature 215: 1043-1044.
216. Prusiner SB (2001) Shattuck lecture--neurodegenerative diseases and prions. N Engl J Med 344: 1516-1526.

217. Beyreuther K, Masters CL (1994) Neurobiology. Catching the culprit prion. Nature 370: 419-420.
218. Calzolai L, Lysek DA, Perez DR, Guntert P, Wuthrich K (2005) Prion protein NMR structures of chickens, turtles, and frogs. Proc Natl Acad Sci U S A 102: 651-655.
219. Diaz-Espinoza R, Soto C (2012) High-resolution structure of infectious prion protein: the final frontier. Nat Struct Mol Biol 19: 370-377.
220. Cobb NJ, Sonnichsen FD, McHaourab H, Surewicz WK (2007) Molecular architecture of human prion protein amyloid: a parallel, in-register beta-structure. Proc Natl Acad Sci U S A 104: 18946-18951.
221. Tycko R, Savtchenko R, Ostapchenko VG, Makarava N, Baskakov IV (2010) The alpha-helical C-terminal domain of full-length recombinant PrP converts to an in-register parallel beta-sheet structure in PrP fibrils: evidence from solid state nuclear magnetic resonance. Biochemistry 49: 9488-9497.
222. Prusiner SB (1994) Biology and genetics of prion diseases. Annu Rev Microbiol 48: 655-686.
223. Pastrana MA, Sajnani G, Onisko B, Castilla J, Morales R, et al. (2006) Isolation and characterization of a proteinase K-sensitive PrPSc fraction. Biochemistry 45: 15710-15717.
224. Safar J, Wille H, Itri V, Groth D, Serban H, et al. (1998) Eight prion strains have PrP(Sc) molecules with different conformations. Nat Med 4: 1157-1165.
225. Safar JG, Scott M, Monaghan J, Deering C, Didorenko S, et al. (2002) Measuring prions causing bovine spongiform encephalopathy or chronic wasting disease by immunoassays and transgenic mice. Nat Biotechnol 20: 1147-1150.
226. Sajnani G, Silva CJ, Ramos A, Pastrana MA, Onisko BC, et al. (2012) PK-sensitive PrP is infectious and shares basic structural features with PK-resistant PrP. PLoS Pathog 8: e1002547.
227. Tzaban S, Friedlander G, Schonberger O, Horonchik L, Yedidia Y, et al. (2002) Protease-sensitive scrapie prion protein in aggregates of heterogeneous sizes. Biochemistry 41: 12868-12875.
228. Colby DW, Giles K, Legname G, Wille H, Baskakov IV, et al. (2009) Design and construction of diverse mammalian prion strains. Proc Natl Acad Sci U S A 106: 20417-20422.
229. Colby DW, Wain R, Baskakov IV, Legname G, Palmer CG, et al. (2010) Protease-sensitive synthetic prions. PLoS Pathog 6: e1000736.
230. Head MW, Knight R, Zeidler M, Yull H, Barlow A, et al. (2009) A case of protease sensitive prionopathy in a patient in the UK. Neuropathol Appl Neurobiol 35: 628-632.
231. Safar JG, Geschwind MD, Deering C, Didorenko S, Sattavat M, et al. (2005) Diagnosis of human prion disease. Proc Natl Acad Sci U S A 102: 3501-3506.
232. Benestad SL, Sarradin P, Thu B, Schonheit J, Tranulis MA, et al. (2003) Cases of scrapie with unusual features in Norway and designation of a new type, Nor98. Vet Rec 153: 202-208.
233. Orge L, Galo A, Machado C, Lima C, Ochoa C, et al. (2004) Identification of putative atypical scrapie in sheep in Portugal. J Gen Virol 85: 3487-3491.

234. Klingeborn M, Wik L, Simonsson M, Renstrom LH, Ottinger T, et al. (2006) Characterization of proteinase K-resistant N- and C-terminally truncated PrP in Nor98 atypical scrapie. J Gen Virol 87: 1751-1760.
235. Fischer MB, Roeckl C, Parizek P, Schwarz HP, Aguzzi A (2000) Binding of disease-associated prion protein to plasminogen. Nature 408: 479-483.
236. Crozet C, Beranger F, Lehmann S (2008) Cellular pathogenesis in prion diseases. Vet Res 39: 44.
237. Dearmond SJ, Bajsarowicz K (2010) PrPSc accumulation in neuronal plasma membranes links Notch-1 activation to dendritic degeneration in prion diseases. Mol Neurodegener 5: 6.
238. Ermolayev V, Cathomen T, Merk J, Friedrich M, Hartig W, et al. (2009) Impaired axonal transport in motor neurons correlates with clinical prion disease. PLoS Pathog 5: e1000558.
239. Ersdal C, Goodsir CM, Simmons MM, McGovern G, Jeffrey M (2009) Abnormal prion protein is associated with changes of plasma membranes and endocytosis in bovine spongiform encephalopathy (BSE)-affected cattle brains. Neuropathol Appl Neurobiol 35: 259-271.
240. Flechsig E, Shmerling D, Hegyi I, Raeber AJ, Fischer M, et al. (2000) Prion protein devoid of the octapeptide repeat region restores susceptibility to scrapie in PrP knockout mice. Neuron 27: 399-408.
241. Lasmezas CI, Deslys JP, Robain O, Jaegly A, Beringue V, et al. (1997) Transmission of the BSE agent to mice in the absence of detectable abnormal prion protein. Science 275: 402-405.
242. Manson JC (1999) Understanding transmission of the prion diseases. Trends Microbiol 7: 465-467.
243. Brown P (1994) The "brave new world" of transmissible spongiform encephalopathy (infectious cerebral amyloidosis). Mol Neurobiol 8: 79-87.
244. Piccardo P, Liepnieks JJ, William A, Dlouhy SR, Farlow MR, et al. (2001) Prion proteins with different conformations accumulate in Gerstmann-Straussler-Scheinker disease caused by A117V and F198S mutations. Am J Pathol 158: 2201-2207.
245. Tateishi J, Kitamoto T (1995) Inherited prion diseases and transmission to rodents. Brain Pathol 5: 53-59.
246. Tateishi J, Kitamoto T, Doh-ura K, Sakaki Y, Steinmetz G, et al. (1990) Immunochemical, molecular genetic, and transmission studies on a case of Gerstmann-Straussler-Scheinker syndrome. Neurology 40: 1578-1581.
247. Tateishi J, Kitamoto T, Kretzschmar H, Mehraein P (1996) Immunhistological evaluation of Creutzfeldt-Jakob disease with reference to the type PrPres deposition. Clin Neuropathol 15: 358-360.
248. Hill AF, Joiner S, Linehan J, Desbruslais M, Lantos PL, et al. (2000) Species-barrier-independent prion replication in apparently resistant species. Proc Natl Acad Sci U S A 97: 10248-10253.
249. Race R, Raines A, Raymond GJ, Caughey B, Chesebro B (2001) Long-term subclinical carrier state precedes scrapie replication and adaptation in a resistant species:

analogies to bovine spongiform encephalopathy and variant Creutzfeldt-Jakob disease in humans. J Virol 75: 10106-10112.
250. Bueler H, Raeber A, Sailer A, Fischer M, Aguzzi A, et al. (1994) High prion and PrPSc levels but delayed onset of disease in scrapie-inoculated mice heterozygous for a disrupted PrP gene. Mol Med 1: 19-30.
251. Brandner S, Isenmann S, Raeber A, Fischer M, Sailer A, et al. (1996) Normal host prion protein necessary for scrapie-induced neurotoxicity. Nature 379: 339-343.
252. Collinge J, Owen F, Poulter M, Leach M, Crow TJ, et al. (1990) Prion dementia without characteristic pathology. Lancet 336: 7-9.
253. Collinge J, Palmer MS, Sidle KC, Hill AF, Gowland I, et al. (1995) Unaltered susceptibility to BSE in transgenic mice expressing human prion protein. Nature 378: 779-783.
254. Weissmann C (1991) A 'unified theory' of prion propagation. Nature 352: 679-683.
255. Saa P, Castilla J, Soto C (2006) Ultra-efficient replication of infectious prions by automated protein misfolding cyclic amplification. J Biol Chem 281: 35245-35252.
256. Soto C (2012) Transmissible proteins: expanding the prion heresy. Cell 149: 968-977.
257. Hathaway LJ, Kraehenbuhl JP (2000) The role of M cells in mucosal immunity. Cell Mol Life Sci 57: 323-332.
258. Heppner FL, Christ AD, Klein MA, Prinz M, Fried M, et al. (2001) Transepithelial prion transport by M cells. Nat Med 7: 976-977.
259. Aucouturier P, Carp RI, Carnaud C, Wisniewski T (2000) Prion diseases and the immune system. Clin Immunol 96: 79-85.
260. Beekes M, McBride PA (2007) The spread of prions through the body in naturally acquired transmissible spongiform encephalopathies. FEBS J 274: 588-605.
261. Mabbott NA, Bruce ME (2003) Prion disease: bridging the spleen-nerve gap. Nat Med 9: 1463-1464.
262. Prinz M, Huber G, Macpherson AJ, Heppner FL, Glatzel M, et al. (2003) Oral prion infection requires normal numbers of Peyer's patches but not of enteric lymphocytes. Am J Pathol 162: 1103-1111.
263. Defaweux V, Dorban G, Antoine N, Piret J, Gabriel A, et al. (2007) Neuroimmune connections in jejunal and ileal Peyer's patches at various bovine ages: potential sites for prion neuroinvasion. Cell Tissue Res 329: 35-44.
264. Andreoletti O, Berthon P, Marc D, Sarradin P, Grosclaude J, et al. (2000) Early accumulation of PrP(Sc) in gut-associated lymphoid and nervous tissues of susceptible sheep from a Romanov flock with natural scrapie. J Gen Virol 81: 3115-3126.
265. Jeffrey M, Gonzalez L (2007) Classical sheep transmissible spongiform encephalopathies: pathogenesis, pathological phenotypes and clinical disease. Neuropathol Appl Neurobiol 33: 373-394.
266. van Keulen LJ, Schreuder BE, Meloen RH, Mooij-Harkes G, Vromans ME, et al. (1996) Immunohistochemical detection of prion protein in lymphoid tissues of sheep with natural scrapie. J Clin Microbiol 34: 1228-1231.
267. van Keulen LJ, Schreuder BE, Vromans ME, Langeveld JP, Smits MA (2000) Pathogenesis of natural scrapie in sheep. Arch Virol Suppl: 57-71.

268. Sigurdson CJ, Spraker TR, Miller MW, Oesch B, Hoover EA (2001) PrP(CWD) in the myenteric plexus, vagosympathetic trunk and endocrine glands of deer with chronic wasting disease. J Gen Virol 82: 2327-2334.
269. Iwata N, Sato Y, Higuchi Y, Nohtomi K, Nagata N, et al. (2006) Distribution of PrP(Sc) in cattle with bovine spongiform encephalopathy slaughtered at abattoirs in Japan. Jpn J Infect Dis 59: 100-107.
270. van Keulen LJ, Vromans ME, van Zijderveld FG (2002) Early and late pathogenesis of natural scrapie infection in sheep. APMIS 110: 23-32.
271. Mabbott NA, Young J, McConnell I, Bruce ME (2003) Follicular dendritic cell dedifferentiation by treatment with an inhibitor of the lymphotoxin pathway dramatically reduces scrapie susceptibility. J Virol 77: 6845-6854.
272. Mabbott NA, Mackay F, Minns F, Bruce ME (2000) Temporary inactivation of follicular dendritic cells delays neuroinvasion of scrapie. Nat Med 6: 719-720.
273. Montrasio F, Frigg R, Glatzel M, Klein MA, Mackay F, et al. (2000) Impaired prion replication in spleens of mice lacking functional follicular dendritic cells. Science 288: 1257-1259.
274. Hetz C, Soto C (2003) Protein misfolding and disease: the case of prion disorders. Cell Mol Life Sci 60: 133-143.
275. Sigurdson CJ, Nilsson KP, Hornemann S, Heikenwalder M, Manco G, et al. (2009) De novo generation of a transmissible spongiform encephalopathy by mouse transgenesis. Proc Natl Acad Sci U S A 106: 304-309.
276. Barria MA, Mukherjee A, Gonzalez-Romero D, Morales R, Soto C (2009) De novo generation of infectious prions in vitro produces a new disease phenotype. PLoS Pathog 5: e1000421.
277. Wang F, Wang X, Yuan CG, Ma J (2010) Generating a prion with bacterially expressed recombinant prion protein. Science 327: 1132-1135.
278. Castilla J, Saa P, Hetz C, Soto C (2005) In vitro generation of infectious scrapie prions. Cell 121: 195-206.
279. Saborio GP, Permanne B, Soto C (2001) Sensitive detection of pathological prion protein by cyclic amplification of protein misfolding. Nature 411: 810-813.
280. Deleault NR, Harris BT, Rees JR, Supattapone S (2007) Formation of native prions from minimal components in vitro. Proc Natl Acad Sci U S A 104: 9741-9746.
281. Edgeworth JA, Gros N, Alden J, Joiner S, Wadsworth JD, et al. (2010) Spontaneous generation of mammalian prions. Proc Natl Acad Sci U S A 107: 14402-14406.
282. Chesebro B, Trifilo M, Race R, Meade-White K, Teng C, et al. (2005) Anchorless prion protein results in infectious amyloid disease without clinical scrapie. Science 308: 1435-1439.
283. Stohr J, Watts JC, Legname G, Oehler A, Lemus A, et al. (2011) Spontaneous generation of anchorless prions in transgenic mice. Proc Natl Acad Sci U S A 108: 21223-21228.
284. Dickinson AG, Fraser H, Outram GW (1975) Scrapie incubation time can exceed natural lifespan. Nature 256: 732-733.
285. Cunningham C, Deacon R, Wells H, Boche D, Waters S, et al. (2003) Synaptic changes characterize early behavioural signs in the ME7 model of murine prion disease. Eur J Neurosci 17: 2147-2155.

286. Guenther K, Deacon RM, Perry VH, Rawlins JN (2001) Early behavioural changes in scrapie-affected mice and the influence of dapsone. Eur J Neurosci 14: 401-409.
287. Jeffrey M, Halliday WG, Bell J, Johnston AR, MacLeod NK, et al. (2000) Synapse loss associated with abnormal PrP precedes neuronal degeneration in the scrapie-infected murine hippocampus. Neuropathol Appl Neurobiol 26: 41-54.
288. Siskova Z, Page A, O'Connor V, Perry VH (2009) Degenerating synaptic boutons in prion disease: microglia activation without synaptic stripping. Am J Pathol 175: 1610-1621.
289. Hill AF, Collinge J (2003) Subclinical prion infection in humans and animals. Br Med Bull 66: 161-170.
290. Frigg R, Klein MA, Hegyi I, Zinkernagel RM, Aguzzi A (1999) Scrapie pathogenesis in subclinically infected B-cell-deficient mice. J Virol 73: 9584-9588.
291. Thackray AM, Klein MA, Aguzzi A, Bujdoso R (2002) Chronic subclinical prion disease induced by low-dose inoculum. J Virol 76: 2510-2517.
292. Klein MA, Frigg R, Raeber AJ, Flechsig E, Hegyi I, et al. (1998) PrP expression in B lymphocytes is not required for prion neuroinvasion. Nat Med 4: 1429-1433.
293. Zou WQ, Gambetti P (2007) Prion: the chameleon protein. Cell Mol Life Sci 64: 3266-3270.
294. Butler DA, Scott MR, Bockman JM, Borchelt DR, Taraboulos A, et al. (1988) Scrapie-infected murine neuroblastoma cells produce protease-resistant prion proteins. J Virol 62: 1558-1564.
295. Schatzl HM, Laszlo L, Holtzman DM, Tatzelt J, DeArmond SJ, et al. (1997) A hypothalamic neuronal cell line persistently infected with scrapie prions exhibits apoptosis. J Virol 71: 8821-8831.
296. Kanu N, Imokawa Y, Drechsel DN, Williamson RA, Birkett CR, et al. (2002) Transfer of scrapie prion infectivity by cell contact in culture. Curr Biol 12: 523-530.
297. Borchelt DR, Taraboulos A, Prusiner SB (1992) Evidence for synthesis of scrapie prion proteins in the endocytic pathway. J Biol Chem 267: 16188-16199.
298. Caughey B, Raymond GJ (1991) The scrapie-associated form of PrP is made from a cell surface precursor that is both protease- and phospholipase-sensitive. J Biol Chem 266: 18217-18223.
299. Caughey B, Raymond GJ, Ernst D, Race RE (1991) N-terminal truncation of the scrapie-associated form of PrP by lysosomal protease(s): implications regarding the site of conversion of PrP to the protease-resistant state. J Virol 65: 6597-6603.
300. Taraboulos A, Raeber AJ, Borchelt DR, Serban D, Prusiner SB (1992) Synthesis and trafficking of prion proteins in cultured cells. Mol Biol Cell 3: 851-863.
301. Xue WF, Hellewell AL, Hewitt EW, Radford SE (2010) Fibril fragmentation in amyloid assembly and cytotoxicity: when size matters. Prion 4: 20-25.
302. Knowles TP, Fitzpatrick AW, Meehan S, Mott HR, Vendruscolo M, et al. (2007) Role of intermolecular forces in defining material properties of protein nanofibrils. Science 318: 1900-1903.
303. Meinhardt J, Fandrich M (2009) [Structure of amyloid fibrils]. Pathologe 30: 175-181.
304. White MD, Mallucci GR (2009) Therapy for prion diseases: Insights from the use of RNA interference. Prion 3: 121-128.

305. Veith NM, Plattner H, Stuermer CA, Schulz-Schaeffer WJ, Burkle A (2009) Immunolocalisation of PrPSc in scrapie-infected N2a mouse neuroblastoma cells by light and electron microscopy. Eur J Cell Biol 88: 45-63.
306. Linse S, Cabaleiro-Lago C, Xue WF, Lynch I, Lindman S, et al. (2007) Nucleation of protein fibrillation by nanoparticles. Proc Natl Acad Sci U S A 104: 8691-8696.
307. Tanaka M, Collins SR, Toyama BH, Weissman JS (2006) The physical basis of how prion conformations determine strain phenotypes. Nature 442: 585-589.
308. Cabaleiro-Lago C, Quinlan-Pluck F, Lynch I, Lindman S, Minogue AM, et al. (2008) Inhibition of amyloid beta protein fibrillation by polymeric nanoparticles. J Am Chem Soc 130: 15437-15443.
309. Smith JF, Knowles TP, Dobson CM, Macphee CE, Welland ME (2006) Characterization of the nanoscale properties of individual amyloid fibrils. Proc Natl Acad Sci U S A 103: 15806-15811.
310. Vilette D, Andreoletti O, Archer F, Madelaine MF, Vilotte JL, et al. (2001) Ex vivo propagation of infectious sheep scrapie agent in heterologous epithelial cells expressing ovine prion protein. Proc Natl Acad Sci U S A 98: 4055-4059.
311. Nishida N, Harris DA, Vilette D, Laude H, Frobert Y, et al. (2000) Successful transmission of three mouse-adapted scrapie strains to murine neuroblastoma cell lines overexpressing wild-type mouse prion protein. J Virol 74: 320-325.
312. Arima K, Nishida N, Sakaguchi S, Shigematsu K, Atarashi R, et al. (2005) Biological and biochemical characteristics of prion strains conserved in persistently infected cell cultures. J Virol 79: 7104-7112.
313. Birkett CR, Hennion RM, Bembridge DA, Clarke MC, Chree A, et al. (2001) Scrapie strains maintain biological phenotypes on propagation in a cell line in culture. EMBO J 20: 3351-3358.
314. Courageot MP, Daude N, Nonno R, Paquet S, Di Bari MA, et al. (2008) A cell line infectible by prion strains from different species. J Gen Virol 89: 341-347.
315. Iwamaru Y, Takenouchi T, Ogihara K, Hoshino M, Takata M, et al. (2007) Microglial cell line established from prion protein-overexpressing mice is susceptible to various murine prion strains. J Virol 81: 1524-1527.
316. Pimpinelli F, Lehmann S, Maridonneau-Parini I (2005) The scrapie prion protein is present in flotillin-1-positive vesicles in central- but not peripheral-derived neuronal cell lines. Eur J Neurosci 21: 2063-2072.
317. Race R (1991) The scrapie agent in vitro. Curr Top Microbiol Immunol 172: 181-193.
318. Race RE, Fadness LH, Chesebro B (1987) Characterization of scrapie infection in mouse neuroblastoma cells. J Gen Virol 68 (Pt 5): 1391-1399.
319. Ostlund P, Lindegren H, Pettersson C, Bedecs K (2001) Altered insulin receptor processing and function in scrapie-infected neuroblastoma cell lines. Brain Res Mol Brain Res 97: 161-170.
320. Haire LF, Whyte SM, Vasisht N, Gill AC, Verma C, et al. (2004) The crystal structure of the globular domain of sheep prion protein. J Mol Biol 336: 1175-1183.
321. Eghiaian F, Grosclaude J, Lesceu S, Debey P, Doublet B, et al. (2004) Insight into the PrPC-->PrPSc conversion from the structures of antibody-bound ovine prion scrapie-susceptibility variants. Proc Natl Acad Sci U S A 101: 10254-10259.

322. Alperovitch A, Zerr I, Pocchiari M, Mitrova E, de Pedro Cuesta J, et al. (1999) Codon 129 prion protein genotype and sporadic Creutzfeldt-Jakob disease. Lancet 353: 1673-1674.
323. Mead S, Stumpf MP, Whitfield J, Beck JA, Poulter M, et al. (2003) Balancing selection at the prion protein gene consistent with prehistoric kurulike epidemics. Science 300: 640-643.
324. Brandel JP, Preece M, Brown P, Croes E, Laplanche JL, et al. (2003) Distribution of codon 129 genotype in human growth hormone-treated CJD patients in France and the UK. Lancet 362: 128-130.
325. Lee S, Eisenberg D (2003) Seeded conversion of recombinant prion protein to a disulfide-bonded oligomer by a reduction-oxidation process. Nat Struct Biol 10: 725-730.
326. Janowski R, Kozak M, Jankowska E, Grzonka Z, Grubb A, et al. (2001) Human cystatin C, an amyloidogenic protein, dimerizes through three-dimensional domain swapping. Nat Struct Biol 8: 316-320.
327. Liu Y, Eisenberg D (2002) 3D domain swapping: as domains continue to swap. Protein Sci 11: 1285-1299.
328. Sambashivan S, Liu Y, Sawaya MR, Gingery M, Eisenberg D (2005) Amyloid-like fibrils of ribonuclease A with three-dimensional domain-swapped and native-like structure. Nature 437: 266-269.
329. Kocisko DA, Come JH, Priola SA, Chesebro B, Raymond GJ, et al. (1994) Cell-free formation of protease-resistant prion protein. Nature 370: 471-474.
330. Ma J, Lindquist S (2002) Conversion of PrP to a self-perpetuating PrPSc-like conformation in the cytosol. Science 298: 1785-1788.
331. Deleault NR, Lucassen RW, Supattapone S (2003) RNA molecules stimulate prion protein conversion. Nature 425: 717-720.
332. Telling GC, Scott M, Mastrianni J, Gabizon R, Torchia M, et al. (1995) Prion propagation in mice expressing human and chimeric PrP transgenes implicates the interaction of cellular PrP with another protein. Cell 83: 79-90.
333. Godsave SF, Wille H, Pierson J, Prusiner SB, Peters PJ (2013) Plasma membrane invaginations containing clusters of full-length PrP(Sc) are an early form of prion-associated neuropathology in vivo. Neurobiol Aging 34: 1621-1631.
334. Kujala P, Raymond CR, Romeijn M, Godsave SF, van Kasteren SI, et al. (2011) Prion uptake in the gut: identification of the first uptake and replication sites. PLoS Pathog 7: e1002449.
335. Goold R, Rabbanian S, Sutton L, Andre R, Arora P, et al. (2011) Rapid cell-surface prion protein conversion revealed using a novel cell system. Nat Commun 2: 281.
336. Marijanovic Z, Caputo A, Campana V, Zurzolo C (2009) Identification of an intracellular site of prion conversion. PLoS Pathog 5: e1000426.
337. Didonna A, Vaccari L, Bek A, Legname G (2011) Infrared microspectroscopy: a multiple-screening platform for investigating single-cell biochemical perturbations upon prion infection. ACS Chem Neurosci 2: 160-174.
338. Soto C, Estrada L, Castilla J (2006) Amyloids, prions and the inherent infectious nature of misfolded protein aggregates. Trends Biochem Sci 31: 150-155.
339. Lansbury PT, Jr., Caughey B (1995) The chemistry of scrapie infection: implications of the 'ice 9' metaphor. Chem Biol 2: 1-5.

340. Sandberg MK, Al-Doujaily H, Sharps B, Clarke AR, Collinge J (2011) Prion propagation and toxicity in vivo occur in two distinct mechanistic phases. Nature 470: 540-542.
341. Baskakov IV (2007) Branched chain mechanism of polymerization and ultrastructure of prion protein amyloid fibrils. FEBS J 274: 3756-3765.
342. Baskakov IV, Bocharova OV (2005) In vitro conversion of mammalian prion protein into amyloid fibrils displays unusual features. Biochemistry 44: 2339-2348.
343. Fevrier B, Vilette D, Archer F, Loew D, Faigle W, et al. (2004) Cells release prions in association with exosomes. Proc Natl Acad Sci U S A 101: 9683-9688.
344. Gousset K, Schiff E, Langevin C, Marijanovic Z, Caputo A, et al. (2009) Prions hijack tunnelling nanotubes for intercellular spread. Nat Cell Biol 11: 328-336.
345. Mattei V, Barenco MG, Tasciotti V, Garofalo T, Longo A, et al. (2009) Paracrine diffusion of PrP(C) and propagation of prion infectivity by plasma membrane-derived microvesicles. PLoS One 4: e5057.
346. Aguzzi A, Rajendran L (2009) The transcellular spread of cytosolic amyloids, prions, and prionoids. Neuron 64: 783-790.
347. Diaz-Espinoza R, Soto C (2010) Generation of prions in vitro and the protein-only hypothesis. Prion 4: 53-59.
348. Bueler H, Aguzzi A, Sailer A, Greiner RA, Autenried P, et al. (1993) Mice devoid of PrP are resistant to scrapie. Cell 73: 1339-1347.
349. Telling GC (2008) Transgenic mouse models of prion diseases. Methods Mol Biol 459: 249-263.
350. Bessen RA, Marsh RF (1994) Distinct PrP properties suggest the molecular basis of strain variation in transmissible mink encephalopathy. J Virol 68: 7859-7868.
351. Telling GC, Parchi P, DeArmond SJ, Cortelli P, Montagna P, et al. (1996) Evidence for the conformation of the pathologic isoform of the prion protein enciphering and propagating prion diversity. Science 274: 2079-2082.
352. Prusiner SB (1989) Creutzfeldt-Jakob disease and scrapie prions. Alzheimer Dis Assoc Disord 3: 52-78.
353. Martin SF, Herva ME, Espinosa JC, Parra B, Castilla J, et al. (2006) Cell expression of a four extra octarepeat mutated PrPC modifies cell structure and cell cycle regulation. FEBS Lett 580: 4097-4104.
354. Pattison IH (1965) Scrapie in the welsh mountain breed of sheep and its experimental transmission to goats. Vet Rec 77: 1388-1390.
355. Lewis V, Hooper NM (2011) The role of lipid rafts in prion protein biology. Front Biosci 16: 151-168.
356. Lantos PL, McGill IS, Janota I, Doey LJ, Collinge J, et al. (1992) Prion protein immunocytochemistry helps to establish the true incidence of prion diseases. Neurosci Lett 147: 67-71.
357. Bruce M, Chree A, McConnell I, Foster J, Pearson G, et al. (1994) Transmission of bovine spongiform encephalopathy and scrapie to mice: strain variation and the species barrier. Philos Trans R Soc Lond B Biol Sci 343: 405-411.
358. Bessen RA, Marsh RF (1992) Biochemical and physical properties of the prion protein from two strains of the transmissible mink encephalopathy agent. J Virol 66: 2096-2101.

359. Hill AF, Desbruslais M, Joiner S, Sidle KC, Gowland I, et al. (1997) The same prion strain causes vCJD and BSE. Nature 389: 448-450, 526.
360. Asante EA, Linehan JM, Desbruslais M, Joiner S, Gowland I, et al. (2002) BSE prions propagate as either variant CJD-like or sporadic CJD-like prion strains in transgenic mice expressing human prion protein. EMBO J 21: 6358-6366.
361. Scott M, Foster D, Mirenda C, Serban D, Coufal F, et al. (1989) Transgenic mice expressing hamster prion protein produce species-specific scrapie infectivity and amyloid plaques. Cell 59: 847-857.
362. Bruce ME, Will RG, Ironside JW, McConnell I, Drummond D, et al. (1997) Transmissions to mice indicate that 'new variant' CJD is caused by the BSE agent. Nature 389: 498-501.
363. Collinge J (1999) Variant Creutzfeldt-Jakob disease. Lancet 354: 317-323.
364. Benetti F, Legname G (2009) De novo mammalian prion synthesis. Prion 3: 213-219.
365. Bessen RA, Kocisko DA, Raymond GJ, Nandan S, Lansbury PT, et al. (1995) Non-genetic propagation of strain-specific properties of scrapie prion protein. Nature 375: 698-700.
366. Hill AF, Antoniou M, Collinge J (1999) Protease-resistant prion protein produced in vitro lacks detectable infectivity. J Gen Virol 80 (Pt 1): 11-14.
367. Dossena S, Imeri L, Mangieri M, Garofoli A, Ferrari L, et al. (2008) Mutant prion protein expression causes motor and memory deficits and abnormal sleep patterns in a transgenic mouse model. Neuron 60: 598-609.
368. Hsiao KK, Scott M, Foster D, Groth DF, DeArmond SJ, et al. (1990) Spontaneous neurodegeneration in transgenic mice with mutant prion protein. Science 250: 1587-1590.
369. Jackson WS, Borkowski AW, Faas H, Steele AD, King OD, et al. (2009) Spontaneous generation of prion infectivity in fatal familial insomnia knockin mice. Neuron 63: 438-450.
370. Ayers JI, Schutt CR, Shikiya RA, Aguzzi A, Kincaid AE, et al. (2011) The strain-encoded relationship between PrP replication, stability and processing in neurons is predictive of the incubation period of disease. PLoS Pathog 7: e1001317.
371. Wang F, Wang X, Ma J (2011) Conversion of bacterially expressed recombinant prion protein. Methods 53: 208-213.
372. Colby DW, Zhang Q, Wang S, Groth D, Legname G, et al. (2007) Prion detection by an amyloid seeding assay. Proc Natl Acad Sci U S A 104: 20914-20919.
373. Legname G, Nguyen HO, Baskakov IV, Cohen FE, Dearmond SJ, et al. (2005) Strain-specified characteristics of mouse synthetic prions. Proc Natl Acad Sci U S A 102: 2168-2173.
374. Legname G, Nguyen HO, Peretz D, Cohen FE, DeArmond SJ, et al. (2006) Continuum of prion protein structures enciphers a multitude of prion isolate-specified phenotypes. Proc Natl Acad Sci U S A 103: 19105-19110.
375. Bocharova OV, Makarava N, Breydo L, Anderson M, Salnikov VV, et al. (2006) Annealing prion protein amyloid fibrils at high temperature results in extension of a proteinase K-resistant core. J Biol Chem 281: 2373-2379.
376. Makarava N, Kovacs GG, Bocharova O, Savtchenko R, Alexeeva I, et al. (2010) Recombinant prion protein induces a new transmissible prion disease in wild-type animals. Acta Neuropathol 119: 177-187.

377. Atarashi R, Moore RA, Sim VL, Hughson AG, Dorward DW, et al. (2007) Ultrasensitive detection of scrapie prion protein using seeded conversion of recombinant prion protein. Nat Methods 4: 645-650.
378. Atarashi R, Wilham JM, Christensen L, Hughson AG, Moore RA, et al. (2008) Simplified ultrasensitive prion detection by recombinant PrP conversion with shaking. Nat Methods 5: 211-212.
379. Chen B, Morales R, Barria MA, Soto C (2010) Estimating prion concentration in fluids and tissues by quantitative PMCA. Nat Methods 7: 519-520.
380. Atarashi R, Sano K, Satoh K, Nishida N (2011) Real-time quaking-induced conversion: a highly sensitive assay for prion detection. Prion 5: 150-153.
381. Orru CD, Caughey B (2011) Prion seeded conversion and amplification assays. Top Curr Chem 305: 121-133.
382. Orru CD, Wilham JM, Raymond LD, Kuhn F, Schroeder B, et al. (2011) Prion disease blood test using immunoprecipitation and improved quaking-induced conversion. MBio 2: e00078-00011.
383. Wilham JM, Orru CD, Bessen RA, Atarashi R, Sano K, et al. (2010) Rapid end-point quantitation of prion seeding activity with sensitivity comparable to bioassays. PLoS Pathog 6: e1001217.
384. Hosszu LL, Tattum MH, Jones S, Trevitt CR, Wells MA, et al. (2010) The H187R mutation of the human prion protein induces conversion of recombinant prion protein to the PrP(Sc)-like form. Biochemistry 49: 8729-8738.
385. Vanik DL, Surewicz WK (2002) Disease-associated F198S mutation increases the propensity of the recombinant prion protein for conformational conversion to scrapie-like form. J Biol Chem 277: 49065-49070.
386. Lehmann S, Harris DA (1996) Two mutant prion proteins expressed in cultured cells acquire biochemical properties reminiscent of the scrapie isoform. Proc Natl Acad Sci U S A 93: 5610-5614.
387. Nazor KE, Kuhn F, Seward T, Green M, Zwald D, et al. (2005) Immunodetection of disease-associated mutant PrP, which accelerates disease in GSS transgenic mice. EMBO J 24: 2472-2480.
388. Brown P, Kenney K, Little B, Ironside J, Will R, et al. (1995) Intracerebral distribution of infectious amyloid protein in spongiform encephalopathy. Ann Neurol 38: 245-253.
389. Little BW, Brown PW, Rodgers-Johnson P, Perl DP, Gajdusek DC (1986) Familial myoclonic dementia masquerading as Creutzfeldt-Jakob disease. Ann Neurol 20: 231-239.
390. Zarranz JJ, Digon A, Atares B, Rodriguez-Martinez AB, Arce A, et al. (2005) Phenotypic variability in familial prion diseases due to the D178N mutation. J Neurol Neurosurg Psychiatry 76: 1491-1496.
391. Gambetti P, Cali I, Notari S, Kong Q, Zou WQ, et al. (2011) Molecular biology and pathology of prion strains in sporadic human prion diseases. Acta Neuropathol 121: 79-90.
392. Fischer M, Rulicke T, Raeber A, Sailer A, Moser M, et al. (1996) Prion protein (PrP) with amino-proximal deletions restoring susceptibility of PrP knockout mice to scrapie. EMBO J 15: 1255-1264.

393. McKinley MP, Bolton DC, Prusiner SB (1983) A protease-resistant protein is a structural component of the scrapie prion. Cell 35: 57-62.
394. Tremblay P, Ball HL, Kaneko K, Groth D, Hegde RS, et al. (2004) Mutant PrPSc conformers induced by a synthetic peptide and several prion strains. J Virol 78: 2088-2099.
395. Perez DR, Damberger FF, Wuthrich K (2010) Horse prion protein NMR structure and comparisons with related variants of the mouse prion protein. J Mol Biol 400: 121-128.
396. Saa P, Castilla J, Soto C (2005) Cyclic amplification of protein misfolding and aggregation. Methods Mol Biol 299: 53-65.
397. Castilla J, Morales R, Saa P, Barria M, Gambetti P, et al. (2008) Cell-free propagation of prion strains. EMBO J 27: 2557-2566.
398. Deleault NR, Geoghegan JC, Nishina K, Kascsak R, Williamson RA, et al. (2005) Protease-resistant prion protein amplification reconstituted with partially purified substrates and synthetic polyanions. J Biol Chem 280: 26873-26879.
399. Geoghegan JC, Valdes PA, Orem NR, Deleault NR, Williamson RA, et al. (2007) Selective incorporation of polyanionic molecules into hamster prions. J Biol Chem 282: 36341-36353.
400. Wang F, Yang F, Hu Y, Wang X, Jin C, et al. (2007) Lipid interaction converts prion protein to a PrPSc-like proteinase K-resistant conformation under physiological conditions. Biochemistry 46: 7045-7053.
401. Baskakov IV, Legname G, Baldwin MA, Prusiner SB, Cohen FE (2002) Pathway complexity of prion protein assembly into amyloid. J Biol Chem 277: 21140-21148.
402. Bjorndahl TC, Zhou GP, Liu X, Perez-Pineiro R, Semenchenko V, et al. (2011) Detailed biophysical characterization of the acid-induced PrP(c) to PrP(beta) conversion process. Biochemistry 50: 1162-1173.
403. Bocharova OV, Breydo L, Parfenov AS, Salnikov VV, Baskakov IV (2005) In vitro conversion of full-length mammalian prion protein produces amyloid form with physical properties of PrP(Sc). J Mol Biol 346: 645-659.
404. Cobb NJ, Apetri AC, Surewicz WK (2008) Prion protein amyloid formation under native-like conditions involves refolding of the C-terminal alpha-helical domain. J Biol Chem 283: 34704-34711.
405. Jackson GS, Hosszu LL, Power A, Hill AF, Kenney J, et al. (1999) Reversible conversion of monomeric human prion protein between native and fibrilogenic conformations. Science 283: 1935-1937.
406. Jones EM, Surewicz WK (2005) Fibril conformation as the basis of species- and strain-dependent seeding specificity of mammalian prion amyloids. Cell 121: 63-72.
407. Polano M, Bek A, Benetti F, Lazzarino M, Legname G (2009) Structural insights into alternate aggregated prion protein forms. J Mol Biol 393: 1033-1042.
408. Kryndushkin DS, Alexandrov IM, Ter-Avanesyan MD, Kushnirov VV (2003) Yeast [PSI+] prion aggregates are formed by small Sup35 polymers fragmented by Hsp104. J Biol Chem 278: 49636-49643.
409. Lee S, Tsai FT (2007) Crystallization and preliminary X-ray crystallographic analysis of a 40 kDa N-terminal fragment of the yeast prion-remodeling factor Hsp104. Acta Crystallogr Sect F Struct Biol Cryst Commun 63: 784-786.

410. Sun Y, Makarava N, Lee CI, Laksanalamai P, Robb FT, et al. (2008) Conformational stability of PrP amyloid fibrils controls their smallest possible fragment size. J Mol Biol 376: 1155-1167.
411. Yonetani M, Nonaka T, Masuda M, Inukai Y, Oikawa T, et al. (2009) Conversion of wild-type alpha-synuclein into mutant-type fibrils and its propagation in the presence of A30P mutant. J Biol Chem 284: 7940-7950.
412. Zhou Z, Fan JB, Zhu HL, Shewmaker F, Yan X, et al. (2009) Crowded cell-like environment accelerates the nucleation step of amyloidogenic protein misfolding. J Biol Chem 284: 30148-30158.
413. Castilla J, Hetz C, Soto C (2004) Molecular mechanisms of neurotoxicity of pathological prion protein. Curr Mol Med 4: 397-403.
414. Westaway D, Cooper C, Turner S, Da Costa M, Carlson GA, et al. (1994) Structure and polymorphism of the mouse prion protein gene. Proc Natl Acad Sci U S A 91: 6418-6422.
415. Soto C, Saborio GP (2001) Prions: disease propagation and disease therapy by conformational transmission. Trends Mol Med 7: 109-114.
416. Silveira JR, Raymond GJ, Hughson AG, Race RE, Sim VL, et al. (2005) The most infectious prion protein particles. Nature 437: 257-261.
417. Polymenidou M, Cleveland DW (2012) Prion-like spread of protein aggregates in neurodegeneration. J Exp Med 209: 889-893.
418. Gajdusek DC, Gibbs CJ, Alpers M (1966) Experimental transmission of a Kuru-like syndrome to chimpanzees. Nature 209: 794-796.
419. Kane MD, Lipinski WJ, Callahan MJ, Bian F, Durham RA, et al. (2000) Evidence for seeding of beta -amyloid by intracerebral infusion of Alzheimer brain extracts in beta -amyloid precursor protein-transgenic mice. J Neurosci 20: 3606-3611.
420. Meyer-Luehmann M, Coomaraswamy J, Bolmont T, Kaeser S, Schaefer C, et al. (2006) Exogenous induction of cerebral beta-amyloidogenesis is governed by agent and host. Science 313: 1781-1784.
421. Langer F, Eisele YS, Fritschi SK, Staufenbiel M, Walker LC, et al. (2011) Soluble Abeta seeds are potent inducers of cerebral beta-amyloid deposition. J Neurosci 31: 14488-14495.
422. Nussbaum JM, Schilling S, Cynis H, Silva A, Swanson E, et al. (2012) Prion-like behaviour and tau-dependent cytotoxicity of pyroglutamylated amyloid-beta. Nature 485: 651-655.
423. Morales R, Duran-Aniotz C, Castilla J, Estrada LD, Soto C (2012) De novo induction of amyloid-beta deposition in vivo. Mol Psychiatry 17: 1347-1353.
424. Rosen RF, Fritz JJ, Dooyema J, Cintron AF, Hamaguchi T, et al. (2012) Exogenous seeding of cerebral beta-amyloid deposition in betaAPP-transgenic rats. J Neurochem 120: 660-666.
425. Eisele YS, Obermuller U, Heilbronner G, Baumann F, Kaeser SA, et al. (2010) Peripherally applied Abeta-containing inoculates induce cerebral beta-amyloidosis. Science 330: 980-982.
426. Clavaguera F, Bolmont T, Crowther RA, Abramowski D, Frank S, et al. (2009) Transmission and spreading of tauopathy in transgenic mouse brain. Nat Cell Biol 11: 909-913.

427. Frost B, Jacks RL, Diamond MI (2009) Propagation of tau misfolding from the outside to the inside of a cell. J Biol Chem 284: 12845-12852.
428. Nonaka T, Watanabe ST, Iwatsubo T, Hasegawa M (2010) Seeded aggregation and toxicity of {alpha}-synuclein and tau: cellular models of neurodegenerative diseases. J Biol Chem 285: 34885-34898.
429. Guo JL, Lee VM (2011) Seeding of normal Tau by pathological Tau conformers drives pathogenesis of Alzheimer-like tangles. J Biol Chem 286: 15317-15331.
430. de Calignon A, Polydoro M, Suarez-Calvet M, William C, Adamowicz DH, et al. (2012) Propagation of tau pathology in a model of early Alzheimer's disease. Neuron 73: 685-697.
431. Liu L, Drouet V, Wu JW, Witter MP, Small SA, et al. (2012) Trans-synaptic spread of tau pathology in vivo. PLoS One 7: e31302.
432. Braak H, Braak E (1991) Demonstration of amyloid deposits and neurofibrillary changes in whole brain sections. Brain Pathol 1: 213-216.
433. Braak H, Braak E, Yilmazer D, de Vos RA, Jansen EN, et al. (1996) Pattern of brain destruction in Parkinson's and Alzheimer's diseases. J Neural Transm 103: 455-490.
434. Brundin P, Li JY, Holton JL, Lindvall O, Revesz T (2008) Research in motion: the enigma of Parkinson's disease pathology spread. Nat Rev Neurosci 9: 741-745.
435. Brundin P, Melki R, Kopito R (2010) Prion-like transmission of protein aggregates in neurodegenerative diseases. Nat Rev Mol Cell Biol 11: 301-307.
436. Desplats P, Lee HJ, Bae EJ, Patrick C, Rockenstein E, et al. (2009) Inclusion formation and neuronal cell death through neuron-to-neuron transmission of alpha-synuclein. Proc Natl Acad Sci U S A 106: 13010-13015.
437. Luk KC, Song C, O'Brien P, Stieber A, Branch JR, et al. (2009) Exogenous alpha-synuclein fibrils seed the formation of Lewy body-like intracellular inclusions in cultured cells. Proc Natl Acad Sci U S A 106: 20051-20056.
438. Volpicelli-Daley LA, Luk KC, Patel TP, Tanik SA, Riddle DM, et al. (2011) Exogenous alpha-synuclein fibrils induce Lewy body pathology leading to synaptic dysfunction and neuron death. Neuron 72: 57-71.
439. Mougenot AL, Nicot S, Bencsik A, Morignat E, Verchere J, et al. (2012) Prion-like acceleration of a synucleinopathy in a transgenic mouse model. Neurobiol Aging 33: 2225-2228.
440. Hansen C, Angot E, Bergstrom AL, Steiner JA, Pieri L, et al. (2011) alpha-Synuclein propagates from mouse brain to grafted dopaminergic neurons and seeds aggregation in cultured human cells. J Clin Invest 121: 715-725.
441. Luk KC, Kehm V, Carroll J, Zhang B, O'Brien P, et al. (2012) Pathological alpha-synuclein transmission initiates Parkinson-like neurodegeneration in nontransgenic mice. Science 338: 949-953.
442. Ren PH, Lauckner JE, Kachirskaia I, Heuser JE, Melki R, et al. (2009) Cytoplasmic penetration and persistent infection of mammalian cells by polyglutamine aggregates. Nat Cell Biol 11: 219-225.
443. Lundmark K, Westermark GT, Nystrom S, Murphy CL, Solomon A, et al. (2002) Transmissibility of systemic amyloidosis by a prion-like mechanism. Proc Natl Acad Sci U S A 99: 6979-6984.

444. Zhang B, Une Y, Fu X, Yan J, Ge F, et al. (2008) Fecal transmission of AA amyloidosis in the cheetah contributes to high incidence of disease. Proc Natl Acad Sci U S A 105: 7263-7268.
445. Xing Y, Nakamura A, Chiba T, Kogishi K, Matsushita T, et al. (2001) Transmission of mouse senile amyloidosis. Lab Invest 81: 493-499.
446. Korenaga T, Yan J, Sawashita J, Matsushita T, Naiki H, et al. (2006) Transmission of amyloidosis in offspring of mice with AApoAII amyloidosis. Am J Pathol 168: 898-906.
447. Polymeropoulos MH, Lavedan C, Leroy E, Ide SE, Dehejia A, et al. (1997) Mutation in the alpha-synuclein gene identified in families with Parkinson's disease. Science 276: 2045-2047.
448. Spillantini MG, Crowther RA, Jakes R, Hasegawa M, Goedert M (1998) alpha-Synuclein in filamentous inclusions of Lewy bodies from Parkinson's disease and dementia with lewy bodies. Proc Natl Acad Sci U S A 95: 6469-6473.
449. Lippa CF, Fujiwara H, Mann DM, Giasson B, Baba M, et al. (1998) Lewy bodies contain altered alpha-synuclein in brains of many familial Alzheimer's disease patients with mutations in presenilin and amyloid precursor protein genes. Am J Pathol 153: 1365-1370.
450. Lippa CF, Smith TW, Saunders AM, Crook R, Pulaski-Salo D, et al. (1995) Apolipoprotein E genotype and Lewy body disease. Neurology 45: 97-103.
451. Spillantini MG, Tolnay M, Love S, Goedert M (1999) Microtubule-associated protein tau, heparan sulphate and alpha-synuclein in several neurodegenerative diseases with dementia. Acta Neuropathol 97: 585-594.
452. Tu PH, Galvin JE, Baba M, Giasson B, Tomita T, et al. (1998) Glial cytoplasmic inclusions in white matter oligodendrocytes of multiple system atrophy brains contain insoluble alpha-synuclein. Ann Neurol 44: 415-422.
453. Arawaka S, Saito Y, Murayama S, Mori H (1998) Lewy body in neurodegeneration with brain iron accumulation type 1 is immunoreactive for alpha-synuclein. Neurology 51: 887-889.
454. Wakabayashi K, Yoshimoto M, Fukushima T, Koide R, Horikawa Y, et al. (1999) Widespread occurrence of alpha-synuclein/NACP-immunoreactive neuronal inclusions in juvenile and adult-onset Hallervorden-Spatz disease with Lewy bodies. Neuropathol Appl Neurobiol 25: 363-368.
455. Wakabayashi K, Yoshimoto M, Tsuji S, Takahashi H (1998) Alpha-synuclein immunoreactivity in glial cytoplasmic inclusions in multiple system atrophy. Neurosci Lett 249: 180-182.
456. Mezey E, Dehejia A, Harta G, Papp MI, Polymeropoulos MH, et al. (1998) Alpha synuclein in neurodegenerative disorders: murderer or accomplice? Nat Med 4: 755-757.
457. Spillantini MG, Crowther RA, Jakes R, Cairns NJ, Lantos PL, et al. (1998) Filamentous alpha-synuclein inclusions link multiple system atrophy with Parkinson's disease and dementia with Lewy bodies. Neurosci Lett 251: 205-208.
458. Gai WP, Power JH, Blumbergs PC, Blessing WW (1998) Multiple-system atrophy: a new alpha-synuclein disease? Lancet 352: 547-548.
459. Marti MJ, Tolosa E, Campdelacreu J (2003) Clinical overview of the synucleinopathies. Mov Disord 18 Suppl 6: S21-27.

460. Polymeropoulos MH, Higgins JJ, Golbe LI, Johnson WG, Ide SE, et al. (1996) Mapping of a gene for Parkinson's disease to chromosome 4q21-q23. Science 274: 1197-1199.
461. Tanner CM (1992) Occupational and environmental causes of parkinsonism. Occup Med 7: 503-513.
462. Dluzen DE, McDermott JL (2000) Gender differences in neurotoxicity of the nigrostriatal dopaminergic system: implications for Parkinson's disease. J Gend Specif Med 3: 36-42.
463. Lotharius J, Brundin P (2002) Pathogenesis of Parkinson's disease: dopamine, vesicles and alpha-synuclein. Nat Rev Neurosci 3: 932-942.
464. Siderowf A, Stern M (2003) Update on Parkinson disease. Ann Intern Med 138: 651-658.
465. Berrios GE, Campbell C, Politynska BE (1995) Autonomic failure, depression and anxiety in Parkinson's disease. Br J Psychiatry 166: 789-792.
466. Gomez-Tortosa E, Newell K, Irizarry MC, Albert M, Growdon JH, et al. (1999) Clinical and quantitative pathologic correlates of dementia with Lewy bodies. Neurology 53: 1284-1291.
467. O'Sullivan SS, Williams DR, Gallagher DA, Massey LA, Silveira-Moriyama L, et al. (2008) Nonmotor symptoms as presenting complaints in Parkinson's disease: a clinicopathological study. Mov Disord 23: 101-106.
468. Doty RL (2012) Olfactory dysfunction in Parkinson disease. Nat Rev Neurol 8: 329-339.
469. Muqit MM, Gandhi S, Wood NW (2006) Mitochondria in Parkinson disease: back in fashion with a little help from genetics. Arch Neurol 63: 649-654.
470. Greenamyre JT, Hastings TG (2004) Biomedicine. Parkinson's--divergent causes, convergent mechanisms. Science 304: 1120-1122.
471. Schiesling C, Kieper N, Seidel K, Kruger R (2008) Review: Familial Parkinson's disease--genetics, clinical phenotype and neuropathology in relation to the common sporadic form of the disease. Neuropathol Appl Neurobiol 34: 255-271.
472. Farrer MJ (2006) Genetics of Parkinson disease: paradigm shifts and future prospects. Nat Rev Genet 7: 306-318.
473. Singleton AB, Farrer M, Johnson J, Singleton A, Hague S, et al. (2003) alpha-Synuclein locus triplication causes Parkinson's disease. Science 302: 841.
474. Ross OA, Braithwaite AT, Skipper LM, Kachergus J, Hulihan MM, et al. (2008) Genomic investigation of alpha-synuclein multiplication and parkinsonism. Ann Neurol 63: 743-750.
475. Chartier-Harlin MC, Kachergus J, Roumier C, Mouroux V, Douay X, et al. (2004) Alpha-synuclein locus duplication as a cause of familial Parkinson's disease. Lancet 364: 1167-1169.
476. Kruger R, Kuhn W, Muller T, Woitalla D, Graeber M, et al. (1998) Ala30Pro mutation in the gene encoding alpha-synuclein in Parkinson's disease. Nat Genet 18: 106-108.
477. Zarranz JJ, Alegre J, Gomez-Esteban JC, Lezcano E, Ros R, et al. (2004) The new mutation, E46K, of alpha-synuclein causes Parkinson and Lewy body dementia. Ann Neurol 55: 164-173.
478. Eriksen JL, Dawson TM, Dickson DW, Petrucelli L (2003) Caught in the act: alpha-synuclein is the culprit in Parkinson's disease. Neuron 40: 453-456.

479. Simon-Sanchez J, Schulte C, Bras JM, Sharma M, Gibbs JR, et al. (2009) Genome-wide association study reveals genetic risk underlying Parkinson's disease. Nat Genet 41: 1308-1312.
480. Farrer M, Kachergus J, Forno L, Lincoln S, Wang DS, et al. (2004) Comparison of kindreds with parkinsonism and alpha-synuclein genomic multiplications. Ann Neurol 55: 174-179.
481. Cookson MR (2009) alpha-Synuclein and neuronal cell death. Mol Neurodegener 4: 9.
482. Pals P, Lincoln S, Manning J, Heckman M, Skipper L, et al. (2004) alpha-Synuclein promoter confers susceptibility to Parkinson's disease. Ann Neurol 56: 591-595.
483. Maraganore DM, de Andrade M, Elbaz A, Farrer MJ, Ioannidis JP, et al. (2006) Collaborative analysis of alpha-synuclein gene promoter variability and Parkinson disease. JAMA 296: 661-670.
484. Mueller JC, Fuchs J, Hofer A, Zimprich A, Lichtner P, et al. (2005) Multiple regions of alpha-synuclein are associated with Parkinson's disease. Ann Neurol 57: 535-541.
485. Satake W, Nakabayashi Y, Mizuta I, Hirota Y, Ito C, et al. (2009) Genome-wide association study identifies common variants at four loci as genetic risk factors for Parkinson's disease. Nat Genet 41: 1303-1307.
486. Kitada T, Asakawa S, Hattori N, Matsumine H, Yamamura Y, et al. (1998) Mutations in the parkin gene cause autosomal recessive juvenile parkinsonism. Nature 392: 605-608.
487. Shimura H, Schlossmacher MG, Hattori N, Frosch MP, Trockenbacher A, et al. (2001) Ubiquitination of a new form of alpha-synuclein by parkin from human brain: implications for Parkinson's disease. Science 293: 263-269.
488. Macedo MG, Anar B, Bronner IF, Cannella M, Squitieri F, et al. (2003) The DJ-1L166P mutant protein associated with early onset Parkinson's disease is unstable and forms higher-order protein complexes. Hum Mol Genet 12: 2807-2816.
489. Leroy E, Boyer R, Auburger G, Leube B, Ulm G, et al. (1998) The ubiquitin pathway in Parkinson's disease. Nature 395: 451-452.
490. Gasser T, Muller-Myhsok B, Wszolek ZK, Oehlmann R, Calne DB, et al. (1998) A susceptibility locus for Parkinson's disease maps to chromosome 2p13. Nat Genet 18: 262-265.
491. Funayama M, Hasegawa K, Kowa H, Saito M, Tsuji S, et al. (2002) A new locus for Parkinson's disease (PARK8) maps to chromosome 12p11.2-q13.1. Ann Neurol 51: 296-301.
492. Hicks AA, Petursson H, Jonsson T, Stefansson H, Johannsdottir HS, et al. (2002) A susceptibility gene for late-onset idiopathic Parkinson's disease. Ann Neurol 52: 549-555.
493. Pankratz N, Nichols WC, Uniacke SK, Halter C, Rudolph A, et al. (2003) Significant linkage of Parkinson disease to chromosome 2q36-37. Am J Hum Genet 72: 1053-1057.
494. Gupta A, Dawson VL, Dawson TM (2008) What causes cell death in Parkinson's disease? Ann Neurol 64 Suppl 2: S3-15.
495. Ransmayr G (2000) Dementia with Lewy bodies: prevalence, clinical spectrum and natural history. J Neural Transm Suppl: 303-314.
496. Quinn N (1989) Multiple system atrophy--the nature of the beast. J Neurol Neurosurg Psychiatry Suppl: 78-89.

497. Graham JG, Oppenheimer DR (1969) Orthostatic hypotension and nicotine sensitivity in a case of multiple system atrophy. J Neurol Neurosurg Psychiatry 32: 28-34.
498. Wenning GK, Tison F, Ben Shlomo Y, Daniel SE, Quinn NP (1997) Multiple system atrophy: a review of 203 pathologically proven cases. Mov Disord 12: 133-147.
499. Gilman S, Low PA, Quinn N, Albanese A, Ben-Shlomo Y, et al. (1999) Consensus statement on the diagnosis of multiple system atrophy. J Neurol Sci 163: 94-98.
500. (1996) Consensus statement on the definition of orthostatic hypotension, pure autonomic failure, and multiple system atrophy. The Consensus Committee of the American Autonomic Society and the American Academy of Neurology. Neurology 46: 1470.
501. Larner AJ, Mathias CJ, Rossor MN (2000) Autonomic failure preceding dementia with Lewy bodies. J Neurol 247: 229-231.
502. Hague K, Lento P, Morgello S, Caro S, Kaufmann H (1997) The distribution of Lewy bodies in pure autonomic failure: autopsy findings and review of the literature. Acta Neuropathol 94: 192-196.
503. Arai K, Kato N, Kashiwado K, Hattori T (2000) Pure autonomic failure in association with human alpha-synucleinopathy. Neurosci Lett 296: 171-173.
504. Kaufmann H, Hague K, Perl D (2001) Accumulation of alpha-synuclein in autonomic nerves in pure autonomic failure. Neurology 56: 980-981.
505. Maroteaux L, Campanelli JT, Scheller RH (1988) Synuclein: a neuron-specific protein localized to the nucleus and presynaptic nerve terminal. J Neurosci 8: 2804-2815.
506. Maroteaux L, Scheller RH (1991) The rat brain synucleins; family of proteins transiently associated with neuronal membrane. Brain Res Mol Brain Res 11: 335-343.
507. Tobe T, Nakajo S, Tanaka A, Mitoya A, Omata K, et al. (1992) Cloning and characterization of the cDNA encoding a novel brain-specific 14-kDa protein. J Neurochem 59: 1624-1629.
508. Ueda K, Fukushima H, Masliah E, Xia Y, Iwai A, et al. (1993) Molecular cloning of cDNA encoding an unrecognized component of amyloid in Alzheimer disease. Proc Natl Acad Sci U S A 90: 11282-11286.
509. Bayer TA, Jakala P, Hartmann T, Havas L, McLean C, et al. (1999) Alpha-synuclein accumulates in Lewy bodies in Parkinson's disease and dementia with Lewy bodies but not in Alzheimer's disease beta-amyloid plaque cores. Neurosci Lett 266: 213-216.
510. Culvenor JG, McLean CA, Cutt S, Campbell BC, Maher F, et al. (1999) Non-Abeta component of Alzheimer's disease amyloid (NAC) revisited. NAC and alpha-synuclein are not associated with Abeta amyloid. Am J Pathol 155: 1173-1181.
511. Jakes R, Spillantini MG, Goedert M (1994) Identification of two distinct synucleins from human brain. FEBS Lett 345: 27-32.
512. George JM, Jin H, Woods WS, Clayton DF (1995) Characterization of a novel protein regulated during the critical period for song learning in the zebra finch. Neuron 15: 361-372.
513. Campion D, Martin C, Heilig R, Charbonnier F, Moreau V, et al. (1995) The NACP/synuclein gene: chromosomal assignment and screening for alterations in Alzheimer disease. Genomics 26: 254-257.

514. Chen X, de Silva HA, Pettenati MJ, Rao PN, St George-Hyslop P, et al. (1995) The human NACP/alpha-synuclein gene: chromosome assignment to 4q21.3-q22 and TaqI RFLP analysis. Genomics 26: 425-427.
515. Spillantini MG, Divane A, Goedert M (1995) Assignment of human alpha-synuclein (SNCA) and beta-synuclein (SNCB) genes to chromosomes 4q21 and 5q35. Genomics 27: 379-381.
516. Shibasaki Y, Baillie DA, St Clair D, Brookes AJ (1995) High-resolution mapping of SNCA encoding alpha-synuclein, the non-A beta component of Alzheimer's disease amyloid precursor, to human chromosome 4q21.3-->q22 by fluorescence in situ hybridization. Cytogenet Cell Genet 71: 54-55.
517. Lavedan C, Leroy E, Torres R, Dehejia A, Dutra A, et al. (1998) Genomic organization and expression of the human beta-synuclein gene (SNCB). Genomics 54: 173-175.
518. Ueda K, Saitoh T, Mori H (1994) Tissue-dependent alternative splicing of mRNA for NACP, the precursor of non-A beta component of Alzheimer's disease amyloid. Biochem Biophys Res Commun 205: 1366-1372.
519. Spillantini MG, Goedert M (2000) The alpha-synucleinopathies: Parkinson's disease, dementia with Lewy bodies, and multiple system atrophy. Ann N Y Acad Sci 920: 16-27.
520. Ji H, Liu YE, Jia T, Wang M, Liu J, et al. (1997) Identification of a breast cancer-specific gene, BCSG1, by direct differential cDNA sequencing. Cancer Res 57: 759-764.
521. Goedert M, Jakes R, Anthony Crowther R, Grazia Spillantini M (2001) Parkinson's Disease, Dementia with Lewy Bodies, and Multiple System Atrophy as alpha-Synucleinopathies. Methods Mol Med 62: 33-59.
522. Buchman VL, Hunter HJ, Pinon LG, Thompson J, Privalova EM, et al. (1998) Persyn, a member of the synuclein family, has a distinct pattern of expression in the developing nervous system. J Neurosci 18: 9335-9341.
523. Lavedan C, Leroy E, Dehejia A, Buchholtz S, Dutra A, et al. (1998) Identification, localization and characterization of the human gamma-synuclein gene. Hum Genet 103: 106-112.
524. Ninkina NN, Alimova-Kost MV, Paterson JW, Delaney L, Cohen BB, et al. (1998) Organization, expression and polymorphism of the human persyn gene. Hum Mol Genet 7: 1417-1424.
525. Surguchov A, Surgucheva I, Solessio E, Baehr W (1999) Synoretin--A new protein belonging to the synuclein family. Mol Cell Neurosci 13: 95-103.
526. Lavedan C (1998) The synuclein family. Genome Res 8: 871-880.
527. George JM (2002) The synucleins. Genome Biol 3: REVIEWS3002.
528. Iwai A, Masliah E, Yoshimoto M, Ge N, Flanagan L, et al. (1995) The precursor protein of non-A beta component of Alzheimer's disease amyloid is a presynaptic protein of the central nervous system. Neuron 14: 467-475.
529. Withers GS, George JM, Banker GA, Clayton DF (1997) Delayed localization of synelfin (synuclein, NACP) to presynaptic terminals in cultured rat hippocampal neurons. Brain Res Dev Brain Res 99: 87-94.
530. Lee VM, Trojanowski JQ (2006) Mechanisms of Parkinson's disease linked to pathological alpha-synuclein: new targets for drug discovery. Neuron 52: 33-38.

531. Bennett MC, Bishop JF, Leng Y, Chock PB, Chase TN, et al. (1999) Degradation of alpha-synuclein by proteasome. J Biol Chem 274: 33855-33858.
532. Tofaris GK, Layfield R, Spillantini MG (2001) alpha-synuclein metabolism and aggregation is linked to ubiquitin-independent degradation by the proteasome. FEBS Lett 509: 22-26.
533. Webb JL, Ravikumar B, Atkins J, Skepper JN, Rubinsztein DC (2003) Alpha-Synuclein is degraded by both autophagy and the proteasome. J Biol Chem 278: 25009-25013.
534. Paxinou E, Chen Q, Weisse M, Giasson BI, Norris EH, et al. (2001) Induction of alpha-synuclein aggregation by intracellular nitrative insult. J Neurosci 21: 8053-8061.
535. Wan OW, Chung KK (2012) The role of alpha-synuclein oligomerization and aggregation in cellular and animal models of Parkinson's disease. PLoS One 7: e38545.
536. Paleologou KE, Kragh CL, Mann DM, Salem SA, Al-Shami R, et al. (2009) Detection of elevated levels of soluble alpha-synuclein oligomers in post-mortem brain extracts from patients with dementia with Lewy bodies. Brain 132: 1093-1101.
537. Tokuda T, Qureshi MM, Ardah MT, Varghese S, Shehab SA, et al. (2010) Detection of elevated levels of alpha-synuclein oligomers in CSF from patients with Parkinson disease. Neurology 75: 1766-1772.
538. Bertoncini CW, Jung YS, Fernandez CO, Hoyer W, Griesinger C, et al. (2005) Release of long-range tertiary interactions potentiates aggregation of natively unstructured alpha-synuclein. Proc Natl Acad Sci U S A 102: 1430-1435.
539. Celej MS, Sarroukh R, Goormaghtigh E, Fidelio GD, Ruysschaert JM, et al. (2012) Toxic prefibrillar alpha-synuclein amyloid oligomers adopt a distinctive antiparallel beta-sheet structure. Biochem J 443: 719-726.
540. Tsigelny IF, Sharikov Y, Wrasidlo W, Gonzalez T, Desplats PA, et al. (2012) Role of alpha-synuclein penetration into the membrane in the mechanisms of oligomer pore formation. FEBS J 279: 1000-1013.
541. Stockl M, Claessens MM, Subramaniam V (2012) Kinetic measurements give new insights into lipid membrane permeabilization by alpha-synuclein oligomers. Mol Biosyst 8: 338-345.
542. Wang S, Xu B, Liou LC, Ren Q, Huang S, et al. (2012) alpha-Synuclein disrupts stress signaling by inhibiting polo-like kinase Cdc5/Plk2. Proc Natl Acad Sci U S A 109: 16119-16124.
543. Ulmer TS, Bax A, Cole NB, Nussbaum RL (2005) Structure and dynamics of micelle-bound human alpha-synuclein. J Biol Chem 280: 9595-9603.
544. Eliezer D, Kutluay E, Bussell R, Jr., Browne G (2001) Conformational properties of alpha-synuclein in its free and lipid-associated states. J Mol Biol 307: 1061-1073.
545. Kahle PJ, Haass C, Kretzschmar HA, Neumann M (2002) Structure/function of alpha-synuclein in health and disease: rational development of animal models for Parkinson's and related diseases. J Neurochem 82: 449-457.
546. Chandra S, Chen X, Rizo J, Jahn R, Sudhof TC (2003) A broken alpha -helix in folded alpha -Synuclein. J Biol Chem 278: 15313-15318.
547. Uversky VN, Fink AL (2002) Amino acid determinants of alpha-synuclein aggregation: putting together pieces of the puzzle. FEBS Lett 522: 9-13.
548. Davidson WS, Jonas A, Clayton DF, George JM (1998) Stabilization of alpha-synuclein secondary structure upon binding to synthetic membranes. J Biol Chem 273: 9443-9449.

549. Li J, Uversky VN, Fink AL (2001) Effect of familial Parkinson's disease point mutations A30P and A53T on the structural properties, aggregation, and fibrillation of human alpha-synuclein. Biochemistry 40: 11604-11613.
550. Conway KA, Rochet JC, Bieganski RM, Lansbury PT, Jr. (2001) Kinetic stabilization of the alpha-synuclein protofibril by a dopamine-alpha-synuclein adduct. Science 294: 1346-1349.
551. Lee HJ, Choi C, Lee SJ (2002) Membrane-bound alpha-synuclein has a high aggregation propensity and the ability to seed the aggregation of the cytosolic form. J Biol Chem 277: 671-678.
552. Lee HJ, Shin SY, Choi C, Lee YH, Lee SJ (2002) Formation and removal of alpha-synuclein aggregates in cells exposed to mitochondrial inhibitors. J Biol Chem 277: 5411-5417.
553. Masliah E, Iwai A, Mallory M, Ueda K, Saitoh T (1996) Altered presynaptic protein NACP is associated with plaque formation and neurodegeneration in Alzheimer's disease. Am J Pathol 148: 201-210.
554. Giasson BI, Murray IV, Trojanowski JQ, Lee VM (2001) A hydrophobic stretch of 12 amino acid residues in the middle of alpha-synuclein is essential for filament assembly. J Biol Chem 276: 2380-2386.
555. el-Agnaf OM, Irvine GB (2002) Aggregation and neurotoxicity of alpha-synuclein and related peptides. Biochem Soc Trans 30: 559-565.
556. Okochi M, Walter J, Koyama A, Nakajo S, Baba M, et al. (2000) Constitutive phosphorylation of the Parkinson's disease associated alpha-synuclein. J Biol Chem 275: 390-397.
557. Hashimoto M, Takenouchi T, Mallory M, Masliah E, Takeda A (2000) The role of NAC in amyloidogenesis in Alzheimer's disease. Am J Pathol 156: 734-736.
558. El-Agnaf OM, Jakes R, Curran MD, Middleton D, Ingenito R, et al. (1998) Aggregates from mutant and wild-type alpha-synuclein proteins and NAC peptide induce apoptotic cell death in human neuroblastoma cells by formation of beta-sheet and amyloid-like filaments. FEBS Lett 440: 71-75.
559. Fauvet B, Mbefo MK, Fares MB, Desobry C, Michael S, et al. (2012) alpha-Synuclein in central nervous system and from erythrocytes, mammalian cells, and Escherichia coli exists predominantly as disordered monomer. J Biol Chem 287: 15345-15364.
560. Bellucci A, Navarria L, Zaltieri M, Missale C, Spano P (2012) alpha-Synuclein synaptic pathology and its implications in the development of novel therapeutic approaches to cure Parkinson's disease. Brain Res 1432: 95-113.
561. Souza JM, Giasson BI, Chen Q, Lee VM, Ischiropoulos H (2000) Dityrosine cross-linking promotes formation of stable alpha -synuclein polymers. Implication of nitrative and oxidative stress in the pathogenesis of neurodegenerative synucleinopathies. J Biol Chem 275: 18344-18349.
562. Kim TD, Paik SR, Yang CH (2002) Structural and functional implications of C-terminal regions of alpha-synuclein. Biochemistry 41: 13782-13790.
563. Park SM, Jung HY, Kim TD, Park JH, Yang CH, et al. (2002) Distinct roles of the N-terminal-binding domain and the C-terminal-solubilizing domain of alpha-synuclein, a molecular chaperone. J Biol Chem 277: 28512-28520.

564. Negro A, Brunati AM, Donella-Deana A, Massimino ML, Pinna LA (2002) Multiple phosphorylation of alpha-synuclein by protein tyrosine kinase Syk prevents eosin-induced aggregation. FASEB J 16: 210-212.
565. Pronin AN, Morris AJ, Surguchov A, Benovic JL (2000) Synucleins are a novel class of substrates for G protein-coupled receptor kinases. J Biol Chem 275: 26515-26522.
566. Fujiwara H, Hasegawa M, Dohmae N, Kawashima A, Masliah E, et al. (2002) alpha-Synuclein is phosphorylated in synucleinopathy lesions. Nat Cell Biol 4: 160-164.
567. McLean PJ, Hyman BT (2002) An alternatively spliced form of rodent alpha-synuclein forms intracellular inclusions in vitro: role of the carboxy-terminus in alpha-synuclein aggregation. Neurosci Lett 323: 219-223.
568. Takahashi T, Yamashita H, Nakamura T, Nagano Y, Nakamura S (2002) Tyrosine 125 of alpha-synuclein plays a critical role for dimerization following nitrative stress. Brain Res 938: 73-80.
569. Rochet JC, Conway KA, Lansbury PT, Jr. (2000) Inhibition of fibrilization and accumulation of prefibrillar oligomers in mixtures of human and mouse alpha-synuclein. Biochemistry 39: 10619-10626.
570. Crowther RA, Jakes R, Spillantini MG, Goedert M (1998) Synthetic filaments assembled from C-terminally truncated alpha-synuclein. FEBS Lett 436: 309-312.
571. Weinreb PH, Zhen W, Poon AW, Conway KA, Lansbury PT, Jr. (1996) NACP, a protein implicated in Alzheimer's disease and learning, is natively unfolded. Biochemistry 35: 13709-13715.
572. Bartels T, Choi JG, Selkoe DJ (2011) alpha-Synuclein occurs physiologically as a helically folded tetramer that resists aggregation. Nature 477: 107-110.
573. Wang W, Perovic I, Chittuluru J, Kaganovich A, Nguyen LT, et al. (2011) A soluble alpha-synuclein construct forms a dynamic tetramer. Proc Natl Acad Sci U S A 108: 17797-17802.
574. Conway KA, Harper JD, Lansbury PT (1998) Accelerated in vitro fibril formation by a mutant alpha-synuclein linked to early-onset Parkinson disease. Nat Med 4: 1318-1320.
575. Ramakrishnan M, Jensen PH, Marsh D (2006) Association of alpha-synuclein and mutants with lipid membranes: spin-label ESR and polarized IR. Biochemistry 45: 3386-3395.
576. Ullman O, Fisher CK, Stultz CM (2011) Explaining the structural plasticity of alpha-synuclein. J Am Chem Soc 133: 19536-19546.
577. Hashimoto M, Hsu LJ, Xia Y, Takeda A, Sisk A, et al. (1999) Oxidative stress induces amyloid-like aggregate formation of NACP/alpha-synuclein in vitro. Neuroreport 10: 717-721.
578. Andringa G, Lam KY, Chegary M, Wang X, Chase TN, et al. (2004) Tissue transglutaminase catalyzes the formation of alpha-synuclein crosslinks in Parkinson's disease. FASEB J 18: 932-934.
579. Paleologou KE, Oueslati A, Shakked G, Rospigliosi CC, Kim HY, et al. (2010) Phosphorylation at S87 is enhanced in synucleinopathies, inhibits alpha-synuclein oligomerization, and influences synuclein-membrane interactions. J Neurosci 30: 3184-3198.

580. Li W, Lee MK (2005) Antiapoptotic property of human alpha-synuclein in neuronal cell lines is associated with the inhibition of caspase-3 but not caspase-9 activity. J Neurochem 93: 1542-1550.
581. Dufty BM, Warner LR, Hou ST, Jiang SX, Gomez-Isla T, et al. (2007) Calpain-cleavage of alpha-synuclein: connecting proteolytic processing to disease-linked aggregation. Am J Pathol 170: 1725-1738.
582. Perrin RJ, Woods WS, Clayton DF, George JM (2001) Exposure to long chain polyunsaturated fatty acids triggers rapid multimerization of synucleins. J Biol Chem 276: 41958-41962.
583. Sharon R, Bar-Joseph I, Frosch MP, Walsh DM, Hamilton JA, et al. (2003) The formation of highly soluble oligomers of alpha-synuclein is regulated by fatty acids and enhanced in Parkinson's disease. Neuron 37: 583-595.
584. Karube H, Sakamoto M, Arawaka S, Hara S, Sato H, et al. (2008) N-terminal region of alpha-synuclein is essential for the fatty acid-induced oligomerization of the molecules. FEBS Lett 582: 3693-3700.
585. Oueslati A, Fournier M, Lashuel HA (2010) Role of post-translational modifications in modulating the structure, function and toxicity of alpha-synuclein: implications for Parkinson's disease pathogenesis and therapies. Prog Brain Res 183: 115-145.
586. Baba M, Nakajo S, Tu PH, Tomita T, Nakaya K, et al. (1998) Aggregation of alpha-synuclein in Lewy bodies of sporadic Parkinson's disease and dementia with Lewy bodies. Am J Pathol 152: 879-884.
587. Masuda-Suzukake M, Nonaka T, Hosokawa M, Oikawa T, Arai T, et al. (2013) Prion-like spreading of pathological alpha-synuclein in brain. Brain 136: 1128-1138.
588. Serpell LC, Berriman J, Jakes R, Goedert M, Crowther RA (2000) Fiber diffraction of synthetic alpha-synuclein filaments shows amyloid-like cross-beta conformation. Proc Natl Acad Sci U S A 97: 4897-4902.
589. Abeliovich A, Schmitz Y, Farinas I, Choi-Lundberg D, Ho WH, et al. (2000) Mice lacking alpha-synuclein display functional deficits in the nigrostriatal dopamine system. Neuron 25: 239-252.
590. Murphy DD, Rueter SM, Trojanowski JQ, Lee VM (2000) Synucleins are developmentally expressed, and alpha-synuclein regulates the size of the presynaptic vesicular pool in primary hippocampal neurons. J Neurosci 20: 3214-3220.
591. Liu S, Ninan I, Antonova I, Battaglia F, Trinchese F, et al. (2004) alpha-Synuclein produces a long-lasting increase in neurotransmitter release. EMBO J 23: 4506-4516.
592. Wersinger C, Sidhu A (2003) Attenuation of dopamine transporter activity by alpha-synuclein. Neurosci Lett 340: 189-192.
593. Chandra S, Gallardo G, Fernandez-Chacon R, Schluter OM, Sudhof TC (2005) Alpha-synuclein cooperates with CSPalpha in preventing neurodegeneration. Cell 123: 383-396.
594. Yavich L, Tanila H, Vepsalainen S, Jakala P (2004) Role of alpha-synuclein in presynaptic dopamine recruitment. J Neurosci 24: 11165-11170.
595. Peng X, Tehranian R, Dietrich P, Stefanis L, Perez RG (2005) Alpha-synuclein activation of protein phosphatase 2A reduces tyrosine hydroxylase phosphorylation in dopaminergic cells. J Cell Sci 118: 3523-3530.

596. Kontopoulos E, Parvin JD, Feany MB (2006) Alpha-synuclein acts in the nucleus to inhibit histone acetylation and promote neurotoxicity. Hum Mol Genet 15: 3012-3023.
597. Iwata A, Maruyama M, Kanazawa I, Nukina N (2001) alpha-Synuclein affects the MAPK pathway and accelerates cell death. J Biol Chem 276: 45320-45329.
598. Ihara M, Yamasaki N, Hagiwara A, Tanigaki A, Kitano A, et al. (2007) Sept4, a component of presynaptic scaffold and Lewy bodies, is required for the suppression of alpha-synuclein neurotoxicity. Neuron 53: 519-533.
599. Ihara M, Tomimoto H, Kitayama H, Morioka Y, Akiguchi I, et al. (2003) Association of the cytoskeletal GTP-binding protein Sept4/H5 with cytoplasmic inclusions found in Parkinson's disease and other synucleinopathies. J Biol Chem 278: 24095-24102.
600. Furukawa K, Matsuzaki-Kobayashi M, Hasegawa T, Kikuchi A, Sugeno N, et al. (2006) Plasma membrane ion permeability induced by mutant alpha-synuclein contributes to the degeneration of neural cells. J Neurochem 97: 1071-1077.
601. Tsigelny IF, Bar-On P, Sharikov Y, Crews L, Hashimoto M, et al. (2007) Dynamics of alpha-synuclein aggregation and inhibition of pore-like oligomer development by beta-synuclein. FEBS J 274: 1862-1877.
602. Cooper AA, Gitler AD, Cashikar A, Haynes CM, Hill KJ, et al. (2006) Alpha-synuclein blocks ER-Golgi traffic and Rab1 rescues neuron loss in Parkinson's models. Science 313: 324-328.
603. Scott DA, Tabarean I, Tang Y, Cartier A, Masliah E, et al. (2010) A pathologic cascade leading to synaptic dysfunction in alpha-synuclein-induced neurodegeneration. J Neurosci 30: 8083-8095.
604. Nemani VM, Lu W, Berge V, Nakamura K, Onoa B, et al. (2010) Increased expression of alpha-synuclein reduces neurotransmitter release by inhibiting synaptic vesicle reclustering after endocytosis. Neuron 65: 66-79.
605. Gaugler MN, Genc O, Bobela W, Mohanna S, Ardah MT, et al. (2012) Nigrostriatal overabundance of alpha-synuclein leads to decreased vesicle density and deficits in dopamine release that correlate with reduced motor activity. Acta Neuropathol 123: 653-669.
606. Lundblad M, Decressac M, Mattsson B, Bjorklund A (2012) Impaired neurotransmission caused by overexpression of alpha-synuclein in nigral dopamine neurons. Proc Natl Acad Sci U S A 109: 3213-3219.
607. Larsen KE, Schmitz Y, Troyer MD, Mosharov E, Dietrich P, et al. (2006) Alpha-synuclein overexpression in PC12 and chromaffin cells impairs catecholamine release by interfering with a late step in exocytosis. J Neurosci 26: 11915-11922.
608. Scott D, Roy S (2012) alpha-Synuclein inhibits intersynaptic vesicle mobility and maintains recycling-pool homeostasis. J Neurosci 32: 10129-10135.
609. Kahle PJ, Neumann M, Ozmen L, Muller V, Jacobsen H, et al. (2000) Subcellular localization of wild-type and Parkinson's disease-associated mutant alpha -synuclein in human and transgenic mouse brain. J Neurosci 20: 6365-6373.
610. Lee HJ, Suk JE, Bae EJ, Lee JH, Paik SR, et al. (2008) Assembly-dependent endocytosis and clearance of extracellular alpha-synuclein. Int J Biochem Cell Biol 40: 1835-1849.
611. Payton JE, Perrin RJ, Woods WS, George JM (2004) Structural determinants of PLD2 inhibition by alpha-synuclein. J Mol Biol 337: 1001-1009.

612. Dalfo E, Ferrer I (2005) Alpha-synuclein binding to rab3a in multiple system atrophy. Neurosci Lett 380: 170-175.
613. Burre J, Sharma M, Tsetsenis T, Buchman V, Etherton MR, et al. (2010) Alpha-synuclein promotes SNARE-complex assembly in vivo and in vitro. Science 329: 1663-1667.
614. Chandra S, Fornai F, Kwon HB, Yazdani U, Atasoy D, et al. (2004) Double-knockout mice for alpha- and beta-synucleins: effect on synaptic functions. Proc Natl Acad Sci U S A 101: 14966-14971.
615. Fitzpatrick KM, Raschke J, Emborg ME (2009) Cell-based therapies for Parkinson's disease: past, present, and future. Antioxid Redox Signal 11: 2189-2208.
616. Eisele YS, Bolmont T, Heikenwalder M, Langer F, Jacobson LH, et al. (2009) Induction of cerebral beta-amyloidosis: intracerebral versus systemic Abeta inoculation. Proc Natl Acad Sci U S A 106: 12926-12931.
617. Frost B, Diamond MI (2010) Prion-like mechanisms in neurodegenerative diseases. Nat Rev Neurosci 11: 155-159.
618. Stohr J, Watts JC, Mensinger ZL, Oehler A, Grillo SK, et al. (2012) Purified and synthetic Alzheimer's amyloid beta (Abeta) prions. Proc Natl Acad Sci U S A 109: 11025-11030.
619. Angot E, Steiner JA, Hansen C, Li JY, Brundin P (2010) Are synucleinopathies prion-like disorders? Lancet Neurol 9: 1128-1138.
620. Tsigelny IF, Crews L, Desplats P, Shaked GM, Sharikov Y, et al. (2008) Mechanisms of hybrid oligomer formation in the pathogenesis of combined Alzheimer's and Parkinson's diseases. PLoS One 3: e3135.
621. Taschenberger G, Garrido M, Tereshchenko Y, Bahr M, Zweckstetter M, et al. (2012) Aggregation of alphaSynuclein promotes progressive in vivo neurotoxicity in adult rat dopaminergic neurons. Acta Neuropathol 123: 671-683.
622. Galvin JE, Lee VM, Trojanowski JQ (2001) Synucleinopathies: clinical and pathological implications. Arch Neurol 58: 186-190.
623. Muller CM, de Vos RA, Maurage CA, Thal DR, Tolnay M, et al. (2005) Staging of sporadic Parkinson disease-related alpha-synuclein pathology: inter- and intra-rater reliability. J Neuropathol Exp Neurol 64: 623-628.
624. Karlsson J, Petersen A, Gido G, Wieloch T, Brundin P (2005) Combining neuroprotective treatment of embryonic nigral donor tissue with mild hypothermia of the graft recipient. Cell Transplant 14: 301-309.
625. Karlsson J, Emgard M, Gido G, Wieloch T, Brundin P (2000) Increased survival of embryonic nigral neurons when grafted to hypothermic rats. Neuroreport 11: 1665-1668.
626. Frodl EM, Duan WM, Sauer H, Kupsch A, Brundin P (1994) Human embryonic dopamine neurons xenografted to the rat: effects of cryopreservation and varying regional source of donor cells on transplant survival, morphology and function. Brain Res 647: 286-298.
627. Li JY, Englund E, Holton JL, Soulet D, Hagell P, et al. (2008) Lewy bodies in grafted neurons in subjects with Parkinson's disease suggest host-to-graft disease propagation. Nat Med 14: 501-503.
628. Kordower JH, Chu Y, Hauser RA, Freeman TB, Olanow CW (2008) Lewy body-like pathology in long-term embryonic nigral transplants in Parkinson's disease. Nat Med 14: 504-506.

629. Kordower JH, Chu Y, Hauser RA, Olanow CW, Freeman TB (2008) Transplanted dopaminergic neurons develop PD pathologic changes: a second case report. Mov Disord 23: 2303-2306.
630. Mendez I, Vinuela A, Astradsson A, Mukhida K, Hallett P, et al. (2008) Dopamine neurons implanted into people with Parkinson's disease survive without pathology for 14 years. Nat Med 14: 507-509.
631. Kordower JH, Freeman TB, Snow BJ, Vingerhoets FJ, Mufson EJ, et al. (1995) Neuropathological evidence of graft survival and striatal reinnervation after the transplantation of fetal mesencephalic tissue in a patient with Parkinson's disease. N Engl J Med 332: 1118-1124.
632. Crews L, Mizuno H, Desplats P, Rockenstein E, Adame A, et al. (2008) Alpha-synuclein alters Notch-1 expression and neurogenesis in mouse embryonic stem cells and in the hippocampus of transgenic mice. J Neurosci 28: 4250-4260.
633. Letarov A, Manival X, Desplats C, Krisch HM (2005) gpwac of the T4-type bacteriophages: structure, function, and evolution of a segmented coiled-coil protein that controls viral infectivity. J Bacteriol 187: 1055-1066.
634. Ekberg H, Qi Z, Pahlman C, Veress B, Bundick RV, et al. (2007) The specific monocarboxylate transporter-1 (MCT-1) inhibitor, AR-C117977, induces donor-specific suppression, reducing acute and chronic allograft rejection in the rat. Transplantation 84: 1191-1199.
635. Emmanouilidou E, Melachroinou K, Roumeliotis T, Garbis SD, Ntzouni M, et al. (2010) Cell-produced alpha-synuclein is secreted in a calcium-dependent manner by exosomes and impacts neuronal survival. J Neurosci 30: 6838-6851.
636. Luk KC, Kehm VM, Zhang B, O'Brien P, Trojanowski JQ, et al. (2012) Intracerebral inoculation of pathological alpha-synuclein initiates a rapidly progressive neurodegenerative alpha-synucleinopathy in mice. J Exp Med 209: 975-986.
637. McKeith IG, Galasko D, Kosaka K, Perry EK, Dickson DW, et al. (1996) Consensus guidelines for the clinical and pathologic diagnosis of dementia with Lewy bodies (DLB): report of the consortium on DLB international workshop. Neurology 47: 1113-1124.
638. Vekrellis K, Xilouri M, Emmanouilidou E, Rideout HJ, Stefanis L (2011) Pathological roles of alpha-synuclein in neurological disorders. Lancet Neurol 10: 1015-1025.
639. Takeda A, Hashimoto M, Mallory M, Sundsumo M, Hansen L, et al. (1998) Abnormal distribution of the non-Abeta component of Alzheimer's disease amyloid precursor/alpha-synuclein in Lewy body disease as revealed by proteinase K and formic acid pretreatment. Lab Invest 78: 1169-1177.
640. Suh YH, Checler F (2002) Amyloid precursor protein, presenilins, and alpha-synuclein: molecular pathogenesis and pharmacological applications in Alzheimer's disease. Pharmacol Rev 54: 469-525.
641. Iwai A, Masliah E, Sundsmo MP, DeTeresa R, Mallory M, et al. (1996) The synaptic protein NACP is abnormally expressed during the progression of Alzheimer's disease. Brain Res 720: 230-234.
642. Kragh CL, Ubhi K, Wyss-Coray T, Masliah E (2012) Autophagy in dementias. Brain Pathol 22: 99-109.

643. Seidel K, Schols L, Nuber S, Petrasch-Parwez E, Gierga K, et al. (2010) First appraisal of brain pathology owing to A30P mutant alpha-synuclein. Ann Neurol 67: 684-689.
644. Iwata A, Maruyama M, Akagi T, Hashikawa T, Kanazawa I, et al. (2003) Alpha-synuclein degradation by serine protease neurosin: implication for pathogenesis of synucleinopathies. Hum Mol Genet 12: 2625-2635.
645. Klucken J, Shin Y, Masliah E, Hyman BT, McLean PJ (2004) Hsp70 Reduces alpha-Synuclein Aggregation and Toxicity. J Biol Chem 279: 25497-25502.
646. McNaught KS, Mytilineou C, Jnobaptiste R, Yabut J, Shashidharan P, et al. (2002) Impairment of the ubiquitin-proteasome system causes dopaminergic cell death and inclusion body formation in ventral mesencephalic cultures. J Neurochem 81: 301-306.
647. McNaught KS, Bjorklund LM, Belizaire R, Isacson O, Jenner P, et al. (2002) Proteasome inhibition causes nigral degeneration with inclusion bodies in rats. Neuroreport 13: 1437-1441.
648. Cuervo AM, Stefanis L, Fredenburg R, Lansbury PT, Sulzer D (2004) Impaired degradation of mutant alpha-synuclein by chaperone-mediated autophagy. Science 305: 1292-1295.
649. Spencer B, Potkar R, Trejo M, Rockenstein E, Patrick C, et al. (2009) Beclin 1 gene transfer activates autophagy and ameliorates the neurodegenerative pathology in alpha-synuclein models of Parkinson's and Lewy body diseases. J Neurosci 29: 13578-13588.
650. Crews L, Spencer B, Desplats P, Patrick C, Paulino A, et al. (2010) Selective molecular alterations in the autophagy pathway in patients with Lewy body disease and in models of alpha-synucleinopathy. PLoS One 5: e9313.
651. Lee HJ, Patel S, Lee SJ (2005) Intravesicular localization and exocytosis of alpha-synuclein and its aggregates. J Neurosci 25: 6016-6024.
652. Vila M, Ramonet D, Perier C (2008) Mitochondrial alterations in Parkinson's disease: new clues. J Neurochem 107: 317-328.
653. Lashuel HA, Overk CR, Oueslati A, Masliah E (2013) The many faces of alpha-synuclein: from structure and toxicity to therapeutic target. Nat Rev Neurosci 14: 38-48.
654. Abbott RD, Petrovitch H, White LR, Masaki KH, Tanner CM, et al. (2001) Frequency of bowel movements and the future risk of Parkinson's disease. Neurology 57: 456-462.
655. Abbott RD, Ross GW, White LR, Sanderson WT, Burchfiel CM, et al. (2003) Environmental, life-style, and physical precursors of clinical Parkinson's disease: recent findings from the Honolulu-Asia Aging Study. J Neurol 250 Suppl 3: III30-39.
656. Kuo YM, Li Z, Jiao Y, Gaborit N, Pani AK, et al. (2010) Extensive enteric nervous system abnormalities in mice transgenic for artificial chromosomes containing Parkinson disease-associated alpha-synuclein gene mutations precede central nervous system changes. Hum Mol Genet 19: 1633-1650.
657. Braak H, Muller CM, Rub U, Ackermann H, Bratzke H, et al. (2006) Pathology associated with sporadic Parkinson's disease--where does it end? J Neural Transm Suppl: 89-97.
658. Braak H, Del Tredici K (2011) Alzheimer's pathogenesis: is there neuron-to-neuron propagation? Acta Neuropathol 121: 589-595.
659. Braak E, Braak H (1999) Silver staining method for demonstrating Lewy bodies in Parkinson's disease and argyrophilic oligodendrocytes in multiple system atrophy. J Neurosci Methods 87: 111-115.

660. Braak H, Del Tredici K, Rub U, de Vos RA, Jansen Steur EN, et al. (2003) Staging of brain pathology related to sporadic Parkinson's disease. Neurobiol Aging 24: 197-211.
661. Beach TG, Adler CH, Sue LI, Vedders L, Lue L, et al. (2010) Multi-organ distribution of phosphorylated alpha-synuclein histopathology in subjects with Lewy body disorders. Acta Neuropathol 119: 689-702.
662. Hawkes CH, Del Tredici K, Braak H (2009) Parkinson's disease: the dual hit theory revisited. Ann N Y Acad Sci 1170: 615-622.
663. Olanow CW, Prusiner SB (2009) Is Parkinson's disease a prion disorder? Proc Natl Acad Sci U S A 106: 12571-12572.
664. Lee SJ, Desplats P, Lee HJ, Spencer B, Masliah E (2012) Cell-to-cell transmission of alpha-synuclein aggregates. Methods Mol Biol 849: 347-359.
665. Munch C, Bertolotti A (2011) Self-propagation and transmission of misfolded mutant SOD1: prion or prion-like phenomenon? Cell Cycle 10: 1711.
666. Grad LI, Guest WC, Yanai A, Pokrishevsky E, O'Neill MA, et al. (2011) Intermolecular transmission of superoxide dismutase 1 misfolding in living cells. Proc Natl Acad Sci U S A 108: 16398-16403.
667. Furukawa Y, Kaneko K, Watanabe S, Yamanaka K, Nukina N (2011) A seeding reaction recapitulates intracellular formation of Sarkosyl-insoluble transactivation response element (TAR) DNA-binding protein-43 inclusions. J Biol Chem 286: 18664-18672.
668. Jang A, Lee HJ, Suk JE, Jung JW, Kim KP, et al. (2010) Non-classical exocytosis of alpha-synuclein is sensitive to folding states and promoted under stress conditions. J Neurochem 113: 1263-1274.
669. Danzer KM, Krebs SK, Wolff M, Birk G, Hengerer B (2009) Seeding induced by alpha-synuclein oligomers provides evidence for spreading of alpha-synuclein pathology. J Neurochem 111: 192-203.
670. Danzer KM, Ruf WP, Putcha P, Joyner D, Hashimoto T, et al. (2011) Heat-shock protein 70 modulates toxic extracellular alpha-synuclein oligomers and rescues trans-synaptic toxicity. FASEB J 25: 326-336.
671. Kordower JH, Freeman TB, Olanow CW (1998) Neuropathology of fetal nigral grafts in patients with Parkinson's disease. Mov Disord 13 Suppl 1: 88-95.
672. Tang Y, Das U, Scott DA, Roy S (2012) The slow axonal transport of alpha-synuclein--mechanistic commonalities amongst diverse cytosolic cargoes. Cytoskeleton (Hoboken) 69: 506-513.
673. Kim JI, Cali I, Surewicz K, Kong Q, Raymond GJ, et al. (2010) Mammalian prions generated from bacterially expressed prion protein in the absence of any mammalian cofactors. J Biol Chem 285: 14083-14087.
674. Makarava N, Kovacs GG, Savtchenko R, Alexeeva I, Budka H, et al. (2011) Genesis of mammalian prions: from non-infectious amyloid fibrils to a transmissible prion disease. PLoS Pathog 7: e1002419.
675. Hardy J, Revesz T (2012) The spread of neurodegenerative disease. N Engl J Med 366: 2126-2128.
676. Conway KA, Lee SJ, Rochet JC, Ding TT, Williamson RE, et al. (2000) Acceleration of oligomerization, not fibrilization, is a shared property of both alpha-synuclein mutations

linked to early-onset Parkinson's disease: implications for pathogenesis and therapy. Proc Natl Acad Sci U S A 97: 571-576.
677. Prusiner SB (1993) Genetic and infectious prion diseases. Arch Neurol 50: 1129-1153.
678. Kosaka K (1990) Diffuse Lewy body disease in Japan. J Neurol 237: 197-204.
679. Dickson DW, Crystal H, Mattiace LA, Kress Y, Schwagerl A, et al. (1989) Diffuse Lewy body disease: light and electron microscopic immunocytochemistry of senile plaques. Acta Neuropathol 78: 572-584.
680. Kahle PJ, Neumann M, Ozmen L, Muller V, Odoy S, et al. (2001) Selective insolubility of alpha-synuclein in human Lewy body diseases is recapitulated in a transgenic mouse model. Am J Pathol 159: 2215-2225.
681. Lee MK, Stirling W, Xu Y, Xu X, Qui D, et al. (2002) Human alpha-synuclein-harboring familial Parkinson's disease-linked Ala-53 --> Thr mutation causes neurodegenerative disease with alpha-synuclein aggregation in transgenic mice. Proc Natl Acad Sci U S A 99: 8968-8973.
682. Schulz-Schaeffer WJ (2010) The synaptic pathology of alpha-synuclein aggregation in dementia with Lewy bodies, Parkinson's disease and Parkinson's disease dementia. Acta Neuropathol 120: 131-143.
683. Garcia-Reitbock P, Anichtchik O, Bellucci A, Iovino M, Ballini C, et al. (2010) SNARE protein redistribution and synaptic failure in a transgenic mouse model of Parkinson's disease. Brain 133: 2032-2044.
684. Horvath I, Weise CF, Andersson EK, Chorell E, Sellstedt M, et al. (2012) Mechanisms of protein oligomerization: inhibitor of functional amyloids templates alpha-synuclein fibrillation. J Am Chem Soc 134: 3439-3444.
685. Conway KA, Lee SJ, Rochet JC, Ding TT, Harper JD, et al. (2000) Accelerated oligomerization by Parkinson's disease linked alpha-synuclein mutants. Ann N Y Acad Sci 920: 42-45.
686. Cremades N, Cohen SI, Deas E, Abramov AY, Chen AY, et al. (2012) Direct observation of the interconversion of normal and toxic forms of alpha-synuclein. Cell 149: 1048-1059.
687. Danzer KM, Haasen D, Karow AR, Moussaud S, Habeck M, et al. (2007) Different species of alpha-synuclein oligomers induce calcium influx and seeding. J Neurosci 27: 9220-9232.
688. Kunze S, Lemke K, Metze J, Bloukas G, Kotta K, et al. (2008) Atomic force microscopy to characterize the molecular size of prion protein. J Microsc 230: 224-232.
689. Weissmann C, Fischer M, Raeber A, Bueler H, Sailer A, et al. (1998) The use of transgenic mice in the investigation of transmissible spongiform encephalopathies. Rev Sci Tech 17: 278-290.
690. Andreoletti O, Orge L, Benestad SL, Beringue V, Litaise C, et al. (2011) Atypical/Nor98 scrapie infectivity in sheep peripheral tissues. PLoS Pathog 7: e1001285.
691. Uro-Coste E, Cassard H, Simon S, Lugan S, Bilheude JM, et al. (2008) Beyond PrP res type 1/type 2 dichotomy in Creutzfeldt-Jakob disease. PLoS Pathog 4: e1000029.
692. Espinosa JC, Morales M, Castilla J, Rogers M, Torres JM (2007) Progression of prion infectivity in asymptomatic cattle after oral bovine spongiform encephalopathy challenge. J Gen Virol 88: 1379-1383.

693. Espinosa JC, Herva ME, Andreoletti O, Padilla D, Lacroux C, et al. (2009) Transgenic mice expressing porcine prion protein resistant to classical scrapie but susceptible to sheep bovine spongiform encephalopathy and atypical scrapie. Emerg Infect Dis 15: 1214-1221.
694. Feraudet C, Morel N, Simon S, Volland H, Frobert Y, et al. (2005) Screening of 145 anti-PrP monoclonal antibodies for their capacity to inhibit PrPSc replication in infected cells. J Biol Chem 280: 11247-11258.
695. Baron GS, Magalhaes AC, Prado MA, Caughey B (2006) Mouse-adapted scrapie infection of SN56 cells: greater efficiency with microsome-associated versus purified PrP-res. J Virol 80: 2106-2117.
696. Ryou C, Legname G, Peretz D, Craig JC, Baldwin MA, et al. (2003) Differential inhibition of prion propagation by enantiomers of quinacrine. Lab Invest 83: 837-843.
697. Kuwahara C, Takeuchi AM, Nishimura T, Haraguchi K, Kubosaki A, et al. (1999) Prions prevent neuronal cell-line death. Nature 400: 225-226.
698. Sakudo A, Onodera T, Suganuma Y, Kobayashi T, Saeki K, et al. (2006) Recent advances in clarifying prion protein functions using knockout mice and derived cell lines. Mini Rev Med Chem 6: 589-601.
699. Nishimura T, Sakudo A, Xue G, Ikuta K, Yukawa M, et al. (2008) Establishment of a new glial cell line from hippocampus of prion protein gene-deficient mice. Biochem Biophys Res Commun 377: 1047-1050.
700. Nishimura T, Sakudo A, Hashiyama Y, Yachi A, Saeki K, et al. (2007) Serum withdrawal-induced apoptosis in ZrchI prion protein (PrP) gene-deficient neuronal cell line is suppressed by PrP, independent of Doppel. Microbiol Immunol 51: 457-466.
701. Mellon PL, Windle JJ, Goldsmith PC, Padula CA, Roberts JL, et al. (1990) Immortalization of hypothalamic GnRH neurons by genetically targeted tumorigenesis. Neuron 5: 1-10.
702. Klebe JG, Bay J (1969) [Measurement of central venous pressure during anesthesia]. Nord Med 81: 12-15.
703. Biedler JL, Helson L, Spengler BA (1973) Morphology and growth, tumorigenicity, and cytogenetics of human neuroblastoma cells in continuous culture. Cancer Res 33: 2643-2652.
704. Latawiec D, Herrera F, Bek A, Losasso V, Candotti M, et al. (2010) Modulation of alpha-synuclein aggregation by dopamine analogs. PLoS One 5: e9234.
705. Huang C, Ren G, Zhou H, Wang CC (2005) A new method for purification of recombinant human alpha-synuclein in Escherichia coli. Protein Expr Purif 42: 173-177.
706. Cohen FE, Prusiner SB (1998) Pathologic conformations of prion proteins. Annu Rev Biochem 67: 793-819.
707. Wiltzius JJ, Landau M, Nelson R, Sawaya MR, Apostol MI, et al. (2009) Molecular mechanisms for protein-encoded inheritance. Nat Struct Mol Biol 16: 973-978.
708. Tanaka M, Chien P, Naber N, Cooke R, Weissman JS (2004) Conformational variations in an infectious protein determine prion strain differences. Nature 428: 323-328.
709. Solassol J, Crozet C, Lehmann S (2003) Prion propagation in cultured cells. Br Med Bull 66: 87-97.
710. Yang S, Levine H, Onuchic JN, Cox DL (2005) Structure of infectious prions: stabilization by domain swapping. FASEB J 19: 1778-1782.

711. Rousseau F, Schymkowitz JWH, Itzhaki LS (2003) The unfolding story of three-dimensional domain swapping. Structure 11: 243-251.
712. Rogers DR (1965) Screening for Amyloid with the Thioflavin-T Fluorescent Method. Am J Clin Pathol 44: 59-61.
713. Khurana R, Coleman C, Ionescu-Zanetti C, Carter SA, Krishna V, et al. (2005) Mechanism of thioflavin T binding to amyloid fibrils. J Struct Biol 151: 229-238.
714. Hamley IW (2007) Peptide fibrilization. Angew Chem Int Ed Engl 46: 8128-8147.
715. Bucciantini M, Calloni G, Chiti F, Formigli L, Nosi D, et al. (2004) Prefibrillar amyloid protein aggregates share common features of cytotoxicity. J Biol Chem 279: 31374-31382.
716. Simoneau S, Rezaei H, Sales N, Kaiser-Schulz G, Lefebvre-Roque M, et al. (2007) In vitro and in vivo neurotoxicity of prion protein oligomers. PLoS Pathog 3: e125.
717. Caughey B, Lansbury PT (2003) Protofibrils, pores, fibrils, and neurodegeneration: separating the responsible protein aggregates from the innocent bystanders. Annu Rev Neurosci 26: 267-298.
718. Abskharon RN, Ramboarina S, El Hassan H, Gad W, Apostol MI, et al. (2012) A novel expression system for production of soluble prion proteins in E. coli. Microb Cell Fact 11: 6.
719. Biljan I, Ilc G, Giachin G, Raspadori A, Zhukov I, et al. (2011) Toward the molecular basis of inherited prion diseases: NMR structure of the human prion protein with V210I mutation. J Mol Biol 412: 660-673.
720. Kosmac M, Koren S, Giachin G, Stoilova T, Gennaro R, et al. (2011) Epitope mapping of a PrP(Sc)-specific monoclonal antibody: identification of a novel C-terminally truncated prion fragment. Mol Immunol 48: 746-750.
721. Rossetti G, Giachin G, Legname G, Carloni P (2010) Structural facets of disease-linked human prion protein mutants: a molecular dynamic study. Proteins 78: 3270-3280.
722. Collinge J, Clarke AR (2007) A general model of prion strains and their pathogenicity. Science 318: 930-936.
723. Chiti F, Dobson CM (2009) Amyloid formation by globular proteins under native conditions. Nat Chem Biol 5: 15-22.
724. Eghiaian F, Daubenfeld T, Quenet Y, van Audenhaege M, Bouin AP, et al. (2007) Diversity in prion protein oligomerization pathways results from domain expansion as revealed by hydrogen/deuterium exchange and disulfide linkage. Proc Natl Acad Sci U S A 104: 7414-7419.
725. Jeffrey M, Goodsir CM, Bruce ME, McBride PA, Scott JR (1994) Infection-specific prion protein (PrP) accumulates on neuronal plasmalemma in scrapie-infected mice. Ann N Y Acad Sci 724: 327-330.
726. Carrell RW, Gooptu B (1998) Conformational changes and disease--serpins, prions and Alzheimer's. Curr Opin Struct Biol 8: 799-809.
727. Chang CC, Su YC, Cheng MS, Kan LS (2002) Protein folding by a quasi-static-like process: a first-order state transition. Phys Rev E Stat Nonlin Soft Matter Phys 66: 021903.
728. Garcia-Mata R, Bebok Z, Sorscher EJ, Sztul ES (1999) Characterization and dynamics of aggresome formation by a cytosolic GFP-chimera. J Cell Biol 146: 1239-1254.

729. Prusiner SB (2012) Cell biology. A unifying role for prions in neurodegenerative diseases. Science 336: 1511-1513.
730. Ashe KH, Aguzzi A (2013) Prions, prionoids and pathogenic proteins in Alzheimer disease. Prion 7: 55-59.
731. Uversky VN, Li J, Fink AL (2001) Evidence for a partially folded intermediate in alpha-synuclein fibril formation. J Biol Chem 276: 10737-10744.
732. Vaughan JR, Farrer MJ, Wszolek ZK, Gasser T, Durr A, et al. (1998) Sequencing of the alpha-synuclein gene in a large series of cases of familial Parkinson's disease fails to reveal any further mutations. The European Consortium on Genetic Susceptibility in Parkinson's Disease (GSPD). Hum Mol Genet 7: 751-753.
733. Guyenet SJ, Furrer SA, Damian VM, Baughan TD, La Spada AR, et al. (2010) A simple composite phenotype scoring system for evaluating mouse models of cerebellar ataxia. J Vis Exp.
734. Thomas PS, Jr., Fraley GS, Damian V, Woodke LB, Zapata F, et al. (2006) Loss of endogenous androgen receptor protein accelerates motor neuron degeneration and accentuates androgen insensitivity in a mouse model of X-linked spinal and bulbar muscular atrophy. Hum Mol Genet 15: 2225-2238.
735. Ghaemmaghami S, Colby DW, Nguyen HO, Hayashi S, Oehler A, et al. (2013) Convergent replication of mouse synthetic prion strains. Am J Pathol 182: 866-874.
736. Kong Q, Surewicz WK, Petersen RB, *et al.* Inherited prion diseases. In: Prusiner SB, ed. Prion biology and disease. 2nd ed. Cold Spring Harbor, NY: Cold Spring Harbor Laboratory Press; 2004:673-776